NDE1 in the DISC1 pathway: Interactions of schizophrenia-related proteins

Nicholas James Bradshaw

PhD

The University of Edinburgh

2009

Declaration

I declare that, except for where noted, all work contained in this thesis was performed and composed by myself. Where others have contributed to elements of the work, this is stated clearly in the text. No element of this work has been submitted for any other degree of professional qualification.

Nicholas J. Bradshaw

Acknowledgements

None of the work I have done over the work I have done over the last three years would have been possible without my supervisors Kirsty Millar and David Porteous, who accepted me for this project and who have been a constant source of support and insight ever since.

All of the DISC1 group have been an enormous amount of support, but I would particularly like to thank Sheila Christie, Shaun Mackie and Sebby Cooper for their help and considerable patience, I dread to think how often I must have pestered each of you for help since I first started. Similarly, I would like to thank Dinesh Soares for all his assistance and ideas in developing the bioinformatics sections of my PhD. Many other people throughout the Medical Genetics section have generously provided me with much appreciated assistance throughout my project and while I could not hope to name them all, I would like to mention in particular Jennifer, Fumiaki, Christoph, Ben, Pippa, Judith and Sarah.

I would also like to acknowledge Dr Nick Brandon, Professor Miles Houslay and Professor Tetsu Akiyama for their kind gifts of the NDEL1 231, PDE4 and α-DISC1 antibodies respectively. Additionally, I would like to thank the Medical Research Council for funding my PhD.

I have enjoyed the vast majority of the last three years working in the Molecular Medicine Centre, and I would like to thank all of the PhD students who I have shared an office with over that time for being a big part of that. I would particularly like to thank Miriam, Becky and Helen for their company and for being willing to trade rants and ravings with me during the more difficult times in our projects.

Away from the lab, however, I have to offer huge amounts of thanks to those who have got me through the last three years:

To Libby, for her seemingly unending support, love and patience ever since we got married and moved to Edinburgh (I promise that in the future we will find somewhere warmer!), and for the inspiration that she has been to me every day since.

To all of my friends and family who have been praying for me, particularly during the harder times of the PhD, and to the guy who has been answering them.

Finally, to little Katie who, despite only being two months old, has already changed my life in ways I never could have expected, and it is to you that I dedicate this thesis.

Abstract

The Disrupted-In-Schizophrenia 1 (*DISC1*) gene is one of the most established risk genes for psychiatric illness currently being studied, having originally been identified as being directly disrupted by a balanced chromosomal translocation that co-segregates with schizophrenia and other major mental illness a large Scottish family. The DISC1 protein is believed to act as a molecular scaffold within the cell, binding to a large number of other proteins. Three of these protein interactors, Phosphodiesterase 4B (PDE4B), Nuclear Distribution Factor E (*Aspergillus nidulans*)-homologue 1 (NDE1) and NDE-Like 1 (NDEL1) all have evidence implicating them as schizophrenia-related proteins in their own right. NDE1 and NDEL1 are highly similar proteins which are known to play cellular roles including microtubule function and mitosis. Their orthologues have also been shown to be important in neurodevelopment within the mouse brain. To date, most work in the literature has investigated NDEL1, with few focusing on NDE1.

In the thesis, I first seek to establish a basic biology for NDE1 by the identification of splice variants expressed in the brain, establishing cellular localisation patterns within the cell and investigating NDE1 multimerisation. The relationship between NDE1 and NDEL1 is also investigated, with the two being found to form complexes together and to have partially over-lapping expression patterns within the cell. That NDE1 and DISC1 directly interact is confirmed. The relationship between NDE1 and PDE4B is then investigated, with the two proteins found to complex within the cell. Additionally, it is shown that NDE1 can be phosphorylated by protein kinase A (PKA). This kinase is cAMP dependant, and is thus indirectly regulated by the cAMP-degrading action of PDE4B protein. Attempts to map and analyse the effect of this phosphorylation on NDE1 are made.

Table of contents

List of figures

List of tables

List of abbreviations used in the thesis

Genes and proteins

Note: For reasons of space, this list does not include proteins listed in table 1.2 unless they also appear elsewhere in the text.

14-3-3ε	Protein encoded by the *YWHAE* gene
AKAP	A-Kinase Anchoring Protein
ATF	Activating Transcription Factor
ATM	Ataxia Telangiectasia Mutated
BBS4	Barde-Biedl Syndrome protein 4
Cdc2	Cell Division Cycle 2
Cdc42GAP	Cell Division Cycle 42 GTPase Activating Protein
Cdk	Cyclin-Dependant Kinase
CENPA	Centromeric Protein A
CENPF	Centromeric Protein F
CHDM	Chromodomain Helicase DNA-binding protein Mi-2 homologue
Clk	Cdc-Like Kinase
COMT	Catechol-O-Methyltransferase
CREB	cAMP Response Element Binding
DAO	D-amino Acid Oxidase (sometimes abbreviated as DAAO, also known as G30)
DAOA	DAO Activator (also known as G72)
DBZ	DISC1-Binding Zinc finger protein (also known as ZNF365 and Su48)
DYNC1H1	Cytoplasmic dynein 1 heavy chain 1
DYNC2H1	Cytoplasmic dynein 2 heavy chain 1
DCTN1	Dynactin 1, gene encoding the dynamitin/p50 subunit
DISC	Disrupted In Schizophrenia
DNA PK	DNA-dependant Protein Kinase
DRD4	Dopamine Receptor D4

DTNBP1	Dystrobrevin-Binding Protein 1 (also known as dysbindin)
Dynactin	Dynein Activator
eIF3 p40	Eukaryotic Initiation Factor 3, 40kDa subunit
EIF3S3	Eukaryotic Initiation Factor 3 Subunit 3 (gene encoding eIF3 p40)
EOPA	Endo-Oligopeptidase A (synonym of NDEL1 in some literature)
EOPARP	Endo-Oligopeptidase A Related Protein (Rabbit homologue of NDEL1 in some literature)
Erk	Extracellular signal-Regulated Kinase
FEZ1	Fasciculation of Elongation factor Zeta 1
IgG	Immunoglobulin G
GFP	Green Fluorescent Protein
GRB2	Growth factor Receptor Bound protein 2
GSK3	Glycogen Synthase Kinase 3
GST	Glutathione S-Transferase
HIPK2	Homeodomain-Interacting Protein Kinase 2
HOM-TES-87	*Homo sapiens* Testis clone 87 (Synonym of NDE1 in some literature)
KATNA1	Katanin A1 (Gene encoding the katanin p60 subunit)
KATNB1	Katanin B1 (Gene encoding the katanin p80 subunit)
KIF	Kinesin Family member
KLC	Kinesin Light Chain
LIS1	Lissencephaly 1
MCRS1	Microspherule protein 1
MAP1A	Microtubule-Associated Protein 1A
MIPT3	Microtubule Interacting Protein that associates with TRAF3
MP43	Mitotic Phosphoprotein 43 (*Xenopus* homologue of NDE1)
N-CoR	Nuclear receptor Corepressor
NDE1	Nuclear Distribution factor E (*Aspergillus nidulans*) homologue 1 (or Nuclear Distribution Element 1 in some literature)
NDEL1	Nuclear Distribution factor E (*Aspergillus nidulans*) homologue-Like 1 (or Nuclear Distribution Element-Like 1 in some literature)
Ndl1	*Saccharomyces cerevisae* homologue of NDE1 and/or NDEL1

NF-L	Neurofilament Light subunit
NMDA	N-Methyl-D-Aspartic acid
NRG1	Neuregulin 1
NPHP6	Nephrocystin Protein 6
NUD-2	*Caenorhabditis elegans* homologue of NDE1 and/or NDEL1
NUDE	Nuclear Distribution factor E (*Aspergillus nidulans* homologue of NDE1/NDEL1) and a synonym for mammalian NDE1 in some literature.
NUDEL	Synonym for NDEL1 in some literature
PAFAH	Platelet-Activating Factor Acetylhydrolase
PAFAH1B1	Platelet-Activating Factor Acetylhydrolase 1B subunit 1, a synonym of the *LIS1* gene
PCM-1	Pericentriolar Material 1
PCTN	Gene encoding pericentrin-A and B
PCTN2	Spliced transcript of *PCTN* encoding pericentrin-B (also known as kendrin)
PDE4	Phosphodiesterase 4
PKA	Protein Kinase A
PKC	Protein Kinase C
PTF	PSE-binding transcription factor
RO-11	*Ro*py 11 (*Neurospora crassa* homologue of NDE1/NDEL1)
Su48	Survivin-related 48kDa
TIAM2	T-cell lymphoma Invasion and Metastasis
TRAF3	TNF Receptor-Associated Factor 3
TRAF3IP1	TRAF3-Interacting Protein 1 (synonym for MIP-T3)
TRAX	Translin-Associated factor X
YWHAE	Tyrosine 3-monooxygenase/Tryptophan 5-monooxygenase Activation protein, Epsilon isoform (Gene encoding the 14-3-3ε protein)
ZNF	Zinc Finger protein

Units

A	Ampere
Å	Angstrom (10^{-10} m)
b	Base (nucleic acid)
°C	Degrees Centigrade
Da	Dalton
g	Gram
l	Litre
m	Meter
mins	Minutes
M	Molar (moles per litre)
mol	Moles
rpm	Revolutions per minute (or Rocks Per Minute)
V	Volt
W	Watt

f	Femto- ($x10^{-15}$)
p	Pico- ($x10^{-12}$)
n	Nano- ($x10^{-9}$)
µ	Micro- ($x10^{-6}$)
m	Milli- ($x10^{-3}$)
c	Centi-($x10^{-2}$)
k	Kilo- ($x10^{3}$)

Amino acids

A	Alanine
C	Cysteine
D	Aspartic acid
E	Glutamic acid

F	Phenylalanine
G	Glycine
H	Histidine
I	Isoleucine
K	Lysine
L	Leucine
M	Methionine
N	Asparagine
P	Proline
Q	Glutamine
R	Arginine
S	Serine
T	Threonine
V	Valine
W	Tryptophan
Y	Tyrosine
pX	Indicates amino acid X is phosphorylated

Nucleotides

A	Adenine
C	Cytosine
G	Guanine
T	Thymidine

Other abbreviations

2xYT	2x Yeast extract Tryptone medium
AMV	Avian Myeloblastosis Virus
AS	Asperger's Syndrome

ATP	Adenosine Triphosphate
AUT	Autism
BSA	Bovine Serum Albumin
BPD	Bipolar Disorder
cAMP	Cyclic Adenosine Monophosphate
cDNA	Complementary DNA
CHAPS	3-[(3-Cholamidopropyl)dimethylammonio]-1-propanesulfonate
CO_2	Carbon Dioxide
CTP	Cytidine Triphosphate
DABCO	1,4-diazabicyclo[2.2.2]octane
DAPI	4',6-diamidino-2-phenylindole
DEPC	Diethylpyrocarbonate
dH_2O	Deionised water
D-MEM	Dulbecco Modified Eagle's minimum essential Medium
DNA	Deoxyribonucleic Acid
DSM-IV	Diagnostic and Statistical manual of Mental disorder (Fourth edition)
DTT	Dithiothreitol
EDTA	Ethylenediaminetetraacetic Acid
ENU	*N*-nitroso-*N*-ethylurea
Es	Extremely Short isoform (of *DISC1*)
Δex3	Lacking exon 3
FL	Full Length
GTP	Guanosine triphosphate
HCl	Hydrochloric Acid
HL	Hot-Loops definition (of the DisEMBL 1.5 program)
H89	N-[2-(p-Bromocinnamylamino)ethyl]-5-soquinolinesulfonamide·2HCl
IBMX	Isobutylmethylxanthine
ICC	Immunocytochemistry
IP	Immunoprecipitation
IPTG	Isopropyl β-D-1-thiogalactopyranoside
L	Long isoform (of *DISC1*)

Lv	Long Variant isoform (of *DISC1*)
LB	Lysogeny Broth
L/C	Loops/Coils definition (of the DisEMBL 1.5 program)
LOD	Logarithm Of Odds
M133	Using the methionine-133 start codon
mRNA	Messenger RNA
MDD	Major Depressive Disorder
MRI	Magnetic Resonance Imaging
M_W	Molecular weight
N/A	Not Applicable
NLS	Nuclear Localisation Signal
NP-40	Nonyl Phenoxylpolyethoxylethanol
OPT	Oct1/PTF/transcription
PBS	Phosphate-Buffered Saline
PCR	Polymerase Chain Reaction
PFA	Paraformaldehyde
pI	Isoelectric point
PSE	Proximal Sequence Element
PVDF	Polyvinylidene Fluoride
R465	Remark-465 definition (of the DisEMBL 1.5 program)
RNA	Ribonucleic Acid
RNAi	RNA Interference
S	Short isoform (of *DISC1*)
SAP	Shrimp Alkaline Phosphatase
SCZ	Schizophrenia
SCZAFF	Schizoaffective disorder
SDS	Sodium Dodecyl Sulphate
SH3	Src Homology 3
SNP	Single Nucleotide Polymorphism
t(1;11)	Translocation between chromosomes 1 and 11 (in the *DISC1* family)
t(1;16)	Translocation between chromosomes 1 and 16 (in a proband with schizophrenia)

TAE	Tris-Acetate-EDTA
TBS	Tris-Buffered Saline
TEMED	Tetramethylethylenediamine
Tris	Tris(hydroxymethyl)aminomethane
TTP	Thymidine triphosphate
WB	Western Blotting

Chapter 1 - Introduction

1.1 Psychiatric illness

1.1.1 The impact of psychiatric illness

In 2004, a report was published in which the leading causes of disability world-wide were analysed (World Health Organisation 2004). The impact of a disability on the global population was measured in terms of "years of life lost", a measure taking into account the prevalence of a condition and also the duration of its effect. Alcohol-related disorders, hearing loss, asthma and osteoarthritis all featured prominently in the list; however the single largest impact was caused by an illness which is far harder to define: depression. Also featuring prominently in the list were two other psychiatric illnesses: schizophrenia (fifth in males, sixth in females) and bipolar disorder (seventh in males, eighth in females). Over an individuals lifetime, their risk of suffering from clinically defined schizophrenia or bipolar disorder has been demonstrated to be approximately 0.4% and 0.8% respectively (Judd and Akiskal 2003; Saha *et al.* 2005). The lifetime risk of suffering from major depressive episodes is significantly higher, ranging from 3% to almost 17% depending on nationality (Andrade *et al.* 2003).

Despite the wide-spread impact of psychiatric illness, progress at treating the conditions has been slow. This is largely because the underlying biology of most mental illnesses is still poorly understood. By attempting to understand these conditions at the subcellular level, it is hoped that better preventative and curative therapies can be devised.

1.1.2 Schizophrenia, bipolar disorder and major depression

Due to the lack of any measurable biomarkers with which to clinically define any major mental illness, diagnosis is instead performed by psychiatrists according to standardised criteria. The *Diagnostic and Statistical Manual of Mental Disorders Fourth Edition* (commonly known as DSM-IV, published by the American Psychiatric Association) is currently the gold standard for such diagnoses and

subdivides major mental illness into discrete conditions. Three of these conditions are briefly described below.

Major depressive disorder, also known as unipolar depression, is characterised by the sufferer experiencing prolonged depressive episodes. During that time a sufferer may feel unusually withdrawn, apathetic, pessimistic and potentially suicidal. Tiredness, appetite loss and insomnia are also common symptoms.

Sufferers of bipolar disorder, like those of major depressive disorder, experience depressive episodes, but additionally experience episodes of mania. During these manic episodes, they can feel euphoric, hyperactive and often lose their inhibitions. Sometimes this can lead to delusions and dangerous behaviour.

Finally, schizophrenia is typically characterised as consisting of both positive symptoms, such as delusion and hallucination, as well as negative symptoms such as social withdrawal and depression. It can also affect the attention and working memory of its sufferers.

1.1.3 Causes of psychiatric illness

Various environmental factors have been suggested to influence the likelihood of a person developing major mental illness. For example, in schizophrenia such risk factors include having used cannabis (Semple *et al.* 2005), having elderly parents (Wohl and Gorwood 2007), being born in the winter or spring (Davies *et al.* 2003), living in an urban area (Pedersen and Mortensen 2001), birth complications such as oxygen deprivation (Cannon *et al.* 2002) and being born to a mother who experienced famine (Susser *et al.* 2008) or suffered from influenza (Byrne *et al.* 2007) during pregnancy.

However, over the course of the last century, evidence has been mounting to suggest that mental illness also has a strong hereditary component. A traditional approach to measuring the effect of genetics on a condition is to compare the monozygotic and dizygotic twins of probands with the condition. Adopted twins can be used, thus

discounting shared environmental effects the study. A meta-analysis of such studies investigating schizophrenia in the period 1920-1978 found that for schizophrenia probands with a monozygotic twin (n = 106) in 44.3% of cases that twin also had a diagnosis of schizophrenia (Gottesman *et al.* 1987). By comparison, the same happened in 12.1% of dizygotic twins (n = 149). This strongly implies that there is a major genetic component to schizophrenia, as sharing your genetic make-up with a schizophrenia sufferer considerably increases your risk of suffering from the same condition. Additionally, when family members of a proband with schizophrenia are investigated, it can be seen that the risk of themselves having schizophrenia diminishes in more distant relatives (Gottesman *et al.* 1987), consistent with disease being caused, at least in part, by their genetic make-up.

1.1.4 Candidate genes for major mental illness

While some inherited conditions, such as cystic fibrosis, can be linked to disruption of a single gene, no such central gene exists to explain psychiatric illnesses. Instead, these conditions are believed to be polygenic, with a large number of genes believed to act together to influence the risk of developing such a condition.

There are two main hypothesises as to how multiple genes can affect a condition like schizophrenia. The first of these is that the condition may be dependent on a number of relatively common gene variants, each of which contributes in a small way to the illness. The illness would then arise due to the cumulative effects of possessing multiple of these disease risk variants. Genome-wide association studies have been undertaken in order to test for such common variants (O'Donovan *et al.* 2008) and larger studies are planned (Psychiatric GWAS Consortium 2008). Such analyses examine haplotypes from throughout the genomes of a population, some of whom are affected by a disease of interest and others who act as healthy controls, in order to determine if any alleles are associated with the disease state. This has the advantage over traditional approaches such as linkage analysis (discussed in section 1.2.1.3) of being able to look at specific gene variants rather than simply identifying chromosomal regions which are likely to contain such variants. Because of the number of different haplotypes which need to be examined in each individual, the

large number of individuals required to detect disease-linked polymorphisms of moderate effect and the computational power needed to analyse all of the data, such studies have only recently become technically practical. A consensus on a list of common variants is, however, still far from being achieved. Notably, one high profile analysis detected only a single variant associated with bipolar disorder, despite achieving significantly better results with other non-psychiatric conditions (Wellcome Trust Case Control Consortium 2007), implying that psychiatric illnesses are amongst the most polygenic illnesses known.

The alternative hypothesis is that mental illness is caused by rare variations in one of a number of genes, each individually conferring a large risk of developing the condition. An established method of studying such rare variants is through cytogenetics (Pickard *et al.* 2005). The theory behind this method is that chromosomal translocations, where sections of chromosome arms break off and reattach in different orientations or on separate chromosomes, will occasionally disrupt expression of a gene critical to mental health. By examining the chromosomes of patients with mental illness, such translocations can be identified. Genes lying on or near the breakpoints can then be viewed as potential candidate genes for mental illness and further analysis, such as by association study, can be used to investigate the wider involvement of variations in this gene in mental illness. The translocations themselves are often very rare, however, and are thus unlikely to be subsequently identified in other populations.

It should be stated however, that the two models are not mutually exclusive, as even if a large proportion of mental illness in the population were to be caused by common variants of small effect, rare large variants would still be expected to exist in at least part of the population, and particularly in families who appear to display a high degree of psychiatric illness heritability.

To date, evidence has been published implicating over 130 genes as being potentially involved in the pathology of schizophrenia, and over 100 in bipolar disorder (Carter 2006, 2007). Attempting to determine which of these genes play the most significant

roles in major mental illness is therefore a matter of great urgency, and also of considerable controversy, with opinions on the validity of different candidate genes varying considerably. Studying reviews written in the past year, the genes most commonly described as being strong candidates for schizophrenia risk factors are *COMT*, *DTNBP1*, *NRG1*, *DISC1*, *DAO*, *DAOA* and *DRD4* (Burmeister *et al.* 2008; Gallinat *et al.* 2008; Maier 2008; Sullivan 2008; Tandon *et al.* 2008). Of these, this thesis will focus on *DISC1*. Definitions of these are other abbreviations can be found on page xx.

1.2 Disrupted-In-Schizophrenia 1 (DISC1)

1.2.1 *DISC1* as a candidate gene for psychiatric illness

1.2.1.1 The t(1;11) family

In 1968 a survey was made of the cytogenetics of boys being admitted to borstals, a type of juvenile detention centre, in Scotland. During the survey, one 18-year old boy was found to possess a chromosomal translocation, which they describe as involving chromosome 1 and one of chromosomes 6-12. Further analysis showed that this translocation was balanced and present across four generations of his family (Jacobs *et al.* 1970). At the time no clinical phenotype was described as being associated with the translocation, and the details of the family were deposited in a cytogenetics registry in Edinburgh.

Twenty years later, a survey of this register was carried out and it was observed that many members of the family had been referred to psychiatrists or mental health hospitals in the intervening years (St Clair *et al.* 1990). Diagnoses within the family included schizophrenia, major and minor depression and, in the case of the original boy, severe adolescent conduct disorder. St Clair and colleagues then studied the translocation, which they identified as being between chromosomes 1 and 11, and found that psychiatric illness was significantly more common in family members with the t(1;11) translocation than in those who appeared cytogenetically normal (St Clair *et al.* 1990).

In a follow-up study a decade later, it was seen that 7 of the 37 t(1;11) translocation carriers suffered from schizophrenia, a condition found in none of their relatives lacking the translocation (Blackwood *et al.* 2001). The translocation was shown to be linked to schizophrenia with a LOD score of 3.6 (Logarithm of Odds, determined by calculating the probability of the linkage occurring by chance, dividing by the probability of it by chance not occuirng and taking log 10 of this ratio). Additionally, when schizophrenia was grouped together with bipolar disorder and major recurrent depression (one and ten cases in the translocation carriers

respectively, no cases of either in the non-carriers) this LOD score increased to 7.1. This was unprecedented evidence that the t(1;11) translocation was linked to, and most probably causative of, psychiatric illness.

1.2.1.2 Identification of genes at the translocation breakpoints

The simplest scenario as to how such a translocation could cause psychiatric illness was that a gene was directly disrupted on chromosome 1 or chromosome 11 at the breakpoint and that disruption of this gene was causative of the illness. A concerted effort was therefore made to map the exact location of the chromosome 1 and 11 breakpoints and to identify potential genes at these locations (Fletcher *et al.* 1993; Evans *et al.* 1995; Muir *et al.* 1995; Devon *et al.* 1997; Millar *et al.* 1998; Semple *et al.* 2001). The breakpoints were determined to be at 1q42.1 and 11q14.3.

Analysis of the breakpoint on chromosome 1 revealed that the translocation directly disrupted two previously unknown genes (Millar *et al.* 2000b) which were named Disrupted-In-Schizophrenia 1 and 2 (*DISC1* and *DISC2*). In contrast no transcripts were shown at the time to be disrupted at the chromosome 11 breakpoints (Millar *et al.* 2000b), although more recent work has identified a potential gene at this location (Zhou *et al.* 2008).

The *DISC1* gene was shown to consist of 13 exons which encode an 854 amino acid protein, DISC1 (Millar *et al.* 2001). The t(1;11) translocation breakpoint lies within intron 8 of this gene. *DISC2* meanwhile lacks any open reading frames (Millar *et al.* 2001). It does however lie anti-sense to *DISC1* and so *DISC2* transcripts have the potential to act as *DISC1* regulators, for example by binding *DISC1* transcripts and blocking translation (Chubb *et al.* 2008). In light of the non-coding nature of *DISC2*, however, the vast majority of work since has instead focused on *DISC1*. Additionally, while *DISC1* orthologues have been reported in a number of organisms, no *DISC2* equivalent has yet been detected in any species other than human (Taylor *et al.* 2003).

The *DISC1* gene has also been shown to form fusion transcripts with another gene, Translin-Associated factor X (*TRAX*) which lies 5' of it on chromosome 1 (Millar *et al.* 2000a). It should therefore be considered that the molecular mechanism of psychiatric illness in the t(1:11) family could technically be due to altered expression of *TRAX* transcripts. Levels of TRAX protein where not, however, seen to be affected by the translocation in lymphoblastoid cell lines derived from t(1;11) family members (Millar *et al.* 2005b).

There are two major theories as to why disruption of one copy of the *DISC1* gene may lead to abnormal phenotypes in the t(1;11) family. The first of these is that the cells of translocation carriers cannot produce DISC1 protein from the translocation-derived chromosome, and that this haploinsufficiency leads to psychiatric illness. This certainly seems to be the case when comparing the levels of both *DISC1* transcripts and various DISC1 protein species in lymphoblastoid cells derived from the blood of translocation carriers and healthy members of the family (Millar *et al.* 2005b). The alternative theory is that a truncated form of DISC1, sometimes known as mutDISC1 and which contains only the N-terminal 597 amino acids of full length DISC1, is instead produced by the translocation-derived chromosome (Morris *et al.* 2003; Ozeki *et al.* 2003). Such a protein has been shown to have a range of dominant negative effects when over-expressed in cell lines (Ozeki *et al.* 2003; Kamiya *et al.* 2005; Pletnikov *et al.* 2007; Taya *et al.* 2007) and to cause phenotypes associated with psychiatric illness in over-expressing transgenic mice (Hikida *et al.* 2007; Pletnikov *et al.* 2008; Shen *et al.* 2008a). To date, however, no sign of such a protein has been detected in the t(1;11) lymphoblastoid cell lines (Millar *et al.* 2005b).

1.2.1.3 The *DISC* locus in global psychiatric illness

The t(1;11) translocation seen in the Scottish family is believed to be unique. Numerous studies, however, have been published implicating the *DISC1* gene as influencing major mental illness in the wider population. The majority of these have focused on attempting to determine one or more common *DISC1* variants which increase the risk of schizophrenia or other psychiatric illnesses.

Two types of study are generally used. Linkage analyses look at either single large families or at sets of families, typically of a common ethnicity. By investigating the inheritance patterns of chromosomal markers it is possible to determine whether one or more such marker co-segregates with a phenotype of interest, such as increased disposition to a specific illness. In this way the approximate locations of disease-causing genes can be mapped. This technique is well suited to the identification of rare variants with a relatively large effect on disease pathology. Figure 1.2.A summarises studies reported to date which display evidence of the *DISC* locus or the chromosomal region surrounding it being linked to major mental illness. The chromosomal region containing the *DISC* locus has therefore been repeatedly demonstrated to be linked to schizophrenia and bipolar disorder, with linkage to schizoaffective disorder and major depressive disorder also reported.

Association analyses meanwhile look at large populations, typically of unrelated individuals. One or more specific single nucleotide polymorphisms (SNPs) or haplotypes of several SNPs are genotyped in each member of the population. Such analyses are performed in a population of individuals suffering from a particular disease and also in a similar population of healthy controls. By doing this it is possible to identify particular genotypes which are more or less common in the affected individuals, and therefore likely to contribute to the pathology of that disease. This technique is well suited to detecting common variants of relatively low effect on disease pathology. Figure 1.2.B summaries studies looking for association of *DISC1* with major mental illness. Association of *DISC1* variants with schizophrenia has been reported now in 15 studies, and association with other psychiatric illnesses has also been detected. To date, however, no individual *DISC1* variant has been robustly demonstrated to be consistently associated with schizophrenia in more than a few of these studies. It therefore appears that while variation in *DISC1* often leads to psychiatric disorder, no individual common variant to account for this. In addition, a number of genome-wide association studies for schizophrenia have been performed in recent years and, while no strong risk factors for psychiatric illness have yet emerged by this approach, it has been

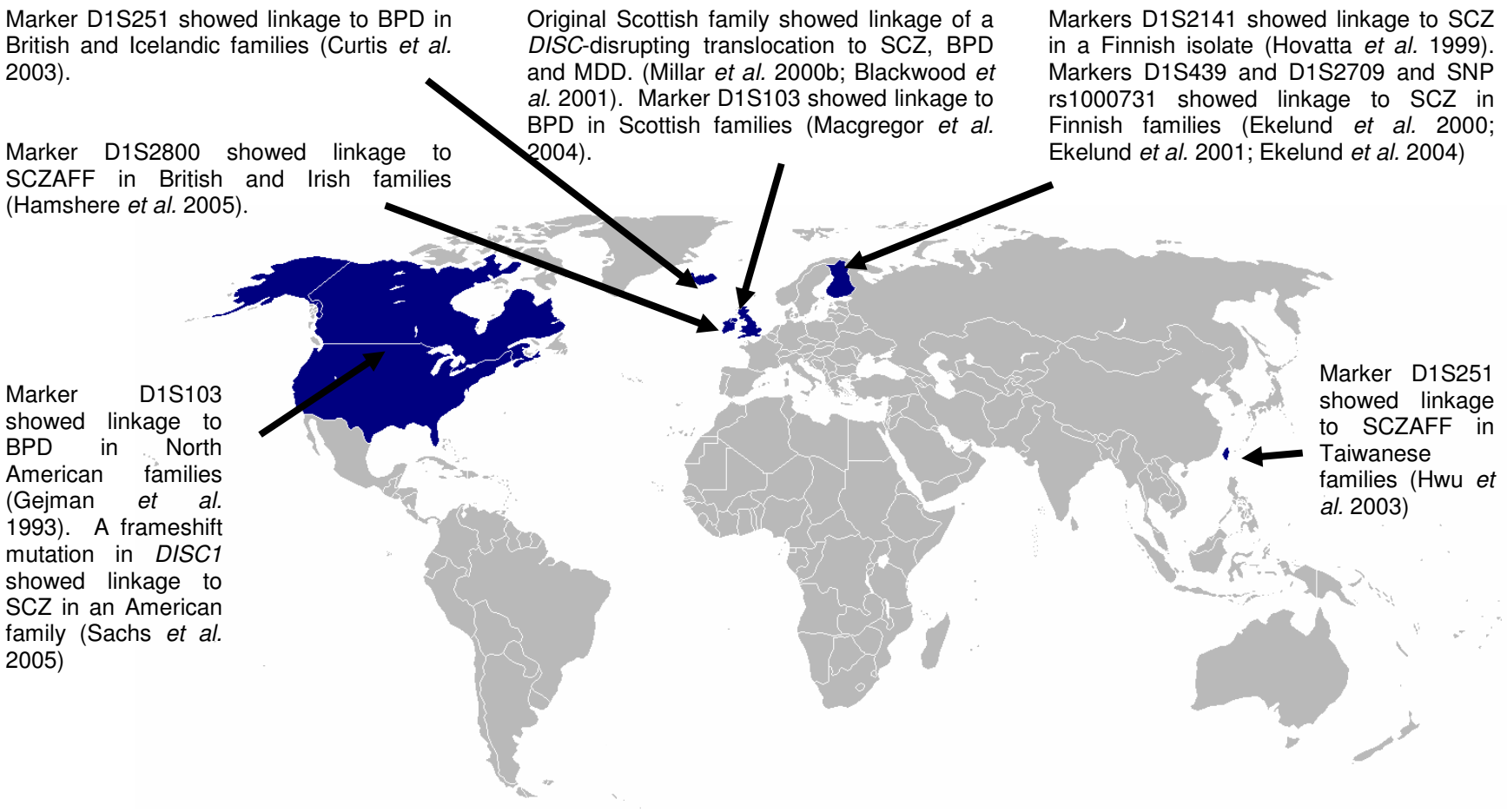

Figure 1.2.A: Summary of studies investigating linkage of chromosomal regions surrounding the *DISC* locus with schizophrenia (SCZ), bipolar disorder (BPD), major depressive disorder (MDD) and schizoaffective disorder (SCZAFF).

A four SNP haplotype was associated with BPD in Scottish females (Thomson *et al.* 2005b) and a three SNP haplotype with SCZ in the Scottish population (Zhang *et al.* 2006). SNP rs821577 was associated with SCZ in an English population (Hennah *et al.* 2008).

Three *DISC1* haplotypes were associated with SCZ in the Finnish population (Hennah *et al.* 2003; Cannon *et al.* 2005), as were SNPs rs1000731 and rs1528979 (Ekelund *et al.* 2004; Hennah *et al.* 2008). A two SNP *DISC1* haplotype was associated with SCZ in males and two *DISC1* and *TSNAX* haplotypes were each associated with BPD (Palo *et al.* 2007). The marker D1S2709 showed association with AUT (Kilpinen *et al.* 2008), while SNP rs1322784 and a three SNP haplotype showed association with AS (Kilpinen *et al.* 2008)

SNPs rs821616 and rs821597 were associated with SCZ in the Han Chinese population. (Qu *et al.* 2007). SNP rs2295959 was also associated , but only in females (Chen *et al.* 2007).

SNPs rs2812393, rs1322784, rs1322783, rs2255340, rs2738864 and S704C showed association with SCZ in Americans of European origin, while rs1934909 was associated in African Americans (Hodgkinson *et al.* 2004; Callicott *et al.* 2005). SNP rs6675281 was associated with SCZAFF in Americans of European origin (Hodgkinson *et al.* 2004).

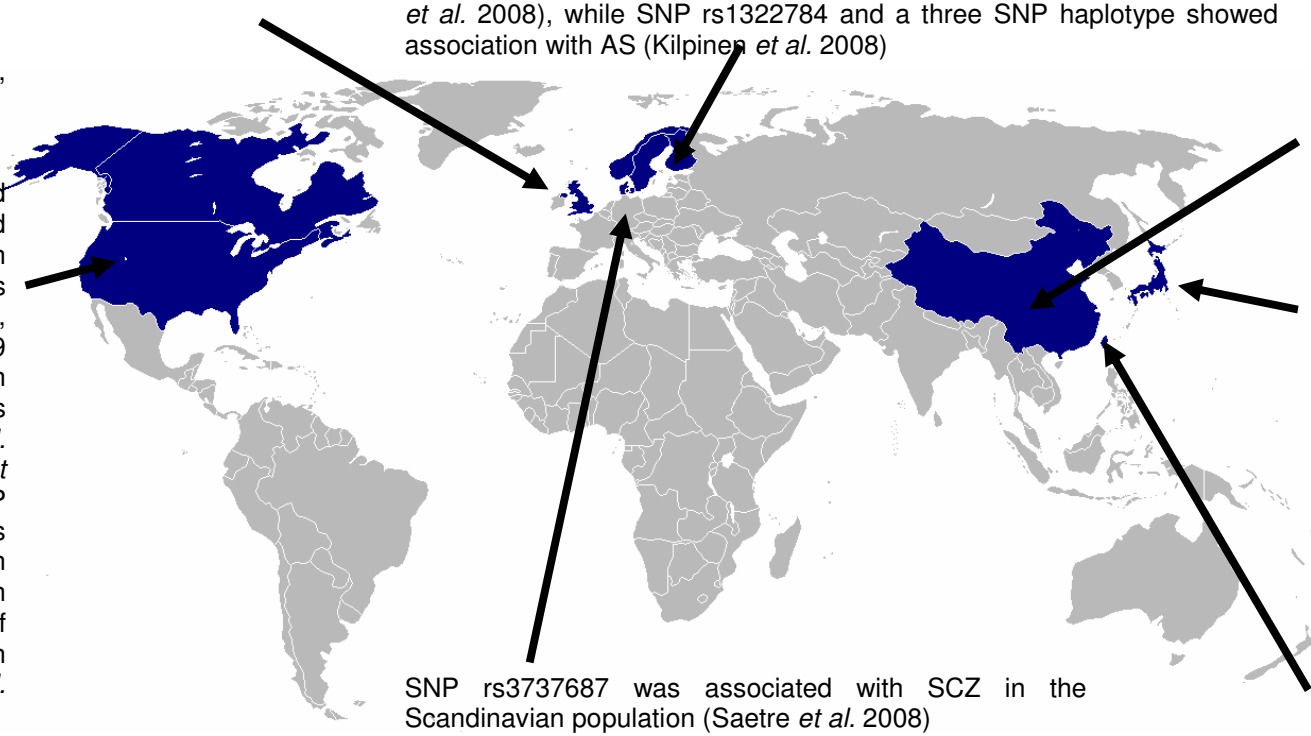

SNP rs999710 was associated with SCZ in the Japanese population. SNP rs821577 was also associated only in females. S704C and rs6541281 were associated with MDD.

SNP rs3737687 was associated with SCZ in the Scandinavian population (Saetre *et al.* 2008)

SNPs rs2793091 and rs2793092 were associated with SCZ in the Taiwanese population (Liu *et al.* 2006)

Figure 1.2.B: Association studies of SNPs in and around the *DISC1* gene with schizophrenia (SCZ), bipolar disorder (BPD), major depressive disorder (MDD), schizoaffective disorder (SCZAFF), autism (AUT) and Asperger's syndrome (AS). Negative results have also been reported (Zhang *et al.* 2005; Hashimoto *et al.* 2006; Arai *et al.* 2007; Kim *et al.* 2007; Sanders *et al.* 2008).

observed that there is at least suggestive evidence for *DISC1* playing such a role (Sullivan 2008).

Two SNPs in *DISC1* exons have been reported and further studied. The first of these variations, leucine-607 to phenylalanine (L607F), has been reported to be over-represented in patients with schizoaffective disorder (Hodgkinson *et al.* 2004) but not schizophrenia (Song *et al.* 2008). Carriers of the Phe allele have been shown to have reduced grey matter volume in the superior frontal gyrus and anterior cingulate gyrus, while schizophrenia patients carrying it suffer from significantly worse hallucinations than those homozygous for the Leu allele (Szeszko *et al.* 2008).

The other common variation, serine-704 to cysteine (S704C), has been reported to be associated with schizophrenia (Callicott *et al.* 2005; Qu *et al.* 2007; Song *et al.* 2008) as well as major depression (Hashimoto *et al.* 2006), although negative results have also been reported (Kim *et al.* 2007). By using MRI to investigate the brains of healthy individuals of known *DISC1* genotype, the two alleles have been demonstrated to affect grey matter volume in the hippocampus (Callicott *et al.* 2005), cingulate cortex (Hashimoto *et al.* 2006) and parahippocampal gyrus (Di Giorgio *et al.* 2008) and to produce visibly different patterns of brain activation on a functional MRI machine during memory-related tests (Callicott *et al.* 2005; Prata *et al.* 2008). The Cys allele has also been linked to reduced cognitive ability in elderly females (Thomson *et al.* 2005a). There is also some evidence to suggest that the S704C variation affects the phosphorylation potential (Hashimoto *et al.* 2006) and the specific protein interaction affinities of the DISC1 protein (Kamiya *et al.* 2006; Burdick *et al.* 2008).

Ultra rare variants have also been reported. One recent study involved the genotyping of the *DISC1* gene of 288 schizophrenia patients. SNPs discovered in this way were then investigated in a large pool of control alleles. By this method, five rare *DISC1* variants were determined, each of which was found in at least one schizophrenia patient, but not in any of 10,000 unaffected controls (Song *et al.*

2008). These mutations were at G14A, R37W, S90L, R418H and T603I. To date, no further work has been reported as to biological implications of these rare variants.

An additional putative pathological rare variant was reported in a trio of American siblings each with schizophrenia or schizoaffective disorder (Sachs *et al.* 2005). This variant consisted of a four base pair deletion near the 3' end of *DISC1* leading to a frame shift mutation. The variant was also present in the trio's unaffected father. The variant was however later discovered in two individuals out of 694 who lacked any psychiatric diagnosis (Green *et al.* 2006), in a study which failed to identify it in any of 655 individuals with schizophrenia. It is therefore uncertain whether or not this variant is pathogenic.

Finally, copy number variation of the *DISC1* gene has been reported, however there is no available evidence to date as to whether or not these are associated with mental illness (Redon *et al.* 2006).

Together, the linkage and association data surrounding the *DISC* locus very strongly implicate it in psychiatric illness globally. However, the sheer variety of *DISC1* SNPs and haplotypes linked to various major mental illnesses implies that it is unlikely that one or more specific *DISC1* variants individually account for more than a fraction of cases world-wide. Nevertheless, it is clear that disruption of the *DISC1* gene considerably increases the chance of an individual having major mental illness. It is also interesting that *DISC1* has been associated with so many clinically distinct psychiatric disorders, adding to the growing body evidence suggesting that the pathology of the conditions is less distinct than had previously been assumed.

1.2.2 The DISC1 protein

1.2.2.1 Characterisation of the DISC1 protein

The full length DISC1 protein is generally described as being of approximately 100kDa in size. It is however known to exist also as a number of smaller species, with a number of distinct Western blot bands having been seen between 70 and

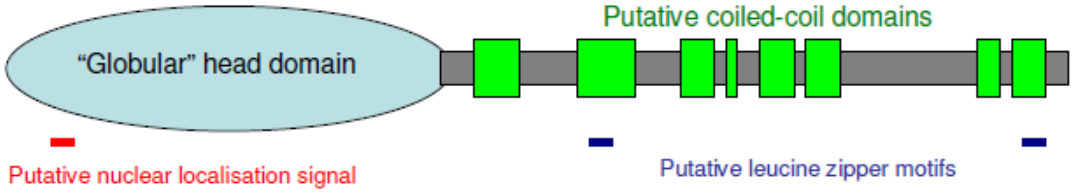

Figure 1.2.C: The predicted secondary structure of DISC1. Predicted coiled coils, nuclear localisation signal and leucine sipper motifs are indicated in green, red and blue respectively. Adapted from (Chubb et al 2008) with additional data from (Taylor *et al.* 2003, Brandon *et al* 2005).

80kDa (Miyoshi *et al.* 2003; James *et al.* 2004; Ogawa *et al.* 2005; Sawamura *et al.* 2005). Bands of other sizes, including 98kDa (James *et al.* 2004) and 45kDa (Koike *et al.* 2006) have also been reported. These are partially accounted for by the existence of a number of splice variants including the full length "long" (L) isoform, a "long variant" (Lv) isoform which lacks 22 amino acids near the C-terminus (Millar *et al.* 2000b), a "short" (S) isoform consisting of exons 1-9 plus an additional exon, and an "extremely short" (Es) isoform consisting on exons 1-3 only (Taylor *et al.* 2003). In addition, it has been suggested that DISC1 protein may be post-translationally truncated within the cell (Millar *et al.* 2005a). Determination of the identity of other isoforms would involve either the use of mass spectroscopy to identify the regions of DISC1 present in each of the remaining undefined DISC1 species, or a thorough analysis of other splice variants and the predicted amino acid sizes of their protein products. The two approaches would be complementary.

The full length DISC1 protein is described as consisting of two parts. The N-terminal region is generally referred to as "globular" due to the lack of a predictable secondary structure, while the C-terminal region is referred to as coiled (Millar *et al.* 2000b). Estimates of the number of distinct coils in this region vary, but may be eight or more (Chubb *et al.* 2008). In addition the existence of two leucine zippers (Brandon *et al.* 2005) and a nuclear localisation signal (Taylor *et al.* 2003) have been predicted. These are shown in figure 1.2.C

The DISC1 protein is most commonly described as being found in punctate structures, the nature of which remains to be determined, within the cytoplasm (Miyoshi *et al.* 2003; James *et al.* 2004). It has also been described as being found at a number of other cellular locations, including the mitochondria (James *et al.* 2004; Millar *et al.* 2005a), the centrosome (Morris *et al.* 2003) and the nucleus (Sawamura *et al.* 2008). The exact cellular localisation pattern is dependent on the specificity of the anti-DISC1 used, with antibodies raised against N-terminal regions of DISC1 producing different results to those raised against C-terminal regions. This probably occurs because different antibodies recognise different DISC1 isoforms. In rat PC12 neurons, DISC1 has been seen in the cell processes (Ozeki *et al.* 2003), and in neurons from the human brain it has been identified in post-synaptic densities using gold-labelling electron microscopy (Kirkpatrick *et al.* 2006). Some antibodies also detect DISC1 as being associated with microtubules (Brandon *et al.* 2005) and found at the nucleus (James *et al.* 2004; Ogawa *et al.* 2005). Subcellular fractionation studies have demonstrated that some DISC1 species display unique patterns of localisation, for example the 71kDa isoform is primarily found in the mitochondria-enriched fraction (Ozeki *et al.* 2003; James *et al.* 2004; Sawamura *et al.* 2005).

1.2.2.2 DISC1 in the brain and neurodevelopment

In both human adults and foetuses, *DISC1* transcripts are expressed in a variety of organs, including the brain (Millar *et al.* 2000b; James *et al.* 2004). Within the human and rodent brain, DISC1 expression is most commonly described as being at the hippocampus within the granular cells of the dentate gyrus (Ma *et al.* 2002; Austin *et al.* 2004; James *et al.* 2004; Lipska *et al.* 2006) and pyramidal cells of the CA3 region (Schurov *et al.* 2004). In the adult mouse cerebral cortex, Disc1 is found primarily in layers II-III, while in the cerebellum it is found at the Purkinje cell layer (Ma *et al.* 2002; Schurov *et al.* 2004). Other regions of the mouse brain where Disc1 expression has been reported include the hypothalamus, olfactory bulb, basolateral amygdala and brain stem (Ma *et al.* 2002; Austin *et al.* 2004; Schurov *et al.* 2004). The expression pattern of Disc1 within the brain appears to alter over the course of development in embryonic mice (Austin *et al.* 2004; Schurov *et al.* 2004).

Interestingly mice exposed to one of two antipsychotics, olanzapine and risperidone, had increased *DISC1* in the frontal cortices (Chiba *et al.* 2006).

DISC1 is known to be found in the cell processes of cultured neurons (Miyoshi *et al.* 2003; Morris *et al.* 2003; Ozeki *et al.* 2003), and has been seen to localise to the synapses of cortical neurons (Kirkpatrick *et al.* 2006). This result is reinforced by the fact that the "interactome" of DISC1 (its list of protein binding partners) resembles that of an essential synaptic protein (Camargo *et al.* 2007). Knock-down of DISC1 within cultured neurons by RNA interference (RNAi) has been shown repeatedly to lead to a reduced rate of neurite outgrowth and a similar effect can be caused by over-expressing a DISC1 dominant negative truncation mutant (Ozeki *et al.* 2003; Kamiya *et al.* 2005; Pletnikov *et al.* 2007; Shinoda *et al.* 2007; Taya *et al.* 2007). Interestingly, in adult neurons, DISC1 knockdown appears to accelerate dendritic development, in contrast to observations made in the developing brain (Duan *et al.* 2007). Neurons in the rodent brain which have their Disc1 level reduced by RNAi, including those of the dentate gyrus, have been shown to localise in an aberrant manner during development (Duan *et al.* 2007; Faulkner *et al.* 2008). That DISC1 is seemingly involved in neuronal differentiation and migration is of exceptional interest when viewing it as a protein related to major mental illness.

1.2.2.3 Mouse models of *DISC1*

In the past few years, a number of mouse models of *DISC1*-related illness have been published. The reasoning behind developing such mouse models is two-fold. Firstly, such models demonstrate that it is possible to induce phenotypes reminiscent of major mental illness simply by altering the workings of the *Disc1* gene. Secondly, by modelling *DISC1*-related psychiatric illness, these mice could be useful in gaining a better understanding of these conditions and ultimately in the development of novel antipsychotics and antidepressants.

The first of these mouse lines came from the serendipitous discovery that all 129 inbred mice strains are homozygous for a natural 25 base pair deletion in their *Disc1* gene (Clapcote and Roder 2006; Koike *et al.* 2006). This is predicted to cause a

frame-shift mutation, introducing a premature stop codon (Koike *et al.* 2006). Indeed, it was reported that the full length Disc1 protein was missing from 129S6/SvEv mice when compared to C57BL/6J mice (Koike *et al.* 2006), although this finding could not be replicated using a number of other anti-Disc1 antibodies (Ishizuka *et al.* 2007). Nevertheless, when this mutant *Disc1* gene was transferred onto a C57BL/6J background and further mutations added to prevent transcription passed exon 8, mice bearing one or more copies of it were shown to have impaired working memory when compared to their wild type littermates (Koike *et al.* 2006; Kvajo *et al.* 2008). These mice displayed smaller pre-frontal cortices and displayed a variety of neuronal abnormalities, including altered migration, stunted dendrite outgrowth and altered short-term plasticity, in specific areas of the brain (Kvajo *et al.* 2008). The presence of this mutation in 129 mouse strains which have previously been used to set up embryonic stem cell lines also means that caution will be needed in any work modelling DISC1 function in such cell lines (Clapcote and Roder 2006).

Clapcote *et al* screened mice which had been subject to ENU-mutagenesis for mutations in exon 2 of *Disc1* (Clapcote *et al.* 2007). They identified two such mutations: a glutamine to leucine substitution (Q31L) and a leucine to proline substitution (L100P). Both homozygous and heterozygous mice carrying each mutation showed significantly reduced total brain size. Q31L mice showed increased immobility in the forced swim test, reduced social interaction and reduced reward responsiveness compared to wild type litter mates. The L100P mice meanwhile had reduced pre-pulse inhibition and latent inhibition compared to wild type litter mates. They also displayed increased locomotive activity and reduced working memory. It was therefore concluded that the Q31L mice have a depressive-like phenotype, while the L100P mice have a schizophrenia-like phenotype. Interestingly both sets of mice showed altered responsiveness to common antidepressants and/or antipsychotics (Clapcote *et al.* 2007).

As an alternative approach, two groups have produced mouse lines which express a transgenic mutant form of human DISC1, encoding amino acids 1-597 only, under a calcium-calmodulin-dependent kinase II-α promoter (Hikida *et al.* 2007; Pletnikov *et*

al. 2008). They suggest that this would reflect the biology of the t(1;11) family, based on a dominant negative model. The mice of Hikida *et al* expressed this mutant DISC1 from birth in the primary neurons of the forebrain (Hikida *et al.* 2007). These mice showed some signs of unusual hyperactivity and were more immobile in a forced swim test, a model of depression, than their wild-type littermates. There was no sign of altered anxiety or social interactions. Minor alterations in the relative sizes of the left and right ventricles of the mutant mice were also reported (Hikida *et al.* 2007). Pletnikov *et al* developed a similar system, but using the Tet system to provide inducible expression of mutant *Disc1* (Pletnikov *et al.* 2008). These mice had increased lateral ventricular size and decreased neurite complexity in their brains. Male mutant mice also showed evidence of increased activity and aggressiveness. Female mutant mice, meanwhile, were seen to have reduced spatial memory (Pletnikov *et al.* 2008).

Shen *et al* used a variation on the approaches of Hikida, Pletnikov *et al*, producing a line of mice expressing two copies of mutated mouse *disc1* as well as the two wild-type copies (Shen *et al.* 2008a). Additionally, Shen *et al* made use of the native *Disc1* promoter in order to express their transgene. They theorised that this should simulate the ratio of the *DISC1* genes in the t(1;11) family, although this would also lead to increased *Disc1* expression, the effect of which is unclear. Multiple brain abnormalities were reported, including enlarged lateral ventricles and a reduced cerebral cortex. Abnormalities and altered localisation of GABAergic neurons in the hippocampus and the parvalbumin cells in the prefrontal cortex were also seen. The mice also had decreased latent inhibition, like the mice of Clapcote *et al* (2007) and displayed some altered behavioural characteristics reminiscent of depression, including reduced vocalisation and mobility in certain tests (Shen *et al.* 2008a).

Finally, Li *et al* also generated a line of mice with inducible expression of a mutant form of DISC1 in the primary forebrain neurons (Li *et al.* 2007). The DISC1 mutant in question consisted of amino acid 671-852, fused to a fragment of an inactive oestrogen receptor. They found that induction of this mutant at postnatal day seven (P7) led to spatial working memory defects, depression-like traits and reduced

sociability, while induction in adulthood had no effect (Li *et al.* 2007). The biological reasons for these behaviours was investigated, and it was found that mice induced at P7 had reduced dendritic density in the dentate gyrus and reduced synaptic transmission in CA1 hippocampal neurons (Li *et al.* 2007).

1.2.2.4 The DISC1 interactome

In order to predict proteins that may be able to interact with DISC1 in the cell, a number of yeast-two-hybrid screens were carried out (Millar *et al.* 2003; Morris *et al.* 2003; Ozeki *et al.* 2003; Brandon *et al.* 2004; Camargo *et al.* 2007). In yeast-two-hybrid screening, plasmids are generated that encode a protein of interest fused to part of a transcription factor. Two such constructs, one referred to as the "bait" the other as the "prey", are used and between them they contain the entire amino acid sequence of a transcription factor. These can then be co-transformed into yeast and the expression of a reporter gene used as a measure of whether the proteins have interacted, thus allowing the transcription factor to function. Libraries of prey proteins can then be used, allowing for the screening of large numbers of protein interactors.

In combination with other techniques, a long list of potential protein interaction partners for DISC1 was built up, which are summarised in table 1.2. It should be noted however that yeast-two-hybrid screens investigate protein-protein interactions in a very artificial manner and therefore have a high false positive rate (Deane *et al.* 2002), meaning that any interaction determined in this way should be confirmed by independent techniques. In order to definitively state that an interaction is genuine, you ideally need both an *in vivo* test, such as co-immunoprecipitation of endogenous protein (to prove that the interaction is of biological relevance) and a separate *in vitro* test to confirm that the interaction is direct. Such confirmations have, to date, only been performed on a relatively small proportion of the proposed DISC1 interactome.

Name	Assays	References
14-3-3ε [YWHAE]	Y2H, AC, IV, IP (E)	(Camargo *et al.* 2007; Taya *et al.* 2007)
14-3-3γ [YHAG]	Y2H	(Ozeki *et al.* 2003)
α-actinin [ACTN family]	Y2H, IP (O)	(Morris *et al.* 2003)
α-tubulin [TUBA family]	IV	(Brandon *et al.* 2004)
AGTPBP1	Y2H	(Camargo *et al.* 2007)
AKAP9	Y2H	(Millar *et al.* 2003)
APAP2	Y2H, IP (O)	(Morris *et al.* 2003)
APLP1	Y2H	(Millar *et al.* 2003)
ARFGEF2	AC	(Taya *et al.* 2007)
ARHGEF11	Y2H	(Millar *et al.* 2003)
ARIH2	Y2H	(Camargo *et al.* 2007)
ATF4	Y2H, IV, IP (O)	(Millar *et al.* 2003; Morris *et al.* 2003; Sawamura *et al.* 2008)
ATF5	Y2H, IP (O)	(Morris *et al.* 2003)
ATF7ip	Y2H	(Morris *et al.* 2003)
B4-Spectrin [SPTBN4]	Y2H, IP (O)	(Morris *et al.* 2003; Ozeki *et al.* 2003)
β-tubulin [TUBB. TUBB2]	Y2H	(Camargo *et al.* 2007)
BBS1 - BBS8	IP (O)	(Kamiya *et al.* 2008)
BICD	Y2H	(Camargo *et al.* 2007)
C14orf135	Y2H	(Camargo *et al.* 2007)
C22orf1	Y2H	(Camargo *et al.* 2007)
C2orf4	Y2H	(Camargo *et al.* 2007)
CDC5L	Y2H	(Camargo *et al.* 2007)
CDK5RAP3	Y2H	(Camargo *et al.* 2007)
CEP63	Y2H, IP (O)	(Morris *et al.* 2003)
CEP170	Y2H	(Camargo *et al.* 2007)
Citron [STK21]	Y2H	(Ozeki *et al.* 2003)
CLU	Y2H	(Camargo *et al.* 2007)
Collagen type IV [COL6A2]	Y2H	(Morris *et al.* 2003)
CRNKL1	Y2H	(Camargo *et al.* 2007)
DBZ / Su48 [ZNF365]	Y2H, IP (O+E)	(Camargo *et al.* 2007; Hattori *et al.* 2007)
DISC1 (Self-association)	IP (O)	(Brandon *et al.* 2005)
DMD	Y2H	(Camargo *et al.* 2007)
DMT1	Y2H	(Millar *et al.* 2003)
DNAJC7	Y2H	(Camargo *et al.* 2007)
DPYSL2	Y2H	(Camargo *et al.* 2007)
DPYSL3	Y2H	(Camargo *et al.* 2007)
DST	Y2H	(Camargo *et al.* 2007)
Dynactin [DCTN1]	Y2H, IP (O+E)	(Ozeki *et al.* 2003; Kamiya *et al.* 2005)
Dynein [DNC1H1, DYNC1I family]	Y2H, AC, IP (E)	(Kamiya *et al.* 2005; Camargo *et al.* 2007; Taya *et al.* 2007)
eEF2	Y2H	(Camargo *et al.* 2007)
eIF3 p40 [EIF3S3]	Y2H, IV, IP (O+E)	(Morris *et al.* 2003; Ogawa *et al.* 2005)
EXOC7	Y2H	(Camargo *et al.* 2007)
FBXO41	Y2H	(Camargo *et al.* 2007)
FEZ1	Y2H, IP (O)	(Miyoshi *et al.* 2003)
FLJ39502	Y2H	(Morris *et al.* 2003)
FRYL	Y2H	(Camargo *et al.* 2007)
γ-actinin [ACTG1]	Y2H	(Camargo *et al.* 2007)
γ-tubulin [TUBG family]	IP (O+E)	(Kamiya *et al.* 2005)

GM130	Y2H	(Millar *et al.* 2003)
GNB1	Y2H	(Camargo *et al.* 2007)
GPRASP2	Y2H	(Camargo *et al.* 2007)
GRB2	AC, IV, IP (O)	(Shinoda *et al.* 2007)
GRIPAP1 (GRASP1)	Y2H	(Millar *et al.* 2003)
HAPIP (Kalirin, DUO) [KALRN]	Y2H	(Millar *et al.* 2003)
HRC1	Y2H	(Morris *et al.* 2003)
KCNQ5	Y2H	(Ozeki *et al.* 2003)
IMMT	Y2H	(Millar *et al.* 2003)
ITSN	Y2H	(Morris *et al.* 2003)
KIAA1377	Y2H	(Morris *et al.* 2003)
KIF3A	Y2H	(Camargo *et al.* 2007)
KIF3C	Y2H	(Camargo *et al.* 2007)
KIF5A	AC, IV, IP (O+E)	(Taya *et al.* 2007)
KIF5B	AC	(Taya *et al.* 2007)
KIF5C	IV	(Taya *et al.* 2007)
KIFAP3	Y2H	(Camargo *et al.* 2007)
KLC1	AC	(Taya *et al.* 2007)
KLC2	AC	(Taya *et al.* 2007)
LIS1 [PAFAH1B1]	Y2H, AC, IV, IP (O+E)	(Brandon *et al.* 2004; Kamiya *et al.* 2005; Camargo *et al.* 2007; Taya *et al.* 2007)
MACF1	Y2H	(Camargo *et al.* 2007)
MAP1A	Y2H, IP (O)	(Morris *et al.* 2003)
MATR3	Y2H	(Camargo *et al.* 2007)
MGAT3	Y2H	(Millar *et al.* 2003)
MGC2599	Y2H	(Millar *et al.* 2003)
MIP-T3 (TRAF3IP1)	Y2H, IP (O)	(Morris *et al.* 2003)
MN7	Y2H	(Camargo *et al.* 2007)
Myosin [MYH7]	Y2H	(Morris *et al.* 2003)
MYT1L	Y2H	(Camargo *et al.* 2007)
N-CoR [NCOR1]	IP (O)	(Sawamura *et al.* 2008)
NDE1	Y2H, IP (O)	(Millar *et al.* 2003; Burdick *et al.* 2008)
NDEL1	Y2H, AC, IV, IP (O+E)	(Millar *et al.* 2003; Morris *et al.* 2003; Ozeki *et al.* 2003; Brandon *et al.* 2004; Taya *et al.* 2007)
NPHP6 [CEP290]	Y2H	(Millar *et al.* 2003)
NUP160	Y2H	(Camargo *et al.* 2007)
OLFM1	Y2H	(Camargo *et al.* 2007)
PACS1	AC	(Taya *et al.* 2007)
PCM1	IP (O)	(Kamiya *et al.* 2008)
PDE4A	IV	(Millar *et al.* 2005a)
PDE4B	Y2H, IV, IP (O+E)	(Millar *et al.* 2005a; Murdoch *et al.* 2007)
PDE4C	IP (O)	(Millar *et al.* 2005a)
PDE4D	IV, IP (O)	(Millar *et al.* 2005a; Murdoch *et al.* 2007)
Pericentrin-B (Kendrin) [PCTN2]	Y2H, IP (E)	(Miyoshi *et al.* 2005)
PGK1	Y2H	(Camargo *et al.* 2007)
PPF1A4	Y2H	(Millar *et al.* 2003)
PPME1	Y2H	(Camargo *et al.* 2007)
PPP4R1	Y2H	(Camargo *et al.* 2007)
RABGAP1	Y2H	(Camargo *et al.* 2007)
RACK1	AC	(Taya *et al.* 2007)
RAD21	Y2H	(Camargo *et al.* 2007)

RanBPM [RANBP9]	Y2H, IP (O)	(Morris *et al.* 2003)
ROGDI	Y2H	(Camargo *et al.* 2007)
SEC3L1	Y2H	(Camargo *et al.* 2007)
SH3BP5	Y2H	(Camargo *et al.* 2007)
SMARCE1 (BAF57)	Y2H	(Millar *et al.* 2003)
SNX3	Y2H	(Camargo *et al.* 2007)
SPTAN1	Y2H	(Millar *et al.* 2003)
SYNE1	Y2H, IP (O)	(Morris *et al.* 2003)
TENC1	Y2H	(Millar *et al.* 2003)
TFIP11	Y2H	(Camargo *et al.* 2007)
TIAM2 (STEF)	Y2H	(Camargo *et al.* 2007)
TNKS	Y2H	(Camargo *et al.* 2007)
TNIK	Y2H	(Camargo *et al.* 2007)
TRAF3IP1	Y2H	(Camargo *et al.* 2007)
TRIO	Y2H	(Camargo *et al.* 2007)
WKL1	Y2H	(Millar *et al.* 2003)
XPNPEP1	Y2H	(Camargo *et al.* 2007)
XRN2	Y2H	(Camargo *et al.* 2007)
ZNF197	Y2H	(Camargo *et al.* 2007)

Table 1.2: A list of published DISC1 interactors. The assays column lists the methods by which an interaction with DISC1 has been demonstrated. Y2H: yeast-two hybrid screen, AC: affinity chromatography, IP: immunoprecipitation using over-expressed (O) or endogenous (E) protein, IV: *in vitro* direct binding assay (including binding of *in vitro* transcribed and translated proteins, binding of bacterially produced proteins and use of peptide arrays). For the sake of space, only the first paper to demonstrate a specific interaction by each individual technique is listed in the reference column, excepting in the case of simultaneous publications. Rounded brackets indicate synonyms while squared brackets indicate gene names where these differ from the name of the protein. Gene families are quoted when it is unclear which gene the protein came from or when interactions were identified using antibodies that detected multiple forms of the protein.

1.2.3 Phosphodiesterase 4B (PDE4B)

1.2.3.1 *PDE4B* in psychosis

One protein interactor which has received much attention in the last few years is phosphodiesterase 4B (PDE4B). Having been identified as a DISC1-interactor in a

yeast-two-hybrid screen PDE4B drew attention when a proband with schizophrenia was identified, who had a balanced t(1;16) translocation, directly disrupting the *PDE4B* gene (Millar *et al.* 2005b). The proband had a cousin with schizophrenia who also carried the t(1;16) translocation. It was suggested that *PDE4B*-deficiency could be the cause of the proband's schizophrenia also on the grounds that the drug rolipram, a known PDE4 inhibitor, is known to act as an antidepressant (Wachtel 1983) and that *Drosophila* with mutations in their *PDE4B* orthologue have learning and memory defects (Dudai *et al.* 1976). That rolipram, a PDE4-inhibitor, has an antidepressant activity furthermore suggests that regulation of the overall activity of PDE4B, rather than specifically reduction in activity due to lowered levels of the protein, may be associated with psychiatric illness. Since the original report, three genetic studies have been published, each providing evidence that different haplotypes of the *PDE4B* gene are associated with an altered risk of schizophrenia in the wider population (Pickard *et al.* 2007; Fatemi *et al.* 2008; Numata *et al.* 2008b). Additionally several *PDE4B* SNPs were found to be associated with major depression, although these results were not replicatable in a second population sample (Numata *et al.* 2008a). *PDE4B* transcript levels were, however, significantly over-represented in major depression sufferers compared to controls, and were reduced in patients on antidepressants compared to drug naïve ones (Numata *et al.* 2008a).

It therefore appears increasingly likely that altered *PDE4B* function is a risk factor in its own right for schizophrenia and potentially wider mental illness. Interactions of the endogenous DISC1 protein with various PDE4B isoforms in the cell have been robustly demonstrated (Millar *et al.* 2005b; Murdoch *et al.* 2007).

1.2.3.2 The role of phosphodiesterases

Cyclic adenosine monophosphate (cAMP) is a versatile secondary messenger within the cell. It is generated from adenosine triphosphate (ATP) by adenylyl cyclase. The only method by which the cell can degrade cAMP is through the use of phosphodiesterases such as PDE4B. Long PDE4 isoforms contain two conserved regulatory regions, and the protein binds in such a way that these two regions interact

with each other. Phosphorylation of one of these regions by PKA leads to a conformational shift, dramatically increasing the phosphodiesterase activity of the molecule. Thus PDE4-activity is PKA dependent. PKA consists of two catalytic subunits as well as two regulatory subunits which bind to the catalytic subunits and inhibit their activity. Binding of cAMP to the regulatory subunits causes them to release the catalytic subunits, activating the protein. Therefore a negative feedback mechanism exists to control the level of cellular cAMP, with cAMP activating PKA, PKA activating PDE4 and PDE4 degrading cAMP. This is summarised in figure 1.2.D.

1.2.3.3 PDE4B and DISC1

PDE4B has been shown to bind to the DISC1 protein at multiple sites (Millar *et al.* 2005b; Murdoch *et al.* 2007). Colocalisation of the two proteins has been seen in both differentiated and undifferentiated neurons, including at the mitochondria (Millar *et al.* 2005b). As stated previously, PDE4B is activated by cAMP-stimulated PKA phosphorylation. It is therefore interesting to note that binding of the 71kDa DISC1 isoform to PDE4B is weakened when drugs are used to boost cellular cAMP levels (Millar *et al.* 2005b), although a similar result was not seen with full length DISC1 (Murdoch *et al.* 2007). It therefore appears that DISC1-PDE4B interactions are regulated in an isoform-specific and cAMP-dependent manner, and which may play an important role in the degradation of cAMP by PDE4B.

PDE4B shows reduced binding affinity for two mutant versions of mouse Disc1, Q31L and L100P, which have been shown to cause depression-like and schizophrenia-like behaviour (Clapcote *et al.* 2007). This is seemingly because the two "pathogenic" mutations lie within two separate PDE4B binding sites (Murdoch *et al.* 2007). Additionally for Q31L mice, the total PDE4B activity in the brain was strikingly reduced compared to wild-type litter mates (Clapcote *et al.* 2007). Together this suggests that the DISC1-PDE4B interaction may be a crucial part of the *DISC1*-induced behavioural phenotypes in the mice.

a)

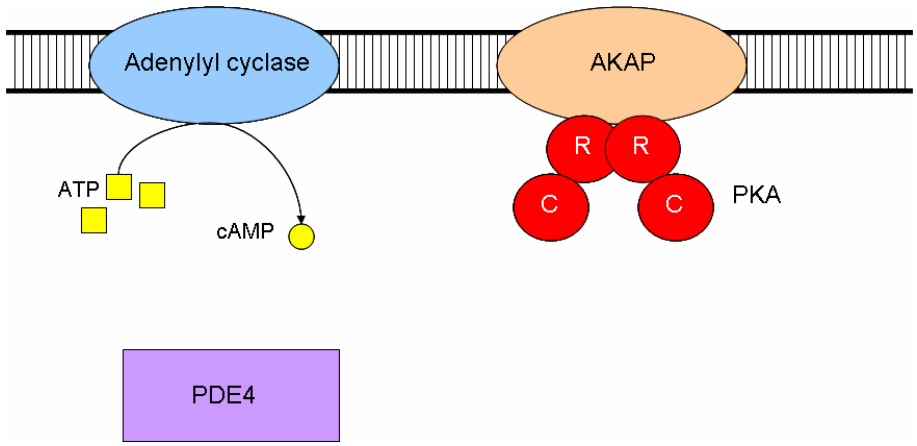
Adenylyl cyclase
AKAP
R
R
C
C
PKA
ATP
cAMP
PDE4

b)

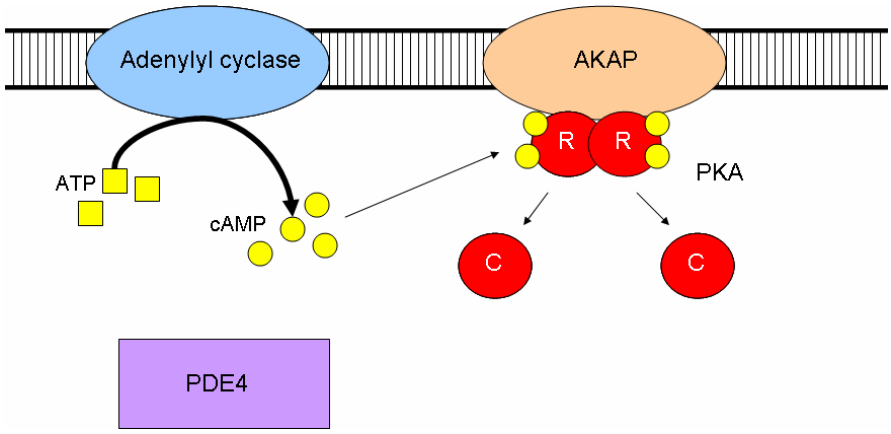
Adenylyl cyclase
AKAP
R
R
PKA
ATP
cAMP
C
C
PDE4

c)

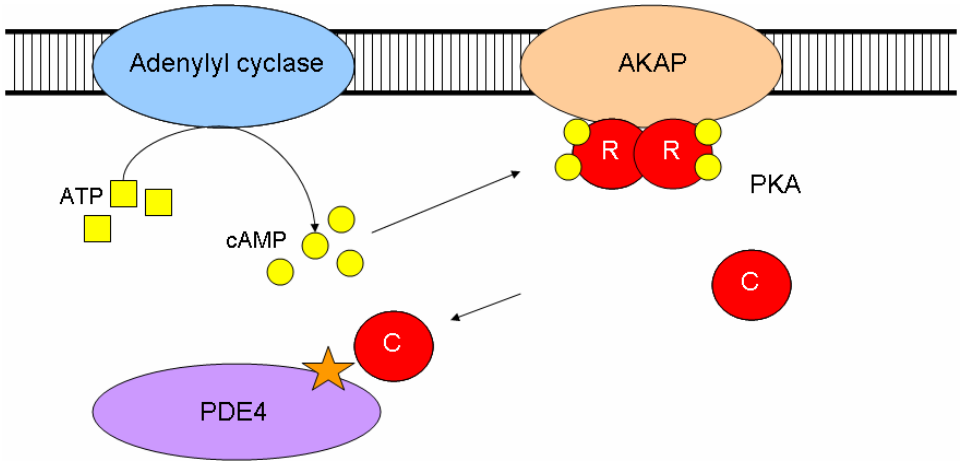
Adenylyl cyclase
AKAP
R
R
PKA
ATP
cAMP
C
C
PDE4

d)

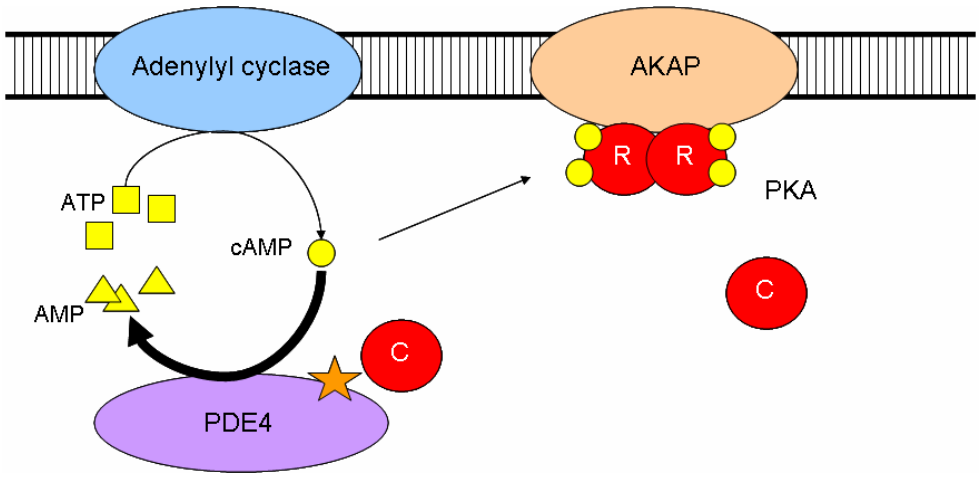
Adenylyl cyclase
AKAP
R
R
PKA
ATP
cAMP
C
AMP
C
PDE4

e)

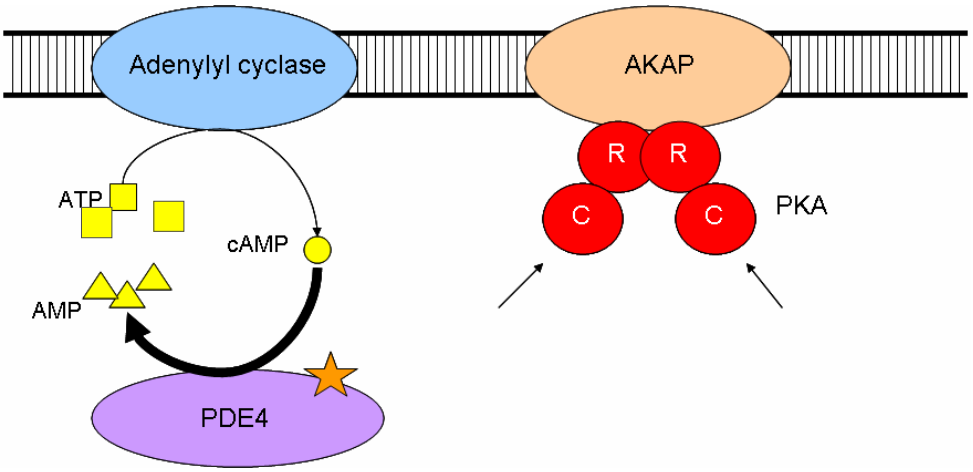
Adenylyl cyclase
AKAP
R
R
C
C
PKA
ATP
cAMP
AMP
PDE4

f)

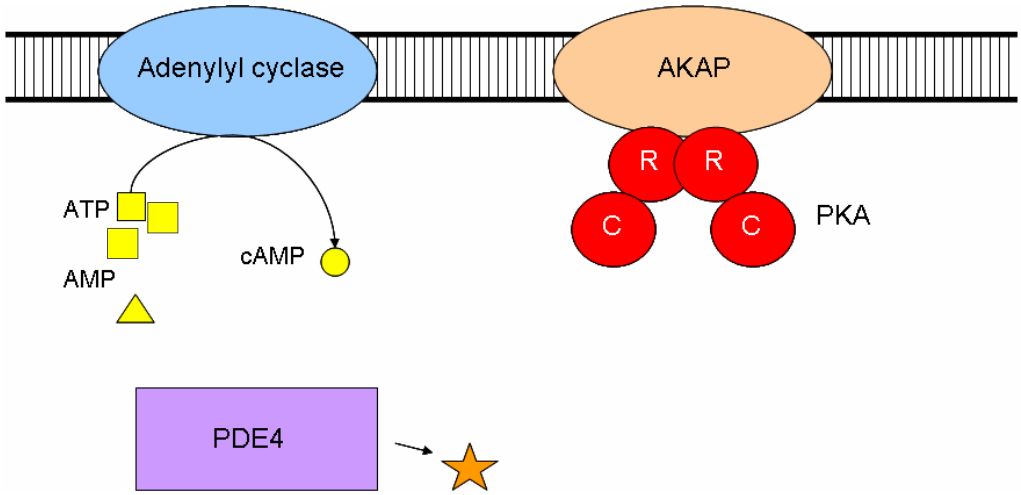
Adenylyl cyclase
AKAP
R
R
C
C
PKA
ATP
cAMP
AMP
PDE4

Figure 1.2.D: The regulation of cyclic AMP (cAMP). a) Adenosine triphosphate (ATP) is converted into cAMP by adenylyl cyclase. The inactive protein kinase A (PKA) holoenzyme is bound to an A-Kinase Anchoring Protein (AKAP). b) Following adenylyl cyclase activation, the rate of cAMP production increases. One function of the cAMP is to bind to the regulatory (R) subunits of PKA, releasing and activating its catalytic (C) subunits. c) PKA can phosphorylate phosphodiesterase 4 (PDE4), causing a conformational shift and activating it. d) PDE4 begins to degrade cAMP to adenosine monophosphate (AMP). e) The reduction in cAMP allows the catalytic PKA subunits to rebind to the regulatory subunits, inactivating the holoenzyme. f) With the cellular PKA activity reduced, PDE4 becomes dephosphorylated, deactivating it. The degradation of cAMP is therefore reduced and cellular homeostasis is restored. Note that, while not shown in the diagram, PDE4s also bind to AKAPs.

1.2.4 Other protein interactors of DISC1

1.2.4.1 ATF4 and 5

Activating Transcription Factors 4 and 5 (ATF4 and ATF5) have both been demonstrated to bind to DISC1 by yeast-two-hybrid analysis (Millar *et al.* 2003; Morris *et al.* 2003) and confirmed by immunoprecipitation of over-expressed protein (Morris *et al.* 2003; Sawamura *et al.* 2008). Both ATF4 and ATF5 are members of the CREB family of proteins, and are transcriptional regulators which play a diverse array of roles within the cell. It has been shown that DISC1 expression can repress the transcriptional activity of ATF4, potentially through interaction with the transcriptional repressor N-CoR (Sawamura *et al.* 2008). ATF4 is also known to be phosphorylated by PKA (Elefteriou *et al.* 2005), providing a potential link between ATF4 and PDE4B.

The *ATF4* gene is located at chromosomal region 22q13, which shows evidence of being linked to psychiatric illness (Pulver *et al.* 1994; Gill *et al.* 1996; Liang *et al.*

2002; Takahashi *et al.* 2005; Zheng *et al.* 2006). However, the evidence directly associating polymorphisms in *ATF4* with psychiatric illness to date is limited (Kakiuchi *et al.* 2007; Qu *et al.* 2008), with at least seven other genes in this region having also been reported to show association (Hong *et al.* 2004; Brennan and Condra 2005; Verma *et al.* 2005a; Verma *et al.* 2005b; Severinsen *et al.* 2006a; Severinsen *et al.* 2006b; Silberberg *et al.* 2008).

1.2.4.2 DBZ/Su48

Zinc finger protein 365 (ZNF365), was identified in two studies as a DISC1 interactor (Camargo *et al.* 2007; Hattori *et al.* 2007). This protein, which Hattori *et al* designated DISC1-Binding Zinc finger protein (DBZ) has also been characterised elsewhere under the name Su48 (Wang *et al.* 2006). DBZ/Su48 is a centrosomal protein (Wang *et al.* 2006) which is known to be expressed primarily in the brain (Nagase *et al.* 1998). Over-expression of both DBZ/Su48 and DISC1 simultaneously in rat PC12 neurons led to diminished neurite outgrowth (Hattori *et al.* 2007). The same effect was not seen when either was over-expressed individually, implicating the DISC1-DBZ/Su48 complex in neuronal development. There is also some limited but intriguing evidence to suggest that the chromosomal region at which it is found, 10q21.2, may play a role in the pathology of bipolar disorder (Liu *et al.* 2003; Segurado *et al.* 2003; Marcheco-Teruel *et al.* 2006; Tastemir *et al.* 2006).

1.2.4.3 eIF3 p40

Eukaryotic Initiation Factor 3 (eIF3) is a complex of at least a dozen protein subunits that acts as a scaffold for the formation of translation initiation complexes (Hinnebusch 2006). DISC1 was shown to bind to the p40 subunit of eIF3 and over-expression of DISC1 led to the production of eIF3 positive stress granules (Ogawa *et al.* 2005). The p40 subunit is encoded by the *EIF3S3* gene, which is found at chromosome 8q24. This region shows linkage to bipolar disorder (Cichon *et al.* 2001; McInnis *et al.* 2003; Macgregor *et al.* 2004; Park *et al.* 2004) and to schizophrenia (Walss-Bass *et al.* 2006; Kaneko *et al.* 2007; Aberg *et al.* 2008), although fine mapping has suggested that the mental illness risk locus may lie away

from the *EIF3S3* gene (Avramopoulos *et al.* 2004; Zandi *et al.* 2007; Zandi *et al.* 2008).

1.2.4.4 FEZ1

Fasciculation and Elongation protein Zeta 1 (FEZ1) is a protein expressed exclusively in the brain (Kuroda *et al.* 1999). Mice which were homozygous negative for *Fez1* showed evidence for increased hyperactivity and increased sensitivity to psychostimulants, but expressed no obvious cognitive impairments (Sakae *et al.* 2008). In combination with PKCζ, FEZ1 has been shown to be involved in neuronal differentiation (Kuroda *et al.* 1999), neurite outgrowth (Fujita *et al.* 2007) and the establishing of neuronal polarity (Ikuta *et al.* 2007), functions which may be related to its ability to activate kinesin-related transport along the microtubules (Blasius *et al.* 2007; Fujita *et al.* 2007).

The DISC1 and FEZ1 proteins have been shown to interact by yeast-two-hybrid screening and by co-immunoprecipitation of over-expressed protein (Miyoshi *et al.* 2003). The two proteins have similarities in their developmental expression profiles in the brain (Honda *et al.* 2004) and their interaction appears to be more abundant during neuronal differentiation (Miyoshi *et al.* 2003). Intriguingly, over-expression of the FEZ1-binding domain of DISC1 leads to stunted neurite outgrowth in PC12 cells, although whether this phenotype is specifically FEZ1-related or not is unclear. The *FEZ1* gene lies close to a translocation breakpoint in a schizophrenia patient, however other genes are directly disrupted by the translocation (Pickard *et al.* 2006). Similarly, there are two reported cases of the chromosomal region surrounding *FEZ1*, 11q24.2, being deleted in individuals with bipolar affective disorder (Böhm *et al.* 2006; Reardon *et al.* 2007). Two *FEZ1* SNPs have been shown to be nominally associated with schizophrenia (Yamada *et al.* 2004), however no significant SNPs were detected in two subsequent studies (Hodgkinson *et al.* 2006; Koga *et al.* 2007).

1.2.4.5 GRB2

Growth factor Receptor Bound protein 2 (GRB2) is a multi-purpose adaptor protein within the cell (Lowenstein *et al.* 1992). DISC1 has been shown to exist in a ternary

complex with both GRB2 and the kinesin heavy chain protein KIF5B (Shinoda *et al.* 2007). DISC1 is involved in kinesin-1-related transport of GRB2 and is required for GRB2-related cellular functions such as the neutrophilin-2-related axonal elongation (Shinoda *et al.* 2007). GRB2 is also known to bind to the PDE4D family of proteins (Beard *et al.* 1999) which, like PDE4B have been independently implicated in schizophrenia (Tomppo *et al.* 2006).

There is a limited amount of evidence that 17q25, the chromosomal region where *GRB2* is found, may be linked schizophrenia (Riley *et al.* 1997; Logue *et al.* 2006) and bipolar disorder (Ewald *et al.* 2005). Interestingly, expression of GRB2 in the dentate gyrus has been shown to increase following electro-convulsive therapy, a treatment for depression (Newton *et al.* 2004).

1.2.4.6 Kinesins

Kinesins are a superfamily of ATP-powered motor protein complexes involved in the transport of cargo, such as vesicles, towards the distal ends of microtubules and the cell periphery (Hirokawa and Noda 2008). By various techniques, the kinesin heavy chains KIF3A, 3C, 5A, 5B and 5C, along with the kinesin light chains KLC1 and KLC2 have all been implicated in DISC1 interaction (Camargo *et al.* 2007; Taya *et al.* 2007). DISC1 plays a role in the localisation of kinesin-1 and may act as a cargo receptor allowing kinesin-1 to transport proteins including GRB2, NDEL1, LIS1 and 14-3-3ε (Shinoda *et al.* 2007; Taya *et al.* 2007). The DISC1-interacting proteins FEZ1 and MIPT3 have also been implicated in kinesin function (Blasius *et al.* 2007; Fujita *et al.* 2007; Li *et al.* 2008). Together this strongly implicates DISC1 as being involved in kinesin-related transport.

1.2.4.7 MAP1A

Microtubule-Associated Protein 1A (MAP1A) was shown to interact with DISC1 in a yeast 2-hybrid screen and by co-immunoprecipitation of over-expressed protein (Morris *et al.* 2003). MAP1A is a large protein known to bind to and be involved in the structural development of both microtubules and the actin cytoskeleton (Shiomura and Hirokawa 1987; Pedrotti *et al.* 1994; Pedrotti and Islam 1994). It is

expressed in the developing brain (Garner *et al.* 1990) and has been implicated as playing roles in neurite outgrowth and dendritic remodelling (Di Giovanni *et al.* 2004; Szebenyi *et al.* 2005). The *MAP1A* gene is located at 15q15, a locus which shows some, currently limited, evidence of linkage to early onset major depressive disorder (Camp *et al.* 2005), bipolar disorder (Marcheco-Teruel *et al.* 2006), schizophrenia (Moon *et al.* 2006) and catatonia (Stöber *et al.* 2000).

1.2.4.8 MIP-T3

Microtubule Interacting Protein that associates with TRAF3 (MIP-T3) is a microtubule-associated protein (Ling and Goeddel 2000) which is suggested to play a role in the assembly of kinesin motor complexes (Li *et al.* 2008). Yeast-two-hybrid screens and co-immunoprecipitation of over-expressed protein have suggested that MIP-T3 is also a DISC1 interactor, with the ability to recruit DISC1 to the microtubules (Morris *et al.* 2003). It is also known as TRAF3-Interacting Protein 1 (TRAF3IP1). The *MIPT-3/TRAF3IP1* gene is found at chromosomal region 2q37, which has been linked to schizophrenia in four studies to date (Paunio *et al.* 2001; Lerer *et al.* 2003; Wijsman *et al.* 2003; Klei *et al.* 2005).

1.2.4.9 PCM1 and BBS4

Pericentriolar Material 1 (PCM1) is a large protein found proximal to, but not at the centrioles (Balczon *et al.* 1994; Kubo *et al.* 1999). It functions as a scaffold protein and is involved in the recruitment of various other proteins, including pericentrin-B, to the centrosome, a process which is essential for correct microtubule organisation (Dammermann and Merdes 2002). PCM1 is itself recruited to the centrosome by Bardet-Biedl Syndrome (BBS) protein 4 (Kim *et al.* 2004). By co-immunoprecipitation, DISC1 has been shown to exist in a complex with PCM-1 and each of BBS proteins 1-8 (Kamiya *et al.* 2008). DISC1 and BBS4 appear to act co-operatively to recruit PCM-1 to the centrosome and affect the rate of radial neuron migration in mouse embryos (Kamiya *et al.* 2008). Two studies have so far reported association between the *PCM1* gene and schizophrenia (Gurling *et al.* 2006; Datta *et al.* 2008). The gene is found at 8p22 in close proximity to *NRG1*, a prominent candidate gene for schizophrenia and bipolar disorder. This makes it difficult to

assess whether or not *PCM1* contributes to linkage signals at this chromosomal location.

1.2.4.10 Pericentrin-B

Pericentrin-B (also known as kendrin) is a large centrosomal protein (Flory *et al.* 2000; Li *et al.* 2001) and is orthologous to a splice variant of the better studied mouse protein pericentrin-A (Doxsey *et al.* 1994; Flory and Davis 2003). Pericentrin-A is among the first proteins to be found at *de novo* generated centrosomes (Khodjakov *et al.* 2002) and appears to act as a molecular scaffold, anchoring proteins such as PKA to the centrosome (Diviani *et al.* 2000). Pericentrin-B was shown to bind to the central regions of DISC1, and the two proteins appear to colocalise at the centrosomes of SH-SY5Y human neuroblastoma cells (Miyoshi *et al.* 2005). Disruption of their interaction has been shown to disrupt the formation of the microtubule network (Shimizu *et al.* 2008).

Pericentrin-B is encoded by the *PCTN* gene, mutations in which have been shown to cause specific forms of dwarfism, characterised by a reduction of brain size in addition to a reduction in general body size (Griffith *et al.* 2008; Rauch *et al.* 2008), thus implicating pericentrin-B in neurodevelopment. Intriguingly, a study of mRNA levels in post-mortem brains revealed *PCTN2* transcripts (the splice form of *PCTN* encoding pericentrin-B) to be over-represented in the brains of bipolar disorder patients compared to controls (Anitha *et al.* 2007). In addition, the *PCTN* gene is found at chromosomal region 21q22.3 which has been repeatably linked to bipolar disorder in various populations (Straub *et al.* 1994; Vallada *et al.* 1996; Smyth *et al.* 1997; Detera-Wadleigh *et al.* 1999; Kwok *et al.* 1999; Liu *et al.* 2001; Ewald *et al.* 2003; Kaneva *et al.* 2004). There are also reported cases of schizophrenia sufferers who possess a chromosomal deletion at 21q22. (Demirhan and Tastemir 2003).

1.2.4.11 14-3-3 proteins

The 14-3-3 proteins are a family of ubiquitously expressed phospho-serine/phosphor-threonine binding proteins involved in a diverse range of signalling pathways and protein interactions within the cell (Dougherty and Morrison 2004). One of these

proteins, 14-3-3ε, has been demonstrated to be a DISC1-interacting protein (Camargo *et al.* 2007; Taya *et al.* 2007). DISC1 is required for the correct localisation of 14-3-3ε to the distal parts of the axon, possibly by facilitating its transport to this location by kinesin-1 (Taya *et al.* 2007). 14-3-3γ has also been seen to bind DISC1 in a yeast-two-hybrid screen (Ozeki *et al.* 2003).

A recent study provided evidence that a SNP in the *YWHAE* gene, which encodes 14-3-3ε, is associated with schizophrenia, as well as demonstrating that *Ywhae* deficient mice display behavioural defects (Ikeda *et al.* 2008). The chromosomal region containing *YWHAE*, 17p13, also contains *LIS1* and is heavily involved in lissencephaly brain malformations (see section 1.3.1). This region has also been linked to schizophrenia in one study (Klei *et al.* 2005).

1.2.4.12 Other interactors from yeast-two-hybrid screens

A number of other DISC1 yeast-two-hybrid interactors, for which further study has not yet been undertaken, also have the potential to link into mental illness pathways. For example, citron forms complexes with NMDA receptors (Furuyashiki *et al.* 1999), TIAM2 is known to be involved in the radial migration of neurons (Kawauchi *et al.* 2003) and the *NPHP6* gene has been repeatedly shown to be linked to the Joubert and Meckel syndromes, both of which include neurological symptoms (Sayer *et al.* 2006; Valente *et al.* 2006; Baala *et al.* 2007).

It can therefore be seen that DISC1 appears to play roles in numerous cellular pathways, several of which have the potential to be involved in the pathology of schizophrenia and other psychiatric conditions. This work will, however, focus on the interactions of DISC1 with two proteins: NDE1 and NDEL1, as well as their relationship with a third DISC1-interactor, LIS1.

1.3 Nuclear Distribution Factor E homologues (NDE1 and NDEL1)

1.3.1 The LIS1 pathway

The Lissencephaly 1 gene (*LIS1*, also known as *PAFAH1B1*) is so named as it was identified as being from a chromosomal region disrupted in sufferers of the brain malformation Miller-Dieker lissencephaly (Reiner *et al.* 1993). The *LIS1* gene has since been shown to be mutated in the majority of cases of the related, but less severe, syndrome isolated lissencephaly (Guerrini and Marini 2006). The LIS1 protein appears to play two major roles in the cell. The first of these is that it is known to be one subunit of the platelet-activating factor acetylhydrolase (PAFAH) complex (Hattori *et al.* 1994). The second occurs through its interactions with the dynein and dynactin protein complexes (Faulkner *et al.* 2000; Tai *et al.* 2002). These two functions appear to be separate as LIS1 cannot bind to both the PAFAH and dynein complexes simultaneously (Tarricone *et al.* 2004). This work will focus on the dynein-related activity of LIS1.

The microtubules function as "conveyer belts" along which cargo (proteins or vesicles) can be trafficked within the cell. This microtubule network spreads throughout the cell from the microtubule organising centre at the centrosome. Trafficking occurs both towards and away from the cell periphery, with separate motor proteins being involved in each direction of traffic. Cytoplasmic dynein is a motor protein complex involved in retrograde transport along the microtubules towards the centrosome, and consists of two heavy chains as well as numerous intermediate chains, light intermediate chains and light chains. In order to function it requires a second protein complex, dynactin (Gill *et al.* 1991). In addition to providing transport of cargo from the cell periphery, this system is involved in a number of other cellular functions, such as facilitating the migration of the nucleus during neuronal development (Shu *et al.* 2004).

LIS1 interacts with this motor complex (Sasaki *et al.* 2000) and may function by aiding in the transport of dynein back to the distal ends of the microtubules (Yamada *et al.* 2008). Use of RNAi to knock down the levels of either LIS1 or dynein proteins

have been shown to impair nuclear movement (Shu *et al.* 2004). Possibly as a result of this, neurons lacking *LIS1* have been shown to have impaired migration (Shu *et al.* 2004; Toyo-Oka *et al.* 2005). In combination with the fact that LIS1 is known to be a DISC1-interacting protein (Brandon *et al.* 2004), it would appear that this pathway may be of significant interest in studying major mental illness.

1.3.2 Identification of nudE homologues

The LIS1-dynein-dynactin pathway has been seen to be strongly conserved even in ancient organisms such as *Aspergillus nidulans*, *Neurospora crassa* and *Saccharomyces cerevisae* (Xiang *et al.* 1995a; Geiser *et al.* 1997; Cockell *et al.* 2004). The homologue of *LIS1* in the fungus *A. nidulans* is one of a series of genes which, when mutated, lead to deficiencies in nuclear migration (Xiang *et al.* 1995a). These nuclear distribution genes include homologues of LIS1 (nudF), dynein subunits (nudA, nudG and nudI) and dynactin subunits (nudK and nudM) (Xiang *et al.* 1995b; Beckwith *et al.* 1998; Xiang *et al.* 1999; Efimov and Morris 2000; Zhang *et al.* 2002; Zhang *et al.* 2003). In addition, a gene nudE, encoded a protein, NUDE, that binds the LIS1/NUDF protein (Efimov and Morris 2000).

In 2000 and 2001, five studies were published that used yeast-two-hybrid screening to predict protein interactors of mammalian LIS1. Three of these studies showed LIS1 to interact with a previously unknown protein that was apparently an orthologue of NUDE (Feng *et al.* 2000; Kitagawa *et al.* 2000; Sasaki *et al.* 2000). This protein was named Nuclear Distribution factor E (*Aspergillus nidulans*) homologue 1 (NDE1). In addition, three of the studies reported LIS1 to interact with a separate protein, a paralogue of NDE1. This second protein was named NDE-Like 1 or NDEL1 (Niethammer *et al.* 2000; Sasaki *et al.* 2000; Sweeney *et al.* 2001).

The NDE1 and NDEL1 proteins have highly similar amino acid sequences (see figure 1.3.A). Conservation is particularly high in the region known to be involved in LIS1-binding (Feng *et al.* 2000; Sweeney *et al.* 2001) and the two genes may have descended from a common ancestral gene, such as nudE in *A. nidulans*. The exact nomenclature of *NDE1* and *NDEL1* has varied since their identification. A complete

```
NDE1            -MEDSGKTFSSEEEEANYWKDLAMTYKQRAENTQEELREFQEGSREYEAELETQLQQIET
NDEL1           MDGEDIPDFSSLKEETAYWKELSLKYKQSFQEARDELVEFQEGSRELEAELEAQLVQAEQ
                   :.   *** :**: ***:*::.***  ::::::** ******** *****:** * *

NDE1            RNRDLLSENNRLRMELETIKEKFEVQHSEGYRQISALEDDLAQTKAIKDQLQKYIRELEQ
NDEL1           RNRDLQADNQRLKYEVEALKEKLEHQYAQSYKQVSVLEDDLSQTRAIKEQLHKYVRELEQ
                ***** ::*:**: *:*::***:* *::::.*:*:*.*****:**:***:**:**:*****

NDE1            ANDDLERAKRATIMSLEDFEQRLNQAIERNAFLESELDEKENLLESVQRLKDEARDLRQE
NDEL1           ANDDLERAKRATIVSLEDFEQRLNQAIERNAFLESELDEKESLLVSVQRLKDEARDLRQE
                *************:**************************.** ***************

NDE1            LAVQQKQE---KPRTPMPSSVEAERTDTAVQATGSVPSTPIAHRGPSSSLNTPGSFRRGL
NDEL1           LAVRERQQEVTRKSAPSSPTLDCEKMDSAVQASLSLPATPVGKGTENTFPSP-----KAI
                ***:::*:   :  :* ..::::.*: *:****: *:*:**:.:   .:  ..     :.:

NDE1            DDSTGGTPLTPAARISALNIVGDLLRKVGALESKLASCRNLVYDQSPNRTGGPASGRSSK
NDEL1           PNGFGTSPLTPSARISALNIVGDLLRKVGALESKLAACRNFAKDQASRKSYISGNVNCGV
                 :. * :****:************************:***:. **:..::  ... ...

NDE1            NRDGGERRPSSTSVPLGDK----GLDTSCRWLSKSTTRSSSSC-------
NDEL1           LNGNGTKFSRSGHTSFFDKGAVNGFDPAPPPPGLGSSRPSSAPGMLPLSV
                 ...* : . *  ..: **    *:*.:    . .::*.**:
```

Figure 1.3.A: Sequence alignment of human NDE1 and NDEL1. Asterisks (*) indicate precisely conserved residues while dots indicate similar residues, while dots (.) and colons (:) indicate ascending degrees of similarity Alignment performed using FASTA Two-Sequence Comparison (Pearson and Lipman 1988)

Gene/Protein	**Names used in the literature**
NDE1	Nde1, NudE, NUDE, HOM-TES-87, mNudE (Mouse), rNUDE (Rat), MP43 (Xenopus)
NDEL1	Ndel1, Nudel, NUDEL, NUDEL-oligopeptidase, EOPA, EOPARP (Rabbit), Ndel1a & Ndel1b (Zebrafish)
NDE1/NDEL1	nudE (A. nidulans), ro-11 (N. crassa), Ndl1 (S. cerevisae), NUD-2 (C. elegans)

Table 1.3: A list of alternate names for NDE1 and/or NDEL1 used in the literature. All names refer to the human genes/proteins unless stated. “NDE1/NDEL1” includes genes for which it is not possible to determine whether they represent direct orthologues specifically of *NDE1* or *NDEL1* or a homologue of their common ancestral gene.

list of the synonyms for the two genes used in the literature is therefore displayed in table 1.3.

Following the initial demonstration of an interaction using yeast-two-hybrid screening, binding of NDEL1 to LIS1 has been robustly demonstrated by co-immunoprecipitation of both endogenous and *in vitro* transcribed and translated protein (Niethammer *et al.* 2000; Sweeney *et al.* 2000). The NDE1-LIS1 interaction has so far only been seen using protein over-expressed in cells (Feng *et al.* 2000; Kitagawa *et al.* 2000). There is also some evidence to suggest that NDE1 can bind to dynein light chains (Feng *et al.* 2000; Stehman *et al.* 2007), while NDEL1 has been robustly demonstrated to complex with the heavy and intermediate chains (Niethammer *et al.* 2000; Sweeney *et al.* 2000; Brandon *et al.* 2004; Kamiya *et al.* 2005). NDE1 and NDEL1 have also both been reported to co-immunoprecipitate with dynactin subunits (Niethammer *et al.* 2000; Brandon *et al.* 2004; Liang *et al.* 2004; Guo *et al.* 2006). Overall, this strongly implies that, as in *A. nidulans*, NDE1 and NDEL1 are likely to exist in the LIS1-dynein-dynactin complex.

1.3.3 Functions of NDE1 and NDEL1 in the cell

NDEL1, and to a lesser extent NDE1, have been demonstrated to play a number of different roles in the cell, most of them related to LIS1 and/or dynein. One of these roles appears to be in the assembly of the LIS1-dynein complex itself. Use of RNAi to block production of the NDEL1 protein leads to reduced association of LIS1 with the dynein intermediate chain in several cell lines (Shu *et al.* 2004; Shim *et al.* 2008), while the expression pattern of endogenous LIS1 matches that of over-expressed NDE1 or NDEL1 (Caspi *et al.* 2003). It therefore appears that NDE1 and NDEL1 act as recruiters for the LIS1 protein.

1.3.3.1 NDE1 and NDEL1 at the centrosome

The NDEL1 protein is consistently found at the centrosome (Niethammer *et al.* 2000; Sasaki *et al.* 2000) and NDE1 appears to do the same when over-expressed in cell lines (Feng *et al.* 2000). These localisations appear to only occur during interphase (Toyo-Oka *et al.* 2005; Hirohashi *et al.* 2006b). NDEL1 has also been seen to be

specific to the mother centriole (Guo *et al.* 2006). Localisation of NDEL1 to the centrosome appears to be regulated by kinases (Yan *et al.* 2003; Toyo-Oka *et al.* 2005; Mori *et al.* 2007) with phosphorylation at sites in the C-terminal half of NDEL1 leading it to be absent from the centrosome. Amino acids 256-291 of NDEL1, found near the C-terminus and containing its dynein binding site (Liang *et al.* 2004), have been shown to be essential for centrosomal localisation (Guo *et al.* 2006).

Over-expression of a mutant form of NDEL1 lacking the centrosomal localisation domain in HeLa cells has been shown to block the localisation of LIS1 and a dynactin subunit to the centrosome while not affecting "core" centrosomal proteins such as γ-tubulin. This implies that NDEL1 is responsible for recruiting LIS1 and dynactin to the centrosome (Guo *et al.* 2006). Knocking down NDEL1 expression using RNAi had a similar effect on LIS1 and NDEL1, but also partially disrupted the centrosomal localisation of pericentrin and γ-tubulin (Guo *et al.* 2006). Over-expression of Nde1 in mouse cell lines has also been seen to lead to γ-tubulin mis-localisation (Feng *et al.* 2000).

1.3.3.2 NDE1 and NDEL1 at the microtubules

Like dynein and LIS1, NDEL1 is known to be anchored to the microtubules of the cell (Sasaki *et al.* 2000), and over-expressed NDE1 appears to do likewise (Coquelle *et al.* 2002). Following the severing of a neuron, mouse Ndel1 was seen at both ends of the microtubules, implying that it is actively transported along it (Sasaki *et al.* 2000).

Expression of mutant versions of NDEL1, lacking the LIS1- or dynein-binding domains, led to the fragmentation of the Golgi apparatus and dispersion of lysosomes and endosomes (Liang *et al.* 2004), in a pattern similar to that which is seen when dynein activity is inhibited (Guo *et al.* 2006). This system was sensitive to the microtubule-destabilising drug nocodazole (Liang *et al.* 2004), implying that NDEL1 is involved in the dynein-related transport of vesicles along microtubules towards the nucleus. Conditional knock-out of Ndel1 in mice again blocked the transport of

vesicles along the microtubules, but interestingly this could be rescued by over-expression of Nde1 (Sasaki *et al.* 2005), suggesting that NDE1 may also be involved in this process.

NDE1 and NDEL1 also appear to play a role in maintaining the structure of microtubules. Over-expression of Nde1 in mouse cell lines leads to the microtubule network taking a disorganised shape (Feng *et al.* 2000). Similarly, cells from conditional knock-out *Ndel1* mice show amorphous microtubule networks (Sasaki *et al.* 2005; Toyo-Oka *et al.* 2005) and are slower to produce new networks after disruption of previous ones with nocodazole (Guo *et al.* 2006). This may be related to the disruption of protein assembly at the centrosomes, which form the organising centre of microtubule networks.

1.3.3.3 NDE1 and NDEL1 in mitosis

Disrupting the functions of either NDE1 or NDEL1 within the cell has been shown to lead to the cell taking longer to undergo mitosis (Feng and Walsh 2004; Liang *et al.* 2007). Expression of truncated mutant versions of NDE1 in cells led to defects in the formation of the spindle (Stehman *et al.* 2007), while expression of NDEL1 mutants led to cells in which the chromosomes failed to disperse correctly (Liang *et al.* 2007).

During mitosis, NDE1 and NDEL1 are both known to be found at the spindle (Yan *et al.* 2003) and the kinetochores (Liang *et al.* 2007; Stehman *et al.* 2007; Vergnolle and Taylor 2007). During normal mitosis, the spindle attaches to the kinetochores at metaphase and various proteins are transported from the spindle to the kinetochores through the action of dynein (Howell *et al.* 2000; Howell *et al.* 2001). Transfer of these proteins may be used as part of a cellular "check" that attachment has occurred successfully before the cell proceeds into anaphase. NDE1 and NDEL1 appear to be among the proteins transported in this way (Yan *et al.* 2003), but interestingly over-expression of a NDEL1 mutant lacking the dynein binding domain actually blocked the transport of itself and other proteins in this manner (Liang *et al.* 2007). That NDEL1 and possibly NDE1 are required for this process provides a mechanism for

NDE1/NDEL1-related mitotic disruption. NDE1 and NDEL1 also appear to play roles in recruiting dynein and/or dynamitin to the kinetochores prior to the binding of the spindle (Liang *et al.* 2007; Vergnolle and Taylor 2007)

1.3.3.4 NDEL1 as an endopeptidase

In addition to these functions, NDEL1 is known to have an additional role as a cysteine endopeptidase (Hayashi *et al.* 2005), having been shown to degrade neuropeptides such as bradykinin in rabbit brain homogenates (Camargo *et al.* 1973; Camargo *et al.* 1983). This function is performed only by the NDEL1 monomer, rather than the dimer which is known to interact with LIS1 (Tarricone *et al.* 2004; Hayashi *et al.* 2005). It is unknown whether NDE1 possesses a similar enzymic activity, although the catalytic cysteine residue of NDEL1 is conserved between the two proteins (Hayashi *et al.* 2005).

1.3.4 NDE1 and NDEL1 in neurodevelopment

1.3.4.1 Nde1 and Ndel1 in the mouse brain

In rodents, Nde1 and Ndel1 are both expressed in numerous parts of the body, with the brain, testes and heart being the most commonly described, although expression has also been seen in the ovary (reported for Ndel1 only), kidney, liver, eye (Ndel1) spleen (Nde1) and muscles (Feng *et al.* 2000; Kitagawa *et al.* 2000; Niethammer *et al.* 2000; Sasaki *et al.* 2000; Sweeney *et al.* 2001; Yamaguchi *et al.* 2004). It should be stressed that a direct comparison of Nde1 with Ndel1 is yet to be performed.

Several studies have investigated the expression pattern of the Ndel1 protein within the rodent brain. Most commonly it is described as being in the cerebral cortex within layers II-IV (Niethammer *et al.* 2000; Sasaki *et al.* 2000; Hayashi *et al.* 2001; Sweeney *et al.* 2001). Expression has also been reported in the hippocampus, where it is found in layers CA1-3 and the dentate gyrus (Niethammer *et al.* 2000; Hayashi *et al.* 2001; Sweeney *et al.* 2001), and at the cerebellum, where it is found in both migrating granular and Purkinje cells (Sasaki *et al.* 2000; Hayashi *et al.* 2001). Other areas where expression has been reported include the entorhinal cortex (Hayashi *et*

al. 2001), the hypothalamus (Niethammer *et al.* 2000), the medulla oblongata (Yamaguchi *et al.* 2004) and the olfactory bulb (Sasaki *et al.* 2000).

In comparison, little work has focused on the localisation of Nde1 within the rodent brain. It has been described as being predominantly located in the cerebral cortex of the embryonic mouse, with weak but specific expression in the ventricular zone, subventricular zone, intermediate zone and cortical plate (Feng *et al.* 2000).

It should be noted that in only one of the studies described above is it stated that the antibodies used were tested in order to ensure specificity for either Nde1 or Ndel1. It is therefore possible that some of these antibodies may in fact cross-react and detect both proteins.

1.3.4.2 Neurodevelopmental phenotypes of *Nde1* and *Ndel1* deficient mice

LIS1 is well known to be linked to brain abnormalities (see section 1.3.1) and is known to play roles in neurite outgrowth (Taya *et al.* 2007) and neuronal migration (Hirotsune *et al.* 1998; Cahana *et al.* 2001; Kholmanskikh *et al.* 2003; Shu *et al.* 2004; Toyo-Oka *et al.* 2005). Therefore, the localisation of its interactors NDE1 and NDEL1 to the brain implicates them also in neurodevelopment.

One dramatic piece of evidence linking NDE1 to neurodevelopment comes from *Nde1* knock-down mice. Mice that were homozygous negative for *Nde1* had a one third smaller total brain mass than their wild type littermates, despite no significant difference in total body mass (Feng and Walsh 2004). This loss of mass was uneven, affecting primarily the cerebral cortex (specifically layers II-IV), with little alteration of the hippocampus, midbrain or cerebellum. This effect was even more significant in mice that were also heterozygous for a *Lis1* knock-out mutation, which die shortly after birth and lack any visible layering in the neocortex (Pawlisz *et al.* 2008).

In contrast, in *Ndel1* knock-out mice, generated by a separate group, embryos die shortly after implantation, although heterozygous and conditional knock-out mutants did show some evidence of aberrant pyramidal neuron localisation (Sasaki *et al.*

2005). This effect was again exaggerated when the mice were crossed with mutants that were heterozygous negative for *Lis1* (Sasaki *et al.* 2005), although these mice did not show the 25% reduction in brain size seen when crossing heterozygous *Nde1* and *Lis1* mutants (Pawlisz *et al.* 2008).

1.3.4.3 The role of NDEL1 in neurite outgrowth and neuronal development

Ndel1 is present in the outgrowing neurites of mouse neurons (Niethammer *et al.* 2000; Sasaki *et al.* 2000). Interestingly, knocking down Ndel1 expression by use of RNAi has been shown to lead to loss of cell processes (Nguyen *et al.* 2004b), reduced axonal length (Taya *et al.* 2007) and dendrites which were both stunted and incorrectly positioned (Duan *et al.* 2007), implying a role for NDEL1 in neuronal differentiation. In contrast, when mouse NIH-3T3 cells were stimulated to differentiate, the amount of Nde1 in the cell processes actually decreased (Mili *et al.* 2008).

In culture, use of RNAi to knockdown Ndel1 levels in mouse NIH-3T3 cells led to cells with reduced motility (Shen *et al.* 2008b) and a similar result has been seen when RNAi was used in the mouse brain (Shu *et al.* 2004). These data fits well with reports that in *Nde1* and *Ndel1* knock-out mice localised sets of neurons show a reduced rate of migration (Feng and Walsh 2004; Sasaki *et al.* 2005; Toyo-Oka *et al.* 2005).

One possible explanation for this reduced rate of neuronal migration is that loss of NDE1 or NDEL1 may prevent the nucleus of the neuron from migrating properly towards the leading edge of the cell, thus inhibiting the cell migration process. Use of RNAi to knock-down NDEL1, LIS1 or dynein also causes such an effect (Shu *et al.* 2004). NDEL1 RNAi has been shown repeatably to enlarge the distance between the centrosome and nucleus within a cell (Shu *et al.* 2004; Toyo-Oka *et al.* 2005; Shen *et al.* 2008b), which may also indicate ineffective nucleokinesis.

1.3.5 NDE1, NDEL1 and psychiatric illness

1.3.5.1 The *NDE1* and *NDEL1* genes and major mental illness

Both the *NDE1* and *NDEL1* genes also show some evidence of their being risk factors for psychiatric illness in their own right. In 2004, a dense genome scan of Eastern Quebec families revealed chromosomal region 16p13, which includes *NDE1*, to show suggestive linkage to schizophrenia (Maziade *et al.* 2004). Meanwhile in studies of Finnish families, two regions of 16p12, D16S769 and D16S764, have been shown to be linked to bipolar disorder (maximum LOD score of 3.4) and schizophrenia (LOD score of 3.17) respectively (Ekholm *et al.* 2003; Hennah *et al.* 2007). On the basis of this evidence, Hennah *et al* went on to look at the association of a particular haplotype, containing four SNPs from *NDE1*, on schizophrenia. They found that in females carrying a known *DISC1* schizophrenia risk haplotype (Cannon *et al.* 2005), this *NDE1* haplotype was significantly associated with an increased risk of schizophrenia, p=0.011 (Hennah *et al.* 2007). This could potentially suggest that disregulation of NDE1 function could exacerbate the psychiatric phenotypes associated with the *DISC1* risk haplotype, resumably as a result of the proteins acting within the same pathway in the cell.

Another study, this time of Americans of European decent, found that a particular four SNP haplotype of *NDEL1* was significantly over-represented in schizophrenia patients compared to healthy controls, p=0.048 (Burdick *et al.* 2008). Each of the four SNPs individually was also associated with disease status. It was found that the effect of the *NDEL1* haplotype was only significant on the background of the Ser/Ser genotype of the *DISC1* schizophrenia risk variant S704C (see section 1.2.1.3) (Burdick *et al.* 2008). Interestingly however, on a Cys carrying background, a SNP in *NDE1* (rs3784859) also showed association with schizophrenia, p=0.049. This SNP, however, showed no significant association unless the population was conditioned for *DISC1* genotype (Burdick *et al.* 2008). Two other association studies have, however, failed to detect any significant association of *NDEL1* SNPs to schizophrenia, although neither of these studies conditioned their sample population on *DISC1* genotype (Ikeda *et al.* 2008; Kähler *et al.* 2008).

It has also been shown that specific *NDEL1* and *LIS1* mRNA species are significantly down-regulated in the brains of schizophrenia patients in America compared to healthy controls, with a more subtle change also visible in the prefrontal cortex (Lipska *et al.* 2006).

1.3.5.2 NDE1 and NDEL1 in other illnesses

In addition to their roles in psychiatric illness, NDE1 and NDEL1 have also been linked to other conditions. The expression of *NDE1* transcripts have been shown to be mis-regulated in seminoma, salivary adenoid cystic carcinoma, glial and glioneural tumours and clear cell renal carcinoma (Türeci *et al.* 2002; Kasamatsu *et al.* 2005; Suzuki *et al.* 2007; Brito *et al.* 2008), as well as in a mouse model of breast cancer (Namba *et al.* 2006). These findings are likely to be related to the role of NDE1 in the cell cycle (see section 1.3.3.3). *NDEL1* transcripts, meanwhile, were down-regulated in a mouse model of motor neuron disease (Nguyen *et al.* 2004b).

1.3.5.3 NDE1 and NDEL1 interactions with DISC1

During the initial DISC1 yeast-two-hybrid screenings, the most commonly reported interaction seen was that of DISC1 with NDEL1 (Millar *et al.* 2003; Morris *et al.* 2003; Ozeki *et al.* 2003; Brandon *et al.* 2004). This interaction has since been extensively investigated, having been shown to occur by co-immunoprecipitation in the mouse brain and also using *in vitro* transcribed and translated protein (Brandon *et al.* 2004). By comparison, the NDE1-DISC1 interaction had been demonstrated only in two yeast-two-hybrid screens (Millar *et al.* 2003; Brandon *et al.* 2004). During the preparation of this thesis, the interaction was also demonstrated using over-expressed protein in HEK293 cells (Burdick *et al.* 2008).

DISC1 binds to amino acids 266-267 of NDEL1 (Kamiya *et al.* 2006), although the location of the NDEL1-binding site of DISC1 has proven more controversial, with two alternative potential sites suggested (Morris *et al.* 2003; Ozeki *et al.* 2003). Several publications have investigated this by attempting to demonstrate complexing of NDEL1 with truncation mutants of DISC1 and the findings of these are

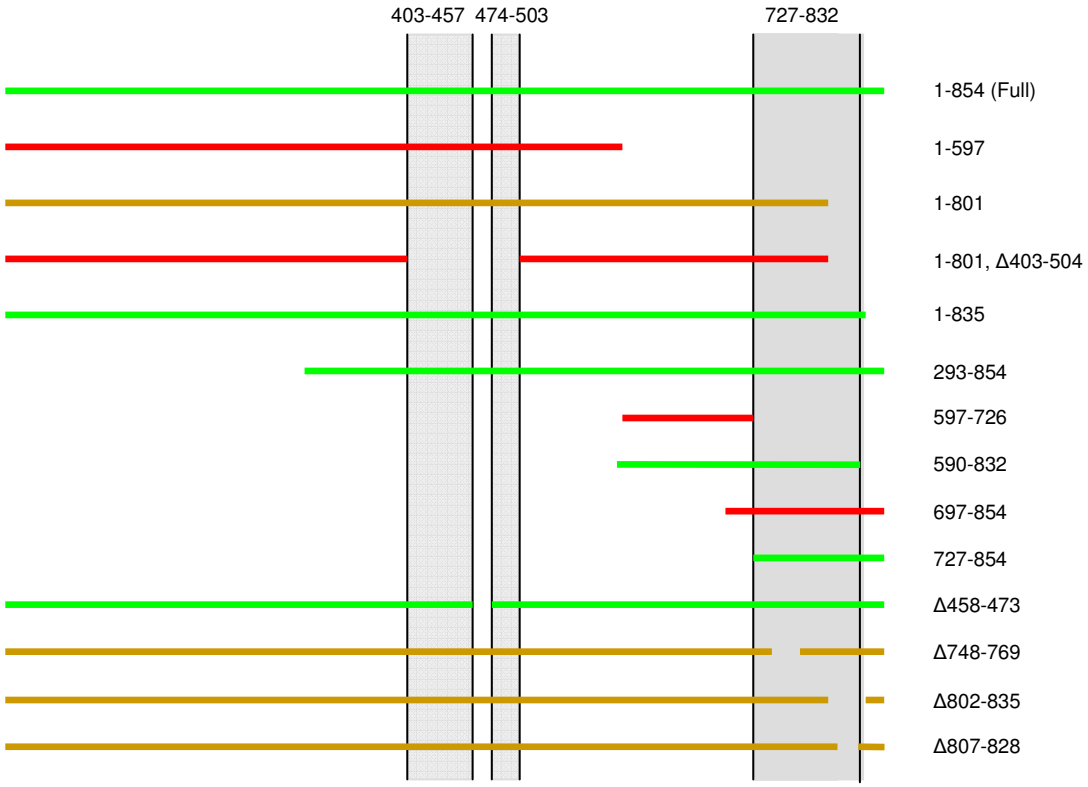

Figure 1.3.B: Determining the location of the NDEL1-binding domain on DISC1. Various studies have used co-immunoprecipitation and GST pull-downs to demonstrate the binding of NDEL1 to truncated versions of DISC1, in order to identify the minimum essential binding region. Data from yeast two-hybrid screening is excluded as potentially less reliable. This figure summarises the DISC1 truncations tested, indicating if DISC1 and NDEL1 could bind (green), could not bind (red) or if binding was greatly reduced relative to other NDEL1-DISC1 interactions tested at the same time (brown). The minimal essential binding region appears to be within amino acids 727-832, although some region of 403-457 and/or 474-503 also appears important. This region, which may contain the DISC1 self-association domain (Kamiya *et al.* 2005), may therefore also be required. Delta (Δ) indicates amino acids that were deleted from the DISC1 construct. It is uncertain why Morris *et al* failed to detect binding of NDEL1 to DISC1 amino acids 697-854, while they could detect binding with 293-854. It is possible that this is related to the lack of the 403-503 region, as they do not demonstrate NDEL1 binding to any construct which lacks this. (Morris *et al.* 2003; Brandon *et al.* 2004; Kamiya *et al.* 2006; Taya *et al.* 2007)

summarised in figure 1.3.B. Based on these, we can postulate that two separate regions are indeed required. The first of these is within amino acids 727-832 of DISC1, as constructs of amino acids 590-832 and 727-854 have both been seen to be sufficient for binding (Brandon *et al.* 2004; Taya *et al.* 2007). However, deletion of DISC1 amino acids 403-503, but not of 458-473, has been shown to disrupt interaction (Brandon *et al.* 2004; Kamiya *et al.* 2006). This second site is known to be the region of DISC1 required for self association (Kamiya *et al.* 2005). Given that NDEL1 has been shown to bind preferentially to DISC1 multimers (Leliveld *et al.* 2008), we can hypothesise that the actual binding site is within 727-832, but that it is also a requirement of binding that DISC1 be able to multimerise. With very short DISC1 segments multimerisation does not appear to be necessary for interaction with NDEL1.

NDEL1 appears to bind primarily to the full length DISC1 variant (Brandon *et al.* 2004). There is also some evidence to suggest that the interaction is weaker in the DISC1 Lv splice variant, which lacks amino acids 748-769 (Kamiya *et al.* 2006). The interaction of DISC1 with NDE1 or NDEL1 has also been reported to be weakened in the DISC1 S704C variant (Kamiya *et al.* 2006; Burdick *et al.* 2008), a mutation previously linked to schizophrenia and major depression (Callicott *et al.* 2005; Hashimoto *et al.* 2006). This data is, however, open to interpretation.

Looking at the various *Disc1* mutant mice described earlier, it is difficult to see how the Q31L and L100P mutants would directly affect interactions with Nde1 or Ndel1 (Clapcote *et al.* 2007). The mice expressing DISC1 amino acids 1-597, however, would lack the Nde1/Ndel1 binding site (Brandon *et al.* 2004) and so the mutant DISC1 species may be able to function as a dominant negative mutant, reducing the number of Disc1-Nde1/Ndel1 interactions within any given cell (Hikida *et al.* 2007; Pletnikov *et al.* 2008). Interestingly, in one of these mouse lines, mutant DISC1 expression was associated with reduced Lis1 expression (Pletnikov *et al.* 2008). The mouse line which inducibly expresses DISC1 amino acids 671-852, meanwhile, would be able to bind to Nde1 or Ndel1 (Li *et al.* 2007). However, this mutant would lack many of the other cellular functions of Disc1 and so its competition with

full length Disc1 for Nde1/Ndel1 binding would have an adverse effect on cellular pathways requiring such an interaction.

1.3.5.4 NDE1 and NDEL1 in the DISC1 pathway

Between them, NDE1 and NDEL1 share a number of protein-interaction partners with DISC1. These are known to include the dynein and dynactin complexes, LIS1, pericentrin B, 14-3-3ε and DBZ/Su48 (Feng *et al.* 2000; Kitagawa *et al.* 2000; Niethammer *et al.* 2000; Sasaki *et al.* 2000; Toyo-Oka *et al.* 2003; Guo *et al.* 2006; Hirohashi *et al.* 2006b). This presents the possibility that NDE1/NDEL1 may exist as part of a larger DISC1 protein complex and participate in different aspects of the DISC1 pathway.

The expression pattern of over-expressed NDEL1 alters when DISC1 is also over-expressed, implying that DISC1 may be able to recruit NDEL1 within the cell (Morris *et al.* 2003). Colocalisation of Disc1 and Ndel1 has been reported in differentiating mouse PC12 neurons, implying that the two may bind during neuronal differentiation (Kamiya *et al.* 2006). Colocalisation of the two proteins has also been reported at the distal ends of PC12 axons (Taya *et al.* 2007). Knockdown of Ndel1 in mice has been shown to lead to the mis-positioning of neurons in the adult dendrite hippocampus (Duan *et al.* 2007). A very similar effect was seen when Disc1 was instead knocked-down, and the effect of knocking down both was cumulative, implying that NDEL1 and DISC1 may co-operate also during neuronal migration (Duan *et al.* 2007).

1.3.6 Contrasting the NDE1 and NDEL1 proteins

NDE1 and NDEL1 share approximately 60% amino acid identity and 80% similarity with each other (see figure 1.3.A), implying that they are likely to have very similar functions within the cell. Notably, several key protein interaction partners of NDEL1, including LIS1, dynein and dynactin are also implicated in NDE1 interaction (Feng *et al.* 2000; Yan *et al.* 2003; Liang *et al.* 2004; Guo *et al.* 2006). However, in spite of these similarities, a number of differences between NDE1 and NDEL1 have been reported in the literature:

1. LIS1 has a higher binding affinity for NDEL1 than it does for NDE1 *in vitro* (Caspi *et al.* 2003).
2. In mice, expression of Nde1 varies with time in the early stages of blastocyst growth, while Ndel1 expression is more consistent (Cahana *et al.* 2003).
3. Homozygous Ndel1 knock-out mice die shortly after implantation (Sasaki *et al.* 2005), while Nde1 homozygous knock-out mice are viable (Feng and Walsh 2004).
4. After treatment with a chemotactic agent, Nde1 from NIH3T3 cells became enriched 4.6-fold in the cell body relative to the cell processes. No significant redistribution of Ndel1 was detected (Mili *et al.* 2008)
5. Use of RNAi to knock-down the levels of NDE1 in the cell blocked recruitment of dynein to the kinetochore during mitosis. Knock-down of NDEL1 in the same way did not have this effect (Vergnolle and Taylor 2007).

It therefore appears that, while NDE1 and NDEL1 are likely to play over-lapping roles in the cell, they nonetheless need to be treated as individual proteins. It therefore cannot be assumed that the wealth of published data surrounding NDEL1 is directly applicable to the lesser studied NDE1 protein.

1.4 Aims of this PhD

Given the intriguing biological and genetic information implicating both NDE1 and NDEL1 in neurodevelopment and potentially psychiatric illness, it seems likely that interactions between these proteins and DISC1 would be critical in major mental illness. This thesis will therefore tackle three main issues:

Firstly, published data relating to the basic biology of NDE1 is limited in comparison to that of NDEL1. Specifically, due to the lack of published antibodies known to specifically detect native NDE1 protein without also cross-reacting with NDEL1, almost nothing is known about the nature and localisation of endogenous NDE1 within the cell. The biology of NDE1 will therefore be studied by investigating the existence of alternatively spliced NDE1 transcripts (chapter 3), bioinformatics analysis of the NDE1 amino acid sequence (chapter 4) and through the generation and use of endogenous anti-NDE1 antibodies (chapter 5).

Secondly, the relationship between NDE1 and NDEL1 in the cell is unclear. Both proteins share considerable amino acid similarity, but it does not clearly follow that they therefore perform the same functions within the cell or that they are regulated in the same way. In order to gain understanding in this area, detailed analyses of the two proteins using bioinformatics will be performed and the results compared (chapter 4). Additionally, known protein interactions of NDEL1, such as that with LIS1 or self-association, will be replicated using NDE1 (chapter 6). Given that NDEL1 self-associates, it will also be investigated whether NDE1 and NDEL1 are capable of complexing together, potentially as a heterodimer (chapter 6).

Thirdly, DISC1 is known to interact with a number of proteins, besides NDE1 and NDEL1, which have been independently implicated in the pathogenesis of psychiatric illness. In the current literature the most prominent of these is PDE4B. Given that it is unlikely that DISC1 would be involved in multiple cellular pathways which independently are involved in major mental illness, the relationships between NDE1, NDEL1, DISC1 and PDE4B will be investigated (chapters 6 and 7).

Chapter 2 - Materials and Methods

2.1 Bioinformatics

2.1.1 Identification of *NDE1* and *NDEL1* splice variants

NDE1 and *NDEL1* splice variants were identified using the UCSC genome browser (http://genome.ucsc.edu/cgi-bin/hgGateway). Variants were carried forward for further analysis if at least three such transcripts were listed on the genome browser, or if they corresponded to a published isoform. The nucleic acid sequence of all coding exons was then entered into the ExPASy translate tool in order to determine an amino acid sequence for the corresponding protein (Gasteiger *et al.* 2005).

2.1.2 Molecular weight and isoelectric point prediction

In order to determine the molecular weight and isoelectric point of a protein, its amino acid sequence was analysed using the ExPASy ProtParam online tool (Gasteiger *et al.* 2005).

2.1.3 Structural prediction

Amino acid sequences of proteins were entered into the online structural prediction programs COILS and PSIPRED (Lupas *et al.* 1991; McGuffin *et al.* 2000) and the results compared. When using COILS, a significance threshold of 0.5 using a seven-amino acid window was used to differentiate coiled from uncoiled residues. When using PSIPRED, predicted helices shorter than 7 amino acids in length (equivalent to one complete turn of an α-helix) were assumed to be false positives.

2.1.4 Disorder prediction

Amino acid sequences of proteins were submitted into nine online protein disorder prediction programs. Each amino acid was then either designated as ordered or disordered based on a simple consensus of the results (i.e. if five or more programs predicted that a given amino acid was disordered then it was considered to be disordered). The programs used were as follows:

1. DisEMBL 1.5 (Linding *et al.* 2003): Facility uses three separate definitions of disorder, Loops/Coil, Hot-Loops and Remark-465. For the purposes of this analysis, all three were considered to be separate programs.
2. DISOPRED2 (Ward *et al.* 2004)
3. DISPROT VSL2 (Obradovic *et al.* 2005; Peng *et al.* 2006)
4. DRIP-PRED (MacCallum)
5. FoldIndex (Prilusky *et al.* 2005)
6. IUPred (Dosztányi *et al.* 2005a, b)
7. PreLink (Coeytaux and Poupon 2005)

2.1.5 Kozak sequence prediction

The programs NetStart 1.0 (Pedersen and Nielsen 1997) and weakAUG (Tikole and Sankararamakrishnan 2008) were used to predict potential Kozak sequences (Kozak 1987) from mRNA transcripts.

2.1.6 Nuclear localisation signal prediction

Two separate techniques were used in order to identify potential nuclear localisation signals (NLS) from amino acids sequences:

1. Complete amino acid sequences of proteins were entered into the online prediction programs PredictNLS and PSORT II (Nakai and Horton 1999; Cokol *et al.* 2000), both of which identify common NLS motifs.
2. Amino acid sequences were manually examined for clusters of basic residues. If a group of basic residues was similar to a known NLS motif then a generalised version of the amino acid sequence was used to search the NLS database (Nair *et al.* 2002) in order to see if it was enriched in nuclear proteins. The "generalised" motif was determined by allowing all residues except for lysines and arginines to vary. For example, a generalised version of the sequence KRCANTADENDTKFMRR, in which the five basic residues are underlined, would be $KRX_{10}KX_2RR$.

2.1.7 Prediction of functional sites

Amino acid sequences of proteins were entered into Scansite 2.0 (Obenauer *et al.* 2003) in order to predict potential phosphorylation and other functional sites. Only sites detected using a "Medium" stringency search were considered. Sites that could also be detected using a "High" stringency search were recorded as such. NetPhosK 1.0 (Blom *et al.* 2004) was also used to investigate more weakly predicted phosphorylation sites.

2.1.8 Web pages of online programs

BLAST http://blast.ncbi.nlm.nih.gov/Blast.cgi

COILS: http://www.ch.embnet.org/software/COILS_form.html

CLUSTALW: http://align.genome.jp/

DisEMBL 1.5: http://dis.embl.de/

DISOPRED 2: http://bioinf.cs.ucl.ac.uk/disopred/disopred.html

DISPROT VSL2: http://www.ist.temple.edu/disprot/predictorVSL2.php

DRIP-PRED: http://www.sbc.su.se/~maccallr/disorder/

ExPASy - ProtParam: http://www.expasy.org/tools/protparam.html

ExPASy - Translate Tool: http://www.expasy.org/tools/dna.html

FASTA Comparison: http://fasta.bioch.virginia.edu/fasta_www2/fasta_list2.shtml

Fold Index: http://bip.weizmann.ac.il/fldbin/findex/

IUPred: http://iupred.enzim.hu/

NetPhosK 1.0: http://www.cbs.dtu.dk/services/NetPhosK/

NetStart 1.0: http://www.cbs.dtu.dk/services/NetStart/

NLS database http://cubic.bioc.columbia.edu/cgi/var/nair/resonline.pl

Operon - Oligo Analysis and Plotting: https://www.operon.com/oligos/toolkit.php

Predict NLS http://cubic.bioc.columbia.edu/cgi/var/nair/resonline.pl

PreLink: http://genomics.eu.org/prelink/

PSIPRED: http://bioinf.cs.ucl.ac.uk/psipred/psiform.html.

PSORT II: http://psort.nibb.ac.jp/form2.html

ScanSite 2.0: http://scansite.mit.edu/motifscan_seq.phtml

WeakAUG: http://bioinfo.iitk.ac.in/AUGPred/

2.2 Materials

2.2.1 Reagents

The following a list of chemical reagents used in this thesis, along with their source and, where appropriate, the buffer in which they were suspended or diluted.

- Acetic acid (Fischer)
- 30% Acrylamide/Bis solution (BioRad)
- Agar (BD Bioscience)
- Agarose (Invitrogen), made up in TAE buffer for most experiments, or in MES SDS running buffer (Invitrogen) for 2-dimensional Western blotting
- Ammonium persulphate (Sigma), made up in dH_2O
- Ampicillin (Sigma), made up in dH_2O
- ATP solution, PCR grade (Sigma)
- Bromophenol blue (Sigma)
- BSA (Sigma), made up in PBS or TBS
- CHAPS (Sigma)
- CTP solution, PCR grade (Sigma)
- DABCO (Sigma)
- DAPI (Sigma), made up in mowiol mounting solution
- DEPC (Sigma)
- DMSO (Sigma)
- D-PBS (Invitrogen)
- DTT (Sigma), made up in dH_2O
- EDTA (Sigma), made up in dH_2O
- Ethanol (Fischer), diluted with dH_2O where appropriate
- Ficoll 40 (Sigma)
- Forskolin (Sigma), made up in DMSO
- Glycerol (Promega)
- Glycine (Sigma)
- Glycogen (Sigma)

- Goat serum (Abcam or Sigma), diluted with PBS
- GTP solution, PCR grade (Sigma)
- H89 (Merck), made up in dH_2O
- Hydrochloric acid (Fischer)
- IBMX (Sigma), made up in absolute ethanol
- IPTG (Melford) in dH_2O
- Iodoacetamide (Sigma), made up in LDS sample buffer (Invitrogen)
- Instant milk powder (Marvel), made up in PBS or TBS wash buffer
- Low melting point agarose (Agarose), made up in TAE buffer
- Magnesium acetate (Fischer), made up in dH_2O
- Magnesium chloride solution, PCR grade (Invitrogen)
- Methanol (Fischer)
- Mowiol (Sigma)
- NP-40 (Sigma)
- Orange G (Sigma)
- PBS (Sigma), made up in dH_2O often as a 10x solution
- Paraformaldehyde (Sigma), made up in PBS
- Phenol/chloroform/isoamyl alcohol (Invitrogen)
- Phosphatase inhibitor cocktail II (Calbiochem)
- Ponceau S (Sigma)
- Protease inhibitor cocktail (Roche), made up in dH_2O
- Rabbit serum (Sigma), diluted with PBS
- SDS (Fischer) made up in dH_2O
- Sodium acetate (BDH Laboratory Supplies), made up in dH_2O and pH adjusted using hydrochloric acid and/or sodium hydroxide
- Sodium chloride (Fischer), made up in dH_2O
- Sodium deoxycholate (Fischer), made up in dH_2O
- Sodium fluoride (Fischer), made up in dH_2O
- Sodium hydroxide (Fischer), made up in dH_2O
- TEMED (Sigma)
- 10x TGS (BioRad), diluted with dH_2O

- Tris (Fischer), made up in dH_2O and pH adjusted using hydrochloric acid and/or sodium hydroxide
- Tris-HCl (Fischer), made up in dH_2O and pH adjusted using hydrochloric acid and/or sodium hydroxide
- Triton X-100 (Sigma), made up in dH_2O
- Tryptone (BD Biosciences)
- TTP solution, PCR grade (Sigma)
- TWEEN-20 (Sigma)
- Urea (Gibco)
- Yeast extract (BD Biosciences)

2.2.2 Solutions and buffers

Below are listed the recipes of all solutions used for the methods described in this chapter.

Coomassie staining solution

200 ml	Methanol
3.5 ml	Acetic acid
Trace	Bromophenol blue
Up to 500 ml	dH_2O

Solution stored at room temperature and was recovered after each stain for re-use.

Coomassie de-staining solution

100 ml	Acetic acid
300 ml	Methanol
600 ml	dH_2O

Solution stored at room temperature

DEPC-treated water

DEPC was added to dH_2O to a final concentration of 0.1% in order to inactivate any RNase in the water. Solution was then left at room temperature overnight and then autoclaved to denature the DEPC. It was stored at room temperature.

dNTP

An equal mix of PCR-grade ATP, CTP, GTP and TTP diluted appropriately in dH_2O. Stored at -20°C.

L Agar/ampicillin

50 g	Tryptone
25 g	Yeast Extract
50 g	Sodium chloride
Up to 5 litres with dH_2O	

Adjust pH to 7.2. Pour into a bottle and add 1.5g Agar per 100ml medium. Stored at 4°C. Before use, melt in a microwave and then stand at room temperature until cool enough to touch with gloved hands and add ampicillin to a final concentration of 50 ng/ml. Used immediately.

L Broth/ampicillin

50 g	Tryptone
25 g	Yeast Extract
25 g	Sodium chloride
Up to 5 litres with dH_2O	

Adjust pH to 7.2. Solution stored at 4°C. Before use add ampicillin to a final concentration of 50 ng/ml.

Membrane blocking buffers

The basic blocking buffer is as follows, and is used both for pre-stain blocking and while applying the primary antibody:

2.5 g	Instant milk powder
5 ml	10x PBS
100 µl	TWEEN-20
Up to 50 ml	dH_2O

Solution was made up immediately prior to use.

When using the PKA substrate antibody (see table 2.4) the following was instead used for pre-stain blocking:

2.5 g	Instant milk powder (Marvel)
5 ml	10x TBS
50 µl	TWEEN-20
Up to 50 ml	dH_2O

Solution was made up immediately prior to use.

When using the PKA substrate antibody, the following was used while applying the primary antibody:

2.5 g	BSA
5 ml	10x TBS
50 µl	TWEEN-20
Up to 50 ml	dH_2O

Solution was stored at 4°C.

Membrane wash buffers

The basic washing buffer was as follows:

100 ml	10x PBS
20 ml	TWEEN-20
Up to 1 litre with dH_2O	

Where TBS-based blocking buffers were used, the following wash buffer was instead used:

100ml	10x TBS
10 ml	TWEEN-20
Up to 1 litre with dH_2O	

Wash buffers were stored at room temperature.

Mowiol mounting solution

7.5 g	Mowiol
10 ml	Glycerol
25 ml	dH_2O

Solution was then incubated overnight at room temperature

50 ml	0.2 M Tris-HCl (pH 8.5)

Solution was then heated at 100°C for 20 minutes and allowed to cool

1.75 g	DABCO

Solution was stored at -20°C, with working aliquots stored at 4°C.

PBS-TX lysis buffer

The following buffer was used to produce lysates for which it was important to maintain the phosphorylation state of the cellular proteins:

5 ml	10x PBS
5 ml	10% Triton X-100
1 ml	0.55 mM sodium fluoride
5 ml	Glycerol
Up to 50ml	dH_2O
0.5 ml	Phosphatase inhibitor cocktail II
1 tablet	Protease inhibitor cocktail

Buffer was stored at 4°C before the addition of the inhibitor cocktails and at -20°C after they had been added.

2x PKA reaction buffer

3 ml	dH_2O
1 ml	0.4M Tris-HCl pH 7.4
1 ml	0.2M Magnesium acetate
20 µl	100mM ATP (PCR quality)

Solution was stored at -20°C.

Ponceau S stain

1 g	Ponceau S
4 ml	Acetic acid
Up to 200 ml	dH_2O

Solution was stored at room temperature and was recovered after each stain for re-use.

Protein sample buffer

6.25 ml	1M Tris pH 6.8
10 ml	Glycerol
10 ml	20% SDS
13.75 ml	dH_2O
1ml	0.1% Bromophenol blue

Solution was stored at room temperate

Recombinant protein storage buffer

40 ml	1M Tris pH 7.5
26.6 ml	3M Sodium chloride
Up to 800 ml	dH_2O

Solution was stored at room temperature.

RIPA buffer

2.5 ml	1M Tris-HCl pH 7.5
2.5 ml	3M Sodium chloride
0.5 ml	NP-40
2.5 ml	10% Sodium deoxycholate
250 µl	20% SDS
Up to 50ml	dH_2O
1 tablet	Protease inhibitor cocktail

Buffer was stored at 4°C before the addition of the inhibitor cocktails and at -20°C after they had been added.

Semi-dry transfer buffer

5.8 g	Tris
2.9g	Glycine
2 ml	20% SDS
200ml	Methanol
Up to 1 litre with dH_2O	

Before use, pH was confirmed to be between 8 and 10. Solution stored at 4°C.

Stop solution

3 g	Ficoll 400
50 µl	20% SDS
800 µl	0.5 M EDTA
25 µg	Orange G
Up to 1 litre with dH_2O	

Solution was stored at room temperature.

TAE buffer

24.2 g	Tris
5.71 ml	Acetic acid
10 ml	0.5 M EDTA
Make up to 5 litres with dH_2O	

Buffer was stored at 4°C

TE buffer

10 ml	1M Tris-HCl pH 7.5
2 ml	500mM EDTA
Make up to 1 litre with dH_2O	

The pH of the buffer was adjusted using hydrochloric acid and/or sodium hydroxide. Buffer was stored at room temperature.

Tris Buffered Saline (TBS)

1x	10x	
8 g	40 g	Sodium chloride
20 ml	100 ml	1M Tris pH 7.5
Up to 1 litre	Up to 500ml	dH_2O

Solution was stored at room temperature.

2xYT medium

16 g	Tryptone
10 g	Yeast extract
5 g	Sodium chloride
Up to 1 litre with dH_2O	

The pH of the buffer was adjusted using hydrochloric acid and/or sodium hydroxide to 7.0. Medium was stored at 4°C.

2-D blot lysis buffer

6 g	Urea
0.25 g	CHAPS
500 µl	Protease inhibitor (one tablet in 2 ml)

Buffer was stored at -20°C.

2-D blot re-hydration buffer

6 g	Urea
0.25 g	CHAPS
62.5 µl	Ampholite solution* (Invitrogen)
1ml	0.1% Bromophenol blue
Up to 12.5ml	dH_2O

*Ampholite solution was chosen to be appropriate for the pI range of the gel system.

Buffer was stored at -20°C.

Cell line	Description	Source	Original paper	Serum
COS7	Monkey, kidney, fibroblast	ECACC	(Gluzman 1981)	D-MEM/10% foetal calf serum
HEK293T	Human, embryonic kidney	Mark Bradley[1]	(Cannon and Strittmatter 1993)	D-MEM/5% foetal calf serum
NIH3T3	Mouse, embryonic	Ian Simpson[2]	(Jainchill *et al.* 1969)	D-MEM/10% newborn calf serum
SH-SY5Y	Human, brain, neuroblastoma	Organon and ECACC	(Biedler *et al.* 1978)	D-MEM/10% foetal calf serum

Table 2.3.A: Media in which each cell line was grown. All chemicals were from Invitrogen. ECACC is the European Collection of Cell Cultures. [1]Bradley Research Group and the [2]Genes and Development Group respectively, University of Edinburgh.

2.3 Cell culture

2.3.1 Cell line maintenance

Cell lines were grown at 37°C, 5% CO_2 in a Galaxy S incubator (Scientific Laboratory Supplies) using the media shown in table 2.3.A and in CellStar T25 or T75 flasks (Greiner Bio-One). Once every 4-7 days the cells were split. To do this, media was removed and cells washed briefly in a 1:1 mix of trypsin and versine (Invitrogen). Cells were then incubated at 37°C for 2-10 minutes in trypsin/versine before having 4 volumes of medium (table 2.3.A) added. This cell suspension was then split 1:5 or more to start new cell cultures. All cell culture manipulations were performed in an Envair Bio2+ Class II Safety Cabinet under containment level 1 conditions.

When protein lysates were to be prepared from a cell line, the cells were split (typically 1:10) into 10cm tissue culture plates (Iwoki) with 10ml of appropriate media. These would then be grown for 1-3 days until the cells were 75-90% confluent. When cells were to be used for immunocytochemistry, 12 well Costar plates (Corning) were set up, each containing a single 16mm sterile glass coverslip (VWR). To each well, 1ml of media and 30-200µl cells were added. These would then be grown overnight.

2.3.2 Transfection of plasmids into eukaryotic cells

In order to exogenously express protein in cultured cells, cells of around 75-90% confluence were washed twice in 37°C OptiMEM (Invitrogen) and then transfected with one or more plasmid constructs using Lipofectamine 2000 (Invitrogen), according to manufacturer's instructions. For a 12-well dish of cells, 0.5-1µg of DNA per well was used, for 10cm plates of cells 10-20µg of DNA was used. Cells were incubated in the transfection media for 6 hours at 37°C and then washed with their normal growth media (table 2.3.A). Cells were then allowed to grow for a further 18-24 hours before proceeding. Details of plasmids used in this thesis are described in table 2.3.B.

2.3.3 Drug treatment

The drugs IBMX and forskolin can be used in combination to raise the level of cAMP within a cell, while H89 is a potent inhibitor of protein kinase A. In order to treat cells with these drugs, the cells were grown in 10cm plates until they were 75-90% confluent and then washed once with media lacking serum. Cells would then be incubated for 30 minutes at 37°C with 5% CO_2 in 10ml of D-MEM containing either 5µM H89 or 250µM IBMX and 100µM forskolin. When all three drugs were to be used, a 30 minute H89 pre-incubation would be performed, followed by a 30 minute IBMX/forskolin incubation. In order to perform control reactions, cells would be treated with equivalent amounts of absolute ethanol or DMSO instead of IBMX and forskolin.

2.4 Protein-related methods

2.4.1 Antibodies

Various antibodies were used in this project. Details of these, and the conditions in which they were used, can be found in table 2.4.

Plasmid	Protein	Tag	Source
pGEX-6P1	Empty vector	(GST)	GE Healthcare
pcDNA3.1-FLAG-DISC1	DISC1	N-terminal FLAG	Nick Brandon[1] (Brandon *et al.* 2004)
pDEST-40-DISC1	DISC1	C-terminal V5	Kirsty Millar & Sheila Christie (Millar *et al.* 2005a)
pDEST-40-NDE1	NDE1-SSSC	C-terminal V5	Kirsty Millar & Sheila Christie (Bradshaw *et al.* 2009)
pDEST-40-NDEL1	NDEL1-PLSV	C-terminal V5	Kirsty Millar & Sheila Christie (Bradshaw *et al.* 2009)
pDEST-53-ATF4	ATF4	N-terminal GFP	Kirsty Millar & Sheila Christie (Bradshaw *et al.* 2008)
pDEST-53-NDE1	NDE1-SSSC	N-terminal GFP	Kirsty Millar & Sheila Christie (Bradshaw *et al.* 2009)
pDEST-53-NDEL1	NDEL1-PLSV	N-terminal GFP	Kirsty Millar & Sheila Christie (Bradshaw *et al.* 2009)
pSV-SPORT-PDE4A10	PDE4A10	None	Miles Houslay[2] (Rena *et al.* 2001)
pEE7-PDE4B1	PDE4B1	None	Miles Houslay[2] (Huston *et al.* 1997)
pEE7-PDE4C2	PDE4C2	None	Miles Houslay[2] (Owens *et al.* 1997)
pcDNA3-PDE4D5	PDE4D5	None	Miles Houslay[2] (Bolger *et al.* 1997)

Table 2.3.B: Pre-existing plasmid constructs used in this thesis. [1]Neuroscience Research Centre, Merck, Sharpe and Dohme (now at Wyeth). [2]Molecular Pharmacology group, University of Glasgow.

Name in text	Specificity	Species	Source	Conditions (WB)	Conditions (ICC)	Amount (IP)	Notes
10233-1-AP	NDE1/NDEL1	Rabbit	Protein Tech Group	x2000 - 2 hours (G)	-	-	
231	NDEL1	Rabbit	Nick Brandon[1]	x5000 - 1 hour	x1000 - 1 hour	-	
92	NDE1	Rabbit	Custom	x500 - 2 hours (G)	x50 - 1 hour	-	See section 5.4
93	NDE1	Rabbit	Custom	x500 - 2 hours	x500 - 1 hour	10µl	See section 5.4
93-488	NDE1	Rabbit	Custom	N/A	x100 - 1½ hours	N/A	Fluorescent (488nm), see sections 5.4 and 6.3.3
94	NDE1 (Mouse)	Rabbit	Custom	x 50 - 2 hours	x100 - 1 hour	-	See section 5.4
95	NDE1 (Mouse)	Rabbit	Custom	x200 - 2 hours	x300 - 1 hour	-	See section 5.4
α-DISC1	DISC1 (C-term)	Rabbit	Tetsu Akiyama[2]	x10,000 - 18 hours	-	-	(Ogawa *et al.* 2005)
Ab57430	NDE1/NDEL1	Mouse	Abcam	x1000 - 2 hours (G)	-	-	
CENPA	CENPA	Mouse	Abcam	-	x500 - 1 hour	-	
GFP	GFP tag	Mouse	Roche	x500 - 2 hours	N/A	-	
GST	GST tag	Goat	GE Healthcare	x2000 - 2 hours (G)	-	-	
γ-tubulin	γ-tubulin	Mouse	Sigma	-	x3000 - 1 hour	-	
FLAG	FLAG tag	Mouse	Sigma	x1000 - 2 hours	x1000 - 1 hour	1µl	
LIS1	LIS1	Mouse	Sigma	x1000 - 2 hours	x100 - 1 hour	-	
H00054820-M01	NDE1/NDEL1	Mouse	Abnova	x10,000 - 2 hours (G)	-	-	
PDE4A (MH)	pan-PDE4A	Sheep	Miles Houslay[3]	x10,000 - 1 hour	-	-	(MacKenzie and Houslay 2000)
PDE4B (MH)	pan-PDE4B	Sheep	Miles Houslay[3]	x10,000 - 1 hour	-	-	(MacKenzie and Houslay 2000)
PDE4C (MH)	pan-PDE4C	Sheep	Miles Houslay[3]	x10,000 - 1 hour	-	-	(McCahill et al. 2005)
PDE4D (MH)	pan-PDE4D	Sheep	Miles Houslay[3]	x10,000 - 1 hour	-	-	(Sette and Conti 1996)
PKA substrate	RRXp(S/T) phospho-peptide	Rabbit	Cell Signalling Technology	x1000 - 18 hours	-	-	Western blots performed using TBS-based buffers.
V5	V5 tag	Mouse	Invitrogen	x1000 - 2 hours	x2000 - 1 hour	3µg	
V5 (MBL)	V5 tag	Rabbit	MBL	-	x2000 - 1 hour	-	The Invitrogen anti-V5 antibody was used unless otherwise stated.

Y12	Smith antigen	Mouse	Gene Tex	-	x500 - 1 hour	-	
Donkey-anti-sheep	Sheep Ig	Donkey	Dako	x10,000 - 20 mins	N/A	N/A	Secondary
Rabbit-anti-goat	Goat Ig	Rabbit	Dako	x5000 - 20 mins	N/A	N/A	Secondary
Rabbit-anti-mouse	Mouse Ig	Rabbit	Dako	x80,000 - 30 mins	N/A	N/A	Secondary
Swine-anti-rabbit	Rabbit Ig	Swine	Dako	x3000 - 20 mins	N/A	N/A	Secondary
Goat-anti-mouse (green)	Mouse Ig	Goat	Invitrogen	N/A	x500 - 1 hour	N/A	Secondary, fluorescent (488nm)
Goat-anti-mouse (red)	Mouse Ig	Goat	Invitrogen	N/A	x800 - 1 hour	N/A	Secondary, fluorescent (594nm)
Goat-anti-rabbit (green)	Rabbit Ig	Goat	Invitrogen	N/A	x500 - 1 hour	N/A	Secondary, fluorescent (488nm)
Goat-anti-rabbit (red)	Rabbit Ig	Goat	Invitrogen	N/A	x800 - 1 hour	N/A	Secondary, fluorescent (594nm)

Table 2.4: A list of all antibodies used in this thesis and the conditions under which they were used for Western blotting (WB) and immunocytochemistry (ICC). "Species" refers to the species in which the antibody was originally raised. A letter G indicates that this is the conditions at which recombinant GST-tagged protein was stained – this requires a far more dilute antibody than would be used for studying endogenous protein. The amount of antibody that is used to immunoprecipitate (IP) protein from a 500µl lysate is also shown. All antibodies detect human antigens unless otherwise stated. All antibody dilutions are for typical experiments and may vary depending on the exact nature of the experiment. [1]Neuroscience Research Centre, Merck, Sharp and Dohme (now at Wyeth). [2]Laboratory of Molecular and Genetic Information, University of Tokyo. [3]Molecular Pharmacology group, University of Glasgow.

It is not possible to use two primary antibodies which were raised in the same species for immunocytochemistry, as an anti-immunoglobulin secondary antibody would bind to both. As a solution to this problem, some antibodies were conjugated directly to green (488nm) fluorescent tags using an Alexa Fluor 488 Monoclonal Antibody Labelling Kit (Invitrogen), according to manufacturer's instructions.

2.4.2 Cell lysates

2.4.2.1 Production of cell lysates

In order to produce cell lysates, cells were grown on 10cm dishes until they were 75-90% confluent. The media was aspirated off and the cells were washed once with 10ml of 4°C D-PBS. Between 300 and 1200µl of a lysis buffer (either RIPA of PBS-TX) was then added and the plate swirled for ~10 seconds. A disposable cell scraper was then used to dislodge all of the remaining adherent cells from the plate into the buffer. This crude lysate was then transferred to a micro-centrifuge tube. The lysates were then mixed at 15-30 rpm for 30 minutes at 4°C on a rotary wheel. After this, the lysates were centrifuged at 13,000 rpm for 30 minutes on a desk-top centrifuge (a Biofuge Fresco, Heraeus Instruments), and the residual pellet discarded. Lysates were typically stored at either -20°C or -70C.

2.4.2.2 Measuring the protein concentration in cell lysates

The concentration of total protein in lysates was measured using a variation on the BioRad protein assay. Six standard reactions of 25µl were prepared containing from 0 to 1.0 mg/ml of protein standard (in 0.2 mg/ml increments). Meanwhile, 2.5µl of each lysate was made up to 25µl with dH_2O. To each of these reactions, both standards and lysates, 125µl of Reagent A and 1ml of Reagent B were added. Reactions were left to stand for 25 minutes at room temperature before their absorbance readings at 750nm (OD750 readings) were measured using an Ultrospec 3000 optical reader (Pharmacia Biotech). The OD750 value for each protein standard was plotted against the corresponding protein concentration in Microsoft Excel, and a standard curve was generated. This curve was then used to determine the concentrations of the protein lysates.

2.4.3 In vitro transcription and translation of protein

The T_NT coupled reticulocyte lysate system (Promega) was used to produce protein from plasmid constructs in a cell-free system. Reactions were set up as follows. All chemicals and solutions were from the T_NT kit, with the exception of the plasmids.

38 µl	dH_2O
4 µl	T_NT buffer
1 µl	Amino acid mix, minus leucine
1 µl	Amino acid mix, minus methionine
4 µl	500 ng/µl plasmid
50 µl	T_NT rabbit reticulocyte lysate
2 µl	T7 polymerase

Reactions were incubated for 90 minutes at 30°C, before being placed on ice. Typically, Reactions were either used immediately for immunoprecipitation. or stored at -20°C or -70°C. These reactions are generally of low yield, but allow for the co-immunoprecipitation of proteins in an environment lacking other confounding cellular factors.

2.4.4 Immunoprecipitation

In order to immunoprecipitate specific proteins, cell lysates or *in vitro* transcribed and translated proteins (both referred to simply as lysates from here on) were first produced as described above. An antibody was added to the lysate (see table 2.4 for concentrations) which was then mixed at 15-30rpm on a rotary wheel at 4°C for 3-18 hours. The antibody should bind to the protein of interest during this time. As a negative control, rabbit or mouse IgG (Dako) was used in place of the antibody. Following the antibody incubation, 30µl of protein G sepharose beads (Sigma) in PBS were added and the samples mixed for a further hour. Thus the antibody-antigen complex should be captured by interaction with protein G. Typically, a 30µl sample of each lysate was removed and stored for use as a loading control.

Once the bead incubation was complete, immunocomplexes were pelleted by spinning at 13,000rpm for 2 minutes on a desk-top centrifuge. The supernatant was then carefully removed using a manual pipette with a glass tip. This tip will have been sharpened by heating and stretching. The beads were then re-suspended in 500ml of PBS-TX lysate buffer and mixed for a further 15 minutes on the rotary wheel at 4°C. This washing procedure was repeated three further times. After the final wash, beads were resuspended in protein sample buffer and prepared for Western blotting (see below).

2.4.5 Western blotting

2.4.5.1 Sample preparation

Cell lysates (see section 2.4.2), *in vitro* transcribed and translated protein (see section 2.4.3) or bacterially purified protein (see section 2.5.7.4) were prepared for Western blotting by mixing 1:1 with protein sample buffer (see section 2.2.2) and 1:10 with 1M DTT. In order to denature the proteins and disrupt protein-protein interactions, samples were then heated at 100°C for 5 minutes.

2.4.5.2 BioRad system

Separating gels were produced using one of the following recipes depending on the molecular weight of the protein under investigation. 7% gels were used to separate proteins of 60kDa or higher (such as DISC1) and 10% gels to separate proteins of 25-60kDa (such as NDE1 and NDEL1).

7%	10%	
1.9ml	2.6ml	30% acrylamide/bis solution
2ml	2ml	1.5M Tris pH 8.8
4.04ml	3.34 ml	dH_2O
40µl	40µl	20% SDS
5µl	5µl	TEMED
20µl	20µl	25% ammonium persulphate

The gel solution was mixed and then poured between two BioRad glass plates, calibrated to produce a 1.0mm gel, leaving 1-2 cm at the top. This gap initially filled with dH_2O. After an hour, when the gel has set, the water was removed from the top and replaced with 4% a stacking gel solution:

870 µl	30% acrylamide/bis solution
1.5 ml	0.5M Tris pH 6.8
3.57 ml	dH_2O
30 µl	20% SDS
3 µl	TEMED
30 µl	25% ammonium persulphate

A comb of either 10 or 15 wells (BioRad) was added to the top and gel left to set for 30 minutes.

Once set, gel(s) were then inserted into a Mini TransBlot Cell (BioRad) which was filled with 400ml 1x TGS. Samples were loaded into the gel along with a standardised protein size maker (BioRad's Precision Plus Protein All Blue Standard). Gels were then run at 150V for between 60 and 100 minutes using a Power Pac 3000 (BioRad) in order to separate the proteins in the sample by molecular weight. Gel(s) were then carefully removed and soaked in semi-dry transfer buffer at room temperature for 30 minutes. Meanwhile, a 6cm by 8cm slice of Hybond-P PVDF membrane (Amersham) was cut out, soaked briefly in methanol and then soaked in semi-dry transfer buffer for 15 minutes. Eight 6cm by 8cm pieces of 1.7mm card (Whatman) were also cut out and soaked briefly in the transfer buffer.

Four pieces of card were then placed onto a Trans-Blot Semi-Dry Transfer Cell (BioRad). On top of them were placed the membrane, the gel (face up) and finally the remaining four pieces of card. This was then run at 20V for 90 minutes in order to transfer the protein, including marker, from the gel to the surface of the membrane.

The membrane was then removed and washed twice briefly with dH_2O. Membrane was then soaked for ~5 minutes with Ponceau S stain in order to confirm the presence of the protein and to facilitate labelling of the membrane. Stain was washed off with dH_2O and the membrane was then blocked with a membrane blocking buffer, either for one hour at room temperature or over-night at 4°C.

2.4.5.3 Invitrogen system

For some experiments, an alternative system was used to run and blot gels. In this case, one or two pre-cast Tris-Acetate 7% gels were inserted into an XCell Surelock Electrophoresis Cell and then loaded with the samples and marker (as above). 400ml of 1x NuPage Tris-Acetate SDS Running Buffer was added to each of the gels and electrophoresis was performed at 150V on a Power Pac 3000 (BioRad) for 60-90 minutes in order to separate proteins in the sample by molecular weight.

After this, 500ml 1x NuPage Transfer Buffer containing 20% methanol (or 40% if two gels were to be transferred at once) was prepared. An Invitrolon PVDF membrane was soaked briefly in methanol and then, along with five sponge pads, was soaked in the transfer buffer for ~5 minutes. Each gel was then extracted from the cell and loaded (face down) into an XCell II Blot Module with the membrane and two sponges below it and the remaining three sponges above it. When two membranes were loaded, one sponge was placed between them and two on either side. The module was then filled with the transfer buffer and placed back in the electrophoresis cell. Exterior of the cell was cooled with water. 30V was then applied from the power pack for 90 minutes in order to transfer proteins from the gel to the membrane. After this, the membranes were washed and blocked as above. All apparatus and buffers used in this section were from Invitrogen.

2.4.5.4 Immunostaining

After blocking, membranes were transferred to an appropriately sized shallow dish or box and incubated with a primary antibody in blocking buffer for between one and 18 hours. Antibody dilutions and conditions are shown in table 2.4. Incubations of two hours or less were carried out at room temperature, longer incubations were

carried out at 4°C. The membrane was then washed five times with wash buffer: once briefly, once for 15 minutes and then three further washes for 5 minutes. The membrane was then incubated with secondary antibody diluted in wash buffer for 20-30 minutes at room temperature. The membrane was then washed five times as before. During all incubations and washes, the membrane was rocked gently at 15-40rpm.

The membrane was then removed from the medium, air-dried on cling film and incubated with ECL Plus solution (Amersham) for five minutes. After removal of the ECL Plus, pieces of photosensitive film (Scientific Laboratory Supplies) were exposed to the membrane for between one second and 16 hours. Films were developed on an Amersham Hyperprocessor, in order to visualise the antibody-labelled proteins on the membrane

2.4.5.5 Densitometry

In order to quantitatively analyse Western blot results, images were transferred to a computer by scanning and the signal intensity of the bands was measured using the program ImageJ (downloaded from http://rsbweb.nih.gov/ij/). These results were then be compared and analysed statistically.

2.4.5.6 Re-probing of membranes

In order to re-probe a membrane with an additional antibody, then the membranes were first cleaned as follows. The membrane was incubated for 30 minutes at room temperature in Restore western blot stripping buffer (Perbio Science) with gentle shaking. The membrane was then washed three times with wash buffer for five minutes each. The membrane was then blocked and stained with the new antibody, as in section 2.4.5.4.

2.4.5.7 Pre-absorption of antibodies

In order to test if an antibody binds to the amino acid sequence against which it was raised, pre-absorption analysis can be used. In order to do this, blocking buffer was prepared, containing the antibody at an appropriate concentration for Western

blotting (see table 2.4) and 100ng/µl of the peptide to which the antibody had originally been raised against. A positive control was also prepared that was identical to the pre-absorption solution, but lacking the antigenic peptide. Solutions were incubated for 18 hours at 4°C, while mixing at 20-30rpm on a rotary wheel. Meanwhile a Western blot was performed with two lanes, each containing an identical amount of the same lysate or recombinant protein. Each of these lanes was then immunostained using either the pre-absorption or positive control antibody solution. If the antibody is working as anticipated, the pre-absorbed antibody should detect significantly less signal on the Western blot than the positive control does.

2.4.5.8 Two-dimensional Western Blotting

A conventional Western blot is unable to differentiate between two protein isoforms of similar molecular weights that are both detectable by the same antibody. In order to get round this problem, two-dimensional (2-D) Western blots can be performed in which the protein species of a lysate are separated both vertically by molecular weight and also horizontally by isoelectric point (pI).

Lysates were prepared as in section 2.4.2.1, but using the 2-D Western blot lysis buffer. The protein concentrations of the lysates were then measured (see section 2.4.2.2). 200-400µg of the sample and 15µl of 1M DTT were then diluted in rehydration buffer to a total volume of 155µl. This solution was then applied to a ZOOM strip which was left to rehydrate in the solution over-night at room temperature in a ZOOM IPGRunner cassette.

An electrode wick was then added over each end of the strip and 650µl of deionised water was added (dH_2O containing 1/60 tap water). The cassette was then loaded into a ZOOM IPGRunner, the external section of which was filled with 600ml deionised water. A current of 500V, 1W and 3mA was then run applied through the strip for four hours using a Power Ease 500 power pack (East Mains Pilot Plant) in order to sort the proteins on the strip by pI. After this the cassette was broken open and the strips removed.

The membrane strips were then each incubated in 4.5ml 1x LDS sample buffer with 500µl sample reducing agent for 15 minutes at room temperature. Strips were then transferred to 5ml 1xLDS containing 116mg iodoacetamide and incubated for a further 15 minutes. The strips were then each inserted into a ZOOM 4-12% Bis-Tris gel. A 50°C 0.5% agarose solution in MES SDS running buffer was the applied and left to cool into a gel around each strip. The gels were then inserted into an XCell Surelock electrophoresis cell and were loaded with a protein marker (BioRad). The cell was filled with MES SDS running buffer. The gel was then subjected to electrophoresis at 200V for 50 minutes on a Power Pac 3000 (BioRad) in order to separate proteins by molecular weight. Following this, the protein was transferred to a membrane which was immunostained as described in section 2.4.5.4. All reagents and apparatus used in this section were from Invitrogen unless otherwise stated.

2.4.5.9 Direct staining of protein on gels

Following electrophoresis, the protein content of a gel could be stained directly by washing in coomassie staining solution at room temperature for 20 minutes with gentle rocking (typically 15rpm). Staining solution was then removed and the gel was washed several times in coomassie de-staining solution in order to remove all of the non-specific blue staining. These washes were typically carried out over a period of 1-2 hours at room temperature to ensure efficient destaining. Gels were then dried on a Drygel Sr gel dryer (Hoefer Scientific).

2.4.6 Immunocytochemistry

A well-established technique for visualising the expression patterns of proteins within individual cells is immunocytochemistry. The procedure involves growing a mono-layer of cells on a glass cover-slip, typically until they are 70-90% confluent, fixing the cells and then applying primary antibodies specific to the protein(s) of interest. Secondary antibodies conjugated to coloured fluorescent molecules can then be applied, allowing the expression patterns of the protein(s) to be viewed using a microscope equipped with appropriate absorption and excitation filters.

2.4.6.1 Cell fixation

Before antibodies can be applied to cells for viewing by immunocytochemistry, the cells must be fixed in order to terminate cellular processes and to expose epitopes for antibody binding. Two separate techniques were used for fixing cells in this thesis.

For the first technique, coverslips were washed once with 37°C D-PBS and then fixed, after removal of media, by the application of -20°C methanol for 10 minutes (500µl methanol per well). Coverslips were then washed three times with room temperature PBS/0.02%BSA before being processed for immunocytochemistry.

In the alternative protocol, coverslips were washed with 37°C D-PBS and then 500µl of room temperature 4% paraformaldehyde (PFA) was added for ten minutes. Coverslips were then washed three times with room temperature PBS/0.02%BSA before being incubated for a further 15 minutes in a solution containing 0.5% Triton. Coverslips were then washed three times as before being processed for immunocytochemistry.

2.4.6.2 Immunostaining

The entire procedure was performed at room temperature. After fixation, coverslips were blocked in 200µl PBS/10% serum each for 20-30 minutes. Serum was selected to match that in which the secondary antibodies were raised (typically goat). Coverslips were then incubated in 100µl of appropriately diluted primary antibodies in PBS/0.02%BSA for 1-2 hours. See table 2.4 for details of antibodies and concentrations. Up to two primary antibodies were incubated with each coverslip at a time. Coverslips were then washed once and then three additional times for 5 minutes with PBS/0.02%BSA. Coverslips were then incubated for one hour with 100µl of appropriately diluted fluorescent secondary antibodies (see table 2.4) in PBS/10% serum. The dishes containing the coverslips were wrapped in foil throughout the secondary incubation in order to keep out light. Coverslips were then washed and given three further 5 minute washes with PBS/0.02%BSA. The coverslips were mounted onto glass slides using mowiol mounting solution containing 250 ng/µl DAPI. Coverslips were then stored in the dark at 4°C. In the

majority of cases, after immunocytochemistry, cells were viewed on a Zeiss Axioskop 2 microscope using Smart Capture 2 software.

One exception to this procedure is when using cells transfected with constructs encoding GFP-tagged proteins. In this case, the GFP group emits green fluorescence on its own and so no antibodies are necessary in order to detect this signal.

For some experiments primary antibodies with conjugated fluorescent tags were used (see section 2.4.1). In this case, the cells were processed exactly as above using any non-fluorescent primary antibodies. After secondary antibody application and washing, cover slips were then blocked for a further 20 minutes with PBS/10% serum. Serum matched that of the animal in which the fluorescent antibody was raised (typically rabbit). Coverslips were then incubated in 100µl of appropriately diluted conjugated antibodies in PBS/10% serum for 90 minutes. Coverslips were then washed and applied to slides as described above.

2.4.6.3 Confocal Microscopy

Some light microscopy results were confirmed by confocal microscopy. This technique involved taking a number of photographs of a cell, each focused on a different vertical "slice" of the cell. By doing this, it can be assumed that any colocalisation of fluorescent antibody signals seen at a specific two-dimensional point is representative of colocalisation in the three-dimensional cell. Typically, the relative intensities of the fluorescent antibodies would be measured along a one-dimensional line within the image, in order to confirm localisation. Confocal microscopy was performed using a Zeiss LSM510 Confocal Microscope and associated software.

2.4.7 *In vitro* phosphorylation by PKA

GST or GST-fusion protein solutions were produced as described in section 2.5.7.4. Reactions were set up as follows:

19.25 µl	dH_2O
25 µl	2x PKA reaction buffer
2 µl	GST or GST-tagged recombinant protein
3.75 µl	Recombinant PKA solution

The PKA solution was made up by diluting recombinant PKA (Promega) 60-fold in 1x PKA reaction buffer. Reactions were then incubated at 30°C for 5 minutes and then placed immediately on ice. To each reaction, 50µl of protein sample buffer (section 2.2.2) and 5µl of 1M DTT was then immediately added and the reactions boiled at 100°C for 5 minutes to denature the PKA and the GST or GST-fusion protein. These reactions were then analysed by Western blotting (section 2.4.5), using the PKA substrate and anti-GST antibodies.

2.5 Molecular biology methods

2.5.1 Primers

A complete list of all oligonucleotude primers used in this thesis can be seen in table 2.5.A. Primers were supplied by Sigma or Invitrogen. Primer design was assisted by use of Operon's Oligo Analysis and Plotting tools and the predicted specificity of primers was investigated using BLAST (Altschul *et al.* 1990).

2.5.2 PCR reactions

It is often necessary to amplify a specific segment of DNA, either because it is needed in the generation of a plasmid construct or in order to determine the extent to which it is present in a cDNA pool. In order to do this, different versions of the polymerase chain reaction (PCR) were used.

Name	Direction	Sequence	Purpose
NDE1 (pan) F	5'	GAAGGATGAAGCCAGAGATTTGCGGC	Detection of all known NDE1 transcripts
NDE1-SSSC R	3'	CAACTCGTGTCCAACCCCTTATCACC	Detection of NDE1-SSSC transcripts
NDE1-KMLL R	3'	GTGTGAAGGCGGCTTCCCAAATTCC	Detection of NDE1-KMLL transcripts
NDE1-KRHS R	3'	CCGCCAGCGAGAGGTTTATTAGAAGG	Detection of NDE1-KRHS transcripts
NDE1-S2 R	3'	GAAGGCACCAAACGCCAGGAAAGTG	Detection of NDE1-S2 transcripts
NDEL1 F	5'	GGAGCGAGCCAAAAGGGCAACAATAG	Detection of all known NDEL1 transcripts
NDEL1-PLSV R	3'	CTGACGATGGACGCGAGGAGC	Detection of NDEL1-PLSV transcripts
NDEL1-FMGQ R	3'	CTGCCCCATGAACAACGTGGGAAATATG	Detection of NDEL1-FMGQ transcripts
NDE1-FL F	5'	GGAGCTGGAAACCATCAAGGAGAAGTTTG	Detection of NDE1 FL transcripts only
NDE1-S1 F	3'	GCTGGAAACCATCAAGCGCCACG	Detection of NDE1-S1 transcripts only
NDE1-BamHI F	5'	GATCGGATCCGAGGACTCCGGAAAGACTTTC	Cloning of NDE1 with a 5' BamHI for insertion into pGEX-6PI
NDE1-SalI R	3'	GATCGTCGACTCAGCAGGAGCTGGACGAC	Cloning of NDE1 with a 3' SalI for insertion into pGEX-6PI
NDEL1-BamHI F	5'	GATCGGATCCGATGGTGAAGATATACCAG	Cloning of NDEL1 with a 5' BamHI for insertion into pGEX-6PI
NDEL1-SalI R	3'	GATCGTCGACTTATCACACACTGAGAGGCAG	Cloning of NDEL1 with a 3' SalI for insertion into pGEX-6PI
NDE1-Seq A	5'	CGAGGAGGAAGAAGCTAACTATTGG	Sequencing of NDE1 from constructs
NDE1-Seq B	5'	GATGACCTCGCGCAGACCAAAG	Sequencing of NDE1 from constructs
NDE1-Seq C	5'	CTTCAGACGTGGCCTGGACG	Sequencing of NDE1 from constructs
NDE1-Seq D	3'	CTTTGGTCTGCGCGAGGTCATC	Sequencing of NDE1 from constructs
NDE1-Seq E	3'	CGTCCAGGCCACGTCTGAAG	Sequencing of NDE1 from constructs
NDE1-Seq F	3'	CTGGACGACCTGGTTGTTGATTTGG	Sequencing of NDE1 from constructs
NDEL1-Seq A	5'	GGAGGAAACTGCTTATTGGAAGG	Sequencing of NDEL1 from constructs
NDEL1-Seq B	5'	GTCAGACTCGGGCCATTAAGGAG	Sequencing of NDEL1 from constructs
NDEL1-Seq C	5'	GTTGGCAAAGGAACGGAGAACAC	Sequencing of NDEL1 from constructs
NDEL1-Seq D	3'	CTCCTTAATGGCCCGAGTCTGAC	Sequencing of NDEL1 from constructs
NDEL1-Seq E	3'	GTGTTCTCCGTTCCTTTGCCAAC	Sequencing of NDEL1 from constructs
NDEL1-Seq F	3'	CATACCCGGCGCTGACGATG	Sequencing of NDEL1 from constructs
6PI-Seq F	5'	GCTGGCAAGCCACGTTTGGTG	Sequencing of pGEX-6PI vectors
6PI-Seq R	3'	GTGTCAGAGGTTTTCACCGTCATCAC	Sequencing of pGEX-6PI vectors
pD40-Seq F	5'	GAGACCCAAGCTGGCTAGTTAAGC	Sequencing of pDEST-40 vectors
pD40-Seq R	3'	GCGTAGAATCGAGACCGAGG	Sequencing of pDEST-40 vectors

T131A F	5’	GGAAAGAGCCAAGCGGGCTGCGATCATGTCTCTCGAAG	Introduction of a T131A mutation into NDE1 constructs and removal of a BssHII site
T131A R	3’	CTTCGAGAGACATGATCGCAGCCCGCTTGGCTCTTTCC	Introduction of a T131A mutation into NDE1 constructs and removal of a BssHII site
T131E F	5’	GGAAAGAGCCAAGCGGGCTGAGATCATGTCTCTCGAAG	Introduction of a T131E mutation into NDE1 constructs and removal of a BssHII site
T131E R	3’	CTTCGAGAGACATGATCTCAGCCCGCTTGGCTCTTTCC	Introduction of a T131E mutation into NDE1 constructs and removal of a BssHII site
S306A F	5’	GAGAGACGGCCAAGCGCCACCAGCGTGCCTTTG	Introduction of an S306A mutation into NDE1 constructs and removal of an AleI site
S306A R	3’	CAAAGGCACGCTGGTGGCGCTTGGCCGTCTCTC	Introduction of an S306A mutation into NDE1 constructs and removal of an AleI site

Table 2.5.A: Details of all primers used in this thesis.

2.5.2.1 Standard PCR reaction

The following PCR reaction was used for the majority of applications. Each PCR reaction was set up using the following:

2 µl	10x PCR reaction buffer (Sigma)
1.2 µl	25 mM magnesium chloride
1.4 µl	10 mM dNTP
1.3 µl	60 ng/µl 5' primer
1.3 µl	60 ng/µl 3' primer
~1 µl	Template (variable depending on the nature and concentration of the template cDNA or plasmid)
10.3 µl	dH_2O
1.5 µl	Taq polymerase (Sigma)

Reactions were then processed on a PTC-225 Peltier Thermal Cycler (MJ Research), using the following program:

1. 93°C 1 minute
2. 93°C 40 seconds
3. 64°C 30 seconds
4. 72°C 30-60 seconds*
5. Repeat steps 2-4 an additional 34 times
6. 72°C 10 minutes
7. 4°C For ever

* The length of the extension step (step 4) varied depending on the expected length of the PCR product. 30 seconds was used for products of 500 base pairs or less, 60 second for products of approximately 1000 base pairs.

2.5.2.2 Touch down PCR

In order to improve the efficiency of amplification of some "problem" PCRs, reactions were set up as above, but the following program was used instead:

1. 93°C 1 minute
2. 93°C 40 seconds
3. 69°C 30 seconds
4. 72°C 30-60 seconds
5. Repeat steps 2-4 an additional 4 times, reducing the temperature of step 3 by 2°C each time.
6. 93°C 40 seconds
7. 59°C 30 seconds
8. 72°C 30-60 seconds
9. Repeat steps 6-8 an additional 29 times
10. 72°C 10 minutes
11. 4°C For ever

2.5.2.3 BigDye pre-sequencing PCR

For the sequencing of existing PCR products, the BigDye Terminator Ready Reaction Mix v3.1 system was used. Each reaction was set up as follows.

1.5 µl	5x Sequencing buffer (Applied Biosystems)
1 µl	2.5x Ready Reaction mix (Applied Biosystems)
1µl	Template (typically a PCR product)
0.5 µl	60 ng/µl primer
6 µl	dH_2O

Reactions were then processed using the following program:

1. 96°C 1 minute
2. 96°C 10 seconds
3. 50°C 5 seconds
4. 60°C 4 minutes
5. Repeat steps 2-4 an additional 24 times
6. 4°C For ever

2.5.2.4 PfU Ultra fusion PCR

In order to amplify open reading frames while simultaneously incorporating a restriction site, PCR reactions were set up as follows:

5 µl	10x PfU Ultra Fusion buffer (Stratagene)
1.25 µl	10 mM dNTP
1.3 µl	300 ng/µl 5' primer
1.3 µl	300 ng/µl 3' primer
1-3 µl	DNA template (plasmid or PCR product)
Up to 49µl	dH_2O
1 µl	PfU Ultra Fusion enzyme (Stratagene)

Reactions were then processed using the following program:

1.	95°C	1 minute
2.	95°C	40 seconds
3.	60°C	30 seconds
4.	72°C	15 seconds
5.	Repeat steps 2-4 an additional 34 times	
6.	72°C	10 minutes
7.	4°C	For ever

2.5.2.5 Site-Directed Mutagenesis PCR

In order to introduce one or more nucleotide substitutions into an existing plasmid construct, PCR reactions were set up using the Quikchange II Site-Directed Mutagenesis kit (Stratagene) as follows:

5 µl	10x Reaction buffer (Stratagene)
1 µl	10-50 ng/µl template plasmid
1µl	125 ng/µl 5' primer
1 µl	125 ng/µl 3' primer
1 µl	dNTP mix (Stratagene)
Up to 49 µl	dH_2O
1 µl	*Pfu* Ultra high fidelity DNA polymerase (Stratagene)

Reactions were then processed using the following program:

1.	95°C	30 seconds
2.	95°C	30 seconds
3.	63°C	1 minute
4.	68°C	10 minutes
5.	Repeat steps 2-4 an additional 15 times	
6.	68°C	10 minutes
7.	4°C	For ever

2.5.3 Sequencing PCR products and plasmids

In order to sequence a plasmid construct or PCR product, the DNA region of interest was first amplified by one or more PCR reactions (sections 2.5.2.1 or 2.5.2.2). Having obtained a pool of the DNA to be sequenced, one or more pre-sequencing PCR reactions were then performed on it using the Big Dye 3.1 system (section 2.5.2.3). Each such PCR reaction would make use of a different single primer (which could be either 5' or 3') in order to amplify different regions of the DNA and hopefully allow the entire section to be included in one or more of the reaction products.

The products of these PCR reactions were then processed as follows. Each product was added to a 0.5ml tube containing 2.5µl of sterilised 125mM EDTA and 30µl absolute ethanol. Tubes were briefly shaken (by hand) to mix them and were then incubated at room temperature for 10-15 minutes. Tubes were spun at 13,000rpm on

a desktop centrifuge for 20 minutes at 4°C and the supernatant was carefully removed with a hand held pipette. The tubes were then spun for an additional two minutes and any remaining supernatant removed. The pellets were then gently resuspended in 30µl of 70% ethanol. These tubes were then centrifuged once for 5 minutes at 13,000rpm and again for two minutes, removing the supernatant carefully after each spin. The tubes were then left to air dry in the dark for 8-10 minutes at room temperature before being stored at -20°C.

The nucleic acid sequence of these DNA samples was then determined by either Agnes Gallacher or Alison Condie (Medical Research Council Human Genetics Unit or Wellcome Trust Clinical Research Facility, University of Edinburgh). Results were viewed using the program Chromas Lite version 2.01 (Technelysium Pty Ltd). The online program ExPASy Translate Tool was used to convert nucleic acid sequences into amino acid sequences (Gasteiger *et al.* 2005), while BLAST, FASTA Sequence Comparison and CLUSTALW were used to compare results to known DNA or protein sequences (Pearson and Lipman 1988; Altschul *et al.* 1990; Thompson *et al.* 1994).

2.5.4 Purification of PCR products

In some circumstances (such as prior to a ligation or recombination reaction), PCR products need to be purified in order to remove other elements of the PCR reaction mix. This was done using a QIAquick PCR Purification kit according to the manufacturers' instructions.

2.5.5 DNA gels

2.5.5.1 Making and running agarose gels

Agarose gels were prepared by adding agarose powder to TAE buffer to a final concentration of 1-2%. This suspension was then heated in a microwave until all the powder had dissolved. Once the solution had cooled down enough to touch, SYBR Safe DNA Gel stain (Invitrogen) was added to a final dilution of 1/5000, and the solution was gently mixed. The solution was then poured into a tray (Bioscience

Service); a comb was added and the gel was allowed to set. The gel was then placed in a tank (Bioscience Service) which was filled with TAE buffer. The comb was removed and the DNA samples, along with a 1kb ladder, were loaded into the wells. Depending on the size of the DNA product to be viewed, gel was run for between 10 minutes and 3 hours at 50-100V. Gels were then viewed under ultra-violet light using a Uvidoc light box (Uvitec) and photographed.

If the gel had been run for longer then 90 minutes and the DNA signal had faded, then the intensity of the DNA signal was restored by washing the gel for 30-120 minutes at room temperature in TAE buffer containing SYBR Safe DNA Gel Stain (Invitrogen) at a dilution of 1/5000.

2.5.5.2 Isolation of DNA fragments from agarose gels

Agarose gels can also be used in order to separate DNA of a certain size from a sample. In order to do this, the sample was run on a gel made using low-melting point agarose, but otherwise as described above. After the gel has been run, the DNA was visualised on a Safe Imager box (Invitrogen), and the band of interest excised using a sterile scalpel. This gel fragment was then transferred to a 1.5ml tube and processed using a QIAquick Gel Extraction kit (QIAGEN), in order to isolate the DNA contained within it. Procedure performed according to manufacturers' instructions (spin protocol).

2.5.6 cDNA production

The First Strand cDNA Synthesis kit (Roche) was used to produce cDNA from RNA as follows. Numbers in brackets refer to the component numbers of the kit. The following reaction was set up:

2 µl	10x Reaction buffer (1)
4 µl	25mM Magnesium chloride (2)
2 µl	Deoxynucleotide mix (3)
1 µl	Oligo-p$(dT)_{15}$ primers (5)
1 µl	Random primers p$(dN)_6$ (6)
1 µl	RNase inhibitor (7)
0.8 µl	AMV reverse transcriptase (8)
1-5 µl	RNA
Up to 20µl	DEPC-treated water

All solutions were from the kit except for the DEPC treated water and RNA. Total RNA from human brain was obtained from Ambion. Reactions were subjected to four incubations as follows and then transferred to -20°C for storage:

1.	Room temperature	10 minutes
2.	42 °C	60 minutes
3.	95 °C	5 minutes
4.	4 °C	5 minutes

Negative controls were processed in exactly the same way, but without the use of the AMV reverse transcriptase.

2.5.7 Culture of bacteria transformed with plasmid constructs

2.5.7.1 Transformation of bacteria with plasmid constructs

1µl of a plasmid construct was transformed into chemically competent JM109 cells (Promega) as follows: Cells were thawed on ice, the plasmid DNA was added to them and the whole mixture was incubated on ice for 30 minutes. Cells were then heat-shocked by incubation at 42°C for 45 seconds, before chilling once again on ice for a further 2 minutes. 900µl of room temperature L Broth/ampicillin media was then added to the cells. This suspension was then immediately incubated at 37°C with 200rpm shaking for 45-120 minutes in an Innova 4300 incubator shaker (New

Brunswick Scientific). After the incubation, 50-150µl of the bacterial culture was placed in the centre of an L Agar/ampicillin plate and spread across the plate using a sterile scraper. Plates were sealed and incubated until colonies were visible (typically 16-22 hours) at 37°C with 5% CO_2 in a Plus II incubator (Gallencamp).

For constructs that had just been subjected to site-directed mutagenesis, XL1-Blue super-competent cells (Stratagene) were instead used, with 2xYT medium being used for the initial growth step.

2.5.7.2 Amplification of plasmid constructs

Cultures of bacteria, transformed as described above, can be set up by selecting a single colony from an L Agar/ampicillin plate and then allowed to grow in L Broth/ampicillin media at 37°C with 200rpm shaking. Small cultures of 1-5 ml media were centrifuged at 13,000rpm for 1 minute in a desktop centrifuge in order to pellet the bacteria. The supernatant was then discarded and the plasmids harvested from the bacterial pellet using a Spin Miniprep Kit (QIAGEN) according to the manufacturer's instructions. Alternatively, 200ml cultures were centrifuged using an Avanti J-20I centrifuge (Beckman Coulter) at 5000rpm, 4°C for 10 minutes. The supernatants were discarded and the bacterial pellet processed using a Plasmid Maxiprep kit (QIAGEN), according to the manufacturer's instructions. After purification, plasmid DNA was suspended in dH_2O (or in some cases pH 7.5 TE buffer) and stored at either 4°C or at -20°C.

2.5.7.3 Measuring plasmid DNA concentration

In order to determine the concentration of a plasmid construct or other DNA solution, an Ultrospec 3000 optical reader (Pharmacia Biotech) was used. The device was set to measure absorbance readings of 260nm (OD260 readings), and calibrated so that dH_2O, or the buffer in which the DNA was dissolved, gave an absorbance reading of zero. The DNA solution was then diluted (typically 50-fold) and an OD260 reading taken. DNA concentration was then calculated using the following equation:

DNA concentration (µg/µl) = OD260 reading x Dilution factor x 0.05

2.5.7.4 Production of bacterially expressed protein

JM109 cells (Promega) were transformed with constructs encoding either GST or GST-tagged proteins and grown overnight on L Agar plates containing ampicillin (see section 2.5.7.1). A 5ml L Broth/ampicillin culture was then set up using one of the colonies and incubated over-night at 37°C. Half of each culture was then diluted to 50 ml with fresh L Broth/ampicillin and incubation was continued for three hours. 50µl of 100mM IPTG was then added in order to induce production of the recombinant protein and cultures were incubated for a further two hours. The culture was then spun on a table-top centrifuge at 13,000rpm for 30 minutes at 4°C in order to pellet the bacterial cells and the supernatant was discarded.

The bacterial pellet was then resuspended in 2.5ml of PBS. 600µl aliquots of the solution were taken, 12µl of lysosyme (Sigma) were added to each and these were then incubated at room temperature for 5 minutes. After this time, 6µl of DNase (Roche) was added to each. Bacteria were then lysed by a freeze-thaw procedure 15 times by snap freezing on dry ice followed by incubation at 37°C. Following this, solutions were spun at 13,000rpm for 10 minutes on a desktop centrifuge and the pellets discarded. The recombinant GST or GST-tagged protein was then purified from the supernatants using GST SpinTrap Purification Modules (GE Healthcare) according to the manufacturers instructions. Finally, the solutions were dialysed in order to transfer the proteins to a suitable recombinant protein storage buffer, using Slide-A-Lyzer Dialysis Cassettes (Pierce) according to manufacturer's instructions.

2.5.8 Cloning techniques

2.5.8.1 Site-directed mutagenesis

Single amino acid point substitutions were introduced to existing plasmid constructs by using the QuikChange II Site-Directed Mutagenesis kit (Stratagene). Primer pairs were designed across the relevant region of the open reading frame so as to introduce one or more nucleotide substitutions. These in would then alter a single amino acid

Enzyme	Target site	Buffer	Source
AleI	C A C N N$^{>}_{<}$N N G T G	4	New England Biolabs
BamHI	G$^{>}$G A T C$_{<}$C	H	Roche
BssHII	G$^{>}$C G C G$_{<}$C	H	Roche
SalI	G$^{>}$T C G A$_{<}$C	H	Roche

Table 2.5.B: Restriction enzymes used in this thesis and the buffers in which they were used.

---

of the derived protein. PCR reactions were performed (section 2.5.2.5) and the PCR product was digested using 1µl DpnI (Stratagene) at 37°C for 90 minutes in order to destroy the template DNA. The PCR products were then transformed into XL1-Blue cells and plated (section 2.5.7.1). Cultures were then grown from individual colonies and the plasmids harvested by Miniprep (section 2.5.7.2). In some cases, primers used for mutagenesis also added or removed a unique restriction site from the protein, allowing the presence of the desired mutation to be tested for by restriction digest (section 2.5.8.2). Mutations were confirmed by sequencing (section 2.5.3).

2.5.8.2 Restriction digests

In order to digest DNA at selective sites, specific restriction enzymes were used. The DNA to be digested was made up in a buffer appropriate for the enzyme and the enzyme was added. The reaction was then incubated at 37°C for 1-18 hours. A list of enzymes used, along with their corresponding buffers, is shown in table 2.5.B. In order to terminate the reaction, EDTA was sometimes added to a final concentration of 10mM. These products could then be run on an agarose gel and the pattern of the digested bands visualised (see section 2.5.5.1).

2.5.8.3 Phenol-Chloroform extraction

In order to precipitate plasmid DNA from solution following a restriction digest (see above) and prior to cloning, proteins were first removed by phenol-chloroform extraction. 100µl of phenol/chloroform/isoamyl alcohol mix was added to the digest. The digest was then briefly vortexed and spun at 13,000 rpm for two minutes on a desk-top centrifuge. 40µl of the aqueous phase was then removed off and stored.

40µl of TE buffer was added to the remaining mixture. This was then vortexed, centrifuged and a further 80µl removed and pooled with the original 40µl fraction.

1.2µl of 3M pH5.2 sodium acetate, 240µl absolute ethanol and 2µl glycogen was then added and the solution frozen at -20°C for at least 15 minutes. Following this, the solution was thawed and spun at 13,000rpm for 30 minutes on a table-top centrifuge. The supernatant was discarded and the DNA pellet resuspended in 70% ethanol. This was then spun at 13,000rpm for a further 5 minutes and the supernatant once again discarded. Finally, the pellet was air dried for 15 minutes and then resuspended in 30µl dH_20.

2.5.8.4 SAP treatment

Following phenol-chloroform extraction and DNA precipitation (see above), DNA was treated with shrimp alkaline phosphatase (SAP) in order to remove any phosphate groups. 10µl of the DNA was made up to 20µl with SAP buffer (USB) and 1.5µl of the SAP enzyme added (USB). The reaction was incubated at 37°C for 30 minutes and terminated by heating at 70°C for a further 10 minutes, denaturing the enzyme.

2.5.8.5 Ligation reaction

In order to ligate DNA inserts containing restriction sites into plasmids, both the insert and plasmid were first restriction digested, phenol-chloroform extracted and SAP treated as described above. A 10µl ligation reaction was then set up containing 1µl T4 ligase (Roche), vector and insert in T4 ligase buffer (Roche). Approximately 2µl of the vector was used, along with insert in a 1:3 molar ratio with it. Reactions were incubated at room temperature for four fours and then transformed into JM109 cells (section 2.5.7.1).

Chapter 3 - Alternate splicing of *NDE1* and *NDEL1*

3.1 Identification of potential *NDE1* and *NDEL1* splice variants

3.1.1 Alternatively spliced *NDE1* and *NDEL1* transcripts

The UCSC genome browser (http://genome.ucsc.edu/) lists a number of alternatively spliced transcripts of both the *NDE1* and *NDEL1* genes. To date, however, only one isoform of each protein has been investigated in the literature for any given species. Three transcripts encoding NDE1 full length isoforms were selected from the genome browser, all of which shared the same N-terminal seven exons but had unique 3' regions (see figure 3.1.A). In addition there is a short *NDE1* transcript which shares exons 4, 5 and 6 of the full length isoforms (see figure 3.1.A). Two *NDEL1* transcripts, encoding proteins which again differed from each other only at the 3' end, were also identified (see figure 3.1.A). These transcripts were selected because they feature three or more times on the genome browser, or because they appear in published literature. The full length species will be referred to by the C-terminal four amino acids they are predicted to encode, while the short NDE1 species will be referred to as NDE1-S2. Figures 3.1.B.a and 3.1.B.b show alignments of all of these isoforms.

3.1.2 A potential alternate start codon in *NDE1*

One early NDE1/NDEL1 publication made reference to a transcript in mouse encoding a 212 amino acid homologue of the *Aspergillus nidulans* protein NUDE (Sasaki *et al.* 2000). This protein appears to be mouse Nde1, but makes use of an alternative methionine, at position 133, as a start codon. Looking at the corresponding transcript (GenBank AF290473) on the UCSC genome browser, this protein was predicted based on a transcript lacking exon 3 and some of the 5' untranslated region (figure 3.1.C). Such a transcript would theoretically be able to produce a protein starting at exon 1, with a premature stop codon shortly into exon 4 as a result of shift in the reading frame (figure 3.1.D). The only functional region of

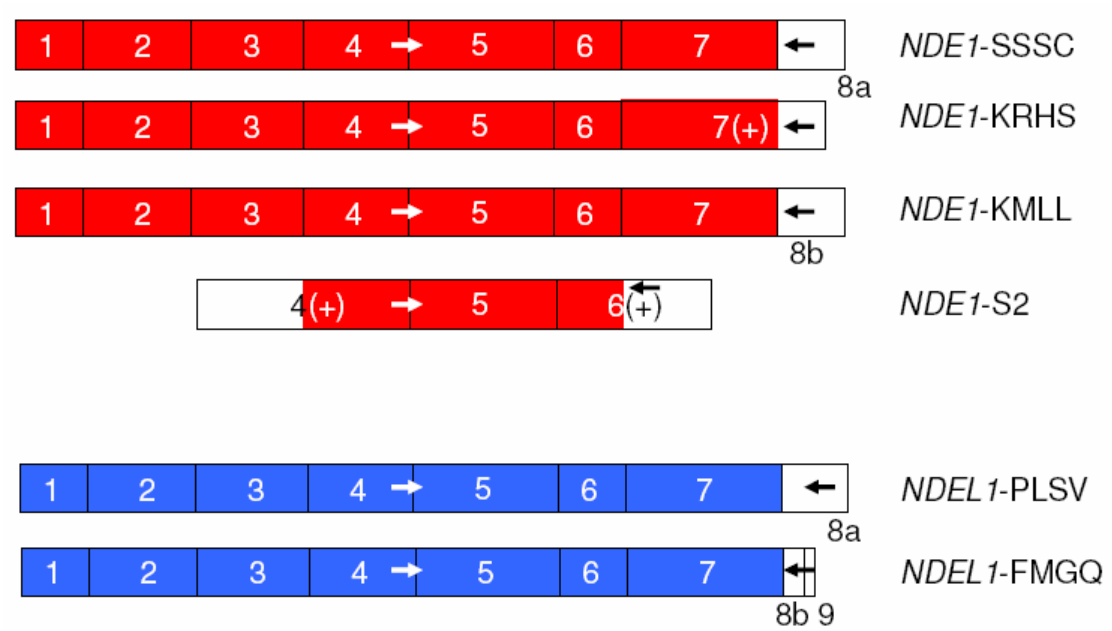

Figure 3.1.A: Exon structure of the NDE1 (red) and NDEL1 (blue) genes. Coloured exons indicate sequence conserved across the isoforms, while white indicates sequence that is unique to that splice variant. Exon 7 of *NDE1*-KMLL, as well as exons 4 and 6 of *NDE1*-S2 contain both conserved and unique sections. Arrows represent the location of the primers used in detecting these isoforms in section 3.2.1.

---

this protein likely to be conserved from the full length variants is the dimerisation site (based on the known corresponding domain in NDEL1 (Sasaki *et al.* 2000)). To date, however, there is no experimental evidence to confirm the implication that, as a result of this, the alternative methionine 133 start codon would be used instead. The use of "internal" start codons is not uncommon however, with one study estimating that 41% of transcripts studied contain at least one unused AUG motif upstream of the actual start codon (Peri and Pandey 2001). As a result of this uncertainty, the transcript will be referred to as *Nde1*-Δex3, while the theoretical methionine-133 based 212-amino acid protein it may encode will be referred to as Nde1-S1a and the alternative short methionine-1 based protein as Nde1-S1b.

a)

```
NDE1-SSSC     MEDSGKTFSSEEEEANYWKDLAMTYKQRAENTQEELREFQEGSREYEAELETQLQQIET
NDE1-KMLL     MEDSGKTFSSEEEEANYWKDLAMTYKQRAENTQEELREFQEGSREYEAELETQLQQIET
NDE1-KRHS     MEDSGKTFSSEEEEANYWKDLAMTYKQRAENTQEELREFQEGSREYEAELETQLQQIET
NDEL1-PLSV  MDGEDIPDFSSLKEETAYWKELSLKYKQSFQEARDELVEFQEGSRELEAELEAQLVQAEQ
NDEL1-FMGQ  MDGEDIPDFSSLKEETAYWKELSLKYKQSFQEARDELVEFQEGSRELEAELEAQLVQAEQ

NDE1-SSSC    RNRDLLSENNRLRMELETIKEKFEVQHSEGYRQISALEDDLAQTKAIKDQLQKYIRELEQ
NDE1-KMLL    RNRDLLSENNRLRMELETIKEKFEVQHSEGYRQISALEDDLAQTKAIKDQLQKYIRELEQ
NDE1-KRHS    RNRDLLSENNRLRMELETIKEKFEVQHSEGYRQISALEDDLAQTKAIKDQLQKYIRELEQ
NDEL1-PLSV   RNRDLQADNQRLKYEVEALKEKLEHQYAQSYKQVSVLEDDLSQTRAIKEQLHKYVRELEQ
NDEL1-FMGQ   RNRDLQADNQRLKYEVEALKEKLEHQYAQSYKQVSVLEDDLSQTRAIKEQLHKYVRELEQ

NDE1-SSSC    ANDDLERAKRATIMSLEDFEQRLNQAIERNAFLESELDEKENLLESVQRLKDEARDLRQE
NDE1-KMLL    ANDDLERAKRATIMSLEDFEQRLNQAIERNAFLESELDEKENLLESVQRLKDEARDLRQE
NDE1-KRHS    ANDDLERAKRATIMSLEDFEQRLNQAIERNAFLESELDEKENLLESVQRLKDEARDLRQE
NDEL1-PLSV   ANDDLERAKRATIVSLEDFEQRLNQAIERNAFLESELDEKESLLVSVQRLKDEARDLRQE
NDEL1-FMGQ   ANDDLERAKRATIVSLEDFEQRLNQAIERNAFLESELDEKESLLVSVQRLKDEARDLRQE

NDE1-SSSC    LAVQQKQE---KPRTPMPSSVEAERTDTAVQATGSVPSTPIAHRGPSSSLNTPGSFRRGL
NDE1-KMLL    LAVQQKQE---KPRTPMPSSVEAERTDTAVQATGSVPSTPIAHRGPSSSLNTPGSFRRGL
NDE1-KRHS    LAVQQKQE---KPRTPMPSSVEAERTDTAVQATGSVPSTPIAHRGPSSSLNTPGSFRRGL
NDEL1-PLSV   LAVRERQQEVTRKSAPSSPTLDCEKMDSAVQASLSLPATPVG-KGTENTFPSP----KAI
NDEL1-FMGQ   LAVRERQQEVTRKSAPSSPTLDCEKMDSAVQASLSLPATPVG-KGTENTFPSP----KAI

NDE1-SSSC    DDSTGGTPLTPAARISALNIVGDLLRKVGALESKLASCRNLVYDQSPNRTGGPASGRSSK
NDE1-KMLL    DDSTGGTPLTPAARISALNIVGDLLRKVGALESKLASCRNLVYDQSPNRTGGPASGRSSK
NDE1-KRHS    DDSTGGTPLTPAARISALNIVGDLLRKVGALESKLASCRNLVYDQSPNRTGGPASGRSSK
NDEL1-PLSV   PNGFGTSPLTPSARISALNIVGDLLRKVGALESKLAACRNFAKDQASRKSYISGNVNCGV
NDEL1-FMGQ   PNGFGTSPLTPSARISALNIVGDLLRKVGALESKLAACRNFAKDQASRKSYISGNVNCGV

NDE1-SSSC    NRDGGERRPSSTSVPLGDKG----LDTSCRWLSKSTTRSSSC-------
NDE1-KMLL    NRDGGERRPSSTSVPLGDKGLGKRLEFGKPPSHMSSSPLPSAQGVVKMLL
NDE1-KRHS    NRDGGERRPSSTSVPLGDKG----SVPSNKPLAGGENPP--APGKRHS--
NDEL1-PLSV   LNGNGTKFSRSGHTSFFDKGAVNGFDPAPPPPGLGSSRPSSAPGMLPLSV
NDEL1-FMGQ   LNGNGTKFSRSGHTSFFDKG---QEKVIFPTLFMGQ--------------
```

b)

```
NDE1-SSSC  MEDSGKTFSSEEEEANYWKDLAMTYKQRAENTQEELREFQEGSREYEAELETQLQQIETR
NDE1-S2

NDE1-SSSC  NRDLLSENNRLRMELETIKEKFEVQHSEGYRQISALEDDLAQTKAIKDQLQKYIRELEQA
NDE1-S2       MMSPILQVKSPCPRRLRDLAHSVASRKFGAGTCAQVCLTLRTSWIRGAGGMLRFVLL

NDE1-SSSC  NDDLERAKRATIMSLEDFEQRLNQAIERNAFLESELDEKENLLESVQRLKDEARDLRQEL
NDE1-S2    DNSAFLFASATIMSLEDFEQRLNQAIERNAFLESELDEKENLLESVQRLKDEARDLRQEL

NDE1-SSSC  AVQQKQEKPRTPMPSSVEAERTDTAVQATGSVPSTPIAHRGPSSSLNTPGSFRRGLDDST
NDE1-S2    AVQQKQEKPRTPMPSSVEAERTDTAVQATGSVPSTPIAHRGPSSSLNTPGSFRRGLDDST

NDE1-SSSC  GGTPLTPAARISALNIVGDLLRKVGALESKLASCRNLVYDQSPNRTGGPASGRSSKNRDG
NDE1-S2    GGTPLTPAARISALNIVGDLLRKVGVRPHFPGVWCLPACLSGCVKGVDLVPSLSSFLFF

NDE1-SSSC  GERRPSSTSVPLGDKGLDTSCRWLSKSTTRSSSSC
NDE1-S2
```

c)

```
NDE1-KMLL          LGKRLEFGKPPSHMSSSPLPSAQGVVKMLL
NDEL1-PLSV         AVNGFDPAPPPPGLGSSRPSSAPGMLPLSV
```

d)

```
NDE1-KRHS          ----SVPSNKPLAGGENPP--APGKRHS--
NDEL1-PLSV         AVNGFDPAPPPPGLGSSRPSSAPGMLPLSV
```

Figure 3.1.B: a) Sequence alignment of all the long isoforms of NDE1 and NDEL1 studied here. Amino acids in red indicate residues conserved between NDE1 and NDEL1. Amino acids in blue indicate residues conserved amongst NDE1 isoforms only. Amino acids in green indicate residues conserved amongst NDEL1 isoforms only. b) Sequence alignment of the long NDE1-SSSC isoform and the short NDE1-flff isoform. Amino acids conserved between the two are shown in red. c) Alignment of the C-terminal regions of NDE1-KMLL and NDEL1-PLSV with identical residues shown in red and similar residues in blue. d) A similar alignment of NDE1-KRHS and NDEL1-PLSV.

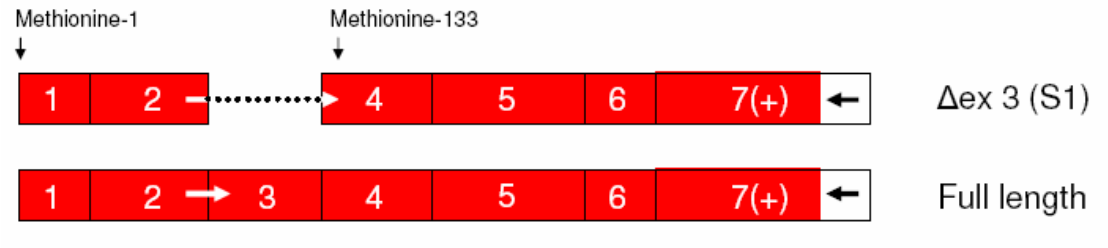

Figure 3.1.C: Exon structure of the NDE1-Δex3 transcript, which is predicted to encode NDE1-S1. Also shown is the exon structure of full length NDE1-KMLL for comparison. The two methionine residues which may be used as start codons are indicated by vertical arrows. Horizontal arrows indicate the regions used as primers to detect these transcripts in section 3.2.3.

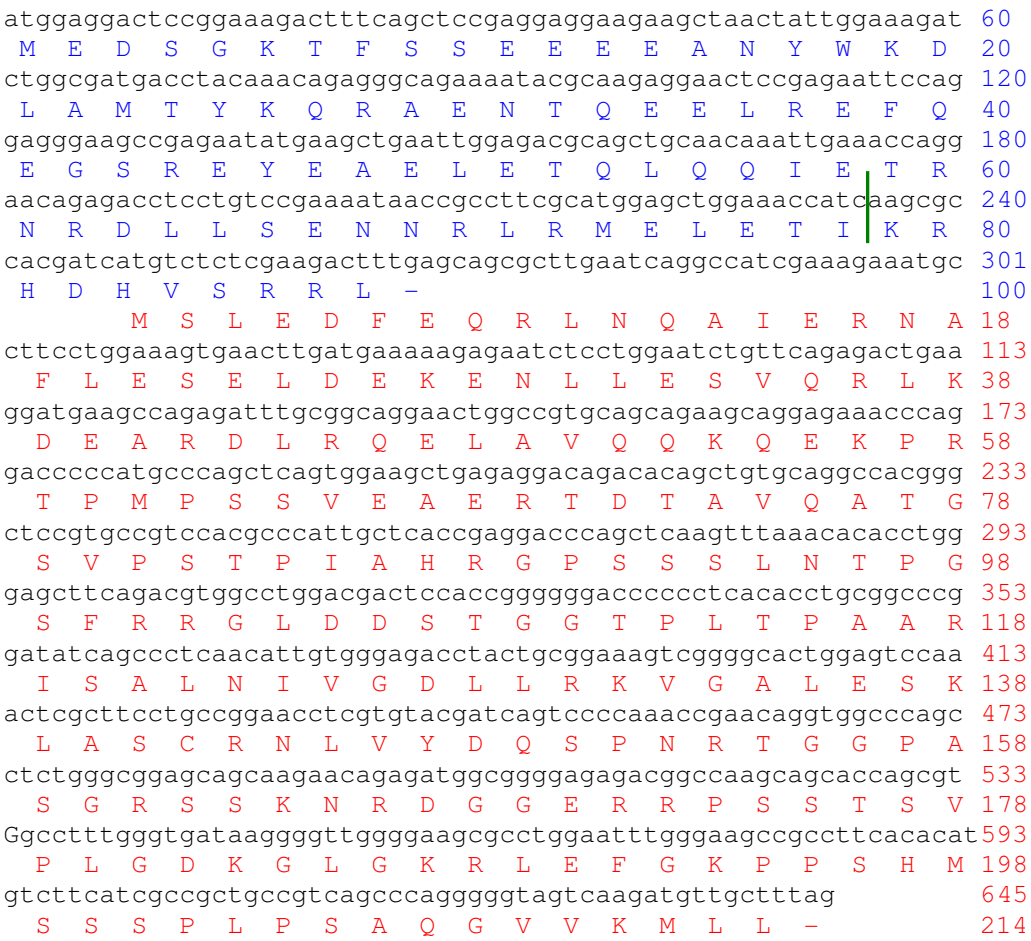

Figure 3.1.D: The nucleic acid sequence of a human NDE1-Δex3 transcript (using the "KMLL" C-terminus) is shown in black. The amino acid sequences of the two potentially derived proteins are shown below in single letter code. The blue sequence makes use of methionine-1 (S1b) and the red sequence makes use of methionine-133 (S1a, numbered based on full length NDE1). The break where exon 3 would otherwise lie is marked with a green line.

NDE1 contains a Kozak sequence (Kozak 1987), conserved in both mouse and human, around methionine-133 (table 3.1.A), Of the five bases preceding the start codon and the one after, only three match the canonical Kozak sequence, however this may well be close enough, as one study found 48.9% of proteins to have four or more mismatches in this region (Peri and Pandey 2001). Thus a NDE1-S1a protein remains a realistic possibility in both organisms. By entering the nucleic acid sequence (including the untranslated regions at the 5' and 3' ends) of *NDE1* into the

		-9	-8	-7	-6	-5	-4	-3	-2	-1	1	2	3	4
Canonical sequence		G	C	C	**G**	C	**C**	**A**	C	**C**	**A**	**T**	**G**	**G**
Methionine-133	Human	G	C	C	A	C	G	**A**	T	**C**	**A**	**T**	**G**	T
Methionine-133	Mouse	G	C	C	A	C	A	**A**	T	**C**	**A**	**T**	**G**	T
Methionine-1	Human	G	T	T	T	T	**C**	**A**	C	A	**A**	**T**	**G**	**G**
Methionine-1	Mouse	C	A	T	T	T	T	**A**	C	**C**	**A**	**T**	**G**	**G**

Table 3.1.A: The canonical Kozak sequence (Kozak 1987), compared to the sequence surrounding the potential start codon at methionine-133 of *NDE1* in mice and humans. The sequence surrounding methionine-1, the canonical start codon, is also shown. Bases in bold indicate those that are most highly conserved in the Kozak sequences of vertebrates. Yellow indicate conservation with the canonical Kozak sequence, while red indicates the essential ATG methionine codon.

---

online program NetStart 1.0 (Pedersen and Nielsen 1997), methionine-133 was rated as the most likely start codon in the protein (more so even than methionine 1). The Kozak sequence is not predictable using the online program weakAUG, however this program cannot detect a Kozak sequence at exon 1 either (Tikole and Sankararamakrishnan 2008).

Methionine-133 of NDE1 is substituted by a valine in NDEL1. Indeed, this is actually the only residue out of amino acids 115-161 of NDE1 which is not precisely conserved in NDEL1. An equivalent isoform of NDEL1 is thus not expected to exist.

3.1.3 Molecular weights and isoelectric points of the isoforms

The predicted amino acid sequences of all theoretical NDE1 and NDEL1 isoforms were entered into the online program ProtParam (Gasteiger *et al.* 2005) which gives theoretical predictions of the molecular weights (M_W) and isoelectric points (pI) of peptides. These are shown in table 3.1.B. Full length NDE1 and NDEL1 isoforms are seen to share similar M_W and pI values, which is expected given their high degree of amino acid similarity. The slightly higher M_W of the NDE1-KMLL and NDEL1-PLSV isoforms may allow them to be distinguished from other isoforms by Western

Protein	Isoform	Mw (kDa)	pI
NDE1	SSSC	37.7	5.09
NDE1	KMLL	38.8	5.20
NDE1	KRHS	37.8	5.14
NDE1	S1a	23.0	9.13
NDE1	S1b	10.7	4.81
NDE1	S2	25.8	8.85
NDEL1	PLSV	38.3	5.16
NDEL1	FMGQ	37.0	5.16

Table 3.1.B: Molecular weights (M_W) and isoelectric points (pI) of theoretical NDE1 and NDEL1 isoforms, predicted by ProtParam (Gasteiger *et al.* 2005).

---

blot. Notably, the short NDE1-S1a and NDE1-S2 splice variants are considerably more basic than the full length species, while the NDE1-S1b protein is slightly more acidic.

3.1.4 Alignment of the unique C-terminal domains

A CLUSTALW (Thompson *et al.* 1994) alignment of the C-terminal isoforms is shown in figure 3.1.B.a. In this region, the highest degree of sequence similarity appears to be between the NDE1-KMLL and NDEL1-PLSV isoforms (figure 3.1.B.c) and the NDE1-KRHS and NDEL1-PLSV isoforms (figure 3.1.B.d). It is therefore possible that these isoforms may therefore have C-terminal regions homologous to the "original" C-terminal region of a common ancestral gene, with the alternative C-terminal regions appearing later in evolution. The short nature of the C-terminal tails prevents the generation of a meaningful phylogenetic tree, however.

3.1.5 *Nde1* transcripts described in other organisms are orthologues of the *NDE1*-KMLL splice variant

The "canonical" human NDE1 protein studied to date in the literature is the NDE1-SSSC isoform (Feng *et al.* 2000). However, when the NDE1-SSSC amino acids sequence was compared to known rodent forms of Nde1 (Feng *et al.* 2000; Kitagawa *et al.* 2000) and other NDE1 orthologues, very little sequence similarity was observed at the extreme C-terminus (see figure 3.1.E.a). A similar comparison was

a)

```
NDE1-SSSC          LRKVGALESKLASCRNLVYDQSPNRTGGPASGRSSKNRDGGERRPSSTSVPLGDKGLDTSCRWLSKSTTRSSSSC----------
Chimpanzee         LRKVGALESKLASCRNLVYDQSPNRTGGPASGRSSKNRDGGERRPSSTSVSLGDKGLGKRLEFGKPPSHMSSSPLPSAQGVVKMLL
Rhesus monkey      LRKVGALESKLASCRNLVYDQSPNRTGGPASGRSSKNRDGGERRPSSSSVPLGDKGLGKCLEFGKPPSHMSSSPLPSAQGVVKMLL
Cattle             LRKVGALESKLASCRNFVYDQSPGRASGPASGRGSKNRDSVDRRPGGSNVPLGDKGLGKRLEFGKPSSNVSSPSLPSAQGVVKMLL
Mouse              LRKVGALESKLASCRNFMYDQSPSRTSGPASGRGTKNRDGVDRRPG--STSVGDKGSGKRLEFGKPASEPASPALPSAQGVVKLLL
Rat                LRKVGALESKLASCKNFMYDQSPSRKSGPALGRGTKNRDGIDRRPG--STAVGDKGSGKRLEFAKPSSQLSSPALPSTQGVVKLLL
Chicken            LRKVGALESKLASCRNFVYDQSPDR----TTVSMYMNRDALETRMSP-HQPLCDTGLVKRLEFGTRPSSTPGPMSHPSQSVVKMLL
Xenopus            LRKVGALESKLASCRNFVHEQSPNRPLTSVSARMNKTREGIENRLSMASGSSVEKGLIKRLEFGSLPSNTPVQGMHSPQGVVKMII
```

b)

```
NDE1-KMLL          LRKVGALESKLASCRNLVYDQSPNRTGGPASGRSSKNRDGGERRPSSTSVPLGDKGLGKRLEFGKPPSHMSSSPLPSAQGVVKMLL
Chimpanzee         LRKVGALESKLASCRNLVYDQSPNRTGGPASGRSSKNRDGGERRPSSTSVSLGDKGLGKRLEFGKPPSHMSSSPLPSAQGVVKMLL
Rhesus monkey      LRKVGALESKLASCRNLVYDQSPNRTGGPASGRSSKNRDGGERRPSSSSVPLGDKGLGKCLEFGKPPSHMSSSPLPSAQGVVKMLL
Cattle             LRKVGALESKLASCRNFVYDQSPGRASGPASGRGSKNRDSVDRRPGGSNVPLGDKGLGKRLEFGKPSSNVSSPSLPSAQGVVKMLL
Mouse              LRKVGALESKLASCRNFMYDQSPSRTSGPASGRGTKNRDGVDRRPG--STSVGDKGSGKRLEFGKPASEPASPALPSAQGVVKLLL
Rat                LRKVGALESKLASCKNFMYDQSPSRKSGPALGRGTKNRDGIDRRPG--STAVGDKGSGKRLEFAKPSSQLSSPALPSTQGVVKLLL
Chicken            LRKVGALESKLASCRNFVYDQSPDR----TTVSMYMNRDALETRMSP-HQPLCDTGLVKRLEFGTRPSSTPGPMSHPSQSVVKMLL
Xenopus            LRKVGALESKLASCRNFVHEQSPNRPLTSVSARMNKTREGIENRLSMASGSSVEKGLIKRLEFGSLPSNTPVQGMHSPQGVVKMII
```

Figure 3.1.E: a) Sequence alignment of the C-terminal region of human NDE1-SSSC with those of known NDE1 homologues from other species demonstrates that there is very little sequence similarity at the extreme C-terminus. b) Sequence alignment of NDE1-KMLL with the same homologues shows far better amino acid similarity. Red amino acids indicate residues which are conserved with the human sequence. Alignment performed using CLUSTALW (Thompson *et al.* 1994).

between NDE1-KMLL and the same orthologues revealed better amino acid conservation (see figure 3.1.E.b). It therefore appears that while *NDE1*-SSSC is the splice variant studied to date in humans, the isoform studied in other organisms is in fact more similar to the *NDE1*-KMLL isoform. At the time of writing, however, GenBank lists four human mRNAs corresponding to NDE1-SSSC, and only one corresponding to NDE1-KMLL, implying that *NDE1*-SSSC may still be the more prominently expressed of the two in humans. While no protein binding domain or phosphorylation site has yet been definitively mapped to the isoform-specific region of the NDE1 protein, the possibility has to be acknowledged that some results in the literature ascribed to "rodent Nde1" may not also apply to "human NDE1" or vice versa simply due to the fact that different isoforms have been studied in each. A theoretical analysis of potential functions of these C-terminal tails will be undertaken in chapter 4.

In contrast, NDEL1-PLSV is the isoform which has been studied to date in all species (Niethammer *et al.* 2000; Sasaki *et al.* 2000; Sweeney *et al.* 2001).

3.2 Splice variants of *NDE1* and *NDEL1* in the human brain

3.2.1 Transcripts of several *NDE1* and *NDEL1* splice variants in human brain cDNA

Four *NDE1* splice variants (SSSC, KMLL, KRHS and S2) and two putative NDEL1 splice variants (PLSV and FMGQ) are predicted. In order to investigate the existence of these transcripts *in vivo*, primers were generated that were specific to each splice variant (see table 2.5.A). 5' primers were selected that spanned introns 4 and 5 of *NDE1* and *NDEL1* (introns 1 and 2 of *NDE1*-S2) in order to ensure detection of only spliced mRNA and not unspliced genomic DNA. 3' primers were selected from the unique sequences at the 3' end of each variant. Figure 3.1.A shows a schematic that includes these primers.

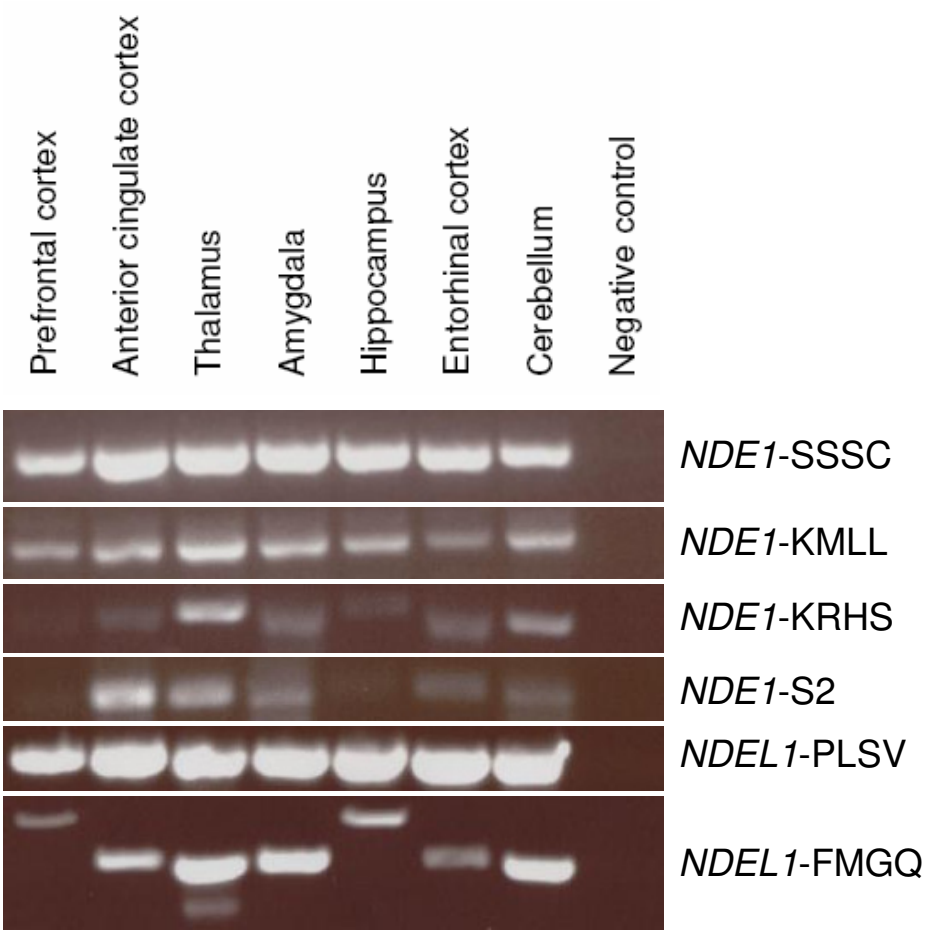

Figure 3.2.A: Expression of transcripts of four *NDE1* and two *NDEL1* splice variants in cDNAs raised from seven different regions of the human brain.

Commercially available RNA from seven different regions of the human brain were reverse transcribed. PCR reactions were then performed on each of these cDNA samples in order to test the presence of the predicted splice variants. As a negative control, a mock reverse transcription reaction was performed that lacked any RNA template. For each splice variant, equal quantities of PCR reaction from each brain region, as well as the negative control, were electrophoresed on an agarose gel (see figure 3.2.A). For each isoform, a sample of the PCR product which yielded the strongest band was then sequenced in order to confirm the specificity of the PCR reaction.

Transcripts encoding all six of the investigated isoforms were detected in cDNA raised from several brain regions. In the case of the three "canonical" splice variants, *NDE1*-SSSC, *NDE1*-KMLL and *NDEL1*-PLSV, transcripts appeared to be expressed in all the brain regions, while for the remaining isoforms, the pattern of staining appeared to be more specialised. It should be noted, however, that these PCR reactions were not quantitative and therefore direct comparisons cannot be definitively made. Nevertheless, this suggests that transcripts encoding each of these isoforms could be expressed in the brain. Given that both the NDE1 and NDEL1 proteins show evidence of neurodevelopmental functions (see section 1.3.4), any or all of these isoforms could therefore potentially play roles in these processes.

3.2.2 Multiple bands of *NDEL1*-FMGQ

The *NDEL1*-FMGQ primers detected PCR products of three distinct sizes (see figure 3.2.A), some of which were specific to certain regions of the brain. These products were run on another gel and eight discrete DNA bands excised (see figure 3.2.B), with each band then being sequenced. Bands B2, C2, D2, F2 and G2 all correspond to full length *NDEL1*-FMGQ transcripts. The anterior cingulate cortex, thalamus, amygdala, entorhinal cortex and cerebellum therefore clearly all express full length *NDEL1*-FMGQ transcripts.

The remaining bands were unfortunately very faint and, in spite of an extensive optimisation effort, it has not yet proven possible to fully sequence these products. Nevertheless, partial sequencing has confirmed that the bands do at least represent genuine *NDEL1* transcripts. It can be speculated that the varying band sizes may be as a result of additional, as yet uncharacterised, splicing of the *NDEL1* gene.

3.2.3 Transcripts of the *NDE1*-Δex3 (S1) splice variant in human brain cDNA

The *NDE1*-Δex3 transcript, which has the potential to encode the NDE1-S1a protein isoform (Sasaki *et al.* 2000), was originally seen in mouse. To investigate if the transcript also exists in human, two primers were designed, one that spans the exon 2-3 splice junction and one that spans exon 2-4 splice junction, as seen in only in the

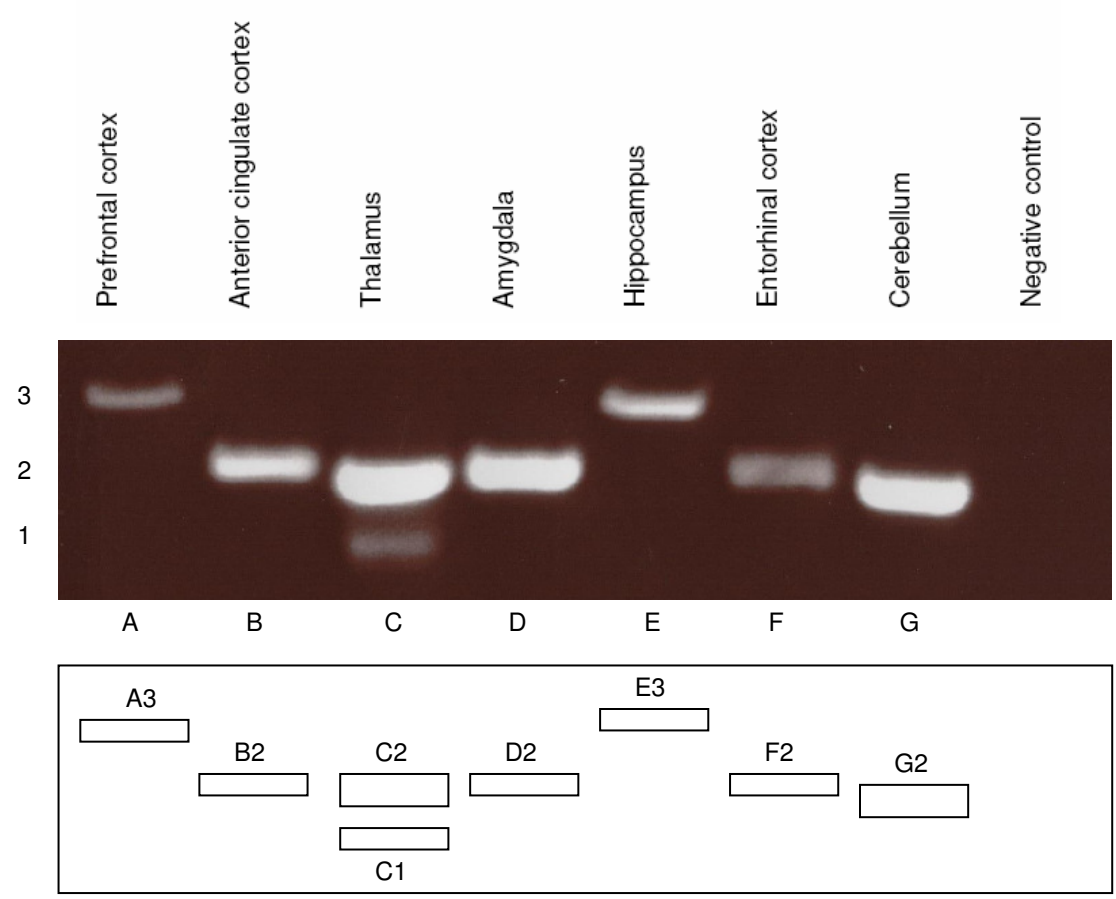

Figure 3.2.B: Eight bands were excised from a gel containing the *NDEL1*-FMGQ PCR products. PCR bands were labelled as shown.

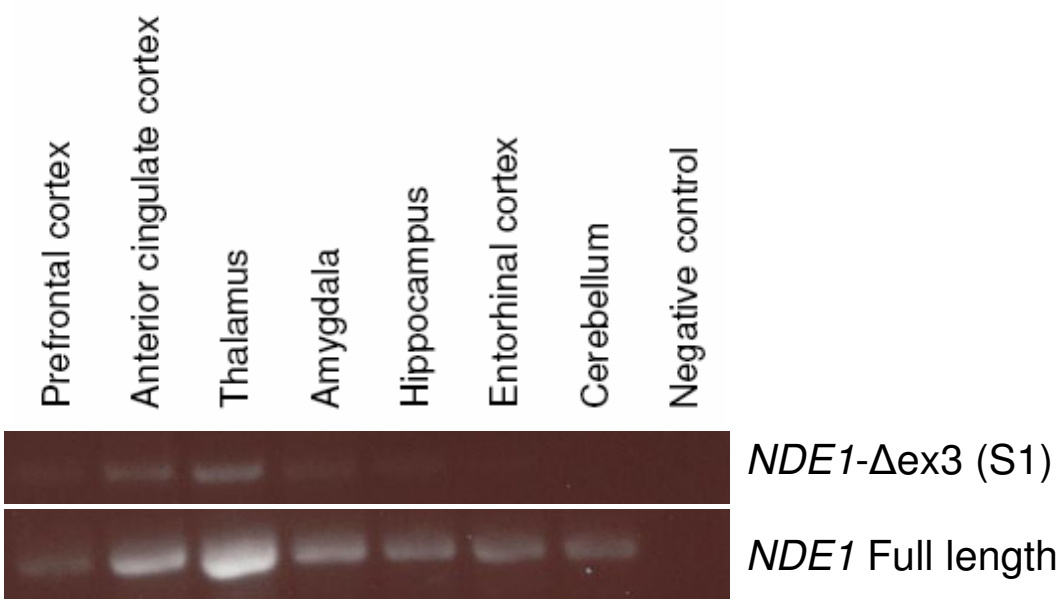

Figure 3.2.C: Expression of the Δex3 splice variant of *NDE1* (with the KMLL C-terminal region) in cDNAs from various regions of the human brain. Full length *NDE1*-KMLL is shown for comparison.

NDE1-Δex3 transcript (see figure 3.1.C). These should therefore detect either Δex3 or full length *NDE1* transcripts respectively. These two primers were then each partnered with a primer that detects the *NDE1*-KMLL 3' end. This 3' end was chosen as it most closely resembled that of the original mouse *Nde1*-Δex3 transcript. When used on the human brain cDNA, the full length transcript was seen throughout the brain, while the Δex3 transcript was seen in at least two locations (see figure 3.2.C). While these PCR reactions were not done in a quantitative manner, it nonetheless appears that the full length transcript is expressed at a greater abundance than the Δex3 transcript in all brain regions tested. It therefore appears that the *NDE1*-Δex3 transcript does exist in the human brain, although the nature of the protein it encodes remains to be determined.

3.3 Discussion

Numerous cDNAs representing potential *NDE1* and *NDEL1* have been listed on the UCSC genome browser for some time, but to date the only published evidence of multiple protein isoforms came from a single early paper which mentioned a NDE1 isoform shorter than that described elsewhere (Sasaki *et al.* 2000). An additional clue to the existence of multiple NDE1 isoforms, however, came from the fact that the canonical human NDE1 isoform (SSSC) did not appear to be a direct orthologue of the Nde1 proteins from other species described in the literature or listed as a standard splice variant on the UCSC Genome Browser. These in fact more closely resemble NDE1-KMLL (see figure 3.1.E).

It is unclear at this time whether these splice variants also exist in other organisms. Certainly the KMLL isoform is well conserved across many species, but in addition *NDE1*-Δex3 transcripts have been described in both human and mouse (Sasaki *et al.* 2000). It therefore seems likely that other mammals may express isoforms equivalent to at least some of these splice variants. Determining which of these splice variants are conserved across species may yield clues as to which of the protein isoforms are likely to play the most essential biological roles. The similarity between the NDE1-KMLL and NDEL1-PLSV C-terminal regions does, however,

suggest that these isoforms are the most closely related to the common gene from which *NDE1* and *NDEL1* diverged. It should be stated that the isoforms described here are unlikely to be the only splice variants of human *NDE1* and *NDEL1* found in the body, with cDNAs containing several other potential splice variants also listed on the genome browser.

A theoretical analysis of potential differences between the isoforms will be performed in chapter 4, while an anti-NDE1 antibody will be used to look for evidence of these isoforms in cell lines in chapter 5. The existence of transcripts encoding multiple NDE1 and NDEL1 isoforms suggests that regulation of their function is likely to be complex. That at least low levels of each of these transcripts appear to be present in the brain furthermore provides the possibility that any of these isoforms could play roles in the neurodevelopmental phenotypes previously ascribed to NDE1 and NDEL1 (Feng and Walsh 2004; Shu *et al.* 2004; Kamiya *et al.* 2006; Duan *et al.* 2007; Taya *et al.* 2007; Shim *et al.* 2008). It would be interesting to, at a later date, perform a quantitative real time PCR experiment in order to determine how prevalent each of these isoforms is in the brain, particularly with regard to NDE1-SSSC which is the most commonly reported on human isoform and NDE1-KMLL which is the most widely reported on in all other species.

Chapter 4 – Predicting the structure and function of the NDE1 and NDEL1 proteins

4.1 Introduction

It is a central dogma of structural biology that the amino acid sequence of a protein determines how it is folded and thus the three-dimensional (3-D) structure of the protein, and that this structure determines the *in vivo* properties of the protein. Therefore in order to understand the cellular roles of the NDE1 and NDEL1 proteins and how those functions may be regulated, it is helpful to build a theoretical model of their structure.

In several of the initial papers characterising NDE1 and NDEL1 it was observed that their N-terminal region had the potential to form a helical or coiled-coil structure (Feng *et al.* 2000; Niethammer *et al.* 2000; Sasaki *et al.* 2000). The 3-D structure of this region of NDEL1 has since been solved and does indeed form a large coiled-coil domain which can interact with the coiled-coils of other NDEL1 monomers (Derewenda *et al.* 2007). To date, a similar structural investigation has not been performed on NDE1 or on the remaining portions of NDEL1. Another key aspect of a protein's structure with respect to function is the location of sites at which it interacts with its protein binding partners. A number of such binding sites have been mapped for both NDE1 and NDEL1 (see table 4.1), but for the majority of interactions, a site has only been established on one or the other of NDE1 and NDEL1. In addition, a number of phosphorylation sites have been identified on each protein, but to date, none of these have been confirmed to exist in both.

Considering that NDE1 and NDEL1 are so similar to each other (approximately 60% amino acid identity, 80% similarity depending on the method of alignment), it is reasonable to assume that many of these features will be shared between them. Comparing the amino acid sequences of the two proteins (figure 1.3.A), it can be seen that certain regions are more closely conserved than others. For example in the

Protein	Binds NDE1?	Binds NDEL1?	NDE1 site	NDEL1 site	References
Self-association	O/E	Yes	22-159	56-104	(Sasaki *et al.* 2000; Feng and Walsh 2004)
14-3-3ε	?	Yes	-	189-256	(Toyo-Oka *et al.* 2003)
Cdc42GAP	?	O/E	-	114-133	(Shen *et al.* 2008b)
CENPF	O/E	O/E	167-287	?	(Yan *et al.* 2003; Soukoulis *et al.* 2005; Vergnolle and Taylor 2007)
DISC1	O/E *	Yes	?	266-267	(Millar *et al.* 2003; Brandon *et al.* 2004; Burdick *et al.* 2008)
DBZ/Su48	O/E	O/E	176-335	?	(Hirohashi *et al.* 2006b)
Dynactin	O/E	Yes	?	256-291	(Liang *et al.* 2004; Guo *et al.* 2006)
Dynein	*In vitro*	Yes	?	256-291	(Sasaki *et al.* 2000; Stehman *et al.* 2007)
Katanin p60	O/E	O/E	?	195-256	(Toyo-Oka *et al.* 2005)
Katanin p80	?	O/E	-	63-189	(Toyo-Oka *et al.* 2005)
LIS1	O/E	Yes	90-159	114-133	(Feng *et al.* 2000; Yan *et al.* 2003)
NF-L	?	Yes	-	191-345	(Nguyen *et al.* 2004b)
Pericentrin	*In vitro*	O/E	?	256-293	(Feng *et al.* 2000; Guo *et al.* 2006)
p78/MCRS1	O/E	O/E	176-335	?	(Hirohashi *et al.* 2006a)

Table 4.1: Binding sites of NDE1 and NDEL1 interactors as mapped experimentally in the literature. "*In vitro*" designates that this interaction has been shown by either yeast-2-hybrid screen or GST *in vitro* pull-down, but has not been demonstrated in the cell. "O/E" designates that this interaction has been seen using over-expressed protein in the cell, but not yet using endogenous protein. * Result published while this thesis was being written

regions of NDE1 containing amino acids 112-181 and 244-276, sequence conservation with NDEL1 is near identical. The region between these two conserved sections, meanwhile, shows only limited conservation with NDEL1. It can therefore be speculated that certain functional properties of NDE1/NDEL1, those lying within the conserved regions, are likely to be shared between the two proteins. The presence of less conserved regions, meanwhile, may imply the existence of protein-specific functions, interactions and/or regulation.

In this chapter bioinformatics software will be utilised in order to predict the structural features of NDE1 and NDEL1, as well as their likely functional domains. These theoretical analyses are intended to aid the generation of a model for the proteins structure, their function and how these functions may be regulated. The hypotheses generated in this way can be used as a framework on which to base future experiments.

4.2 Coiled-coil and α-helix forming potential of NDE1 and NDEL1

4.2.1 Introduction to α-helices and coiled-coils

The α-helix is a common protein secondary structure in which an amino acid chain is arranged as a spiral. These helices make one complete rotation every 3.4 amino acids and are held together by hydrogen bonding between the C=O group of a residue and the N-H group of the residue four amino acids in front of it.

In some proteins, two α-helices spiral around each other to form a structure known as a coiled coil. Such structures serve a variety of biological roles, as well as often being the sites of protein-protein interactions. In a coiled-coil, some residues (typically hydrophilic) will be facing outwards of the coiled coil, while those involved in the interaction of the two helices and typically hydrophobic, will be internal. The amino acid sequence of the coiled-coil is thought of as existing in units of seven residues (each known as a heptad repeat) as each residue occupies an equivalent position in the coil (internal or external) to the residue seven amino acids ahead of it.

4.2.2 COILS analysis of full length NDE1 and NDEL1

Given the fact that NDEL1 possesses a long N-terminal coiled-coil region (Derewenda *et al.* 2007), the online program COILS (Lupas *et al.* 1991) was used to evaluate the helix-forming potential of a NDE1-SSSC monomer. An equivalent helix was indeed strongly predicted (see figure 4.2.A.a), in agreement with a previously published prediction (Feng *et al.* 2000), implying that NDE1 would also be able to form coiled-coil structures. In addition, the COILS program also shows the potential, albeit at a lower probability, for an additional short helical domain nearer the C-terminus, around amino acids 252-278. This feature is also seen when the amino acid sequence of NDEL1-PLSV was investigated in the same way (see figure 4.2.A.b). However, this C-terminal helix is only detectable when the sequence is analysed using a "sliding window" of 14 amino acid "blocks". The helix is weak when a 21 amino acid "window" is used and not detectable at all with a 28 amino acid one. This may be due to the short length, approximately 36 amino acids, of this region or may indicate that the result is a false positive.

4.2.3 PSIPRED analysis of full length NDE1 and NDEL1

In order to assess the reliability of these helix predictions, the sequences of NDE1-SSSC and NDEL-PLSV were analysed using the PSIPRED protein structure prediction server (McGuffin *et al.* 2000). This program predicts the secondary structure of each amino acid in a sequence, with an accuracy independently measured at 77.3% (Moult *et al.* 1999). Results are shown in figure 4.2.B. Both proteins are predicted to have α-helical domains covering most of their N-terminal regions, matching the coiled-coil predicted using the COILS program. A short C-terminal helix is predicted in both proteins, running from amino acids 247-278 of full length NDE1 and 246-278 of NDEL1, matching the coiled-coil predicted using COILS. Interestingly, this region is extremely well conserved between NDE1 and NDEL1 (figure 1.3.A), implying that it may have an evolutionarily conserved function.

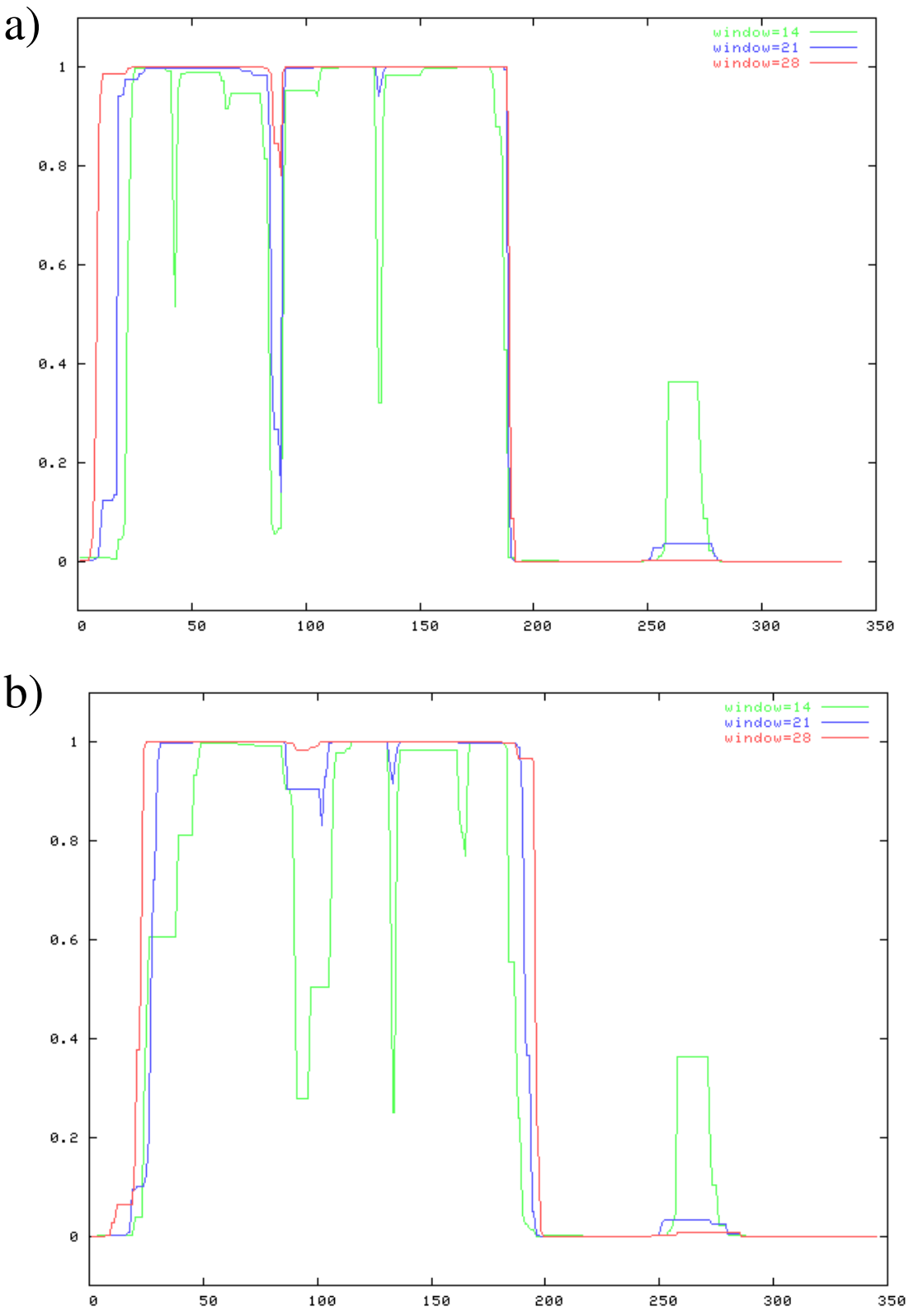

Figure 4.2.A: Regions of a) NDE1-SSSC and b) NDEL1-PLSV with coil-forming potential, predicted using the program COILS (Lupas *et al.* 1991).

a)

NDE1

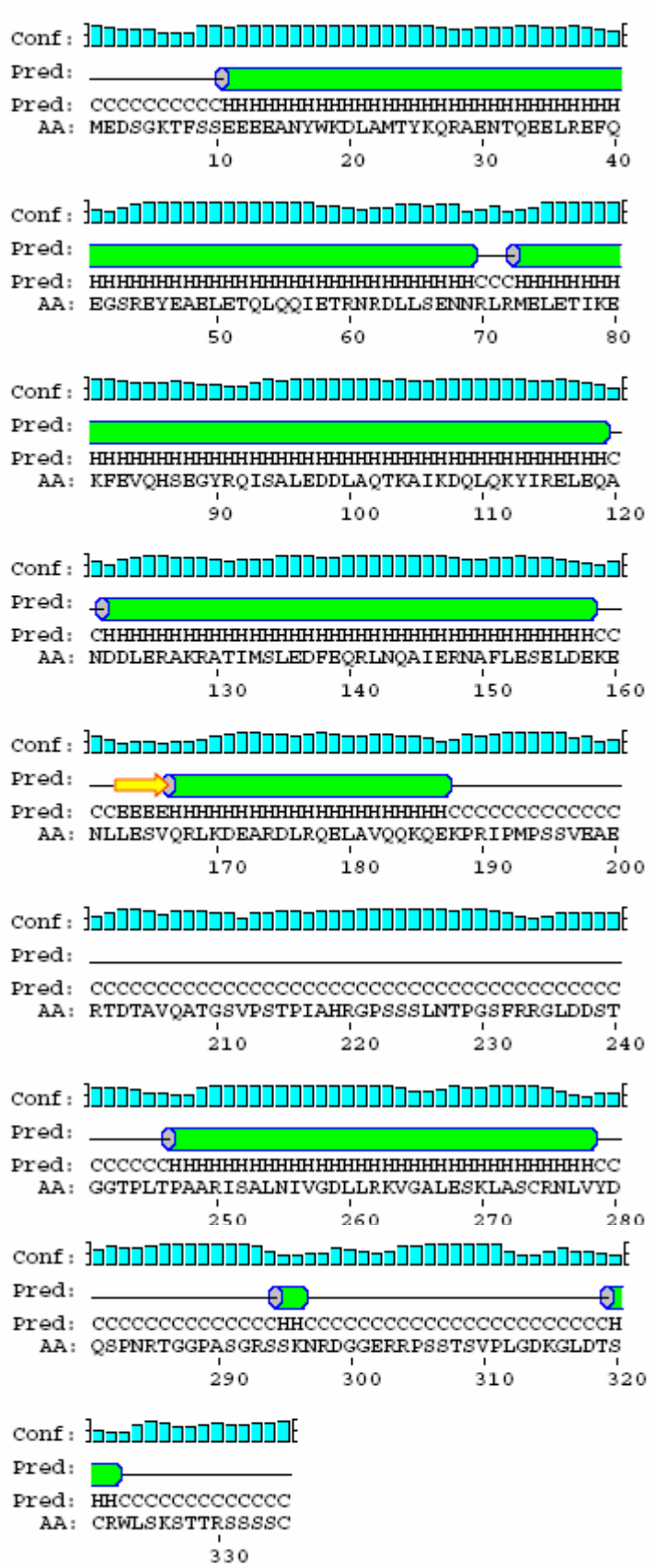
Conf:
Pred:
Pred: CCCCCCCCCCHHHHHHHHHHHHHHHHHHHHHHHHHHHHHH
AA: MEDSGKTFSSEEEEANYWKDLAMTYKQRAENTQEELREFQ
10 20 30 40
Conf:
Pred:
Pred: HHHHHHHHHHHHHHHHHHHHHHHHHHHHHHCCCHHHHHHH
AA: EGSREYEAELETQLQQIETRNRDLLSENNRLRMELETIKE
50 60 70 80
Conf:
Pred:
Pred: HHHHHHHHHHHHHHHHHHHHHHHHHHHHHHHHHHHHHHHC
AA: KFEVQHSEGYRQISALEDDLAQTKAIKDQLQKYIRELEQA
90 100 110 120
Conf:
Pred:
Pred: CHHHHHHHHHHHHHHHHHHHHHHHHHHHHHHHHHHHHHCC
AA: NDDLERAKRATIMSLEDFEQRLNQAIERNAFLESELDEKE
130 140 150 160
Conf:
Pred:
Pred: CCEEEEHHHHHHHHHHHHHHHHHHHHCCCCCCCCCCCCC
AA: NLLESVQRLKDEARDLRQELAVQQKQEKPRIPMPSSVEAE
170 180 190 200
Conf:
Pred:
Pred: CCCCCCCCCCCCCCCCCCCCCCCCCCCCCCCCCCCCCCC
AA: RTDTAVQATGSVPSTPIAHRGPSSSLNTPGSFRRGLDDST
210 220 230 240
Conf:
Pred:
Pred: CCCCCCHHHHHHHHHHHHHHHHHHHHHHHHHHHHHHCC
AA: GGTPLTPAARISALNIVGDLLRKVGALESKLASCRNLVYD
250 260 270 280
Conf:
Pred:
Pred: CCCCCCCCCCCCCCHHCCCCCCCCCCCCCCCCCCCCCCH
AA: QSPNRTGGPASGRSSKNRDGGERRPSSTSVPLGDKGLDTS
290 300 310 320
Conf:
Pred:
Pred: HHCCCCCCCCCCCCC
AA: CRWLSKSTTRSSSSC
330

b)

NDEL1

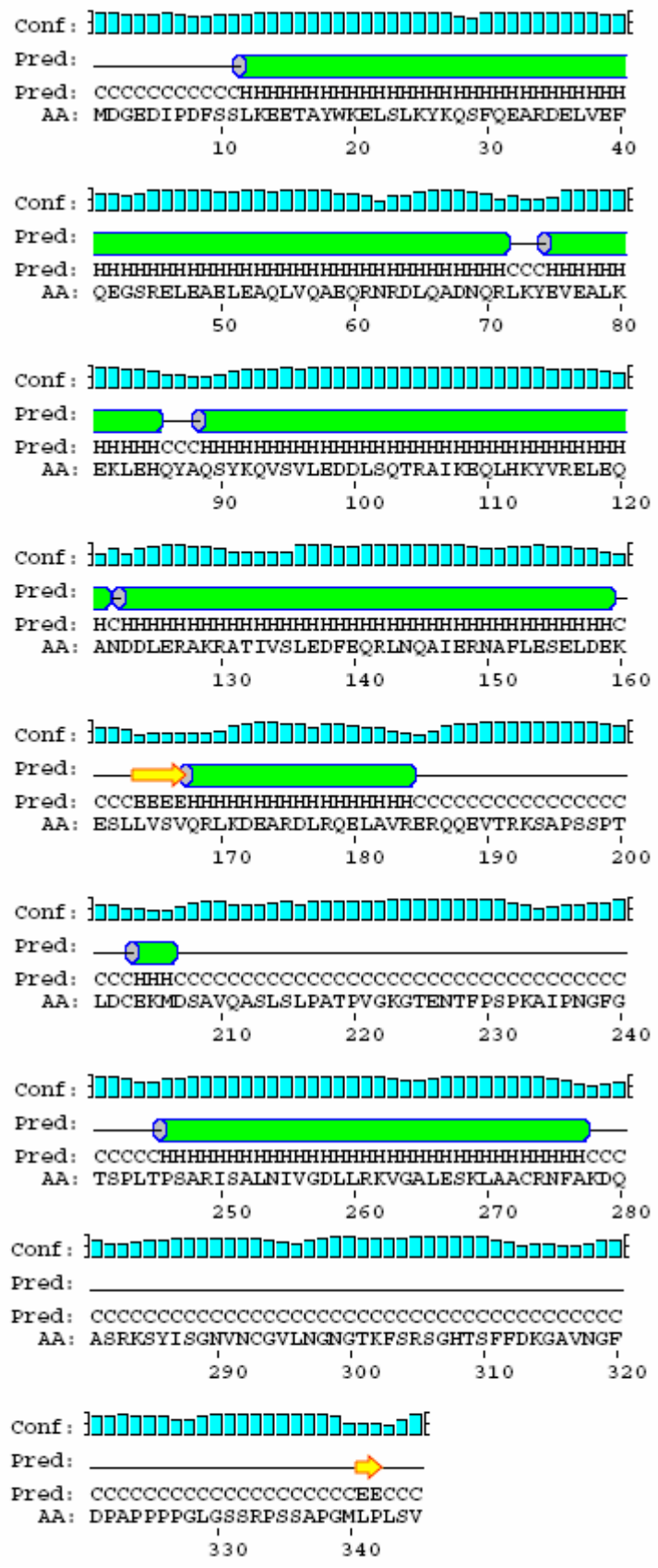
Conf:
Pred:
Pred: CCCCCCCCCCCHHHHHHHHHHHHHHHHHHHHHHHHHHHH
AA: MDGEDIPDFSSLKEETAYWKELSLKYKQSFQEARDELVEF
10 20 30 40
Conf:
Pred:
Pred: HHHHHHHHHHHHHHHHHHHHHHHHHHHHHHHHCCCHHHHHH
AA: QEGSRELEAELEAQLVQAEQRNRDLQADNQRLKYEVEALK
50 60 70 80
Conf:
Pred:
Pred: HHHHHCCCHHHHHHHHHHHHHHHHHHHHHHHHHHHHHHHH
AA: EKLEHQYAQSYKQVSVLEDDLSQTRAIKEQLHKYVRELEQ
90 100 110 120
Conf:
Pred:
Pred: HCHHHHHHHHHHHHHHHHHHHHHHHHHHHHHHHHHHHHHC
AA: ANDDLERAKRATIVSLEDFEQRLNQAIERNAFLESELDEK
130 140 150 160
Conf:
Pred:
Pred: CCCEEEEHHHHHHHHHHHHHHHHHCCCCCCCCCCCCCCCC
AA: ESLLVSVQRLKDEARDLRQELAVRERQQEVTRKSAPSSPT
170 180 190 200
Conf:
Pred:
Pred: CCCHHHCCCCCCCCCCCCCCCCCCCCCCCCCCCCCCCCC
AA: LDCEKMDSAVQASLSLPATPVGKGTENTFPSPKAIPNGFG
210 220 230 240
Conf:
Pred:
Pred: CCCCCHHHHHHHHHHHHHHHHHHHHHHHHHHHHHHHCCC
AA: TSPLTPSARISALNIVGDLLRKVGALESKLAACRNFAKDQ
250 260 270 280
Conf:
Pred:
Pred: CCCCCCCCCCCCCCCCCCCCCCCCCCCCCCCCCCCCCCC
AA: ASRKSYISGNVNCGVLNGNGTKFSRSGHTSFPDKGAVNGF
290 300 310 320
Conf:
Pred:
Pred: CCCCCCCCCCCCCCCCCCCCEECCC
AA: DPAPPPPGLGSSRPSSAPGMLPLSV
330 340

Figure 4.2.B: Predictions of the secondary structure of a) NDE1-SSSC and b) NDEL1-PLSV made using the program PSIPRED (McGuffin *et al.* 2000). "Conf" is the level of confidence the program has in its position (from 0% with no blue bar to 100% with a full height bar). "H" or a green cylinder indicates that the residue is predicted to be part of an α-helix. "E" or a yellow arrow indicates that the amino acid is part a β-strand. "C" or a thin black line indicates that this amino acid is classified by the program as "coiled", in this case meaning a loose structure (as opposed to a helical coiled-coil).

There are some differences between the predicted NDE1-SSSC and NDE1-KMLL structures, such as the presence of a couple of 2-3 amino acid "helices" near the C-terminus of NDE1. Given the extremely short nature of these predicted structures, less than the 3.6 residues required for one turn of an α-helix, it is doubtful that these correspond to genuine structures.

4.2.4 Lack of isoform specific α-helices in the full length isoforms

The amino acid sequences of the remaining three full length NDE1/NDEL1 isoforms (described in chapter 3) were investigated using PSIPRED. The results at the C-terminal tails of all five isoforms are shown in figure 4.2.C. None of the three NDE1 full length isoforms contains any predicted α-helixes within their unique C-terminal domains. With NDEL1, there are only minor predicted differences between the two isoforms, consisting of very short "structured" regions which may be false positives.

4.2.5 Helical structure of the NDE1-S2 isoform

The amino acid sequence of NDE1-S2 was analysed using PSIPRED. At least three separate α-helical regions were predicted to exist (see figure 4.2.D.a). One of these is found in the N-terminal half of the protein (amino acids 62-122) and is a fragment of the major coiled-coil seen in the full length NDE1 isoforms. In addition, two or more distinct α-helical regions were predicted at the extreme N- and C-termini of the protein (amino acids 13-46 and 184-235). Analysis of the same amino acid sequence using COILS however, detected only the one region with helix-forming potential, the

a)

b)

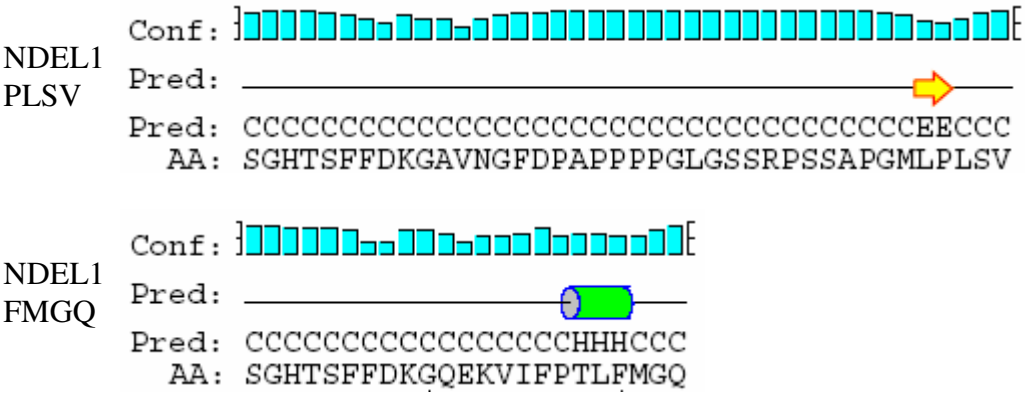

Figure 4.2.C: a) The complete amino acid sequences of each of the three full length NDE1 isoforms were analysed using PSIPRED. Only the results from the extreme C-terminus (amino acid 307 onwards) are displayed here. b) The two NDEL1 isoforms were analysed in the same way. Sequence is shown from amino acid 306 onwards. Green cylinders indicate α-helices, while yellow arrows indicate β-strands.

a)

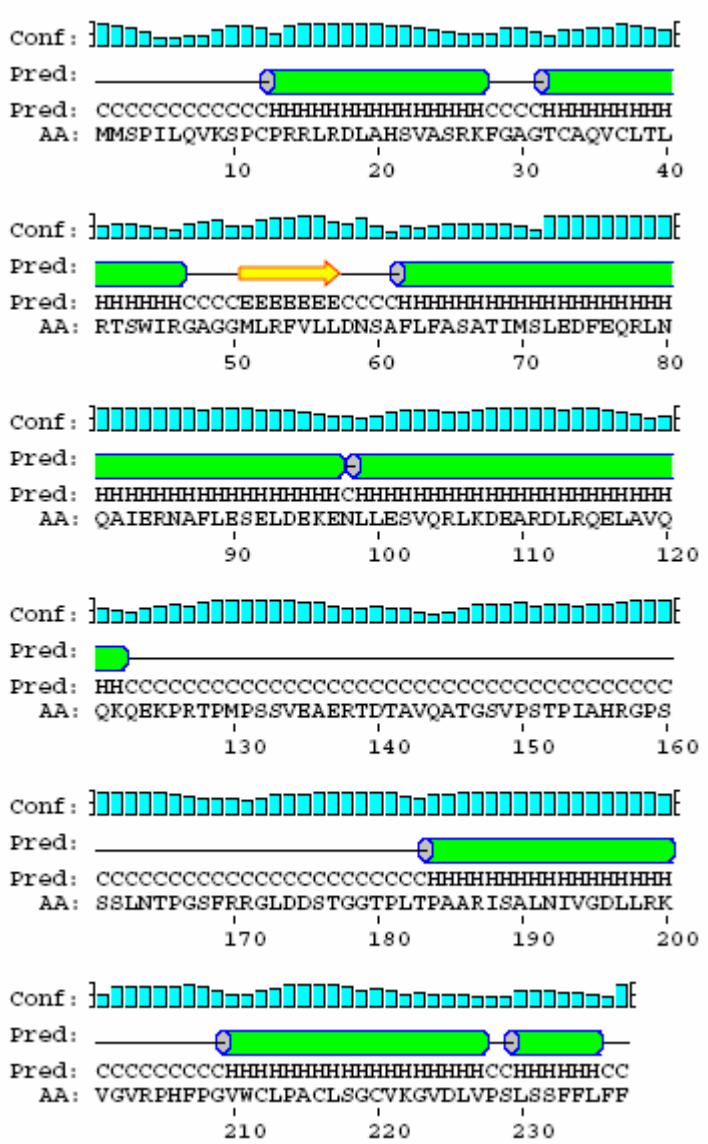

b)

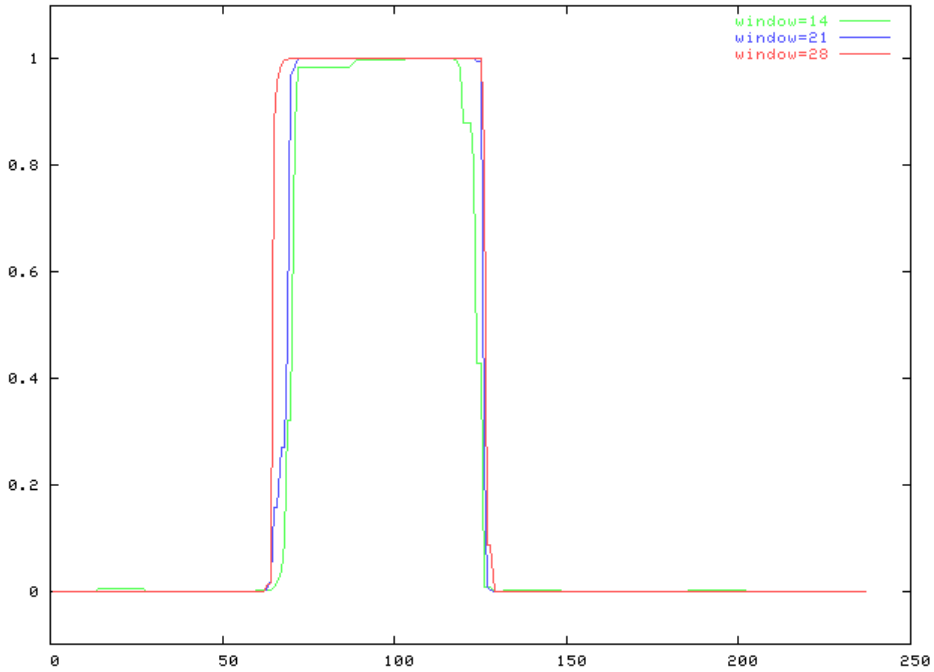

Figure 4.2.D: a) The secondary structure of NDE1-S2 as predicted by PSIPRED (McGuffin *et al.* 2000). Green cylinders indicate α-helices, yellow arrows indicate β-strands. b) The coil structure of NDE1-S2 as predicted by COILS (Lupas *et al.* 1991).

central coiled-coil which is conserved in full length NDE1 (see figure 4.2.D.b). Whether or not the remaining two helical regions exist *in vivo* is therefore unclear.

4.2.6 Helical structure of the theoretical NDE1-S1 isoforms

In order to investigate the potential effects of the *NDE1*-Δex3 transcript (see section 3.1.2) on the secondary structure of NDE1, a NDE1-S1a amino acid sequence was created by removing the first 132 amino acids from NDE1-KMLL. The KMLL C-terminal domain was chosen as it is homologous to that of the originally reported *Nde1*-Δex3 transcript in mouse (Sasaki *et al.* 2000). When this sequence was analysed using PSIPRED (figure 4.2.E.a) a structure similar to that of full length NDE1 was seen, with an α-helix at the extreme N-terminus, corresponding to the large N-terminal coiled-coil of full length NDE1. There are a few minor differences between this and the corresponding sections of full length NDE1, but none more than a few amino acids long. Analysis of the alternative S1a protein reveals it to be almost entirely formed of α-helices (figure 4.2.E.b), matching the corresponding regions of full length NDE1.

4.3 NDE1 and NDEL1 are predicted to have intrinsically unstructured regions

4.3.1 Introduction to intrinsically unstructured proteins

As stated previously, the rationale behind structural biology is that the function of a protein is derived form its 3-D structure. However many protein regions lack a definitive structure and are difficult or impossible to crystallise, as they are intrinsically unstructured or "disordered". It has been predicted that a third or more of eukaryotic proteins may have such "disordered" regions of 30 amino acids or longer (Dunker *et al.* 2000; Ward *et al.* 2004). Such regions are often flexible and are likely to aid in protein binding (Wright and Dyson 1999). Indeed the presence of disordered regions is enriched in "hub" proteins, those with many binding partners (Haynes *et al.* 2006), particularly those that are involved in large protein complexes (Hegyi *et al.* 2007), but possess few distinct protein binding sites themselves (Kim *et al.* 2008).

a) NDE1-S1a


Conf:
Pred:
Pred: CCHHHHHHHHHHHHHHHHHHHHHHHHHHHHHHHHHHHHHH
AA: MSLEDFEQRLNQAIERNAFLESELDEKENLLESVQRLKDE
10 20 30 40
Conf:
Pred:
Pred: HHHHHHHHHCCCCCCCCCCCCCCCCCCCCCHHHHCCCCC
AA: ARDLRQELAVQQKQEKPRTPMPSSVEAERTDTAVQATGSV
50 60 70 80
Conf:
Pred:
Pred: CCCCCCCCCCCCCCCCCCCCCCCCCCCCCCCCCCHHHHH
AA: PSTPIAHRGPSSSLNTPGSFRRGLDDSTGGTPLTPAARIS
90 100 110 120
Conf:
Pred:
Pred: HHHHHHHHHHHHHHHHHHHHHHHHHHHHCCCCCCCCCCC
AA: ALNIVGDLLRKVGALESKLASCRNLVYDQSPNRTGGPASG
130 140 150 160
Conf:
Pred:
Pred: CCCCCCCCCCCCCCCCCCCCCCCCCCCCCCCCCCCCCCC
AA: RSSKNRDGGERRPSSTSVPLGDKGLGKRLEFGKPPSHMSS
170 180 190 200
Conf:
Pred:
Pred: CCCCCCCCCCCCCC
AA: SPLPSAQGVVKMLL
210

b) NDE1-S1b

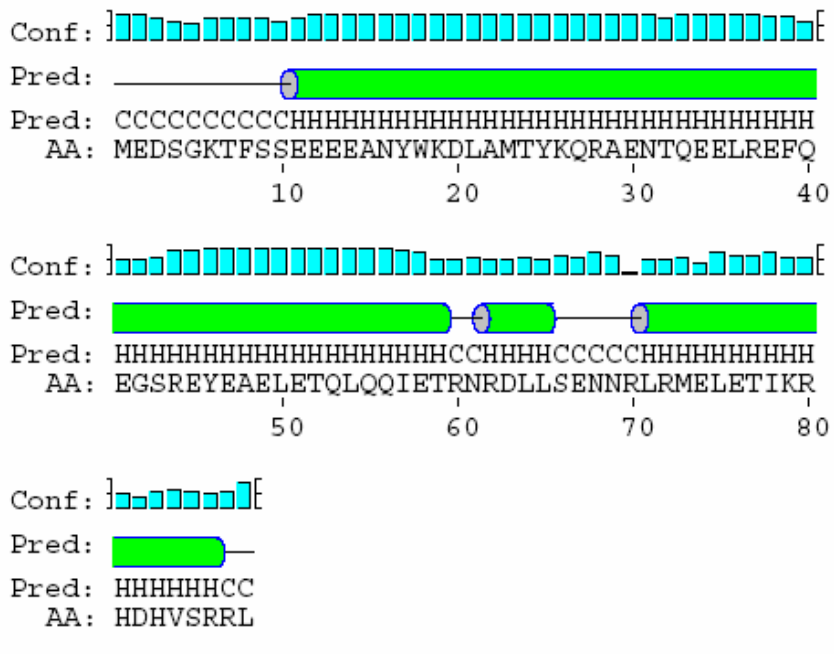

Figure 4.2.E: The secondary structure of a) NDE1-S1a and b) NDE1-S1b as predicted by PSIPRED (McGuffin *et al.* 2000). Green cylinders indicate α-helices.

Given that NDE1 and NDEL1 both have numerous protein interactors and at least two distinct protein binding sites (Sasaki *et al.* 2000), it would be interesting to know if they also possess intrinsically disordered regions.

4.3.2 Disordered regions of full length NDE1 and NDEL1

Various programs exist in order to predict disorder based on the amino acid sequence of a protein. As many of these work by comparing the amino acid sequence to large datasets of proteins known to have such intrinsic disorder, it is difficult to generate an independent dataset with which to analyse their accuracy. One technique which can be used to minimise the false positive rate of such analyses, however, is to analyse the same protein with a variety of different disorder prediction programs, which define disorder in a variety of different ways, and to look for regions which

are consistently predicted to be disordered by a majority of the programs (Dosztányi and Tompa 2008).

The amino acid sequences of NDE1-SSSC and NDEL1-PLSV were entered into nine online predictors of protein disorder (MacCallum; Linding *et al.* 2003; Ward *et al.* 2004; Coeytaux and Poupon 2005; Dosztányi *et al.* 2005b, a; Obradovic *et al.* 2005; Prilusky *et al.* 2005; Peng *et al.* 2006). Based on these results, a consensus was determined as to whether each amino acid position is predicted to be ordered or disordered in each of the two proteins. These results are shown in figure 4.3.A.

The predicted pattern of order and disorder in NDE1 and NDEL1 is similar. Each has a short predicted region of disorder at their immediate N-terminus, followed by two more substantial ones in the C-terminal half of the protein. Interestingly, these regions all corresponds to regions of poor sequence homology between NDE1 and NDEL1 (see figure 1.3.A). It therefore appears that the location of disordered regions in NDE1 and NDEL1 is evolutionarily conserved, while the exact amino acid composition of these regions is not. These variations in the disordered regions could potentially lead to differences in the functions of the two proteins.

4.3.3 Disorder variation across the full length isoforms

The complete amino acid sequences of NDE1-KMLL, NDE1-KRHS and NDEL1-FMGQ were next analysed using the disorder predictors, the C-terminal regions of which are shown in figure 4.3.B. Comparing these to the NDE1-SSSC and NDEL1-PLSV, variations in the level of disorder at the isoform specific C-terminal regions can be seen. Specifically a short predicted ordered region near the C-terminus of NDE1-SSSC is reduced in NDE1-KMLL and absent completely from NDE1-KRHS. Additionally, while NDEL1-PLSV has a disordered C-terminus, NDEL1-FMGQ has an ordered one.

4.3.4 Disorder in the short NDE1 isoforms

Given that much of the amino acid sequence of the NDE1-S2 isoform is not conserved in the full length variants (see figure 3.1.A), its sequence was also

a) NDE1-SSSC

```
Sequence      MEDSGKTFSSEEEEANYWKDLAMTYKQRAENTQEELREFQEGSREYEAELETQLQQIETR
Consensus     DDDDDDDDDDDDD-------------------------------------------------
DisEMBL HL    DDDDDDDDDDDDDDDD-----------------------------------------DDDD
DisEMBL L/C   DDDDDDDDDDDDD-----------------------------------------------
DisEMBL R465  DDDDDDDDDDDDDDD---------------------------------------------
DISO-PRED     DDDDDD-DDD-----------------------------------------------------
DISPROT VSL2  DDDDDDDDDDDDDDDDDDDDDDDDDDDDDDDDDDDDDDDDDDDDDDDDDDDDDDDDDDDD
DRIP-PRED     D-------------------------------------------------------------
FoldIndex     DDDDDDDDDDDDDDDDDDDDDDDDDDDDDDDDDDDDDDDDDDDDDDDDDDDDDDDDDDDD
IUPRED        DDDDDDDDDDDDD-----DDDDDD----DDDDDDDDDDDDDDDDD-DDDDDDD---DDD-
PreLink       -------------------------------------------------------------
                      10        20        30        40        50        60

Sequence      NRDLLSENNRLRMELETIKEKFEVQHSEGYRQISALEDDLAQTKAIKDQLQKYIRELEQA
Consensus     ------------------------------------------------------------
DisEMBL HL    DDDDDDDD------------------------------------------------------
DisEMBL L/C   ------------------------------------------------------------
DisEMBL R465  ------------------------------------------------------------
DISOPRED      ------------------------------------------------------------
DISPROT VSL2  DDDDDDDDDDDDDDDDDDDDDDDDDDDDDDDDDDDDDDDDDDDDDDDDDDDDDDDDDDDD
DRIP-PRED     ------------------------------------------------------------
FoldIndex     DDDDDDDDDDDDDDDDDDDDDDDDDDDDDDDDDDDDDDDDDDDDDDDDDDDDDDDDDDDD
IUPRED        DDD-DD-DD-------DD--------------DDDDDD-------------D----DD--
PreLink       ------------------------------------------------------------
                      70        80        90       100       110       120

Sequence      NDDLERAKRATIMSLEDFEQRLNQAIERNAFLESELDEKENLLESVQRLKDEARDLRQEL
Consensus     ------------------------------------------------------------
DosEMBL HL    ------------------------------------------------------------
DisEMBL L/C   ------------------------------------------------------------
DisEMBL R465  ------------------------------------------------------------
DISOPRED      ------------------------------------------------------------
DISPROT VSL2  DDDDDDDDDDDDDDDDDDDDDDDDDDDDDDDDDDDDDDDDDDDDDDDDDDDDDDDDDDDD
DRIP-PRED     ------------------------------------------------------------
FoldIndex     DDDDDDDDDDDDDDDDDDDDDDDDDDDDDDDDDDDDDDDDDDDDDDDDDDDDDDDDDDDD
IUPRED        ----DDDDDDDDD----D----------DD--D---D----DDDDDDD-----DDDDDDD
PreLink       ------------------------------------------------------------
                     130       140       150       160       170       180

Sequence      AVQQKQEKPRIPMPSSVEAERTDTAVQATGSVPSTPIAHRGPSSSLNTPGSFRRGLDDST
Consensus     DDDDDDDDDDDDDDDDDDDDDDDDDDDDDDDDDDDDDDDDDDDDDDDDDDD-----DDDD-
DisEMBL HL    DDDDDDDDDDDDDDDDDDDD----------DDDDDDDDDDDDDDDDDDDD----------
DisEMBL L/C   ----DDDDDDDDDDDDDDDDDDDDDDDDDDDDDDDDDDDDDDDDDDDDDDDDDDDDDDDD
DisEMBL R465  DDDDDDDDDDDDDDDDDDDDDDDDD---------------------------------
DISOPRED      ----DDDDDDDDDDDDDDDDDDDDDDDDDDD-DDDDDDDDDDDDDDDDDDDDDDDDD-
DISPROT VSL2  DDDDDDDDDDDDDDDDDDDDDDDDDDDDDDDDDDDDDDDDDDDDDDDDDDDDDDDDDDDD
DRIP-PRED     ---------------------------DDDDDDDDDDDDDDDDDDDD------DDDDD
FoldIndex     DDDDDDDDDDDDDDDDDDDD----DDDDDD-------------------------------
IUPRED        DDDDDDDDDDDDDDDDDDDDDDDDDDDDDDDDDDDDDDDDDDDDDDDDDDDDDDDDDDDD
PreLink       --DDDDDDDDDDDDDDDDDDDDDDDDDDDDDDDDDDDDDDDDDDDD--------------
                     190       200       210       220       230       240
```

```
Sequence      GGTPLTPAARISALNIVGDLLRKVGALESKLASCRNLVYDQSPNRTGGPASGRSSKNRDG
Consensus     ------------------------------------DDDDDDDDDDDDDDDDDDDDDDD
DisEMBL HL    ------------------------------------DDDDDDDDDDDDDDDDDDDDDDD
DisEMBL L/C   DDDDDDDD----------------------------DDDDDDDDDDDDDDDDDDDDDDD
DiSEMBL R465  ------------------------------------------DDDDDDDDDDDDDDDD
DISOPRED      ----------------------------------------DDDDDDDDDDDDDDDDDDD
DISPROT VSL2  DDDDDDD--------------------------DDDDDDDDDDDDDDDDDDDDDDDDD
DRIP-PRED     DDDDDDDDD--------------------------DDDDDDDDDDDDDDDDDDDD
FoldIndex     ----------------------------------DDDDDDDDDDDDDDDDDDDDDDDD
IUPRED        DDDDDDDDDDDDDD--------------------DDDDDDDDDDDDDDDDDDDDDDDD
PreLink       ------------------------------------------DDDDDDDDDDDDDDD
                     250       260       270       280       290       300

Sequence      GERRPSSTSVPLGDKGLDTSCRWLSKSTTRSSSSC
Consensus     DDDDDDDDDDDDD----------DDDDDDDDDDD
DISEMBL HL    DDDDDDDDDDDDDDDDDDDDDDDDDDDDDDDDDD
DisEMBL L/C   DDDDDDDDDDDDDDDDDDDDDDDDDDDDDDDDDD
DisEMBL R465  DDDDDDDDDDD-------------DDDDDDDDDD
DISOPRED      DDDDDDDDDDDD------------DDDDDDDDDD
DISPROT VSL2  DDDDDDDDDDDDDDDDDDDDDDDDDDDDDDDDDD
DRIP-PRED     DDDDDDDDDDDDD-----------DDDDDDDDDD
FoldIndex     ----------------------------------
IUPRED        DDDDDDDDDDDDD-------D-D----------DD
PreLink       DDDDDD-----------------DDDDDDDDDDD
                     310       320       330
```

b) NDEL1-PLSV

```
Sequence      MDGEDIPDFSSLKEETAYWKELSLKYKQSFQEARDELVEFQEGSRELEAELEAQLVQAEQ
Consensus     DDDDDD-------------------------------------------------------
DisEMBL HL    DDDDDDDDDDDDDDD-----------------------------------------------D
DisEMBL L/C   DDDDDDDDDDDDD-------------------------------------------------
DisEMBL R465  -------------------------------------------------------------
DISO-PRED     DDDDDD-D------------------------------------------------------
DISPROT VSL2  DDDDDDDDDDDDDDDDDDDDDDDDDDDDDDDDDDDDDDDDDDDDDDDDDDDDDDDDDDDD
DRIP-PRED     -------------------------------------------------------------
FoldIndex     -------------------------------------------------------------
IUPRED        DDDDDDD-----------------------------------------DDD----DDD
PreLink       -------------------------------------------------------------
                      10        20        30        40        50        60

Sequence      RNRDLQADNQRLKYEVEALKEKLEHQYAQSYKQVSVLEDDLSQTRAIKEQLHKYVRELEQ
Consensus     ------------------------------------------------------------
DisEMBL HL    DDDDDDDD------------------------------------------------------
DisEMBL L/C   -------------------------------------------------------------
DisEMBL R465  -------------------------------------------------------------
DISO-PRED     -------------------------------------------------------------
DISPROT VSL2  DDDDDDDDDDDDDDDDDDDDDDDDDDDDDDDDDDDDDDDDDDDDDDDDDDDDDDDDDDDD
DRIP-PRED     -------------------------------------------------------------
FoldIndex     -------------------------------------------------------------
IUPRED        -D----D-------------------------------------------------------
PreLink       -------------------------------------------------------------
                      70        80        90       100       110       120
```

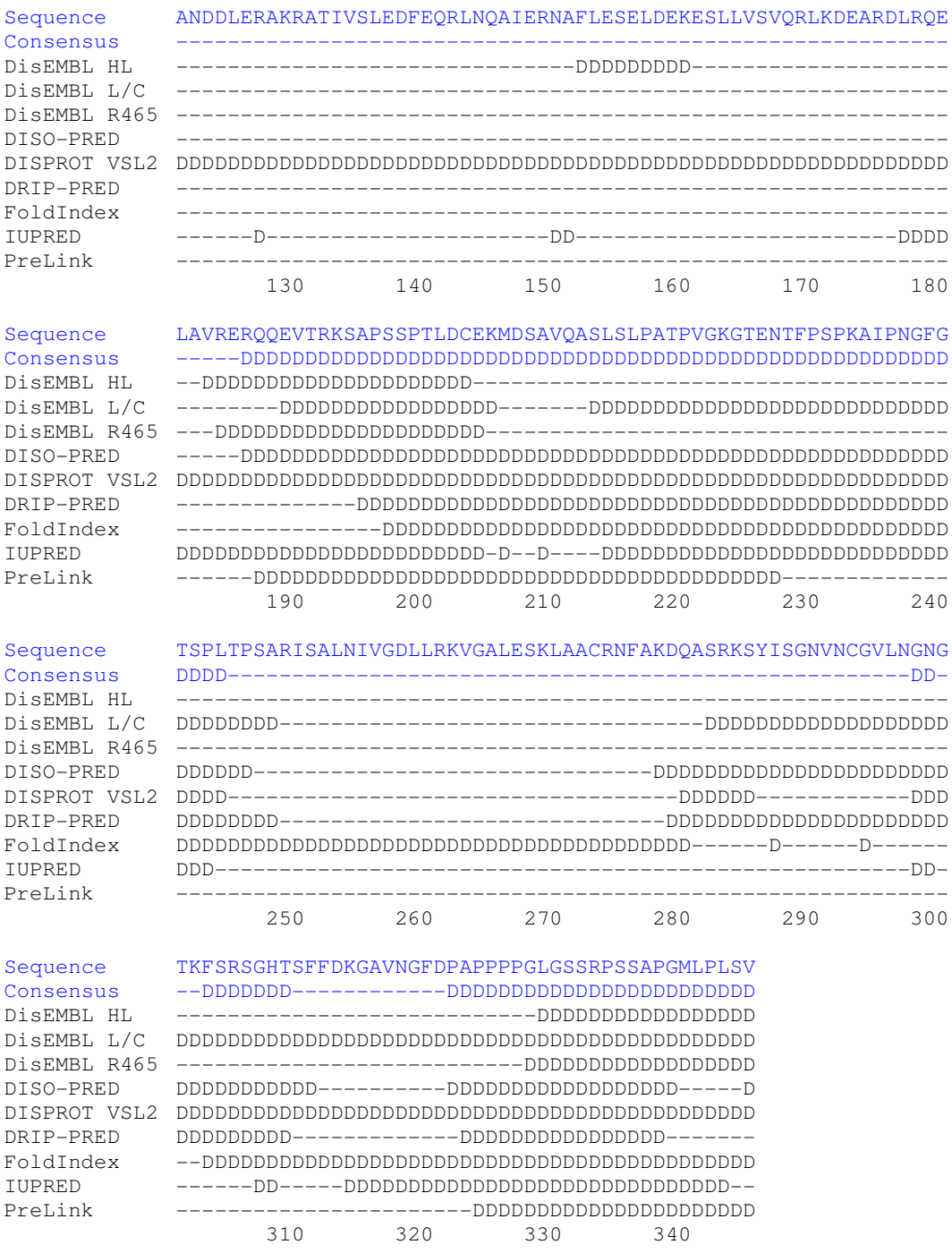

Figure 4.3.A: Predicted regions of order (-) and disorder (D) in a) NDE1-SSSC and b) NDEL1-PLSV. Predictions were made using nine separate programs and for each amino acid a consensus of either ordered or disordered was determined (shown in blue).

a)

NDE1-SSSC

```
Sequence     GERRPSSTSVPLGDKGLDTSCRWLSKSTTRSSSSC
Consensus    DDDDDDDDDDDDD----------DDDDDDDDDDDD
DISEMBL HL   DDDDDDDDDDDDDDDDDDDDDDDDDDDDDDDDDDD
DisEMBL L/C  DDDDDDDDDDDDDDDDDDDDDDDDDDDDDDDDDDD
DisEMBL R465 DDDDDDDDDDD-------------DDDDDDDDDDD
DISOPRED     DDDDDDDDDDDD-----------DDDDDDDDDDD
DISPROT VSL2 DDDDDDDDDDDDDDDDDDDDDDDDDDDDDDDDDDD
DRIP-PRED    DDDDDDDDDDDDD----------DDDDDDDDDDD
FoldIndex    -----------------------------------
IUPRED       DDDDDDDDDDDDD-------D-D----------DD
PreLink      DDDDDD-----------------DDDDDDDDDDD
                    310       320       330
```

NDE1-KMLL

```
Sequence     GERRPSSTSVPLGDKGLGKRLEFGKPPSHMSSSPLPSAQGVVKMLL
Consensus    DDDDDDDDDDDDDDDDD-----DDDDDDDDDDDDDDDDDDDDDDD
DISEMBL HL   DDDDDDDDDDDDDDDDD------DDDDDDDDDDDDDDDDDDDDDD
DisEMBL L/C  DDDDDDDDDDDDDDDDDDDDDDDDDDDDDDDDDDDDDDDDDDDDD
DisEMBL R465 DDDDDDDDDD---------------DDDDDDDDDDD---------
DISOPRED     DDDDDDDDDD-----------DDDDDDDDDDDDDDDD-------
DISPROT VSL2 DDDDDDDDDDDDDDDDDDDDDDDDDDDDDDDDDDDDDDDDDDDDD
DRIP-PRED    DDDDDDDDDDDDDDDD-------DDDDDDDDDDDDDDD-------D
FoldIndex    DDDDDDDDDDDDDDDDDDDDDDDDDDDDDDDDDDDDDDDDDDDDD
IUPRED       DDDDDDDDDDDDDDDDDDDDDDDDDDDDDDDDDDDDDDDDD----
PreLink      DDDDDD-----------------DDDDDDDDDDDDDDDDDDDDD
                    310       320       330       340
```

NDE1-KRHS

```
Sequence     GERRPSSTSVPLGDKGSVPSNKPLAGGENPPAPGKRHS
Consensus    DDDDDDDDDDDDDDDDDDDDDDDDDDDDDDDDDDDDD
DISEMBL HL   DDDDDDDDDDDDDDDDDDDDDDDDDDDDDDDDDDDDD
DisEMBL L/C  DDDDDDDDDDDDDDDDDDDDDDDDDDDDDDDDDDDDD
DisEMBL R465 DDDDDDDDDDDDDDD---------DDDDDDDDDDDDD
DISOPRED     DDDDDDDDDD----------DDDDDDDDDDDDDDDD
DISPROT VSL2 DDDDDDDDDDDDDDDDDDDDDDDDDDDDDDDDDDDDD
DRIP-PRED    DDDDDDDDDDDD----DDDDDDDDDDDDDDDDDDDDD
FoldIndex    DDDDDDDDDDDDDDDDDDDDDDDDDDDDDDDDDDDDD
IUPRED       DDDDDDDDDDDDDDDDDDDDDDDDDDDDDDDDDDDDD
PreLink      DDDDDDDDDDDDDDDDDDDDDDDDDDDDDDDDDDDDD
                    310       320       330
```

b)

NDEL1-PLSV

```
Sequence     TKFSRSGHTSFFDKGAVNGFDPAPPPPGLGSSRPSSAPGMLPLSV
Consensus    --DDDDDDD-----------DDDDDDDDDDDDDDDDDDDDDDD
DisEMBL HL   ----------------------------DDDDDDDDDDDDDDDDD
DisEMBL L/C  DDDDDDDDDDDDDDDDDDDDDDDDDDDDDDDDDDDDDDDDDDDD
DisEMBL R465 ---------------------------DDDDDDDDDDDDDDDDD
DISO-PRED    DDDDDDDDDDD----------DDDDDDDDDDDDDDDDDD-----D
DISPROT VSL2 DDDDDDDDDDDDDDDDDDDDDDDDDDDDDDDDDDDDDDDDDDDD
DRIP-PRED    DDDDDDDDD------------DDDDDDDDDDDDDDDD-------
FoldIndex    --DDDDDDDDDDDDDDDDDDDDDDDDDDDDDDDDDDDDDDDDD
IUPRED       ------DD-----DDDDDDDDDDDDDDDDDDDDDDDDDDDD--
PreLink      ----------------------DDDDDDDDDDDDDDDDDDDDD
                    310       320       330       340
```

NDEL1-FMGQ

```
Sequence     TKFSRSGHTSFFDKGQEKVIFPTLFMGQ
Consensus    D-----DDDD-----------------
DisEMBL HL   ------DDDDDDDDDDDDDDDDDDD
DisEMBL L/C  DDDDDDDDDDDDDDDDDDDDDDDDDD
DisEMBL R465 ---------------------------
DISO-PRED    DDDDDDDDDD-----------------
DISPROT VSL2 DDDDDDDDDDDDD------------DDD
DRIP-PRED    DDDDDDDDDDDD--------------DD
FoldIndex    D--------------------------
IUPRED       ------D--------------------
PreLink      ---------------------------
```

Figure 4.3.B: Disorder predictions for the unique C-terminal regions of the full length a) NDE1 and b) NDEL1 isoforms. All amino acid sequences are shown from residue 301 to the C-terminus.

---

analysed using the disorder prediction programs. Results are shown in figure 4.3.C.a. With the exception of a few amino acids at the extreme N-terminus, this splice form does not appear to have any novel predicted regions of disorder. It does however possess the central disordered region seen in the full length isoforms.

The potential for disorder in the theoretical NDE1-S1 proteins was also investigated. NDE1-S1b had short disordered regions at each end of the protein (see figure 4.3.C.a). NDE1-S1a had two distinct regions of disorder (see figure 4.3.C.c) which correspond to the central and C-terminal disordered regions of full-length NDE1-KMLL.

a) NDE1-S2

```
Sequence      MMSPILQVKSPCPRRLRDLAHSVASRKFGAGTCAQVCLTLRTSWIRGAGGMLRFVLLDNS
Consensus     DDDD------------------------------------------------------------
DisEMBL HL    DDDDDDDDDDDDDDDD-------DDDDDDDDDD--------------------------
DisEMBL L/C   DDDDDDDDDDDDDDDDD-----------------------------------------------
DisEMBL R465  ------------------------------------------------------------
DISO-PRED     DDDD-D------------------------------------------------------
DISPROT VSL2  DDDDDDDDDDDDDDDDDD-----------------------------------------
DRIP-PRED     DDDD----------------------DDDDDDDDD---------DD--------------
FoldIndex     ------------------------------------------------------------
IUPRED        ------------------------------------------------------------
PreLink       ------------------------------------------------------------
                      10        20        30        40        50        60

Sequence      AFLFASATIMSLEDFEQRLNQAIERNAFLESELDEKENLLESVQRLKDEARDLRQELAVQ
Consensus     ------------------------------------------------------------DDD
DisEMBL HL    ------------------------------------------------------------DDD
DisEMBL L/C   ------------------------------------------------------------
DisEMBL R465  ------------------------------------------------------------DDD
DISO-PRED     ------------------------------------------------------------DDD
DISPROT VSL2  ------------------DDDDDDDDDDDDDDDDDDDDDDDDDDDDDDDDDDDDDDDDDDD
DRIP-PRED     ------------------------------------------------------------
FoldIndex     ----------------------DDDDDDDDDDDDDDDDDDDDDDDDDDDDDDDDDDDDDDD
IUPRED        --------------------------DD------------DD--DD-----D-DDDDDDDD
PreLink       ------------------------------------------------------------DD
                      70        80        90       100       110       120

Sequence      QKQEKPRTPMPSSVEAERTDTAVQATGSVPSTPIAHRGPSSSLNTPGSFRRGLDDSTGGT
Consensus     DDDDDDDDDDDDDDDDDDDDDDDDDDDDDDDDDDDDDDDDDDDDDDDDDDDDDDDDD----
DisEMBL HL    DDDDDDDDDDDDDDDDDD---------DDDDDDDDDDDDDDDDDDDD-------------
DisEMBL L/C   -DDDDDDDDDDDDDDDDDDDDDDDDDDDDDDDDDDDDDDDDDDDDDDDDDDDDDDDDDDD
DisEMBL R465  DDDDDDDDDDDDDDDDDDDDDD-----------------------------------------
DISO-PRED     DDDDDDDDDDDDDDDDDDDDDDDD------DDDDDDDDDDDDDDDDDDDDDDDDD----
DISPROT VSL2  DDDDDDDDDDDDDDDDDDDDDDDDDDDDDDDDDDDDDDDDDDDDDDDDDDDDDDDDDDDD
DRIP-PRED     ---DDDDDDDDDDDDDDDDDDDDDDDDDDDDDDDDDDDDDDDDDDDDDDDDDDDDDDDD
FoldIndex     DDDDDDDDDDDDDDDDDDDDDDDDDDDD------------------------------
IUPRED        DDDDDDDDDDDDDDDDDDDDDDDDDDDDDDDDDDDDDDDDDDDDDDDDDDDDDDDDDDD
PreLink       DDDDDDDDDDDDDDDDDDDDDDDDDDDDDDDDDDDDDDDDDDDD----------------
                     130       140       150       160       170       180

Sequence      PLTPAARISALNIVGDLLRKVGVRPHFPGVWCLPACLSGCVKGVDLVPSLSSFFLFF
Consensus     ------------------------------------------------------------
DisEMBL HL    ------------------------------------------------------------
DisEMBL L/C   DDDDD------------DDDDDDDDDDDDDDDDDDDDDDDDDDDDDDDDDDDDDDD
DisEMBL R465  ------------------------------------------------------------
DISO-PRED     ------------------------------------------------------------
DISPROT VSL2  DDD-----------------------------------------------------DD
DRIP-PRED     DDDD------------------------DD----------------DDDDDDDDD
FoldIndex     ------------------------------------------------------------
IUPRED        D-----------------------------------------------------------
PreLink       ------------------------------------------------------------
                     190       200       210       220       230
```

b) NDE1-S1a

```
Sequence      MSLEDFEQRLNQAIERNAFLESELDEKENLLESVQRLKDEARDLRQELAVQQKQEKPRTP
Consensus     ----------------------------------------------------DDDDDDDDDDDD
Full length   ----------------------------------------------------DDDDDDDDDDDD
DisEMBL HL    ---------------DDDDDDDDDD----------------------DDDDDDDDDDDD
DisEMBL L/C   ---------------------------------------------------DDDDDDDD
DisEMBL R465  ----------------------------------------------------DDDDDDDDDDDD
DISO-PRED     DDDDDDD-----------------------------------------------DDDDDDDDDD
DISPROT VSL2  DDDDDDDDDDDDDDDDDDDDDDDDDDDDDDDDDDDDDDDDDDDDDDDDDDDDDDDDDDDDDDD
DRIP-PRED     ----------------------------------------------------------DDDDDDD
FoldIndex     DDDDDDDDDDDDDDDDDDDDDDDDDDDDDDDDDDDDDDDDDDDDDDDDDDDDDDDDDDDDDDDD
IUPRED        DDDDDDDD-DDDD-DDDDDDDDDDDDDDDDDDDDDDDD--DDDDDDDDDDDDDDDDDDDD
PreLink       ----------------------------------------------------DDDDDDDDDD
                      10        20        30        40        50        60

Sequence      MPSSVEAERTDTAVQATGSVPSTPIAHRGPSSSLNTPGSFRRGLDDSTGGTPLTPAARIS
Consensus     DDDDDDDDDDDDDDDDDDDDDDDDDDDDDDDDDDDDDDDDDDDDD---------------
Full length   DDDDDDDDDDDDDDDDDDDDDDDDDDDDDDDDDDDDD-----DDDD-------------
DisEMBL HL    DDDDDDDDD---------DDDDDDDDDDDDDDDDDDDD----------------------
DisEMBL L/C   DDDDDDDDDDDDDDDDDDDDDDDDDDDDDDDDDDDDDDDDDDDDDDDDDDDDDDDDD----
DisEMBL R465  DDDDDDDDDDDDDD-------------------------------------------------
DISO-PRED     DDDDDDDDDDDDDDD--------DDDDDDDDDDDDDDDDDDDDDDD---------------
DISPROT VSL2  DDDDDDDDDDDDDDDDDDDDDDDDDDDDDDDDDDDDDDDDDDDDDDDDDDDDDDDDD-----
DRIP-PRED     DDDDDDDDDDDDDDDDDDDDDDDDDDDDDDDDDDDDDDDDDDDDDDDDDDDDDDDDDD--
FoldIndex     DDDDDDDDDDDDDDDDDDDD-----------------------------------------
IUPRED        DDDDDDDDDDDDDDDDDDDDDDDDDDDDDDDDDDDDDDDDDDDDDDDDDDDDDDDDDDDD
PreLink       DDDDDDDDDDDDDDDDDDDDDDDDDDDDDDDDD--------------------------
                      70        80        90       100       110       120

Sequence      ALNIVGDLLRKVGALESKLASCRNLVYDQSPNRTGGPASGRSSKNRDGGERRPSSTSVPL
Consensus     ------------------------DDDDDDDDDDDDDDDDDDDDDDDDDDDDDDDDDD
Full length   ------------------------DDDDDDDDDDDDDDDDDDDDDDDDDDDDDDDDDD
DisEMBL HL    -------------------------DDDDDDDDDDDDDDDDDDDDDDDDDDDDDDDDD
DisEMBL L/C   -------------------------DDDDDDDDDDDDDDDDDDDDDDDDDDDDDDDDD
DisEMBL R465  ---------------------------------DDDDDDDDDDDDDDDDDDDDDDDDD--
DISO-PRED     ---------------------------------DDDDDDDDDDDDDDDDDDDDDDDDD--
DISPROT VSL2  ----------------------DDDDDDDDDDDDDDDDDDDDDDDDDDDDDDDDDDD
DRIP-PRED     ----------------------DDDDDDDDDDDDDDDDDDDDDDDDDDDDDDDDDDD
FoldIndex     ----------------------DDDDDDDDDDDDDDDDDDDDDDDDDDDDDDDDDDD
IUPRED        --------------------DDDDDDDDDDDDDDDDDDDDDDDDDDDDDDDDDDDD
PreLink       ---------------------------------DDDDDDDDDDDDDDDDDDDD------
                     130       140       150       160       170       180

Sequence      GDKGLGKRLEFGKPPSHMSSSPLPSAQGVVKMLL
Consensus     DDDDD-----DDDDDDDDDDDDDDDDDDDDDDD
Full length   DDDDD-----DDDDDDDDDDDDDDDDDDDDDDD
DisEMBL HL    DDDDD------DDDDDDDDDDDDDDDDDDDDDD
DisEMBL L/C   DDDDDDDDDDDDDDDDDDDDDDDDDDDDDDDDD
DisEMBL R465  --------------DDDDDDDDDDDD---------
DISO-PRED     ----------DDDDDDDDDDDDDDDDD-------
DISPROT VSL2  DDDDDDDDDDDDDDDDDDDDDDDDDDDDDDDDD
DRIP-PRED     D-----------DDDDDDDDDDDDDD--------
FoldIndex     DDDDDDDDDDDDDDDDDDDDDDDDDDDDDDDDD
IUPRED        DDDDDDDDDDDDDDDDDDDDDDDDDDDDDD----
PreLink       -----------DDDDDDDDDDDDDDDDDDDDDD
                    190       200       210
```

c) NDE1-S1b

```
Sequence      MEDSGKTFSSEEEEANYWKDLAMTYKQRAENTQEELREFQEGSREYEAELETQLQQIETR
Consensus     DDDDDDDDDDDDDD----------------------------------------------
Full length   DDDDDDDDDDDDDD----------------------------------------------
DisEMBL HL    DDDDDDDDDDDDDDD---------------------------------------DDDD
DisEMBL L/C   DDDDDDDDDDDD----------------------------------------------
DisEMBL R465  DDDDDDDDDDDDDDD-------------------------------------------
DISO-PRED     DDDDDD-D----------------------------------------------------
DISPROT VSL2  DDDDDDDDDDDDDDDDDDDDDDDDDDDDDDDDDDDDDDDDDDDDDDDDDDDDDDDDDD
DRIP-PRED     DDDDDDDD----------------------------------------------------
FoldIndex     DDDDDDDDDDDDDDDDDDDDDDDDDDDDDDDDDDDDDDDDDDDDDDDDDDDDDDDDDD
IUPRED        DDDDDDDDDDDDDD----DDDDDD----DDDDDDDDDDDDDDDDDDDDDDDDDDDDDD
PreLink       ----------------------------------------------------------
                       10        20        30        40        50        60

Sequence      NRDLLSENNRLRMELETIKRHDHVSRRL
Consensus     -----------------D---DDDDDDD
Full length   -------------------
DisEMBL HL    DDDDDDDDDDDDDDDDDDDDDDDDDDDD
DisEMBL L/C   -----------------DDDDDDDDDDD
DisEMBL R465  ----------------------------
DISO-PRED     ---------------------DDDDDDD
DISPROT VSL2  DDDDDDDDDDDDDDDDDDDDDDDDDDDD
DRIP-PRED     ---------------------DD--DDD
FoldIndex     DDDDDDDDDDDDDDDDDDDDDDDDDDDD
IUPRED        DDDDDDDDDDDDDDDDDD----D--D--
PreLink       ----------------------------
                       70        80
```

Figure 4.3.C: Predicted regions of order (-) and disorder (D) in a) NDE1-S2, b) NDE1-S1a and c) NDE1-S1b. For the NDE1-S1 isoforms, the order/disorder in the corresponding sections of full-length NDE1-KMLL is shown in red for comparison. Predictions were made using nine separate programs and for each amino acid a consensus of either ordered or disordered was determined (shown in blue).

4.4 Phosphorylation potential of NDE1 and NDEL1

4.4.1 Introduction to NDE1 and NDEL1 phosphorylation

Both NDE1 and NDEL1 have been predicted to have multiple phosphorylation sites (Feng *et al.* 2000; Kitagawa *et al.* 2000; Niethammer *et al.* 2000; Sweeney *et al.* 2001), and a number of these have been experimentally demonstrated (Niethammer *et al.* 2000; Yan *et al.* 2003; Rush *et al.* 2005; Beausoleil *et al.* 2006; Larkin *et al.* 2007; Mori *et al.* 2007). These are all summarised in table 4.4.A. The known effects

Site	Protein	Kinases	Reference
S198	NDEL1	cdc2	(Niethammer *et al.* 2000; Mori *et al.* 2007)
T219	NDEL1	cdc2, erk2	(Niethammer *et al.* 2000; Yan *et al.* 2003; Mori *et al.* 2007; Toyo-Oka *et al.* 2008)
S231	NDEL1	cdc2	(Niethammer *et al.* 2000; Mori *et al.* 2007)
S242	NDEL1	cdc2	(Yan *et al.* 2003)
T245	NDEL1	cdc2, erk2	(Yan *et al.* 2003)
S251	NDEL1	Aurora-A kinase	(Mori *et al.* 2007)
T279	NDE1	?	(Rush *et al.* 2005)
S282	NDE1	?	(Beausoleil *et al.* 2006)
*	NDE1	cdc2	(Yan *et al.* 2003)
?	NDEL1	cdk5	(Niethammer *et al.* 2000)
?	NDE1	erk2	(Yan *et al.* 2003)

Table 4.4.A: Known phosphorylation sites of the NDE1 and NDEL1 proteins from the literature. * NDE1 is known to be phosphorylated by cdc2 at one or more sites out of S196, T215, S231, S239 and T246, which correspond to S198, T219, S231, S242 and T245 of NDEL1.

---

of these phosphorylations in NDEL1 vary and include regulating its protein-protein interactions and cellular localisation (Niethammer *et al.* 2000; Yan *et al.* 2003; Toyo-Oka *et al.* 2005; Hirohashi *et al.* 2006a; Hirohashi *et al.* 2006b). Some are also known to be specific to certain points in the cell cycle (Toyo-Oka *et al.* 2005; Mori *et al.* 2007). It still remains to be determined, however, whether these phosphorylations are conserved between NDE1 and NDEL1, and we cannot rule out the existence of additional phosphorylation sites.

4.4.2 ScanSite analysis of full length NDE1 and NDEL1

In order to predict potential phosphorylation and other functional sites, the amino acid sequences of all five full length NDE1/NDEL1 isoforms were analysed using the online program ScanSite Motif Scan (Obenauer *et al.* 2003). The results are shown in table 4.4.B. A large number of potential phosphorylation sites were predicted, including two that have been demonstrated experimentally (Yan *et al.* 2003). Interestingly, no more than a third of these are conserved between NDE1 and NDEL1, in spite of their high amino acid similarity. Additionally, each of the unique

	NDE1 SSSC	NDE1 KMLL	NDE1 KRHS	NDEL1 PLSV	NDEL1 FMGQ
GSK3 Kinase (kinase site)	S10	S10	S10	-	-
PKC delta (kinase site)	-	-	-	S23	S23
PKC epsilon (kinase site)	-	-	-	S29	S29
DNA PK (kinase site)	**T32**	**T32**	**T32**	-	-
ATM kinase (kinase site)	T32	T32	T32	-	-
Calmodulin dependent kinase (kinase site)	-	-	-	S95	S95
ATM kinase (kinase site)	-	-	-	**S102**	**S102**
DNA PK (kinase site)	-	-	-	S102	S102
PKC delta (kinase site)	**T131**	**T131**	**T131**	T132	T132
PKA (kinase site)	T131	T131	T131	T132	T132
Erk D-domain (kinase binding group)	-	-	-	**V134**	**V134**
PKC epsilon (kinase site)	S134	S134	S134	-	-
Casein kinase 2 (kinase site)	**S154**	**S154**	**S154**	**S155**	**S155**
GSK3 Kinase (kinase site)	**T191**	**T191**	**T191**	-	-
Erk1 (kinase site)	-	-	-	S198	S198
Abl SH3 (SH3 site)	-	-	-	P217	P217
Cdk5 (kinase site)	T215	T215	T215	-	-
Cdc2 kinase (kinase site)	T215	T215	T215	*T219*	T219
Erk1 (kinase site)	T228	T228	T228	-	-
PKC alpha/beta/gamma (kinase site)	**S231**	**S231**	**S231**	-	-
Erk1 binding (kinase binding site)	-	-	-	P232	P232
GSK3 Kinase (kinase site)	-	-	-	T241	T241
Casein kinase 1 (kinase site)	T243	T243	T243	-	-
Cdk5 (kinase site)	T246	T246	T246	T245	T245
Cdc2 kinase (kinase site)	**T246**	**T246**	**T246**	*T245*	T245
Erk1 (kinase site)	T246	T246	T246	**T245**	**T245**
PKA (kinase site)	S306	S306	S306	-	-
Ajt kinase (kinase site)	S309	S309	S309	-	-
Erk D-domain (kinase binding group)	**V310**	**V310**	**V310**	-	-
PKC epsilon (kinase site)	-	-	-	S310	S310
PKC delta (kinase site)	-	-	-	S310	S310
PKC alpha/beta/gamma (kinase site)	-	-	-	-	S310
Clk2 kinase (kinase site)	-	-	-	-	S310
Itk SH3 (SH3 site)	-	-	-	P324	-
Nck 2nd SH3 (SH3 site)	-	-	-	**P324**	-
Src SH3 (SH3 site)	-	-	-	P324	-
Cb1-assocaited protein SH3 (SH3 site)	-	-	-	**P327**	-
PKC alpha/beta/gamma (kinase site)	**T328**	-	-	-	-
GSK3 Kinase (kinase site)	-	-	-	S331	-
Itk SH3 (SH3 site)	-	-	**P331**	-	-
Nck 2nd SH3 (SH3 site)	-	-	P331	P332	-
14-3-3 (pS/T binding group)	-	-	-	**S336**	-

Table 4.4.B: Predicted phosphorylation sites and functional residues of full length NDE1 and NDEL1 isoforms, according to Scansite (Obenauer *et al.* 2003) on a stringency setting of “Medium” (normal type) or “High” (bold).

Conservation across orthologues of NDE1 (green), NDEL1 (yellow), both (blue) or between individual isoforms only (purple) are indicated. * Phosphorylation has been demonstrated experimentally (Yan *et al.* 2003).

C-termini is distinct in its predicted functional sites from the others, although one potential SH3-binding site appears to be shared between the NDE1-KRHS and NDEL1-PLSV isoforms.

4.4.3 Many of the potential phosphorylation sites are evolutionarily conserved

Potential phosphorylation sites and other motifs that are conserved throughout various species are likely to serve an evolutionarily conserved function *in vivo*. The amino acid sequences of homologues of NDE1-KMLL and NDEL1-PLSV from various species were therefore analysed using ScanSite. The majority of the predicted sites are conserved across most of the mammals studied, and some are seen in additional species (table 4.4.C).

4.4.4 Phosphorylation of the short NDE1 isoforms

The amino acid sequences of NDE1-S2, NDE1-S1a and NDE1-S1b were also investigated using ScanSite (see table 4.4.D). All three proteins are predicted to be phosphorylated in the same manner as the corresponding sections of full length NDE1. In addition, NDE1-S2 is predicted to contain two unique phosphorylatable serine residues in its N-terminal region while NDE1-S1b has such a site near its C-terminus.

a) NDE1-KMLL

Site / Motif	Human	Monkey	Cow	Mouse	Rat	Chicken	Xenopus
Casein kinase 2	S10	S10	S10	**S10**	S10	-	-
DNA PK	**T32**	**T32**	**T32**	**T32**	**T32**	-	-
ATM kinase	T32	T32	T32	T32	T32	-	-
PKC delta	**T131**	**T131**	**T131**	**T131**	**T131**	-	**T132**
PKA	T131	T131	T131	T131	T131	-	T132
PKC epsilon	S134	S134	S134	S134	S134	-	S135
Casein kinase 2	**S154**	**S154**	**S154**	**S154**	**S154**	**S155**	**S155**
GSK3 Kinase	**T191**	**T191**	T191	-	**T191**	-	-
Cdk5	T215	T215	T215	T215	T215	T216	-
Cdc2 kinase	T215	T215	T215	T215	T215	T216	-
Erk1	T228	T228	T228	T228	T228	-	S231
PKC alpha/beta/gamma	**S231**	**S231**	**S231**	-	-	-	S234
Casein kinase 1	T243	T243	T243	T243	-	-	-
Cdk5	T246	T246	T246	T246	T246	-	T249
Cdc2 kinase	**T246**	**T246**	**T246**	**T246**	**T246**	T247	T249
Erk1	T246	T246	T246	T246	T246	-	-
PKA	S306	S306	-	-	-	-	-
Ajt kinase	S309	S309	-	-	-	-	-
Erk D-domain	**V310**	**V310**	**V310**	V310	V310	-	-

Table 4.4.C: Predicted phosphorylation and other functional sites in orthologues of a) NDE1-KMLL and b) NDEL1-PLSV from various species. All sites shown were predicted by Scansite (Obenauer *et al.* 2003) on a stringency setting of "Medium". Sites in bold were also detectable using the "High" setting. Blue indicates conservation in primates, yellow conservation in other mammals and green conservation in other species. Functional sites found only in non-human species were excluded from the table.

b) NDEL1-PLSV

Site / Motif	Human	Chimp	Orangutan	Monkey	Dog	Rabbit	Mouse	Rat	Chicken	Xenopus	Zebrafish	Bee
PKC delta	S23	S23	S23	S88	S87	S23	S23	S23	S23	-	-	-
PKC epsilon	S29	S29	S29	S94	S93	S29	S29	S29	S29	-	-	-
Calmodulin-dependent kinase	S95	S95	S95	S160	S159	S95	S95	S95	-	-	-	-
ATM kinase	**S102**	**S102**	**S102**	**S167**	**S166**	**S102**	**S102**	**S102**	**S102**	-	-	-
DNA PK	S102	S102	S102	S167	S166	S102	S102	S102	S102	-	-	-
PKC delta	T132	T132	T132	T197	T196	T132	T132	T132	T132	T132	T132	-
PKA	T132	T132	T132	T197	T196	T132	T132	T132	T132	T132	T132	-
Erk D-domain	**V134**	**V134**	**V134**	**V199**	**V198**	**V134**	**V134**	**V134**	**V134**	**V134**	-	-
Casein kinase 2	**S155**	**S155**	**S155**	**S220**	**S219**	**S155**	**S155**	**S155**	S155	**S155**	**S155**	S151
Erk1	S198	S198	S198	S263	S262	S198	S198	S198	S198	S198	S198	-
Abl SH3	P217	P217	P217	P282	P281	P217	P217	P217	P217	-	P217	-
Cdc2 kinase	T219	T219	T219	T284	T283	T219	T219	T219	T219	-	T219	-
Erk1 binding	P232	P232	P232	P297	P296	P232	P232	P232	P232	P232	-	-
GSK3 Kinase	T241	T241	T241	T306	-	T241	T241	T241	T241	T241	-	-
Cdk5	T245	T245	T245	T310	-	T245	T245	T245	T245	T245	T246	T257
Cdc2	T245	T245	T245	T310	T309	T245	T245	T245	T245	T245	**T246**	T257
Erk1	**T245**	**T245**	**T245**	**T310**	T309	**T245**	**T245**	**T245**	**T245**	**T245**	T246	T257
PKC	S310	S310	S310	S375	S374	S310	-	-	-	-	-	-
PKC	S310	S310	S310	S375	S374	S310	**T310**	**T310**	-	-	-	-
Itk	P324	P324	P324	-	P324	P324	P324	P324	-	-	-	-
Nck 2nd SH3	**P324**	**P324**	**P324**	-	**P388**	**P324**	**P324**	**P324**	-	-	-	-
Src SH3	P324	P324	P324	-	P388	P324	P324	P324	-	-	-	-
Cb1-assocaited protein SH3	**P327**	**P327**	**P327**	-	**P391**	**P327**	**P327**	**P327**	-	-	-	-
GSK3 Kinase	S331	S331	S331	-	S395	S332	S331	S331	-	S332	-	-
Nck 2nd SH3	P332	-	-	P387	-	-	-	-	-	P335	-	-
14-3-3 binding	**S336**	**S336**	**S336**	**S403**	**S400**	**S336**	**S336**	**S336**	**S334**	-	S335	-

	KMLL	S1a	S1b	S2
Casein kinase 2 (kinase site)	S10	-	S10	-
DNA PK (kinase site)	**T32**	-	**T32**	-
ATM kinase (kinase site)	T32	-	T32	-
PKC alpha/beta/gamma (kinase site)	-	-	T77	-
Cdk5 (kinase site)	-	-	-	S10
Cdc2 kinase (kinase site)	-	-	-	S10
PKC zeta (kinase site)	-	-	-	S22
PKC delta (kinase site)	**T131**	-	-	-
PKA (kinase site)	T131	-	-	-
PKC epsilon (kinase site)	S134	-	-	-
Casein kinase 2 (kinase site)	**S154**	**S22**	**-**	**S91**
GSK3 Kinase (kinase site)	**T191**	**T59**	**-**	**T128**
Cdk5 (kinase site)	T215	T83	-	T152
Cdc2 kinase (kinase site)	T215	T83	-	T152
Erk1 (kinase site)	T228	T96	-	T165
PKC alpha/beta/gamma (kinase site)	**S231**	**S99**	**-**	**S168**
Casein kinase 1 (kinase site)	T243	T111	-	T180
Cdk5 (kinase site)	T246	T114	-	T183
Cdc2 kinase (kinase site)	**T246**	**T114**	**-**	**T183**
Erk1 (kinase site)	T246	T114	-	T183
PKA (kinase site)	S306	S174	-	-
Ajt kinase (kinase site)	S309	S177	-	-
Erk D-domain (kinase binding group)	**V310**	**V178**	-	-

Table 4.4.D: Predicted phosphorylation and other functional sites in full length NDE1-KMLL, NDE1-S1a, NDE1-S1b and NDE1-S2. All sites shown were predicted by Scansite (Obenauer *et al.* 2003) on a stringency setting of "Medium" (normal type) or "High" (bold).

4.5 Specific NDE1 isoforms have potential nuclear localisation signals

4.5.1 Introduction to nuclear localisation

To date most studies have described NDE1 and NDEL1 as being found at the cytoplasm or at the centrosome (see section 1.3.3.1), however two papers have mentioned low levels of NDE1 and/or NDEL1 being seen at the nucleus (Yan *et al.* 2003; Suzuki *et al.* 2007). In both papers antibodies were used that were unable to differentiate between NDE1 and NDEL1. One interpretation of these results is that one or more isoforms of NDE1 or NDEL1 localise to the nucleus, but that these isoforms are undetectable using the antibodies used to date by other research groups. An indication of whether a protein has the ability to enter the nucleus can be gained

by searching for a nuclear localisation signal (NLS). These are conserved motifs consisting of a number of basic amino acids which are recognised by karyopherins, a class of transport receptor which are required to transport proteins through the nuclear pore complex and into the nucleus (Sorokin *et al.* 2007).

4.5.2 NDE1-KMLL may localise to the nucleus

Analysis of the full length sequences of the NDE1 isoforms using the online signal prediction programs PredictNLS and PSORT II (Nakai and Horton 1999; Cokol *et al.* 2000) detected no potential canonical NLS sequences. However, NDE1-KMLL does contain an $RRX_{10}KX_3KR$ motif that is very similar to a bipartite NLS (Dinesh Soares, personal communication). Such an NLS typically consists of two basic residues, followed 10 residues later by at least three basic amino acids out of five (Robbins *et al.* 1991). The NDE1-KMLL motif follows a similar pattern, except that its C-terminal three basic amino acids are spread over six. Searching the NLS database (Nair *et al.* 2002), it can be seen that this exact motif is also present in at least two other proteins, CHDM and HIPK2, both of which are also found in the nucleus (Kim *et al.* 1999; Khattak *et al.* 2002). In the latter example the motif contains the only basic residues of a 61 amino acid fragment which is known to be essential for nuclear localisation. When a more generalised $(K/R)_2X_{10}(K/R)X_3(K/R)_2$ motif is searched for, the NLS database yields 620 proteins from various species (including multiple orthologues of some proteins), of which 76.6% are known to be found at the nucleus. This proportion of nuclear proteins is considerably higher than that across the complete database of 21,498 proteins, of which 21.9% are known to localise to the nucleus (Nair *et al.* 2002).

It therefore appears likely that this motif is capable of acting as a functional NLS. Interestingly, the final two basic amino acids of the NDE1-KMLL NLS are found only in the isoform-specific exon 8 and not in any other NDE1 or NDEL1 isoform examined. Looking at homologues of NDE1 from other species, these basic residues are conserved in several mammals (although the exact spacing between the basic residues varies slightly in rodents) adding evidence that the motif may have an *in vivo* function (figure 4.5).

```
Homo sapiens          RRPSSTSVPLGDKGLGKR
Pan troglodytes       RRPSSTSVSLGDKGLGKR
Bos taurus            RRPGGSNVPLGDKGLGKR
Mus musculus          RRPG--STSVGDKGSGKR
Rattus norvegicus     RRPG--STAVGDKGSGKR
Gallus gallus         ETRMSPHQPLCDTGLVKR
Xenopus tropicallis   NRLSMASGSSVEKGLIKR
Aspergillus nidulans TRTQGDSRPSSRTSFSSS
NDEL1 (Human)         KFSRSGHTSFFDKGAVNG
```

Figure 4.5: The five basic residues (shown in red) that make up the potential NLS in human NDE1-KMLL are seen to be conserved in orthologues from several mammalian species. They are not conserved in orthologues from some other species or in human NDEL1-PLSV. Alignment performed using CLUSTALW (Thompson *et al.* 1994)

4.5.3 NDE1-S2 may localise to the nucleus

Analysis by eye of the NDE1-S2 sequence revealed a PRRXR motif at amino acids 13-17. This motif, consisting of a proline followed shortly by three basic residues out of four is similar to a classic NLS signal. It is found in a region that is not conserved with any of the full length isoforms. NDE1-S2 may therefore have a unique function in the nucleus. This motif could be detected using PSORT II, but not PredictNLS (Nakai and Horton 1999; Cokol *et al.* 2000). A search for "PRRXR" on the NLS database yielded 216 proteins (including multiple orthologues of some proteins) of which 52.8% are known to localise to the nucleus, a greater than two fold enrichment compared to the 21.9% seen in the complete database (Nair *et al.* 2002).

4.5.4 No sign of localisation signals in NDEL1

The amino acid sequences of NDEL1-PLSV and NDEL1-FMGQ were investigated for potential NLS sequences, however none were found either by manual examination or using the NLS prediction software.

4.6 Discussion

4.6.1 The secondary structure of full-length NDE1 and NDEL1

NDEL1 is known to have a large N-terminal coiled-coil (Derewenda *et al.* 2007), and from this analysis NDE1 is predicted to possess a similar structure. This coiled-coil is known to be the site of self-association in NDEL1 (Sasaki *et al.* 2000), and also contains the LIS1 binding site of both NDE1 and NDEL1 (Feng *et al.* 2000; Yan *et al.* 2003). In addition, both proteins are predicted to have a shorter helical or coiled-coil region near the C-terminus. This region also appears to be involved in protein interactions, with NDEL1 known to bind DISC1 as well as probably cytoplasmic dynein heavy chain and dynamitin at this site (Sasaki *et al.* 2000; Brandon *et al.* 2004; Liang *et al.* 2004). This structure is very well conserved between NDE1 and NDEL1, in spite of poor conservation in the surrounding regions, implying it to be of evolutionary significance.

In both proteins, the two coiled-coils/helices appear to be separated by a disordered region. The lack of overlap between predicted helices and predicted disordered regions reinforces the validity of both analyses. This central disordered region could theoretically act as a flexible "linker", potentially allowing the protein to adjust its structure to accommodate the interactions of different protein binding partners. This fits well with a previously published observation that "hub" proteins (those with numerous protein interactors) frequently have sizable regions of disorder, but that their interaction domains themselves are often structured (Kim *et al.* 2008). This region is known to contain phosphorylation sites in both NDE1 and NDEL1 (Niethammer *et al.* 2000; Yan *et al.* 2003; Mori *et al.* 2007). Several proteins may also bind in this region, notably 14-3-3ε and katanin p60, the protein products of the *YWHAE* and *KATNA1* genes respectively (Toyo-Oka *et al.* 2003; Toyo-Oka *et al.* 2005). Binding of these proteins could potentially impart structure on this region.

Previously published analyses of the location and function of disordered proteins showed that they are most commonly found in the nucleus, however they are also enriched among microtubule-bound proteins and in those involved in mitosis,

neurogenesis and protein transport (Vucetic *et al.* 2007; Xie *et al.* 2007). Thus the identification of disordered regions within NDE1 and NDEL1 fits well with their roles in these processes.

The crystal structure of the N-terminal coiled-coil of NDEL1 has already been solved (Derewenda *et al.* 2007). However, as a consequence of these disordered regions, it is unlikely that a complete structure for full length of NDE1 or NDEL1 will be producible using these techniques.

It is interesting to note that the helical regions of NDE1 and NDEL1 are exceptionally well conserved, suggesting that these regions contain the "core" functional elements of the proteins e.g. self association, LIS1 binding and potentially dynein, dynactin and/or DISC1 binding. In comparison, the disordered regions show poor amino acid similarity between the two proteins. In both proteins, the disordered regions are of similar length which, combined with the flexible nature of such regions, suggests NDE1 and NDEL1 are likely to be of a similar basic structure. However any protein interactors which bind in this region, such as 14-3-3ε or katanin p60 (Toyo-Oka *et al.* 2003; Toyo-Oka *et al.* 2005) may be specific to one or the other of NDE1 and NDEL1 and may impose specific three-dimensional configurations on the region, thus altering the relative positions of the two helical regions. All of this information is summarised in figure 4.6.A.

4.6.2 NDE1 and NDEL1 are predicted to be heavily phosphorylated

Full length NDE1 and NDEL1 are both predicted to be phosphorylated by a variety of kinases and at a number of different sites. A summary of all the predicted phosphorylation sites and their conservation is shown in table 4.6 and figure 4.6.A. Only two of the previously demonstrated phosphorylations (cdc2 at threonine residues 219 and 245 of NDEL1) are predicted by this analysis, although changing the stringency of the prediction program to "Low" does predict the remaining experimentally demonstrated cdc2 sites. This implies a high false negative rate, and also emphasises that experimental data is needed to confirm these predictions.

a) NDE1

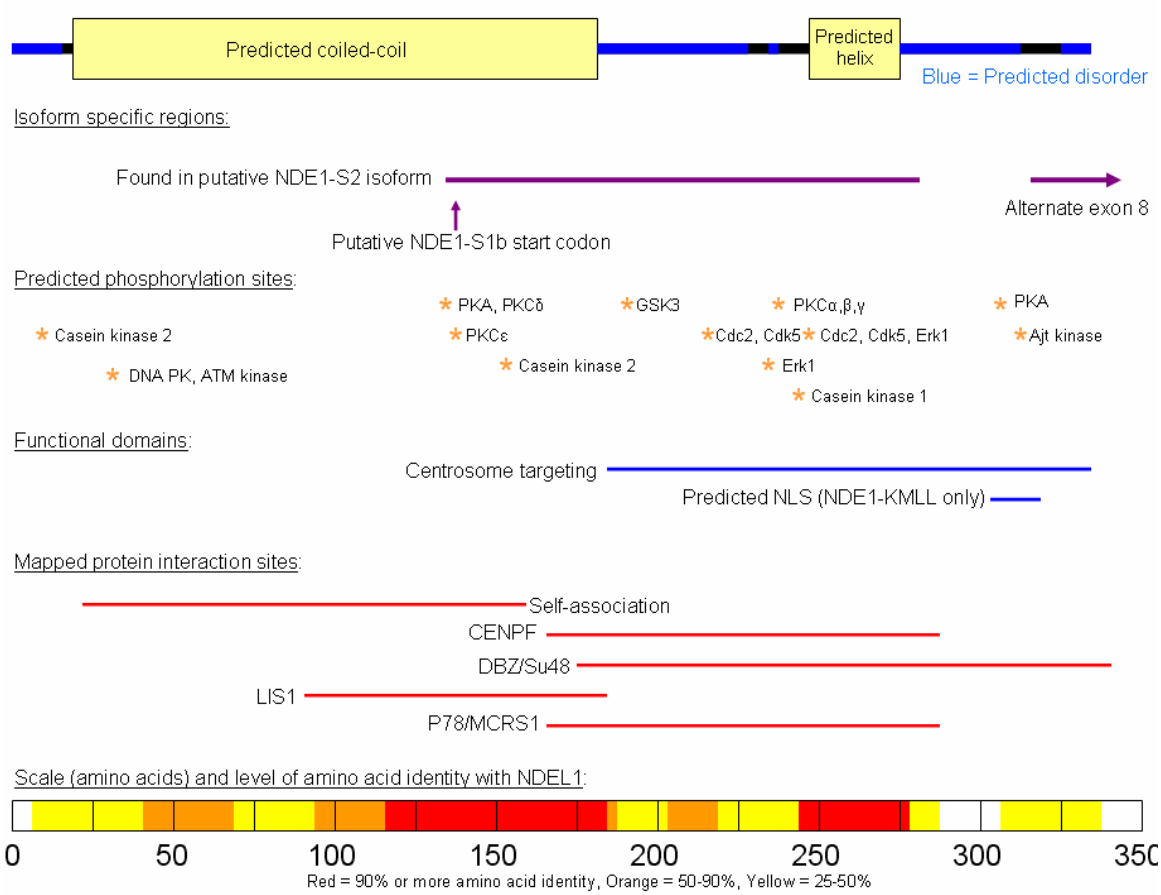

Figure 4.6.A Schematics of the structural and functional regions of a) NDE1 and b) NDEL1, derived from both this analysis and from published experimental evidence. Isoforms shown are human NDE1-SSSC and NDEL1-PLSV. Data was taken from the following papers: (Feng *et al.* 2000; Niethammer *et al.* 2000; Sasaki *et al.* 2000; Toyo-Oka *et al.* 2003; Yan *et al.* 2003; Brandon *et al.* 2004; Liang *et al.* 2004; Nguyen *et al.* 2004a; Hayashi *et al.* 2005; Soukoulis *et al.* 2005; Toyo-Oka *et al.* 2005; Guo *et al.* 2006; Hirohashi *et al.* 2006a; Hirohashi *et al.* 2006b; Derewenda *et al.* 2007; Mori *et al.* 2007; Shen *et al.* 2008b)

b) NDEL1

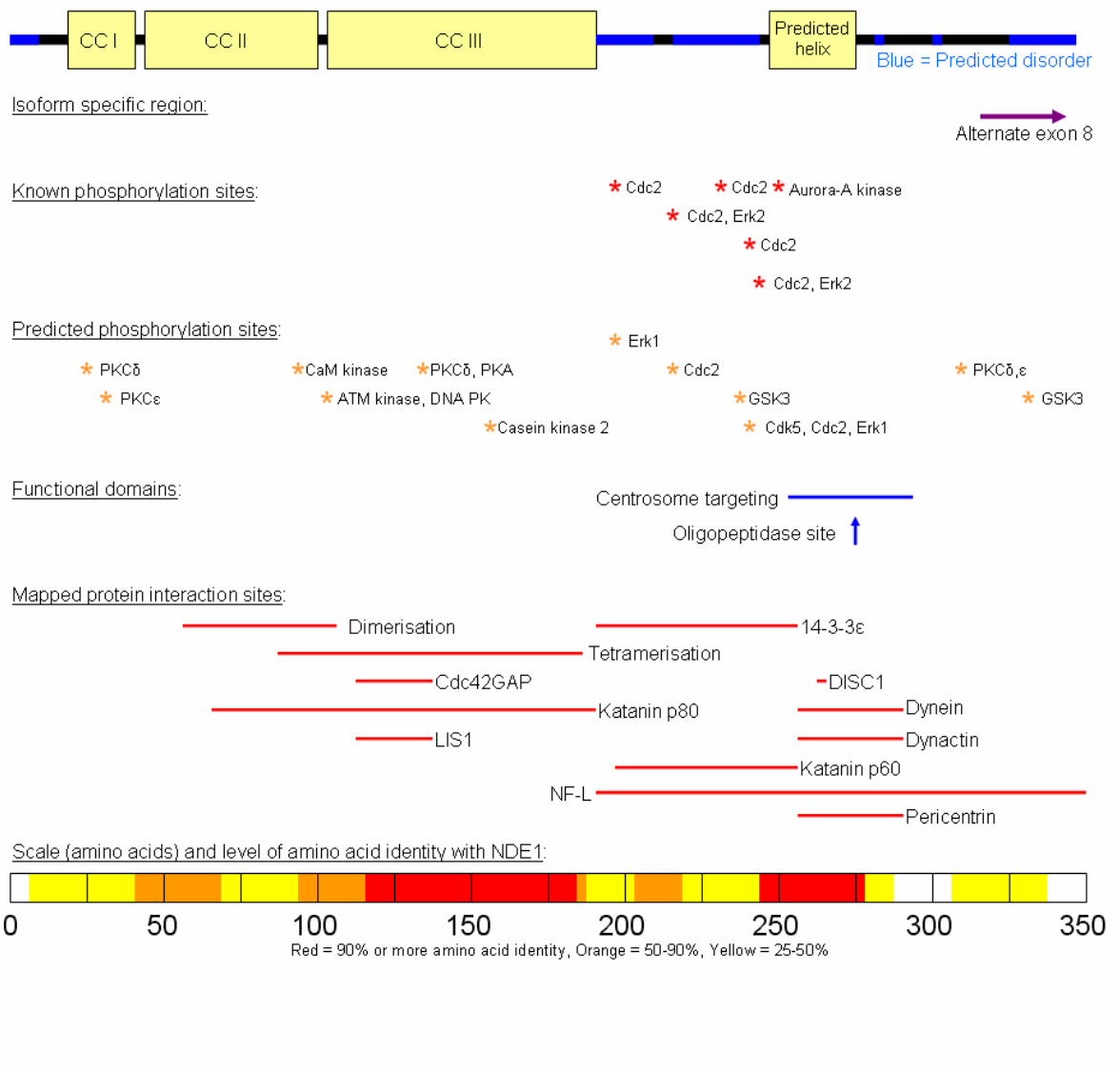
CC I
CC II
CC III
Predicted helix
Blue = Predicted disorder
Isoform specific region:
Alternate exon 8
Known phosphorylation sites:
Cdc2
Cdc2
Aurora-A kinase
Cdc2, Erk2
Cdc2
Cdc2, Erk2
Predicted phosphorylation sites:
Erk1
PKCδ
CaM kinase
PKCδ, PKA
Cdc2
PKCδ,ε
PKCε
ATM kinase, DNA PK
GSK3
GSK3
Casein kinase 2
Cdk5, Cdc2, Erk1
Functional domains:
Centrosome targeting
Oligopeptidase site
Mapped protein interaction sites:
Dimerisation
14-3-3ε
Tetramerisation
Cdc42GAP
DISC1
Katanin p80
Dynein
LIS1
Dynactin
Katanin p60
NF-L
Pericentrin
Scale (amino acids) and level of amino acid identity with NDE1:
0
50
100
150
200
250
300
350
Red = 90% or more amino acid identity, Orange = 50-90%, Yellow = 25-50%

a) NDE1

Site	Potential kinases	Conserved in NDEL1?	Species conservation
S10	Casein kinase 2	-	++
T32	**DNA PK**, ATM kinase	-	++
T131	PKA, **PKCδ**	+	+++
S134	PKCε	-	+++
S154	**Casein kinase 2**	+	+++
T191	**GSK3**	-	++
T215	Cdc2, Cdk5	+	++
T228	Erk1	-	+++
S231	PKCα,β,γ	-	+
T243	Casein kinase 1	-	++
T246	**Cdc2**, Cdk5, Erk1	+	+++
S306	PKA	-	+
S309	Ajt kinase	-	++

b) NDEL1

Site	Potential kinases	Conserved in NDE1?	Species conservation
S23	PKCδ	-	++
S29	PKCε	-	++
S95	CaM kinase	-	++
S102	**ATM kinase**, DNA PK	-	++
T132	PKCδ, PKA	+	+++
S155	**Casein kinase 2**	+	+++
S198	Erk1	-	+++
T219	Cdc2	+	+++
T241	GSK3	-	++
T245	Cdk5, Cdc2, **Erk1**	+	+++
S310	PKCδ,ε	-	++
S331	GSK3	-	++

Table 4.6: Summary of predicted phosphorylation sites in full length a) NDE1 and b) NDEL1. Kinases in bold type indicates this site was predictable by a "High" stringency scan, sites in bold type indicates that this has been demonstrated experimentally in the literature. Species conservation of a given site is rated as "+" if it is conserved in primates, "++" if it is conserved in mammals and "+++" if it is conserved more widely.

Four potential phosphorylation sites are conserved between NDE1 and NDEL1, all of which show good conservation across species, implying that these residues are of potential evolutionary importance. However at least twice as many such predicted sites on each protein are not present in the other one, and this includes a number of sites with strong species conservation. Given the high degree of amino acid similarity between NDE1 and NDEL1, this could imply that they perform similar functions within the cell, but that each has its own evolutionarily conserved mechanisms of post-translational regulation.

One result of particular interest it that NDE1 is predicted to be phosphorylated by protein kinase A (PKA) on two sites, one of which is also present in NDEL1. PKA is a cAMP-dependent kinase and is regulated by a negative feedback system involving PDE4B (see figure 1.2.D), a known DISC1-interactor and independent candidate gene for major mental illness (Millar *et al.* 2005b; Pickard *et al.* 2007; Fatemi *et al.* 2008; Numata *et al.* 2008a; Numata *et al.* 2008b). One of these sites (T131) is well conserved across species and so may play a key regulatory function. The other (S306) is found only in primates and so, if genuine, is likely to supply an extra level of regulation that has only developed recently in evolution.

Such phosphorylation prediction programs have a high false positive rate, normally calculated on a kinase-by-kinase basis. For example, Scansite on a stringency setting of medium has been reported to return 98.1% of serine and threonine residues as not being substrate sites for PKA correctly, i.e. 1.9% of such residues are reported as false positives. Therefore as NDE1-SSSC and NDEL1-PLSV contain 58 and 43 serine/threonine residues respectively, this analysis could be expected to incorrectly predict 1.10 sites on NDE1 and 0.87 sites on NDEL1 as being phosphorylatable by PKA. Therefore the fact that NDEL1 is predicted to contain a single PKA phosphorylation site is unremarkable, while the fact that NDE1 was predicted to contain two such sites warrants further attention.

Such theoretical analysis of phosphorylation should therefore be treated primarily as hypothesis-generating, revealing the locations of potential sites which should then be

investigated experimentally in order to determine whether or not they are genuine. The two putative PKA sites described in NDE1, T131 and S306, will be subjected to such an investigation in chapter 7.

4.6.3 Potential roles of the isoform specific C-terminal tails

In chapter 3, six NDE1/NDEL1 full length isoforms were described, each with a unique C-terminal "tail" domain. To date, no protein has been shown to definitively bind NDE1 or NDEL1 in these regions, although for a few proteins it is a possibility (Nguyen *et al.* 2004b; Hirohashi *et al.* 2006a; Hirohashi *et al.* 2006b).

Interestingly two of the isoforms, NDE1-KRHS and NDEL1-PLSV are also predicted to have isoform-specific aliphatic-proline-X-aliphatic-proline motifs which may allow them to bind to proteins with SH3 domains. NDEL1-PLSV is also predicted to have a 14-3-3 binding region. Other potential differences between the isoforms include the potential for protein kinase C α, β and γ to phosphorylate NDE1-SSSC and glycogen synthase kinase 3 to phosphorylate NDE1-PLSV. One major difference in the NDE1-KMLL isoform is the presence of a putative conserved NLS, suggesting that this isoform may perform unique cellular functions within the nucleus.

Together these analyses point to the isoform-specific C-terminal tails having little effect on the basic functions of NDE1 and NDEL1. However, they are likely to add an extra layer of regulation, in terms of phosphorylation, localisation and potentially protein binding, that would affect only a subpopulation of full length NDE1 or NDEL1 proteins in any given cell. In order to determine whether these predicted features are genuine or not, the isoforms should be cloned into expression vectors, so that these putative isoform-specific features can be investigated experimentally, for example by the use of site-directed mutagenesis to knock-out potential kinase sites.

4.6.4 A model of full length NDE1 and NDEL1 in the cell

NDEL1 is well established to exist as a dimer, forming a parallel coiled-coil with its N-terminal coiled domain (Efimov and Morris 2000; Sasaki *et al.* 2000; Maiolica *et al.* 2007). More recently, it has been shown that NDEL1 dimers can multimerise further *in vitro*, with the coiled coils of two dimers binding in an anti-parallel manner to form a tetramer (Derewenda *et al.* 2007). The existence of an *in vivo* tetramer remains to be investigated. NDE1 is also believed to dimerise (Feng and Walsh 2004), and the high conservation of sequence with NDEL1 suggests tetramerisation is also likely. Due to the conserved structure and amino acid sequence of the multimerisation domains of NDE1 and NDEL1, it may even be possible that they form heterodimers or heterotetramers. Regardless, the basic structure of any NDE1 and/or NDEL1 multimer is likely or be similar. Figure 4.6.B shows predicted models of such dimers and tetramers based on the analyses performed in this chapter and experimental evidence from the literature.

The dimer and tetramer both appear to consist of a "backbone" coiled-coil domain, the centre of which may bind LIS1. At the end of the dimer backbone are two flexible "arms", each containing a protein binding helix. In the tetramer, four such arms come out from part-way along the backbone. The positioning of these arms is likely to be phosphorylation-dependent, facilitating the binding of various combinations of proteins. At the tip of each arm is an exposed isoform-specific region which is likely to provide regulation.

In a NDE1/NDEL1 heteromultimer, it is also possible that the extreme N-terminus, which varies between the two proteins, may provide some additional regulatory function, as NDE1 and NDEL1 are predicted to have unique phosphorylation sites in this region. Similarly the unique natures of the NDE1/NDEL1 "arms" may provide for protein-specific phosphorylation and binding partner interactions in these regions, thus imposing three-dimensional structures on these arms which are specific for NDE1 or NDEL1.

a)

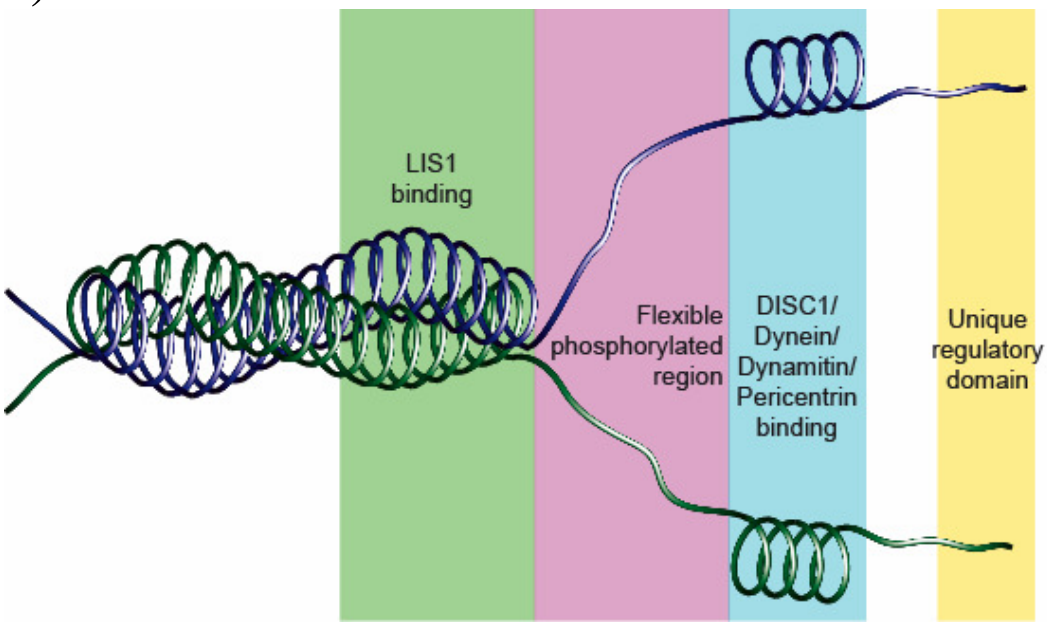

b)

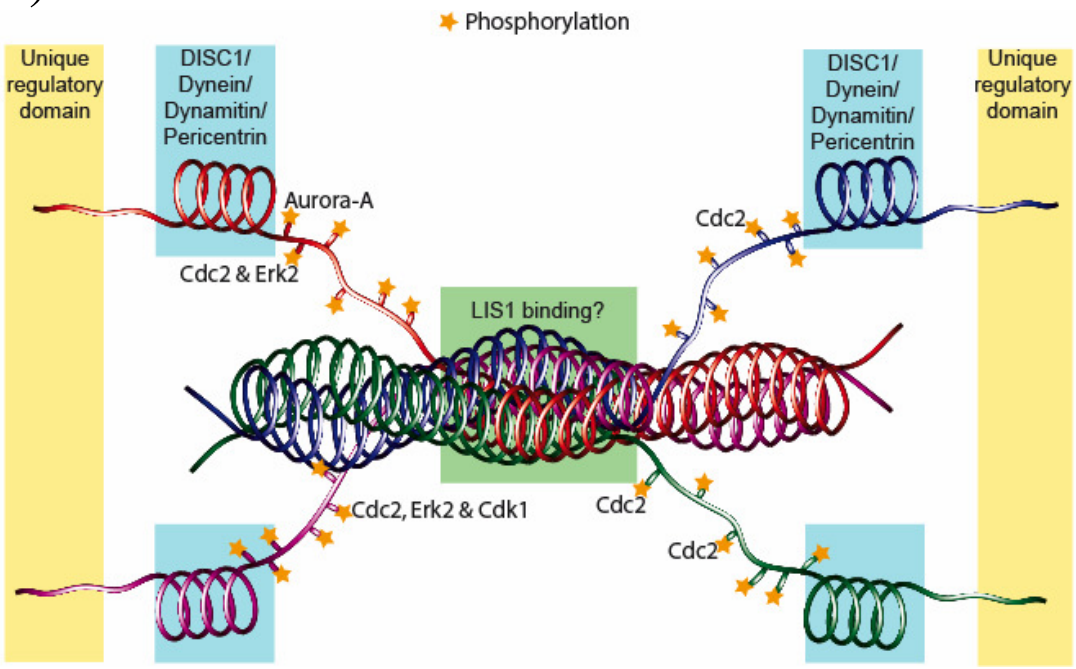

Figure 4.6.B: A model of NDE1/NDEL1 dimers (a) and tetramers (b). The binding domain information on the diagram incorporates known protein-binding sites from both NDEL1. On the tetramer, experimentally demonstrated NDEL1 phosphorylation sites are shown. "LIS1", "dynein", "dynactin" and "pericentrin" refer to the protein products of the *PAFAH1B1*, *DYNC1H1/DYNC2H1*, *DCTN2* and *PCTN2* genes respectively. Graphics by Sarah West.

4.6.5 The NDE1-S1 isoforms

In the previous chapter, PCR was used to detect the *NDE1*-Δex3 transcript in several cDNA samples. This demonstrates that at least some examples of such alternatively spliced transcripts exist, although such an analysis is not quantitative and does not demonstrate whether or not expression is substantial compared to the full length NDE1 variants. In order to investigate potential functions for *NDE1*-Δex3, the hypothetical NDE1-S1a protein, which uses methionine-133 as an alternate start site and is based on this transcript, was analysed. Alternatively, the NDE1-S1b protein could be translated, consisting of exons 1 and 2 of full length NDE1, plus a short amount of novel sequence derived from exon 4 (see figure 3.1.D). This too was analysed. There were no significant predicted secondary structure differences between either of these and the corresponding sections of full length NDE1.

The LIS1-binding site on NDEL1 is within amino acids 114-133 (Yan *et al.* 2003). Assuming that this site is conserved in NDE1 (and the amino acid sequence here is virtually identical), then it can be presumed that both NDE1-S1a and NDE1-S1b should be unable to bind LIS1. It is thus interesting to note that *Nde1*-Δex3 was identified in a yeast-2-hybrid screen for mouse Lis1 interactors (Sasaki *et al.* 2000). The reason for this anomaly remains a mystery. The most likely explanation is that the interaction was a false positive, possibly due to contamination by other *Nde1* transcripts.

Additionally, based on the corresponding region on NDEL1 (Sasaki *et al.* 2000), loss of the N-terminal 132 amino acids is likely to prevent NDE1 homodimerisation. Should NDE1 possess any cellular functions that can only occur when it is in a monomeric state, such as the ability of the NDEL1 monomer to act as an oligopeptidase (Hayashi *et al.* 2005), then these would occur preferentially in the NDE1-S1a isoform.

Looking at the NDE1-S1b isoform, based on the known binding sites of full length NDE1 and NDEL1 (see table 4.1), it should still be able to form dimers with itself and/or full length NDE1. It would not be able to bind any of the NDE1/NDEL1

protein interactors for which a binding site has been described to date, however. Theoretically it could therefore compete for dimer-formation with full length NDE1. It is difficult to predict the properties of a full length/S1b heterodimer, but interaction with LIS1 is unlikely, as it is known to bind preferentially to NDEL1 dimers (Tarricone *et al.* 2004). It can be theorised that this heterodimer may therefore have similar cellular properties to a full length NDE1 monomer, except that it would be unable to easily convert to a conventional dimer. In addition, NDE1-S1b is predicted to contain a unique residue which can be phosphorylated by PKC, providing an additional layer of regulation.

4.6.6 The NDE1-S2 isoform

The NDE1-S2 protein is predicted to consist of one or more helical regions (figure 4.2.D), separated by a central disordered region (figure 4.3.C). As was the case with the full length isoforms, this suggests that it may bind multiple protein interactors (probably using both helical regions) with the disordered region allowing for additional flexibility. Many of the potential phosphorylation sites of full length NDE1 are conserved in NDE1-S2, implying that post-translational regulation is likely to be similar (see table 4.4.D). The remainder of NDE1-S2 is predicted to be sparsely phosphorylated by comparison, although two potential unique phosphorylation sites are seen.

No NDE1-interactors have been mapped entirely to the regions contained within NDE1-S2, but it is likely that CENPF would be able to bind it (Soukoulis *et al.* 2005). Based on known NDEL1 interactors in this region, it is also possible that NDE1-S2 may be able to bind 14-3-3ε and katanin p60 (Toyo-Oka *et al.* 2003; Toyo-Oka *et al.* 2005). However, based on their established NDEL1 binding sites, dynein, LIS1 and DISC1 are all unlikely to be NDE1-S2 interactors (Sasaki *et al.* 2000; Yan *et al.* 2003; Brandon *et al.* 2004). The presence of a putative NLS, however, implies that this short variant may well be a nuclear protein and therefore perform different functions to those of many of the full length isoforms. This is consistent with the potential loss of binding regions related to microtubule and centrosome-based proteins.

Chapter 5 - The cellular localisation of the endogenous NDE1 protein

5.1 Introduction

The cellular localisation of NDEL1 has been well studied, with the protein being reported most commonly at the centrosome (Niethammer *et al.* 2000; Toyo-Oka *et al.* 2003; Toyo-Oka *et al.* 2005; Guo *et al.* 2006; Kamiya *et al.* 2006; Toyo-Oka *et al.* 2008), along the microtubule network (Sasaki *et al.* 2000; Yamaguchi *et al.* 2004) and in cell processes (Niethammer *et al.* 2000; Sasaki *et al.* 2000; Toyo-Oka *et al.* 2003; Nguyen *et al.* 2004b; Toth *et al.* 2008). Localisation of NDEL1 to the synapse (Niethammer *et al.* 2000) and the mitochondria (Brandon *et al.* 2005) has also been reported.

In contrast, data regarding NDE1 localisation is currently limited to studies which made use of over-expressed protein. Such studies have suggested that, like NDEL1, NDE1 is found primarily at the centrosome of interphase cells (Feng *et al.* 2000; Feng and Walsh 2004; Hirohashi *et al.* 2006a; Hirohashi *et al.* 2006b), although large cytoplasmic puncta of NDE1 have also been reported (Yan *et al.* 2003). A thorough study of the localisation of endogenous NDE1 has yet to be performed.

5.2 Generation of novel NDE1 and NDEL1 constructs

NDE1-SSSC and NDEL1-PLSV inserts were cloned from pDEST-40-NDE1-SSSC and pDEST-40-NDEL1-PLSV vectors (see table 2.3.B), using primers that added a *BamHI* restriction digest site to the 5' end of the cDNA and a *SalI* site at the 3' end (see table 2.5.A for primer details). These inserts and the pGEX-6PI vector, were then digested using *BamHI* and *SalI* enzymes. Phenol-chloroform extraction was then performed on the clones and vector. The vector was treated with shrimp alkaline phosphatase (SAP) and the clones were inserted into the vector through a ligation reaction. The resulting constructs were named pGEX-6PI-NDE1 and pGEX-

6PI-NDEL1. Sequencing was performed in order to confirm the nature of the derived plasmid vectors using the NDE1-Seq, NDEL1-Seq and 6PI-Seq primers as appropriate. These vectors when then used to produce GST-NDE1 and GST-NDEL1 protein in bacteria.

5.3 Investigating NDE1 localisation using commercial antibodies

5.3.1 The localisation of over-expressed NDE1

Before attempting to analyse the cellular distribution of endogenous NDE1, previously published investigations of the expression patterns of over-expressed NDE1 were replicated. V5-tagged NDE1-SSSC was over-expressed in COS7 cells and immunocytochemistry was performed. In these cells NDE1 localised to a number of large structures in the cell body (see figure 5.3.A.a) which do not resemble any reported NDEL1 localisation. These structures may therefore be protein aggregates, an artefact of protein over-expression, and thus not represent the expression pattern of endogenous NDE1.

When the protein was instead over-expressed in HEK293T cells, a pattern more resembling that of endogenous NDEL1 was seen (see figure 5.3.A.b). In these cells the V5-NDE1-SSSC took on a primarily diffuse pattern in the cell body, often with a large peri-nuclear puncta. Given the known expression patterns of endogenous NDEL1, this is likely to be the centrosome, although co-staining with a marker would be required in order to be certain. Other punctate structures, similar to those in COS7 but smaller and less abundant, were sometimes also seen. A similar expression pattern was seen when V5-NDE1-SSSC was instead over-expressed in SH-SY5Y cells, except that in approximately 10% of cells there were also signs of large nuclear NDE1 structures (see figure 5.3.A.c).

5.3.2 Commercially available NDE1 antibodies cross-react with NDEL1

A difficulty in studying endogenous NDE1 and NDEL1 is the problem of antibody cross-reactivity. That is, because of their highly similar amino acid sequences, many antibodies raised against NDE1 will also detect NDEL1 and vice versa. Indeed, of

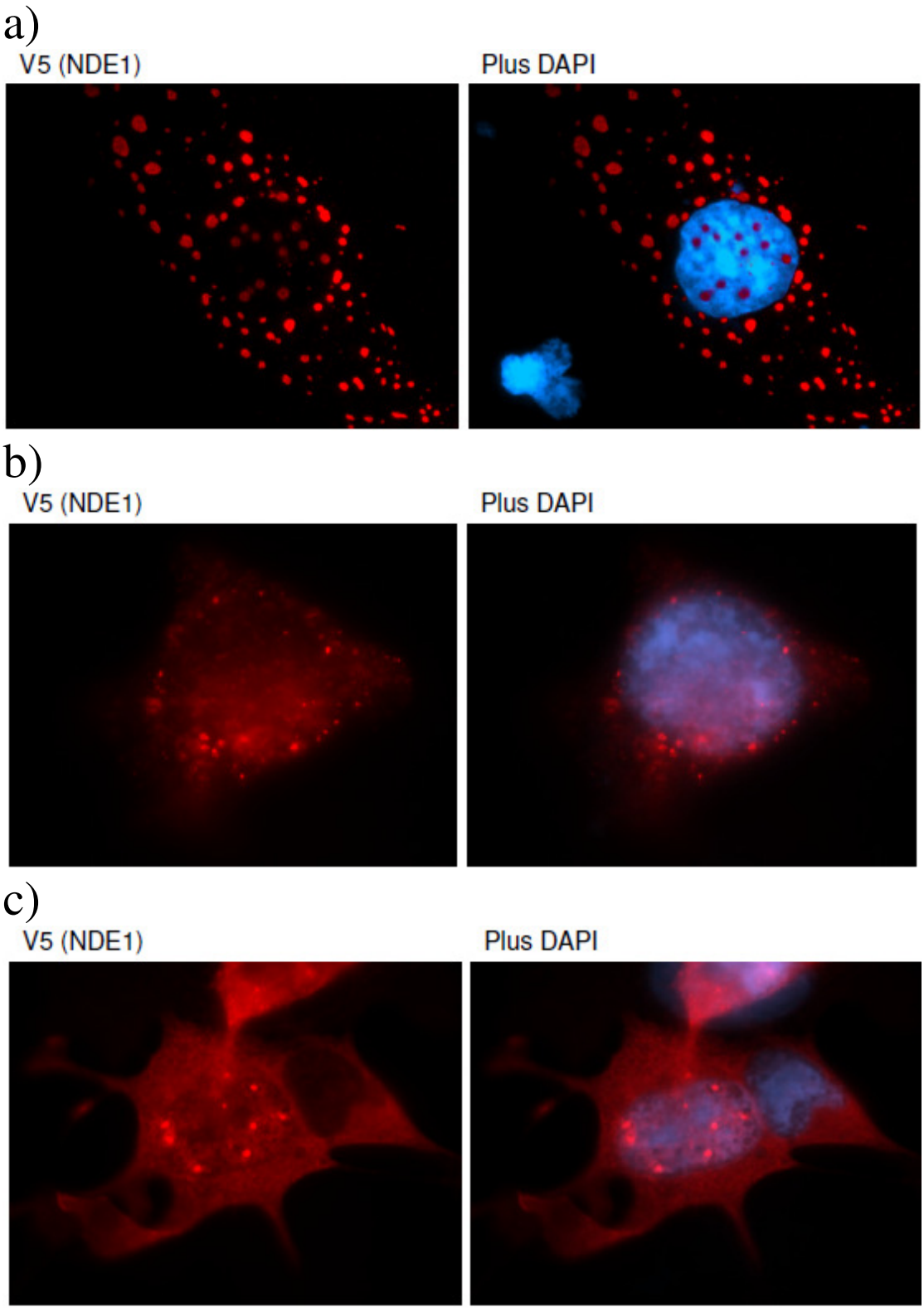

Figure 5.3.A: Localisation of over-expressed V5-NDE1-SSSC in the following cell lines: a) COS7, b) HEK293T and c) SH-SY5Y. Parts (a) and (c) are shown at 50% and 70% respectively of the magnification of part (b).

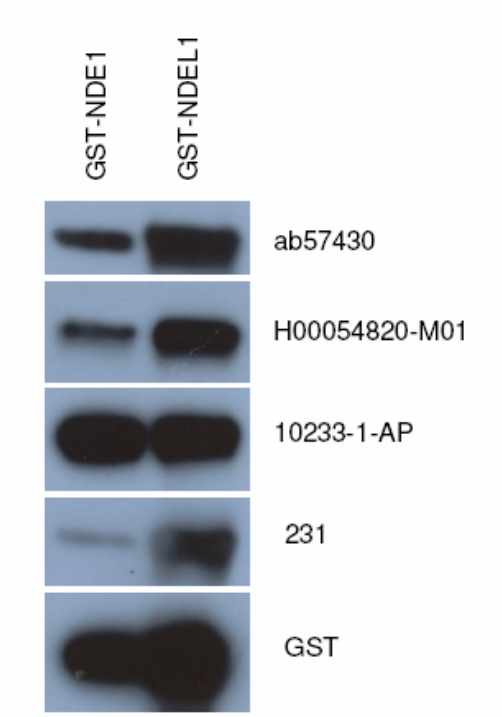

Figure 5.3.B: Equal amounts of GST-NDE1-SSSC and GST-NDEL1-PLSV were subjected to Western blotting. Three commercial anti-NDE1 antibodies showed immunoreactivity to GST-NDEL1 as well as to GST-NDE1. The anti-NDEL1 231 antibody was largely specific to GST-NDEL1. The possibility that one or more of these antibodies detects GST cannot be formally excluded.

---

the four published papers that describe testing the specificity of their NDE1 antibodies, only two report no NDEL1 cross-reactivity and of these, only one shows data to back this up (Yan *et al.* 2003; Yamaguchi *et al.* 2004; Stehman *et al.* 2007; Burdick *et al.* 2008).

The three commercially available anti-NDE1 antibodies (as of time of writing) were tested to see whether they cross-reacted with NDEL1 or not. To do this, equal amounts of bacterially produced GST-NDE1-SSSC and GST-NDEL-PLSV were run on an acrylamide gel, Western blotted and the membrane stained with the three antibodies: ab57430 (Abcam), H00054820-M01 (Abnova) and 10233-1-AP (Protein Tech Group). All three antibodies cross-reacted substantially with NDEL1 (see figure 5.3.B) and are therefore of limited use in investigating exogenous NDE1. In

Antibody	Peptide label	Peptide sequence	Species	Species conservation	Amino acids
92	EP072192	GRSSKNRDGGERRPS	Human	9/15, 14/15	292-306
93	EP072193	EKPRTPMPSSVEAERT	Human	10/15, 13/15	187-201
94	EP072194	MTYKQRAENTQE	Mouse	12/12, 12/12	23-34
95	EP072195	GKRLEFGKPASEPAS	Mouse	11/15, 13/15	316-330

Table 5.4.A: Peptides used as antigens to produce the NDE1 antibodies 92, 93, 94 and 95. In the case of the mouse antibodies, the peptides were from the mouse homologue of NDE1-kmll. "Species conservation" indicates amino acid identity and similarity between mouse and human NDE1 at this peptide.

contrast the NDEL1 231 antibody (a gift from Dr. Nick Brandon) was largely specific for NDEL1.

5.4 Generation and testing of NDE1-specific antibodies

5.4.1 Selection of antigenic peptides and production of antibodies

In order to investigate endogenous NDE1, four new antibodies were produced, two against human NDE1 and two against mouse Nde1. As stated previously it is always a danger that NDEL1 will also be detected by any anti-NDE1 antibody. In order to minimise the risk of this, antibodies were raised against short peptides taken from NDE1, rather than using full length NDE1 itself as the antigen. Several regions of NDE1 were therefore identified that shared limited homology with the corresponding regions of NDEL1. These were amino acids 1-37, 65-95, 183-243 and 277-313 of human NDE1-SSSC and 1-34, 182-243 and 282-344 of mouse Nde1-KMLL. From these regions, and following consultation with Eurogentec, four antigenic peptides were selected. These are shown in table 5.4.A.

Antibodies were raised and purified by Eurogentec according to the following schedule, summarised in figure 5.4.A. In total four rabbits were immunised: rabbits 5069 and 5070 were immunised with both of peptides EP072192 and EP072193 (see table 5.4.A), while rabbits 5041 and 5042 were immunised with peptides EP072194 and EP072195. Further "booster" immunisations, using the same pair of peptides per animal, were performed after 2, 4 and 8 weeks. At 12 weeks the animals were bled.

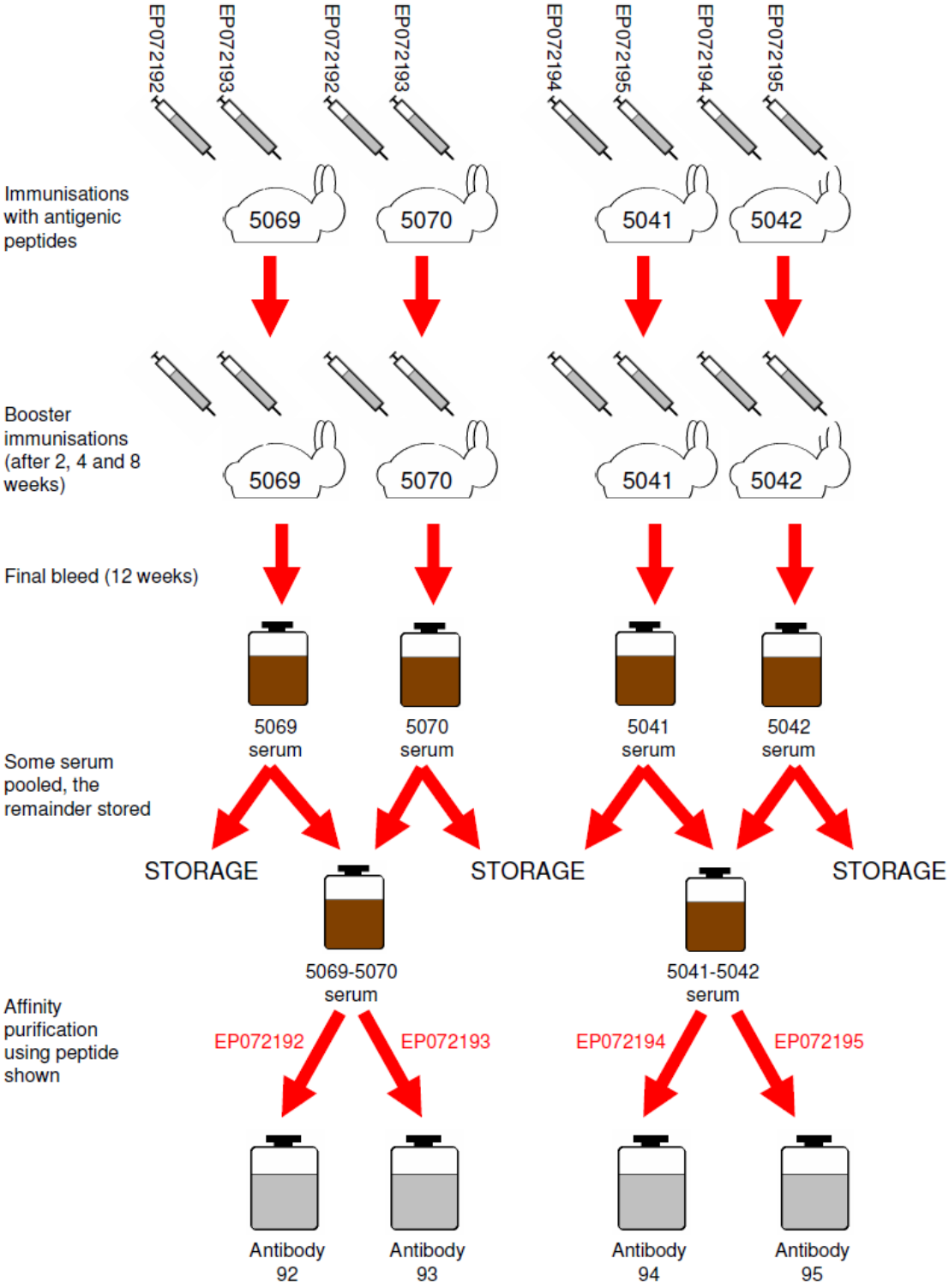

Figure 5.4.A: Schematic of the generation of the four anti-NDE1 antibodies

---

Samples of the serum from rabbit 5069 and 5070 were pooled together, as was serum from rabbits 5041 and 5042. The remainder of the serum was stored. The pooled serum from rabbits 5069 and 5070 was divided in half. One half was affinity

purified using peptide EP072192 to generate an antibody entitled "92", while the other half was affinity purified using peptide EP072193 to generate antibody 93. Similarly, samples of the 5041-5042 pooled serum were affinity purified using either peptides EP072194 or EP072195 to generate antibodies 94 or 95 respectively.

Antibodies 92, 93 and 95 were raised against peptides with some similarity between human and mouse and so may potentially detect both the human and mouse versions of NDE1. The peptide from which antibody 94 was raised is identical in both species and therefore can be expected to react with both. Based on the regions of NDE1 that they were raised against, antibody 93 should be able to detect all full length NDE1 variants as well as the S1a and S2 short variants. 92 should be able to detect all of these except for NDE1 S2. 95 should be specific to NDE1-KMLL and NDE1-S1b. 94 should be able to detect S1b and the full length variants only.

5.4.2 The new antibodies detect over-expressed NDE1

In order to determine whether the antibodies do indeed detect NDE1 in the cell, COS7 cells were transfected with V5-NDE1-SSSC and their lysates Western blotted. All four of the 92-95 antibodies correctly detected a band of slightly over 37kDa (see figure 5.4.B). To reinforce this result, further transfected cells were analysed, this time by immunocytochemistry. All four antibodies displayed the same expression pattern of large cytoplasmic puncta as did an anti-V5 antibody (see figure 5.4.C). The V5 antibody also detected additional staining in the cell body that none of the anti-NDE1 antibodies could detect and so this may represent non-speific staining. Together these results suggest that all four antibodies can detect human NDE1.

5.4.3 Pre-absorption testing of the NDE1 antibodies

As this work will focus on primarily on human NDE1, the 92 and 93 antibodies were subjected to further testing. As an initial test of antibody specificity, pre-absorption tests were carried out. Antibodies 92 and 93 were incubated over-night at an appropriate experimental concentration with their corresponding antigenic peptide (EP072192 or EP072193, see table 5.4.A). As a control, equal amounts of the antibodies were also incubated in the same way, but minus the peptide. Two lanes of

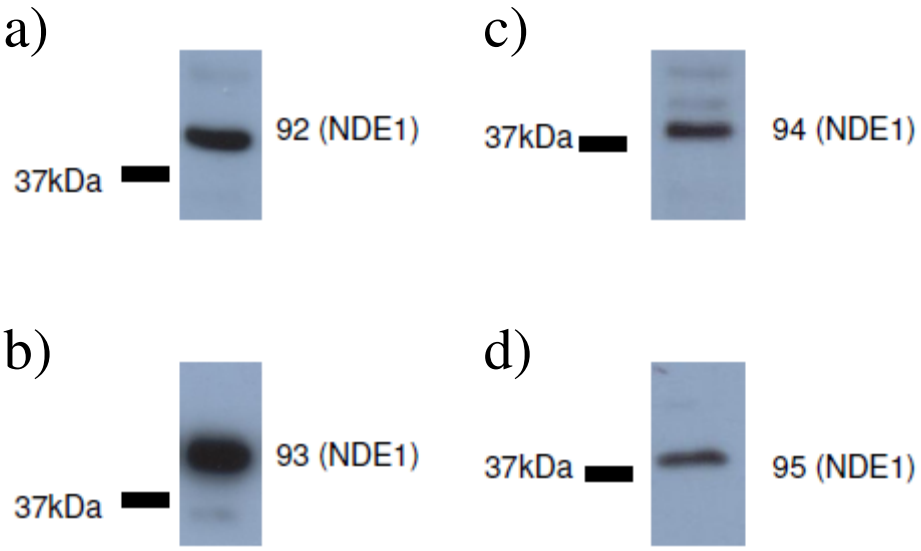

Figure 5.4.B: All four of the novel NDE1 antibodies can detect a band of approximately the expected size of 38kDa when used to blot COS7 cell lysates containing V5-NDE1-SSSC. Some antibodies also detect weaker minor bands, which may represent endogenous NDE1 isoforms.

GST-NDE1-SSSC were run on a Western blot per antibody, and then the 92 and 93 antibodies (both pre-absorbed and mock absorbed) were used to stain them. Both antibodies detected a much stronger signal in the absence of the antigenic peptide (see figure 5.4.D). This demonstrates that the antibodies are capable of being blocked by their antigenic peptides and therefore have immunoreactivity to them.

5.4.4 The human NDE1 antibodies do not cross-react with NDEL1

Previously produced NDE1 antibodies more often than not also detected NDEL1 (see section 5.3.2). Based on the choice of antigenic peptide, these novel anti-NDE1 antibodies should not detect NDEL1, but in order to be certain equal amounts of bacterially expressed GST-NDE1-SSSC and GST-NDEL1-PLSV were Western blotted and stained using the 92 and 93 antibodies. Both antibodies detected the GST-NDE1, but not the GST-NDEL1, while an anti-GST antibody detected both (see figure 5.4.E). It therefore appears that these antibodies are specific for NDE1, and do not cross-react with NDEL1.

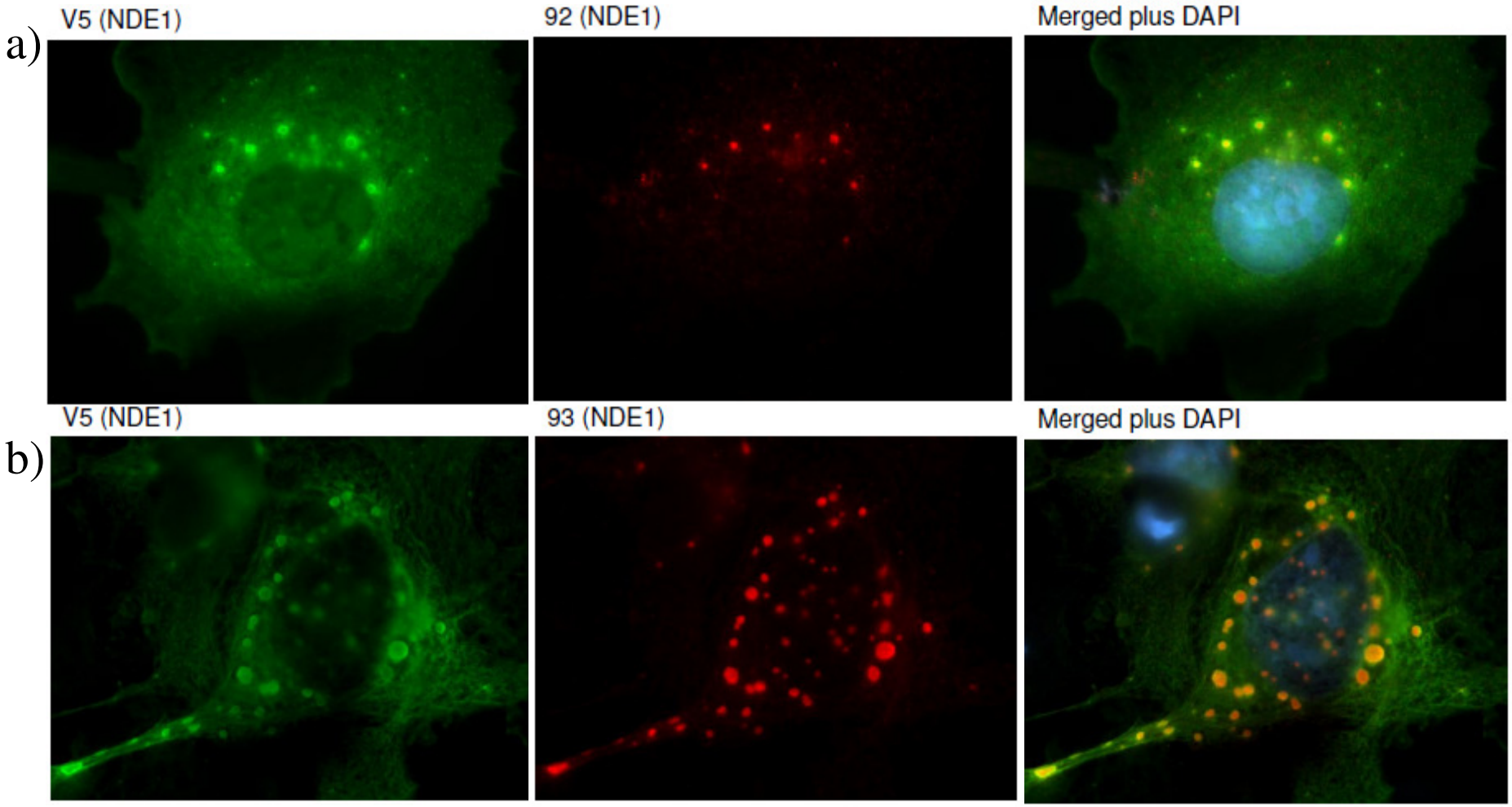

Figure 5.4.C: The novel NDE1 antibodies all detect V5-NDE1-SSSC when it is over-expressed in COS7 cells. a) Antibody 92, b) Antibody 93, c) Antibody 94, d) Antibody 95.

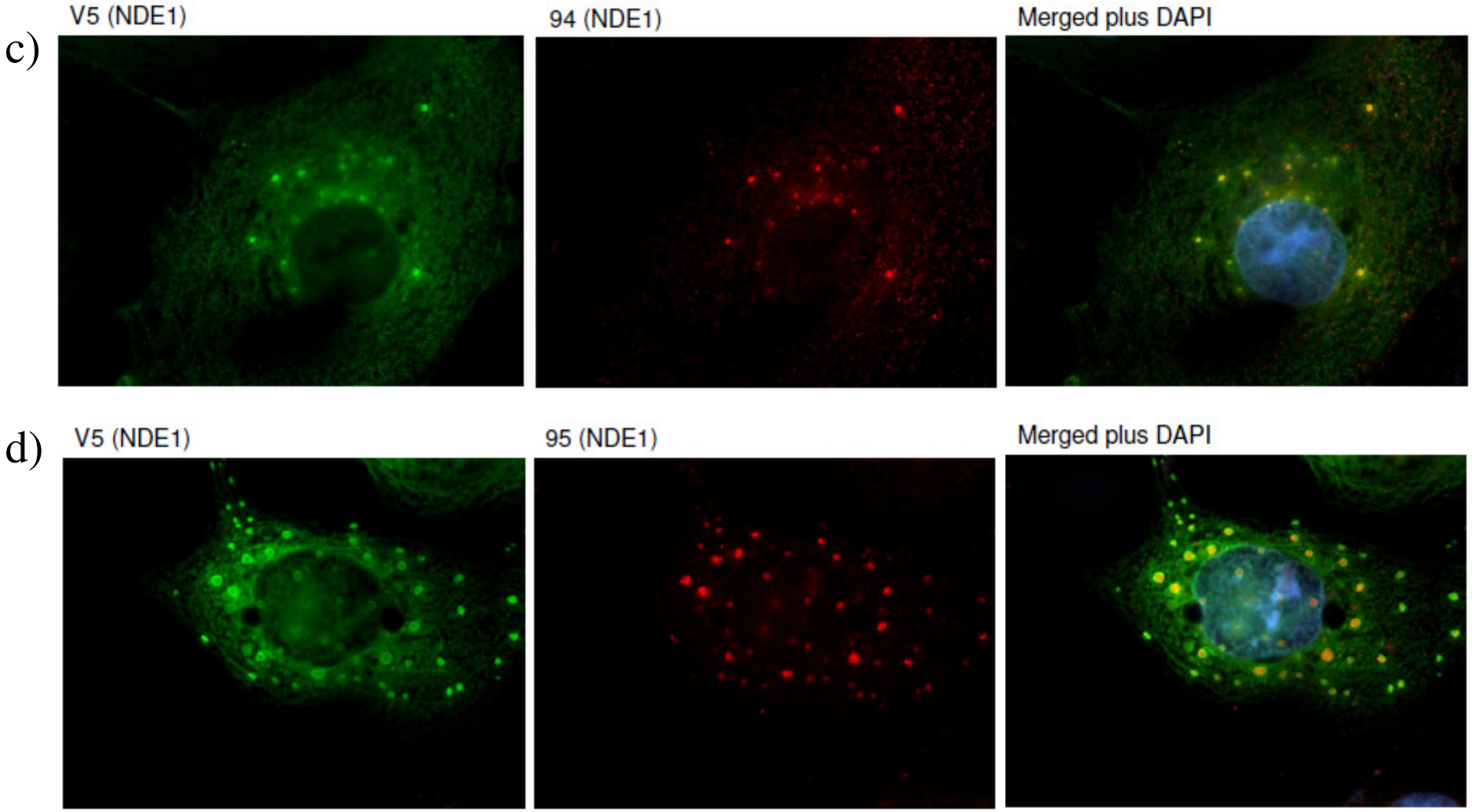
c)
V5 (NDE1)
94 (NDE1)
Merged plus DAPI
d)
V5 (NDE1)
95 (NDE1)
Merged plus DAPI

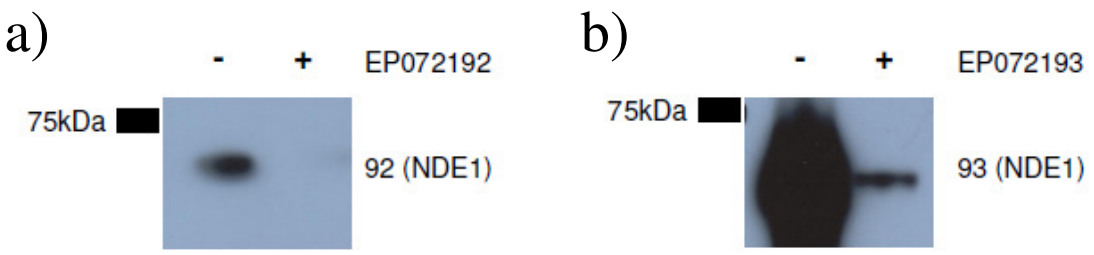

Figure 5.4.D: a) The 92 antibody can detect GST-NDE1-SSSC *in vitro* (-) but this effect is considerably weaker when it has been incubated over-night with peptide EP072192 (+). This shows that the 92 antibody does indeed bind the peptide which it was originally raised against. b) The peptide EP072193 can similarly limit immunoreactivity of the 93 antibody.

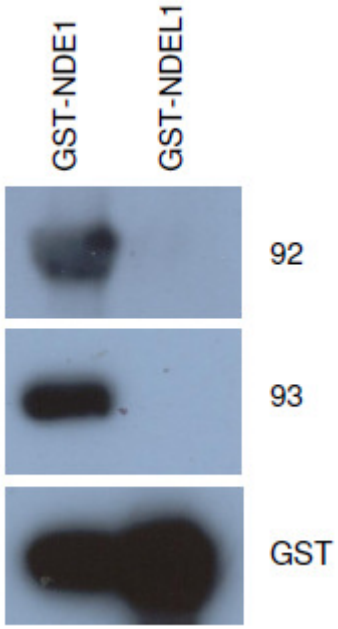

Figure 5.4.E: The 92 and 93 antibodies can both detect GST-NDE1-SSSC, but not GST-NDEL1-PLSV *in vitro*. See figure 5.3.B for similar testing of various commercial anti-NDE1 antibodies and NDEL1 antibody 231.

Amino acids	pI
1-50	4.24
50-100	4.67
100-150	5.28
150-200	4.65
200-250	11.40
250-300	10.02
300-335	9.50

Table 5.4.B: Isoelectric points of different section of the NDE1-SSSC protein as determined by ExPASy ProtPatam tool (Gasteiger *et al.* 2005) demonstrate that the N-terminal region of NDE1 is considerably more acidic than the C-terminal region.

5.4.5 Detection of multiple NDE1 isoforms in SH-SY5Y cells

In chapter 3, the existence of transcripts encoding various *NDE1* and *NDEL1* splice variants in human brain cDNA was demonstrated. In order to test if multiple isoforms of NDE1 also exist at the protein level, an SH-SY5Y cell lysate (prepared by Sheila Christie) was subjected to two-dimensional Western blotting. SH-SY5Y cells are derived from a human neuroblastoma and therefore can serve as a crude model for human neuronal tissue. By blotting in this manner, proteins can be separated from each other both by molecular mass (vertically) and by isoelectric point (horizontally). The 93 antibody was then used to investigate NDE1 protein expression in the lysate. Molecular weight and isoelectric points of the NDE1 isoforms are described in table 3.1.B.

Multiple NDE1 immunoreactive species are indeed detected (see figure 5.4.F.a). These include at least two distinct species of approximately the correct size and pI value to be NDE1-SSSC, NDE1-KMLL and/or NDE1-KRHS (see figures 5.4.F.b and 5.4.E.c). Note that this technique regularly slightly over-estimated the molecular mass of proteins. Several smaller and more acidic species are also visible. If it is assumed that these also represent genuine NDE1, then given that the N-terminal domain of NDE1 is acidic, while the C-terminal end is basic (see table 5.4.B) it can

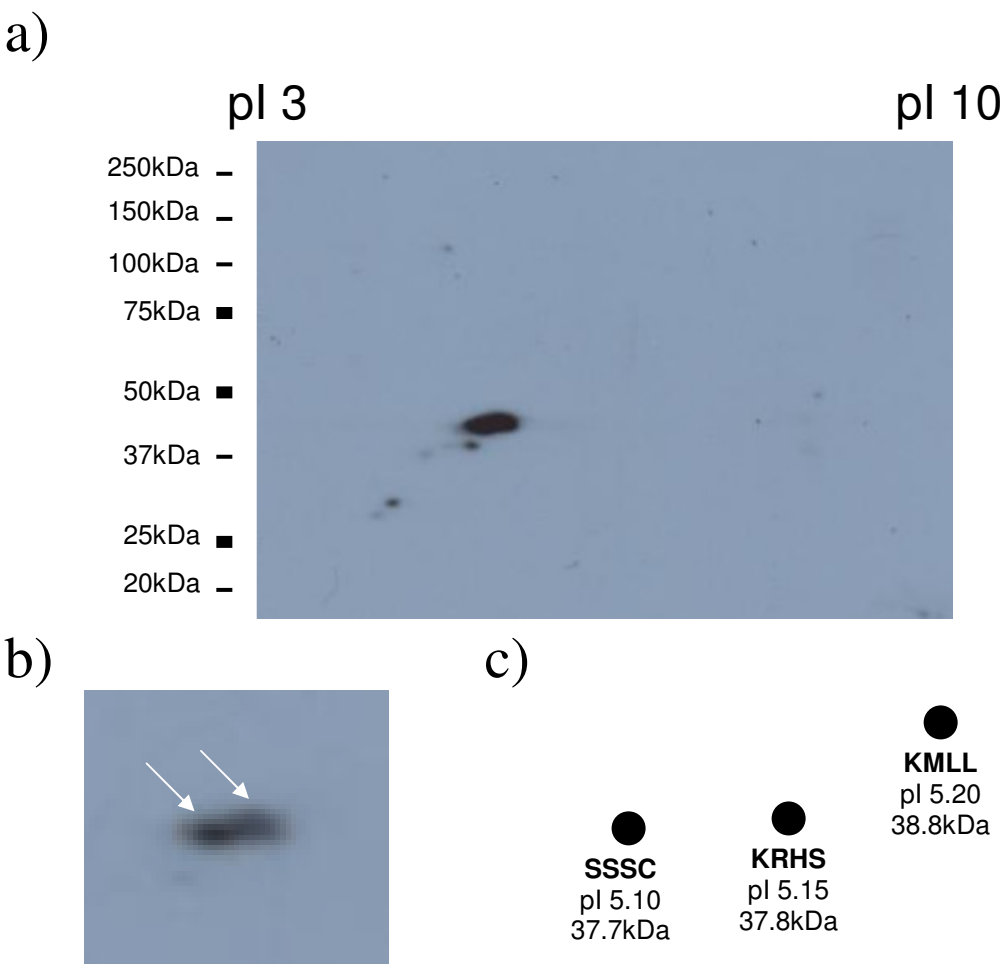

Figure 5.4.F: a) 2-D Western blot of an SH-SY5Y cell lysate which has been stained using the 93 (NDE1) antibody. b) Reduced exposure and enlargement of the most prominent signal, demonstrating that it includes at least two distinct species, shown by white arrows. c) The theoretical relative positions of NDE1-SSSC, KRHS and KMLL on a 2-D Western blot. These closely resemble the pattern of isoforms in part b, suggesting that at least two of these isoforms exist in SH-SY5Y cells.

---

be hypothesised that these NDE1 species lack sections of the C-terminus, either due to alternative splicing, post-translational modification or protein degradation. There is no sign of any signal corresponding to either the NDE1-S1a or S2 proteins and so it appears that these are not expressed to any significant degree in SH-SY5Y cells. The epitope to which this antibody was raised means that it would be unable to detect the S1b isoform.

5.5 The cellular localisation of NDE1 determined using specific antibodies

5.5.1 Detection of NDE1 nuclear puncta in SH-SY5Y cells using the 93 antibody

Initially, the expression pattern of NDE1 was investigated in SH-SY5Y. The cells were fixed using methanol and stained using the 93 antibody, as it was the most avid of the two human NDE1 antibodies produced. A large proportion of cells displayed staining at the nucleus, as confirmed by colocalisation with the nuclear stain DAPI, an expression pattern not widely reported of NDEL1. The exact nature of this nuclear staining varied. Many cells displayed one or more large punctate structures within the nucleus, while some displayed a more diffuse pattern of smaller NDE1 puncta. Some staining was also seen in the cell body, although this tended to be diffuse and did not resemble a microtubule-like pattern.

In an attempt to quantify these expression patterns, SH-SY5Y cells were grown on coverslips and stained using antibody 93. Cells with intact nuclei were located and photographs taken of them on the microscope without first looking at the NDE1 expression pattern in these cells. Photos were taken from seven coverslips, with 10-14 cells photographed per coverslip, for a total of n=86 cells. Afterwards these images were analysed and every cell that was completely contained in any of the images was tallied based on the number of large nuclear puncta present and whether or not it contained diffuse background puncta. Figure 5.5.A shows sample images and table 5.5.A shows the data. 87.2% of the cells contained at least one strong NDE1 nuclear puncta, with 33.7% having three or more. In addition, 94.2% had a diffuse staining of smaller NDE1 puncta in the nucleus.

In a similar way, n=70 SH-SY5Y cells were counted to determine if their 93 staining pattern was primarily nuclear, in the cell body or whether they were similarly expressed in both locations. Figure 5.5.B shows sample images and table 5.5.B shows the data. In 52.9% of cells, NDE1 was primarily in the nucleus, while in only 15.7% was it seen to be primarily in the cell body.

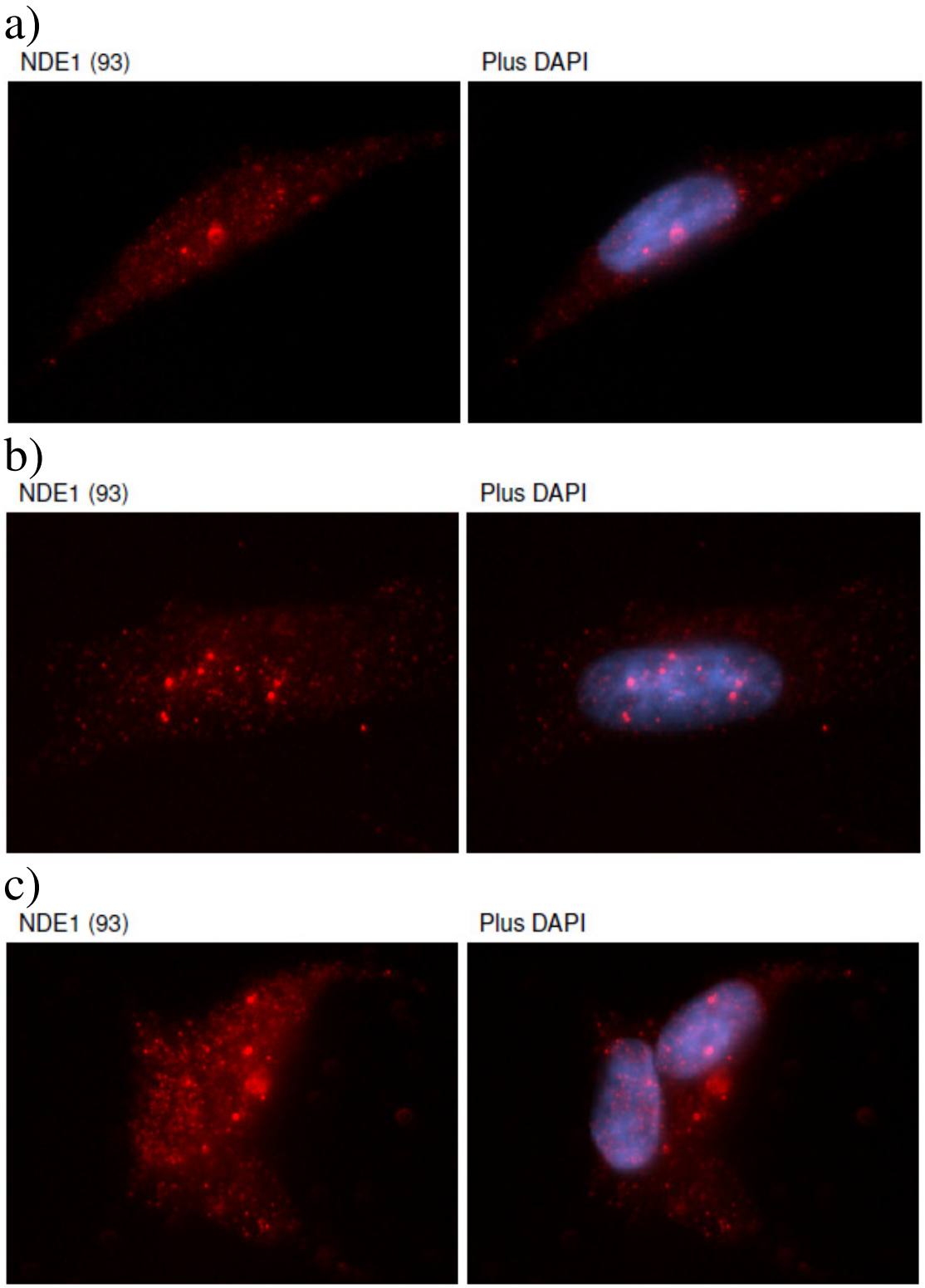

Figure 5.5.A: Examples of 93 (NDE1) antibody staining in SH-SY5Y cells. a) A cell with two strong nuclear puncta. b) A cell with many strong nuclear puncta. c) A cell (on left) with no strong nuclear puncta.

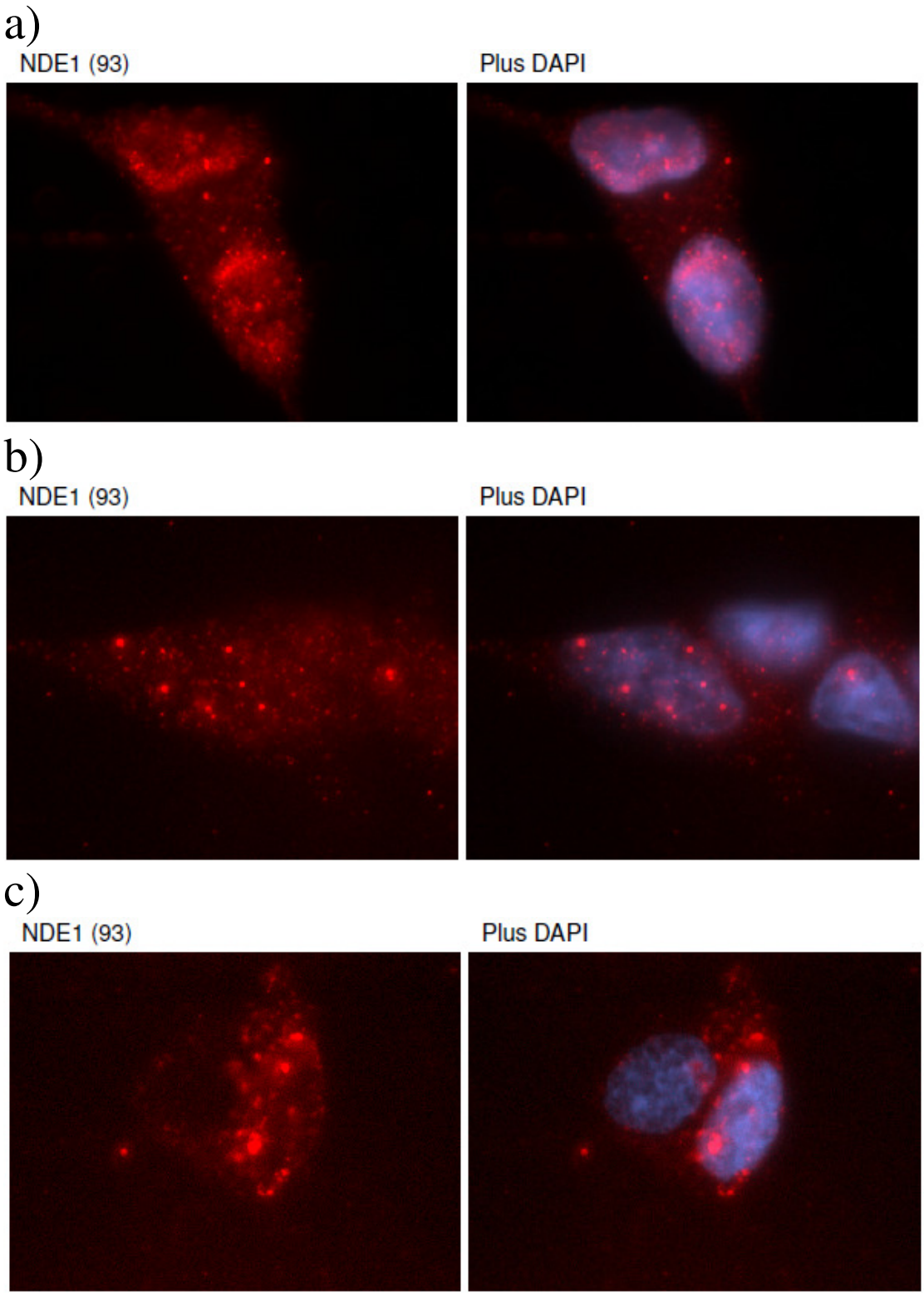

Figure 5.5.B: Examples of 93 (NDE1) antibody staining in SH-SY5Y cells. The amount of diffuse staining in the nucleus (N) and cytoplasm (C) is compared. a) Cells where N > C. b) Cells where N = C. c) Cells where N < C.

Large Puncta	Number of cells	Percentage of cells
0	11	12.8
1	24	27.9
2	22	25.6
3-5	21	24.4
6+	8	9.3
Diffuse puncta	**Number of cells**	**Percentage of cells**
Yes	81	94.2
No	5	5.6

Table 5.5.A: The proportion of n=86 SH-SY5Y cells in which the NDE1 93 antibody detected NDE1 puncta in the nucleus.

NDE1 (93) localisation	Number of cells	Percentage of cells
Primarily nucleus	37	52.9
Primarily cell body	22	31.4
Nucleus and cell body	11	15.7

Table 5.5.B: The proportion of n=70 SH-SY5Y cells in which the NDE1 93 antibody detected staining primarily in the nucleus, in the cell body or comparably in both locations.

As shown in section 5.3.1, when V5-NDE1 was over-expressed in SH-SY5Y cells a number of nuclear puncta were seen using an anti-V5 antibody. These puncta are also detectable using the 93 antibody (see figure 5.5.C).

5.5.1.1 The NDE1 93 nuclear structures do not appear to be centromeric nucleosomes

The large NDE1 puncta within the nucleus resemble the expression pattern seen using markers of centromeric nucleosomes (Orthaus *et al.* 2008). These are histone-based structures found at the centres of each chromosome and which form the bases of kinetochores during mitosis. The protein CENPA is a core element of this type of nucleosome, and antibodies raised against it can be used to identify the locations of centromeric nucleosomes within the cell.

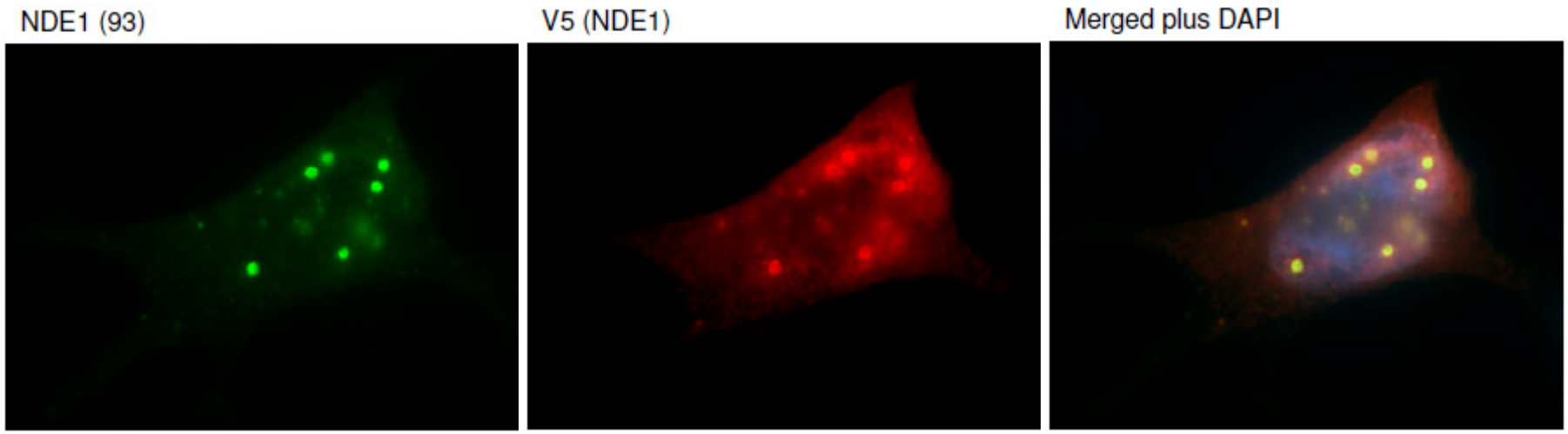

Figure 5.5.C: The anti-NDE1 93 antibody can detect the V5 punctate structures seen in the nucleus when V5-NDE1-SSSC is over-expressed in SH-SY5Y cells (see figure 5.3.A.c)

SH-SY5Y cells were examined by immunocytochemistry using the 93 antibody and an anti-CENPA antibody (see figure 5.5.D). The CENPA antibody revealed a number of distinct nuclear puncta. In some of the cells, one or two of the large NDE1 nuclear puncta colocalised with CENPA puncta, however, the majority of the puncta did not colocalise. It can therefore be assumed that the NDE1 puncta do not simply represent centromeric nucleosomes.

5.5.1.2 The small NDE1 93 nuclear structures are related to splicing speckles

In addition to the large punctate structures, a more diffuse set of smaller structures were seen in the nucleus. This staining bears some resemblance to that of nuclear speckles (Lamond and Spector 2003). These structures contain machinery related to the splicing process and can be detected using antibodies against the Smith antigen, which consists of small nuclear riboprotein particles. Such an antibody, Y12, was therefore used to investigate the localisation of splicing speckles in relation to NDE1. The staining pattern of antibody 93 showed considerable colocalisation with that of the Y12 antibody in SH-SY5Y cells (see 5.5.E). This colocalisation occurs at numerous small semi-diffuse punctate structures throughout the nucleus, and appears to account for a large part of the "background" NDE1 nuclear staining. This suggests that NDE1 may have a previously uncharacterised role either in splicing itself or in a related process.

5.5.2 A putative NDE1 nuclear structure and the nucleus using the 94 antibody

The 94 antibody was raised against a peptide which is found in both human NDE1 and mouse Nde1. Its localisation was therefore tested in both human SH-SY5Y and mouse NIH-3T3 cells, using methanol to fix both. In both cell lines, 94 showed a nuclear staining pattern (see figure 5.5.F), but interestingly this was distinct from the nuclear pattern seen using antibody 93 (as will be discussed in section 5.6.4). Rather than showing an array of puncta in the nucleus, antibody 94 stained between one and three small cloud-like structures in each cell. These bear some resemblance to nuclear stress bodies (Biamonti 2004) or potentially Oct1/PTF/transcription (OPT) domains (Pombo *et al.* 1998).

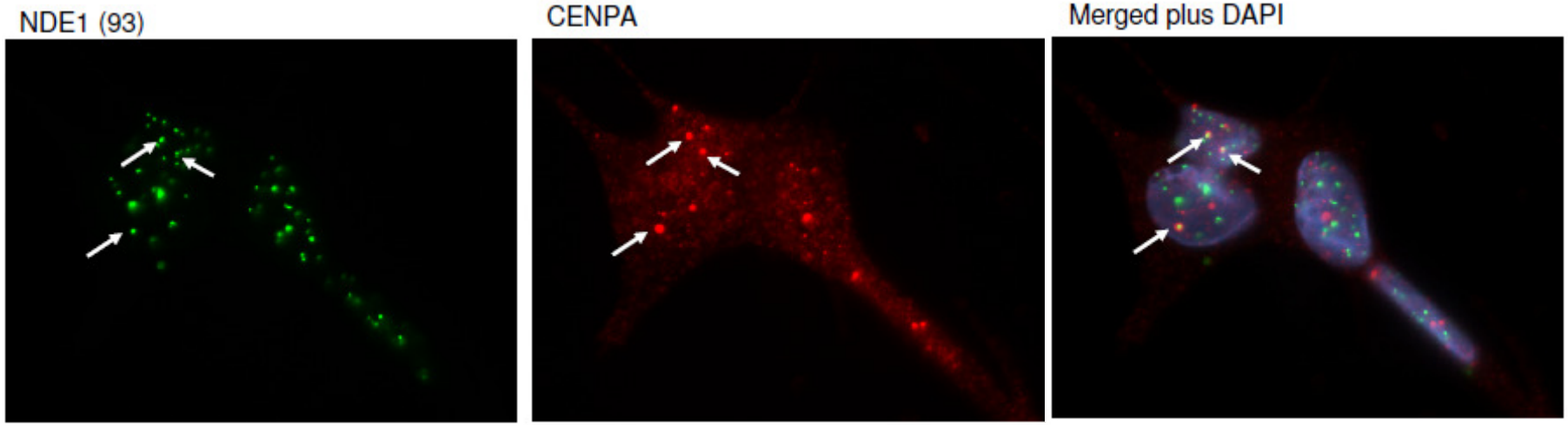

Figure 5.5.D: NDE1 (93) colocalises with the centromeric nucleosome marker protein CENPA at individual punctate structures in some SH-SY5Y cells.

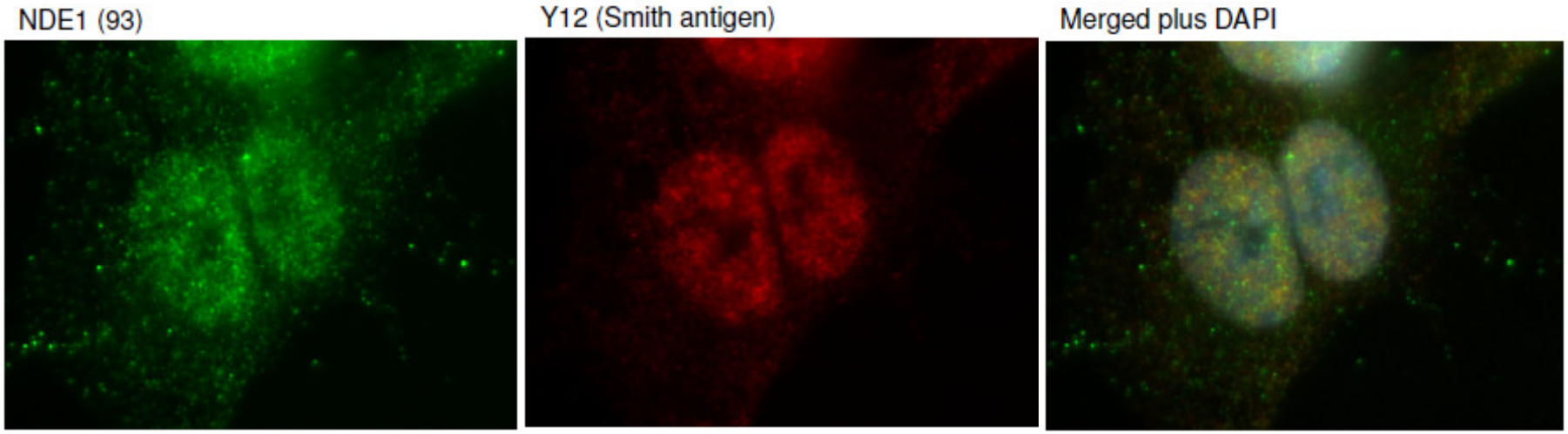

Figure 5.5.E: The staining pattern of the anti-NDE1 93 antibody consistently overlaps with that of the anti-Smith antigen Y12 antibody in the nuclei of SH-SY5Y cells, suggesting that NDE1 is present at splicing speckles.

a)

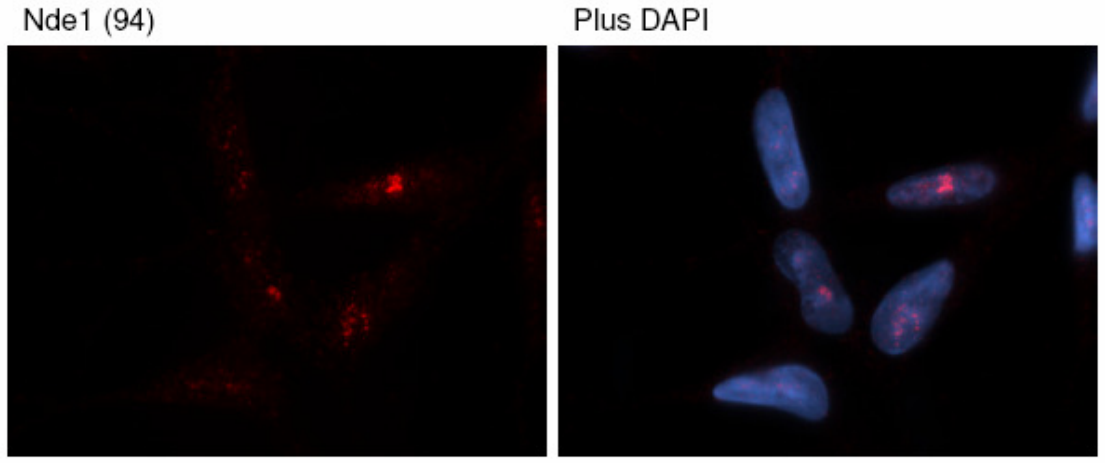

b)

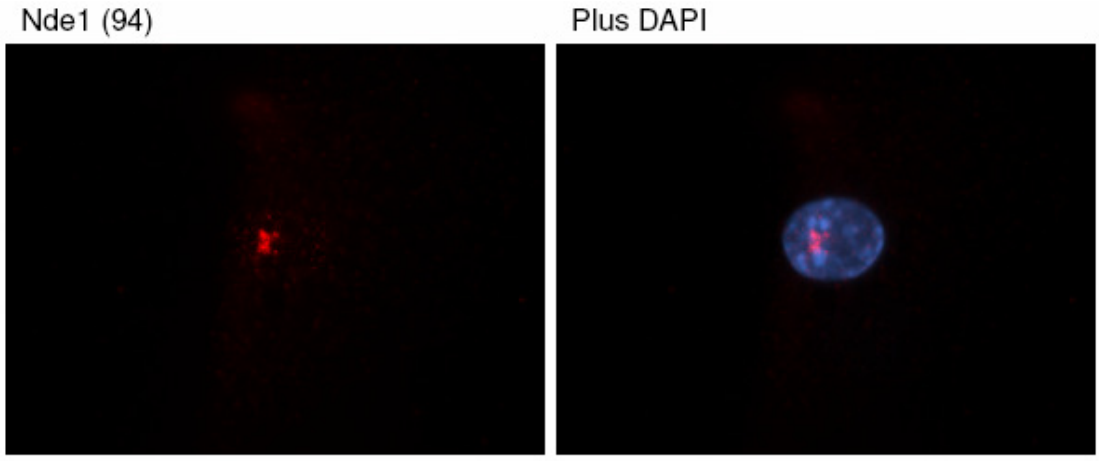

Figure 5.5.F: a) Expression pattern of the mouse Nde1 94 antibody in SH-SY5Y cells. b) Expression pattern of the mouse Nde1 94 antibody in NIH-3T3 cells.

5.5.3 NDE1 at the nucleus using the 95 antibody

The mouse Nde1 95 antibody was used initially to stain NIH-3T3 cells. Strikingly, the antibody showed Nde1 to be associated with the nuclear membrane, as well as potentially at structures within the nucleus (see 5.5.G.a). This pattern may be specific to NIH-3T3 cells, or may be due to the fact that 95 was raised against an epitope found only in one specific splice variant (the mouse orthologue of NDE1-KMLL). This was, however, only visible following methanol fixation. After paraformaldehyde fixation however, this nuclear membrane-like pattern was not seen

a)

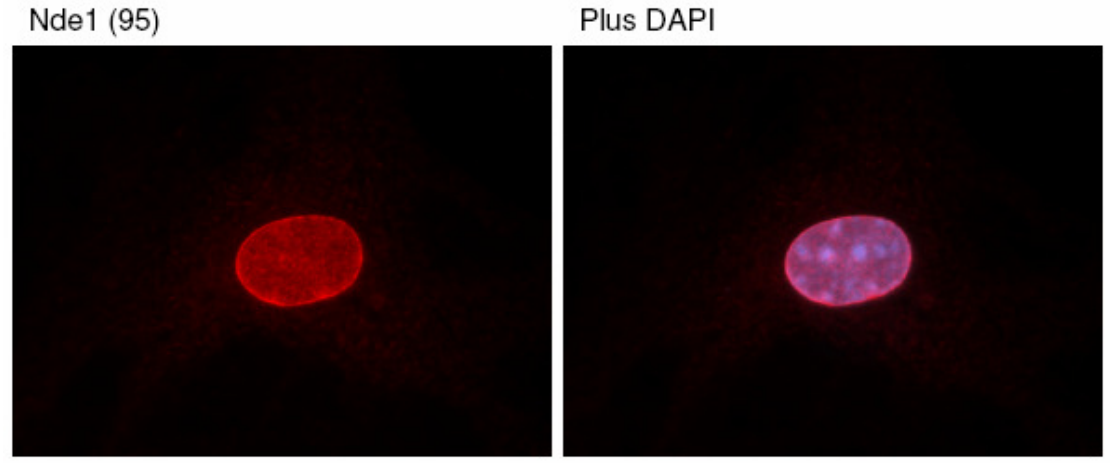

b)

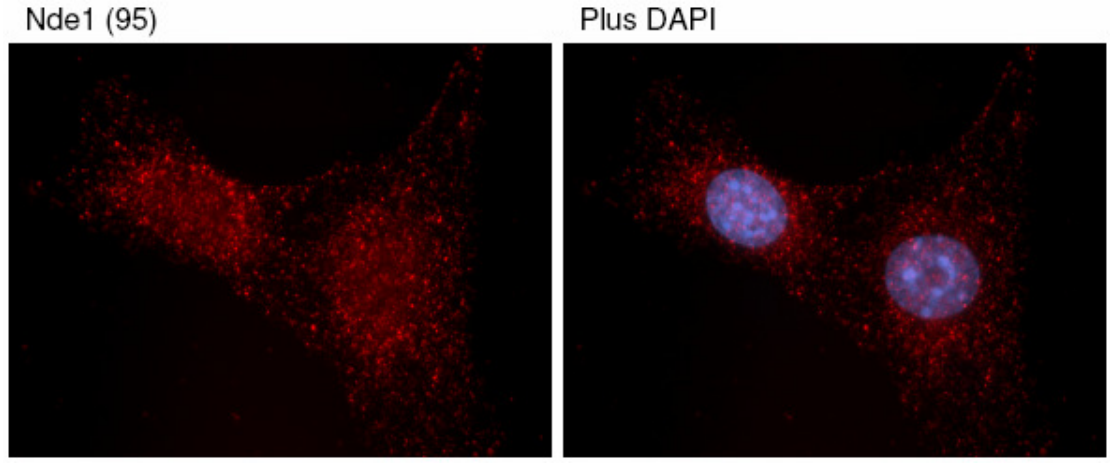

Figure 5.5.G: a) Expression pattern of the mouse Nde1 95 antibody in NIH-3T3 cells following methanol fixation. b) Expression pattern of the mouse Nde1 95 antibody in NIH-3T3 cells following paraformaldehyde fixation.

---

and instead Nde1 was seen to be primarily cytoplasmic, with some nuclear puncta (see figure 5.5.G.b). Methanol can be more effective at revealing epitopes than paraformaldehyde fixation, providing a potential explanation for this effect, although whether of not either expression pattern can be replicated in an independent mouse cell line should be determined.

When used on SH-SY5Y cells, only a very faint, primarily cytoplasmic stain was seen. This signal is probably non-specific, as the 95 antigenic peptide bears limited sequence similarity to the corresponding section of human NDE1.

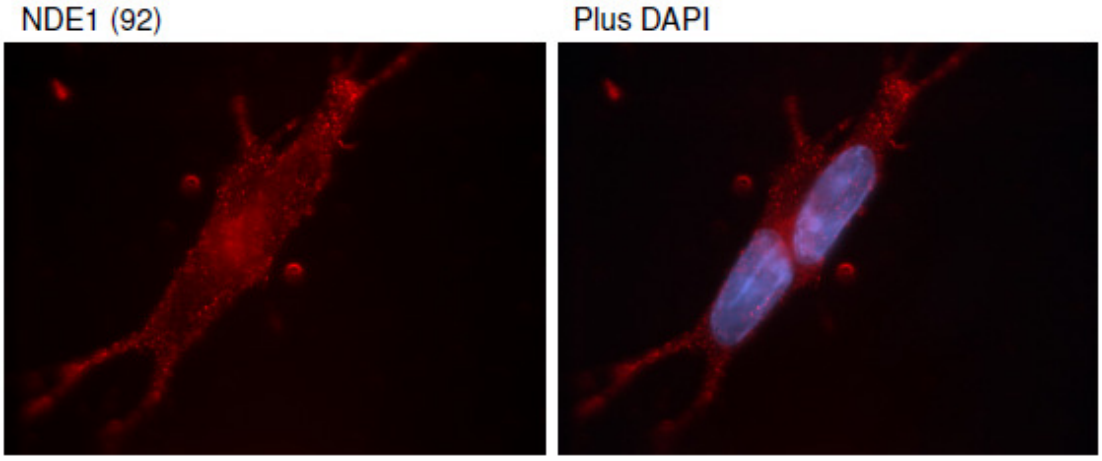

Figure 5.5.H: Expression pattern of the anti-NDE1 92 antibody in SH-SY5Y cells.

	Colocalisation	Centrosome but no colocalisation	No detectable centrosome
Number of cells	22	41	50
Percentage of cells with centrosomes	34.9	65.1	0
Percentage of total cells	19.5	36.3	44.2

Table 5.5.C: Number of SH-SY5Y cells in which NDE1 (93) colocalised with γ-tubulin. When no colocalisation was seen, cells were counted based on whether a centrosome-like γ-tubulin puncta was visible.

5.5.4 The 92 antibody does not obviously detect endogenous NDE1

When antibody 92 was used to stain SH-SY5Y cells, only a faint punctate pattern in the cytoplasm was seen with no obvious sign of signal within the nucleus. The pattern of expression does not resemble the published expression patterns of NDEL1 or over-expressed NDE1 (see figure 5.5.H). Given the high concentration of this antibody required to detect recombinant NDE1 (see table 2.4), which was detected considerably more easily by antibody 93, it is possible that the signal seen here does not represent endogenous NDE1, and may instead be non-specific staining. Similarly, it has not proved possible to detect endogenous NDE1 by Western blotting using this antibody. Due to this uncertainty, the 93 antibody will be used instead for the remainder of the thesis.

5.5.5 Endogenous NDE1 associates with the centrosome

It has been widely reported that NDEL1 is a centrosomal protein and over-expressed NDE1 is also known to localise there (see section 1.3.3.1). To confirm that endogenous NDE1 also shows this localisation, SH-SY5Y cells were co-stained with the NDE1 93 antibody and an antibody against γ-tubulin, a commonly used marker of the centrosome. In some cells NDE1 was indeed seen to colocalise with γ-tubulin (see figure 5.5.I). Centrosomes were not visible in all cells, however. Of n=63 cells with visible centrosomes, 34.9% had NDE1 present at them (see table 5.5.C). It therefore appears that endogenous NDE1 is indeed found at the centrosome, but not in all cells.

Colocalisation between NDE1 and γ-tubulin was also seen in some mouse NIH-3T3 cells using the Nde1 95 antibody (see figure 5.5.J.a), but could not obviously be seen using the Nde1 94 antibody (see figure 5.5.J.b).

5.5.6 NDE1 colocalisation with γ-tubulin confirmed using confocal microscopy

In order to further confirm the localisation of endogenous NDE1 to the centrosome in SH-SY5Y cells, confocal microscopy was used. This technique allows the user to generate a "stack" of two-dimensional immunofluorescence images from each cell, each taken at a different depth. Therefore it can be determined whether two proteins colocalise within the cell's three-dimensional shape. It is also possible using the Zeiss LSM510 system to gather quantitative values for the intensity of the immunofluorescence at a given point on the image. SH-SY5Y cells were therefore once again stained with the NDE1 93 and anti-γ-tubulin antibodies. These were then viewed by confocal microscopy with the assistance of Becky Carlyle. Again, colocalisation of the two proteins was visible at the centrosome (see figure 5.5.K) although the NDE1 staining appeared to be centred to one side of the γ-tubulin-defined centrosome.

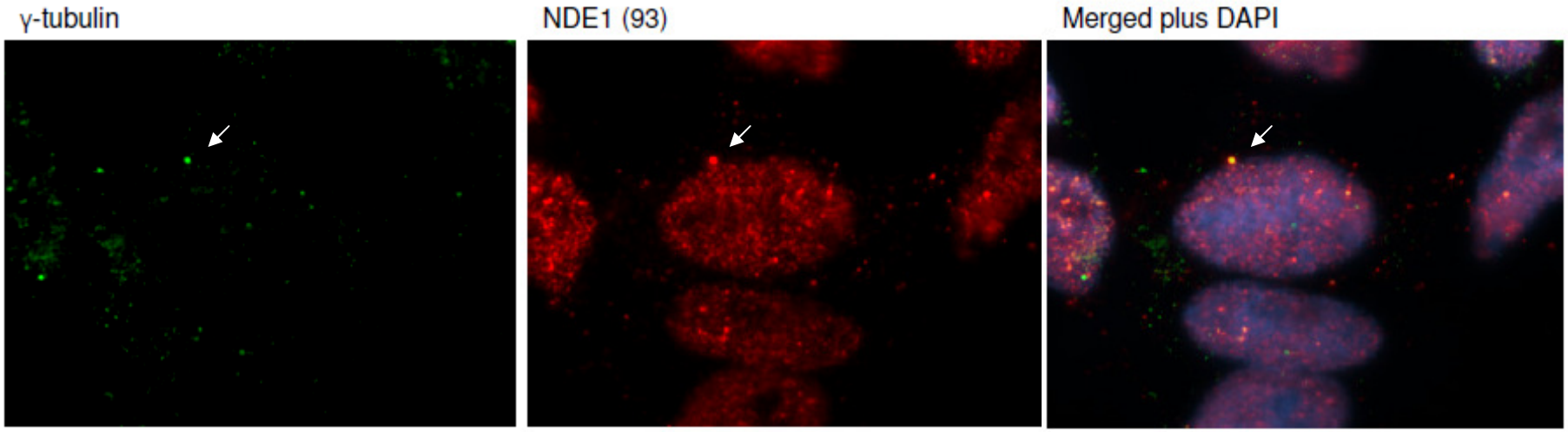

Figure 5.5.I: NDE1 (93) is seen to co-localise with γ-tubulin in a subset of SH-SY5Y cells at peri-nuclear punctate structure (white arrow), suggesting that endogenous NDE1 is found at the centrosome.

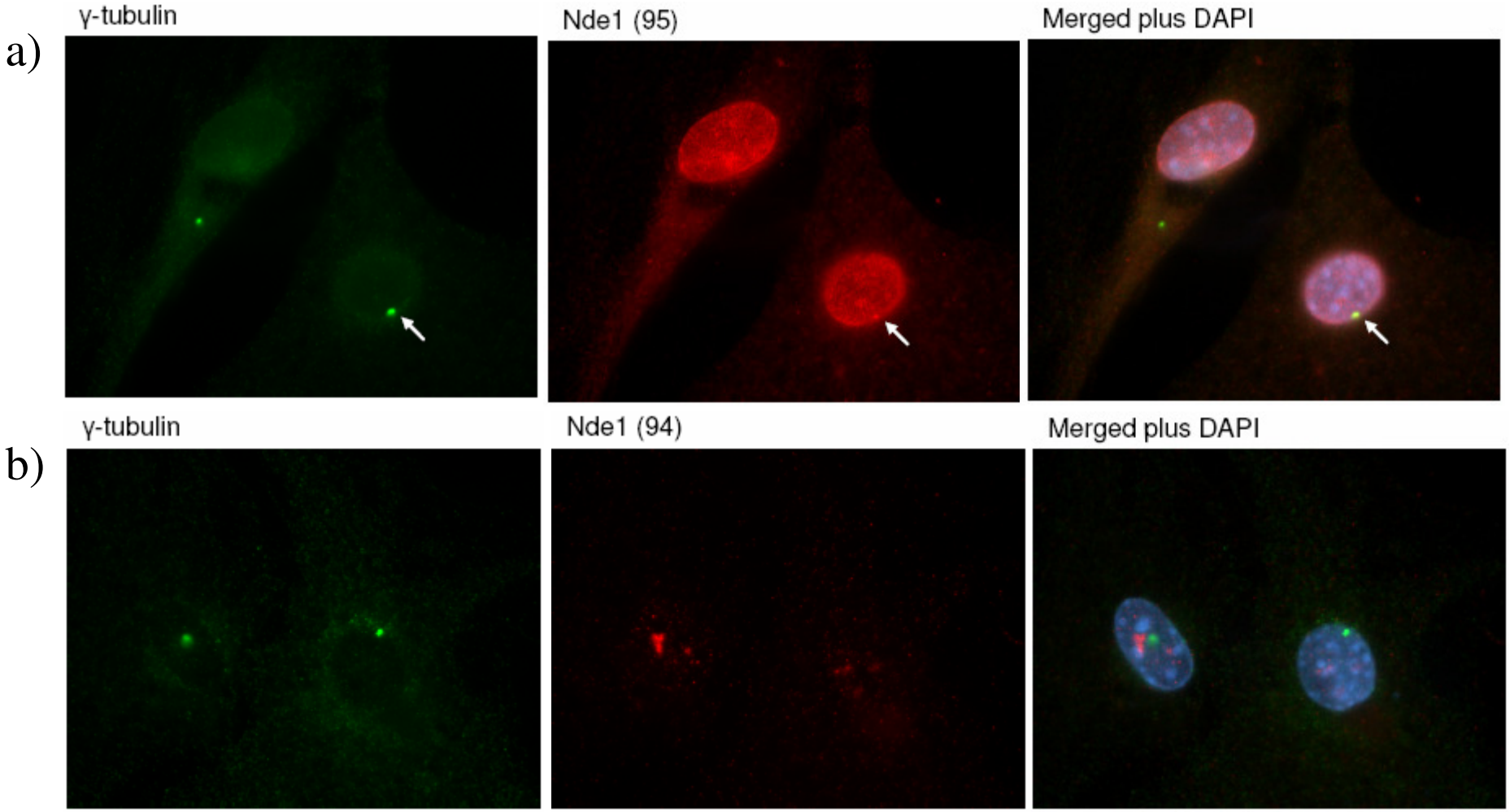

Figure 5.5.J: a) Nde1 95 stains the centrosome (white arrow, as defined by γ-tubulin) in some but not all NIH-3T3 cells. b) Nde1 94 does not stain the centrosome, as defined by γ-tubulin of NIH-3T3 cells.

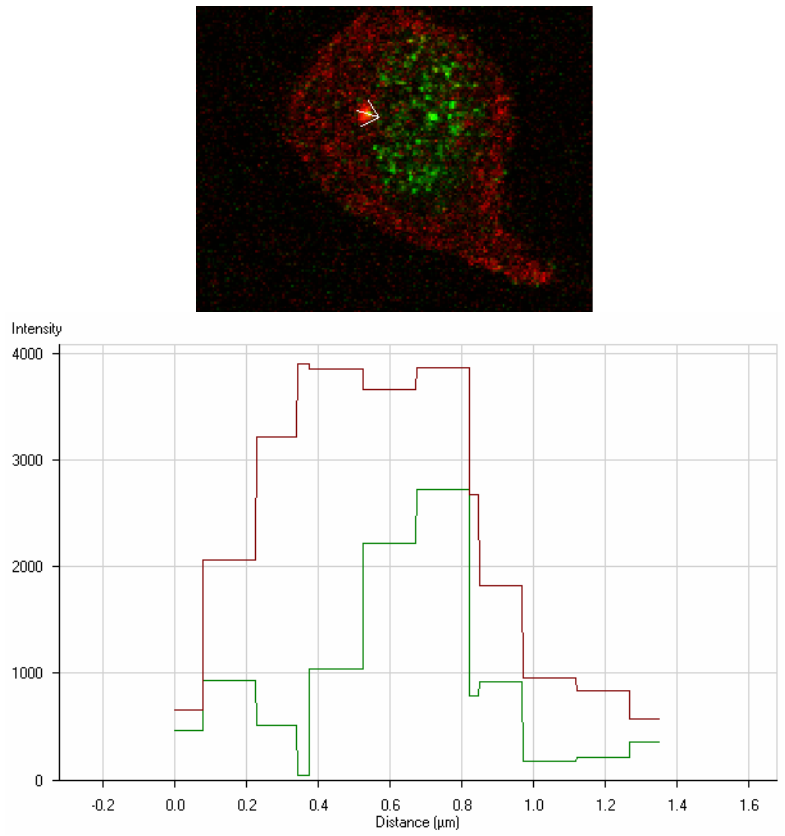

Figure 5.5.K: Confocal microscopy analysis of NDE1 93 (green) and γ-tubulin (red) in an SH-SY5Y cell. Image shows a slice of the cell. Graph shows the intensity of each antibody along the one-dimensional white line from the above image. The two staining patterns colocalise, indicating NDE1 is at the centrosome, but NDE1 is off-centre relative to γ-tubulin.

5.6 Discussion

5.6.1 The subcellular localisation of endogenous NDE1

In this chapter, four novel anti-NDE1 antibodies were used to investigate the expression pattern of endogenous NDE1 protein within the cell. While the expression patterns shown by the antibodies varied, there were two recurring themes: Expression of NDE1 at the nucleus (although the type of nuclear expression pattern seen did vary between antibodies) and expression at the centrosome. These will now be discussed in turn, before discussing the differences between and reliability of the antibodies.

5.6.2 NDE1 at the nucleus

There are two published reports in which a faint nuclear NDE1/NDEL1 expression pattern was reported (Yan *et al.* 2003; Suzuki *et al.* 2007). Both of these were seen using antibodies that detected both endogenous NDE1 and NDEL1. It was therefore unclear whether the expression pattern represented NDE1, NDEL1 or specific isoforms of one of them. The new 93 antibody described here, which does not detect NDEL1, demonstrates that this signal is due, at least in part, to NDE1. This is consistent with the identification of potential NLS in two NDE1 isoforms (see section 4.5), although such puncta have been seen using over-expressed NDE1-SSSC which does not have such a sequence.

Within the nucleus, two distinct expression patterns of NDE1 are seen - a large number of small puncta throughout the nucleus, and a smaller number of discreet larger puncta. In any given cell, one such large puncta is likely to represent the centrosome, while the nature of the remaining ones remains a mystery. These structures are not centromeric nucleosomes, but may represent other nuclear bodies such as paraspeckles (Fox *et al.* 2002). A promising possibility, however, comes from the recent identification of a subpopulation of DISC1 which resides at promyelocytic leukaemia bodies (Kamiya *et al.* 2008), raising the possibility that NDE1 may also be present here. Promyelocytic leukaemia bodies are nuclear structures with diverse functions, including involvement in the phosphorylation and acetylation of proteins, transcriptional regulation and heterochromatin formation (Bernardi and Pandolfi 2007). These large puncta are also seen in some SH-SY5Y cells that had been transfected with over-expressed NDE1 and, based on this work, Fumiaki Ogawa has gone on to observe similar structures when NDE1 was over-expressed in mouse hippocampal neurons (Bradshaw *et al.* 2008).

The smaller, more dispersed, NDE1 structures in the nucleus, meanwhile, overlap with the signal detected using the Y12 antibody. This antibody was raised against the Smith antigen, a collection of small nuclear riboprotein particles, and marks splicing speckles within the nucleus. These structures contain splicing factors, kinases and phosphatases and have therefore been suggested to be involved in the regulation of mRNA splicing (Lamond and Spector 2003). The presence of one or more NDE1 isoforms at this location, therefore, suggests that NDE1 may play a, previously

unknown, role in this or a related process. Further work is required in order to better understand this.

5.6.3 NDE1 at the centrosome

That NDE1 is seen at the centrosome is not surprising, given that NDEL1 is well known to localise here (see section 1.3.3.1). What is more surprising is that colocalisation of NDE1 with γ-tubulin was only seen in a relatively small fraction of the cells, with mouse Ndel1 having been reported to be found "predominantly" at the centrosome (Sasaki *et al.* 2000). A more direct comparison is required, but this may suggest that NDE1 plays a role at the centrosomes of a lower proportion of cells than does NDEL1.

Using confocal microscopy, NDE1 was seen to be predominantly on one side of the centrosome (as defined by γ-tubulin staining). This may imply that NDE1 binds predominantly or exclusively to one of the two centrioles, and fits in well with a previously published observation that NDEL1 binds only to the mother centriole of COS7 cells (Guo *et al.* 2006).

5.6.4 Differing staining patterns of the NDE1 antibodies

The variations in the staining patterns of the different NDE1 antibodies may be indicative of different NDE1 isoforms adopting differing cellular localisations. For example, the novel nuclear structure detected using isoform 94 may be due to the NDE1-S1b isoform, which would not be detectable by any of the other antibodies. Similarly, the 95 antibody can detect only the NDE1-KMLL isoform or its mouse orthologue, and so its prominent nuclear localisation pattern must be due to this isoform. Finally, the 93 antibody is the only one which can theoretically detect NDE1-S2, although this was not observable by two-dimensional Western blotting, and so its prominent nuclear staining pattern could theoretically be in part due to this NDE1 variant. The two-dimensional Western blot also suggests the existence of other NDE1 isoforms besides the ones described in chapter 3. These may be due to additional splice variants or due to post-translational modification of variants already investigated.

A more pragmatic possibility, however, would be that one or more of the antibodies cross-reacts with proteins other than NDE1, and that these may be responsible for one or more of the localisation patterns seen. Specifically, the unique nuclear localisation patterns of the 94 and 95 antibodies must be viewed with a degree of suspicion at the present time, as they do not represent anything seen either with over-expressed protein or with other antibodies.

In order to test whether these patterns are specific or not, constructs could be generated encoding the suspected NDE1 nuclear isoforms, and their cellular localisations viewed. Another approach would be to make use of RNAi to specifically knock-down expression of NDE1. If the antibodies are indeed specific to NDE1, then such a treatment should dramatically decrease the signal seen by both immunofluoresence and Western blotting using the antibodies. Isoform-specific RNAi constructs could even be used to determine if the varying expression patterns of the antibodies are a direct result of *NDE1* alternate-splicing or not. Antigen recovery techniques could also be used. Finally, the antibodies should be tested in a larger variety of cell lines and also in primary cultures, in order to confirm that the expression patterns seen are consistent and not cell line-specific. In particular, the mouse 94 and 95 antibodies have so far been tested in only one mouse cell line, NIH-3T3, and could be tested in mouse primary neuron cultures. Until analyses such as those described above have been performed, the data presented in this chapter should be regarded as preliminary.

Nevertheless, the best demonstration that a protein exhibits a specific localisation pattern is through replication with independently produced antibodies, raised against non-overlapping regions of the protein. Therefore, while the data described here cannot be taken as definitive, it does provide a benchmark for future investigation.

5.6.5 The problem of antibody cross-reactivity

As has been demonstrated, all three commercially available NDE1 antibodies (at time of writing) are unable to distinguish between NDE1 and NDEL1. Interestingly, a recent paper also investigated one of these antibodies (10233-1-AP) and concluded that it was largely NDE1-specific (Vergnolle and Taylor 2007). They did this through

Antibody	Target	Original paper	Cross-reactivity?
mNudE	Mouse NDE1	(Feng *et al.* 2000)	(Not stated)
210 + 211	NDEL1	(Niethammer *et al.* 2000)	(Not stated)
C-6	NDEL1	(Sasaki *et al.* 2000)	(Not stated)
Nudel	NDEL1	(Yan *et al.* 2003)	Yes
4-9C	Rat NDEL1	(Yamaguchi *et al.* 2004)	No
NO_{AB}	Rat NDEL1	(Hayashi *et al.* 2005)	(Not stated)
NudE	Mouse NDE1	(Soukoulis *et al.* 2005)	(Not stated)
P-NDEL1	Phospho-NDEL1	(Toyo-Oka *et al.* 2005)	(Not stated)
Nudel	NDEL1	(Guo *et al.* 2006)	(Not stated)
NDEL1	NDEL1	(Kamiya *et al.* 2006)	No (Burdick *et al.* 2008)
NudE	NDE1	(Liang *et al.* 2007)	(Not stated)
Nudel	NDEL1	(Liang *et al.* 2007)	(Not stated)
α-P-251	Phospho-NDEL1	(Mori *et al.* 2007)	(Not stated)
mNudE	Mouse NDE1	(Stehman *et al.* 2007)	Yes
NDE1	NDE1	(Burdick *et al.* 2008)	No

Table 5.6: A list of non-commercial NDE1 and NDEL1 antibodies published in the literature. Only five have, to date, been reported to have been tested for cross-reactivity between NDE1 and NDEL1.

---

use of NDE1 RNAi, which greatly reduced the signal detected by the antibody. Some NDE1 signal did remain however, implying that the antibody may also detect NDEL1 to some degree, in agreement with the results reported here. The difference in the degree to which the antibody appears NDE1-specific in the two studies is likely due to a combination of the different methods used (knocking down of endogenous NDE1 expression as opposed to direct detection of NDE1 and NDEL1 *in vitro*) and the fact the relationship between the strength of signal on a Western blot, used in both studies, and the amount of a protein present is not linear, especially once the signal becomes saturated.

Given the high level of amino acid similarity between the NDE1 and NDEL1 proteins, it is likely that other NDE1/NDEL1 antibodies would also cross-react in a similar way to the commercial antibodies described above. Table 5.6 shows a list of novel NDE1 and NDEL1 antibodies described in the literature to date. As can be seen, only a fraction of these are reported as having been tested in order to determine whether they are specific to NDE1 or NDEL1. Based on these results, it appears reasonable to assume that a substantial proportion of these antibodies will cross-react, making it difficult to fully interpret results gained whilst using them.

Chapter 6 - Protein binding partners of NDE1 include DISC1 and members of its pathway

6.1 Introduction

NDEL1 is known to have at least two distinct protein-protein interaction sites. These correspond to a short predicted C-terminal helix, where proteins including DISC1 and dynein bind (Sasaki *et al.* 2000; Millar *et al.* 2003; Brandon *et al.* 2004), and parts of a longer N-terminal coiled-coil where LIS1 binds and self-association occurs (Sasaki *et al.* 2000; Yan *et al.* 2003). These putative structures appear to be conserved in NDE1 as well as NDEL1 (see chapter 4). NDEL1 can form multimers (Sasaki *et al.* 2000; Derewenda *et al.* 2007) and NDE1 has been seen to do the same. Such multimers therefore have the potential to bind to several proteins simultaneously. This suggests that NDE1 and NDEL1 may be able to act as interaction hubs, binding simultaneously to more than one protein, possibly as part of a larger protein complex. The most studied protein interaction partners of NDEL1 to date are LIS1 and DISC1, however study of these proteins as potential NDE1 interactors has been very limited.

DISC1 is implicated in binding to over 100 separate proteins; mostly as a result of yeast-two-hybrid screening (see section 1.2.2.4). One DISC1 interactor of particular interest is phosphodiesterase 4B (PDE4B), which was found to be disrupted by a chromosomal translocation in a proband with schizophrenia (Millar *et al.* 2005b), and which has since been associated with schizophrenia in several populations (Pickard *et al.* 2007; Fatemi *et al.* 2008; Numata *et al.* 2008b) and with major depression (Numata *et al.* 2008a).

Multiple protein interaction sites within DISC1 have been mapped and occur along the length of DISC1 suggesting that DISC1 is also likely to be a hub protein. For example, the sites known to be involved in PDE4B binding are primarily in the N-terminal quarter of DISC1 (Millar *et al.* 2005b; Murdoch *et al.* 2007), while the NDEL1 binding site is near the C-terminus (see figure 1.3.B). This therefore raises the interesting possibility that PDE4B, encoded by a gene with known links to psychiatric illness, may bind to DISC1 at the same time as NDE1 and/or NDEL1.

6.2 Confirmation that endogenous NDE1 interacts with LIS1

6.2.1 Endogenous LIS1 and NDE1 co-immunoprecipitate

Mammalian NDE1 was originally characterised after it was found to bind to LIS1 in a series of yeast-two-hybrid screens (Feng *et al.* 2000; Kitagawa *et al.* 2000; Sasaki *et al.* 2000). The authors then went on to demonstrate that, in rodents, these proteins were also capable of co-immunoprecipitating each other when over-expressed in cell lines. To date, however, complexing of endogenous NDE1 and LIS1 has not been demonstrated.

The 93 antibody, generated in chapter 5, was therefore used to immunoprecipitate NDE1 from a COS7 cell lysate. Using a commercial antibody, LIS1 was seen to be co-immunoprecipitated (see figure 6.2.A). It therefore appears that endogenous NDE1 and LIS1 can complex together in the mammalian cell.

6.2.2 Endogenous LIS1 and NDE1 colocalise in some cells at a centrosome-like structure

In order to further confirm the LIS1-NDE1 interaction, their expression patterns were compared. Immunocytochemistry was therefore used to visualise endogenous LIS1 and NDE1 (antibody 93) within SH-SY5Y cells. The expression patterns of the two proteins differed considerably, with LIS1 being found primarily in the cell body, while NDE1 was primarily nuclear (see figure 6.2.B). Colocalisation was seen, however, in a subset of cells (less than one quarter). This was seen usually at a bright puncta either at or adjacent to the nucleus. Given that LIS1 is known to be at the centrosome (Feng *et al.* 2000; Niethammer *et al.* 2000) and endogenous NDE1 has now been seen there also (see section 5.5.5), it can reasonably be assumed that NDE1 and LIS1 are colocalising at this location.

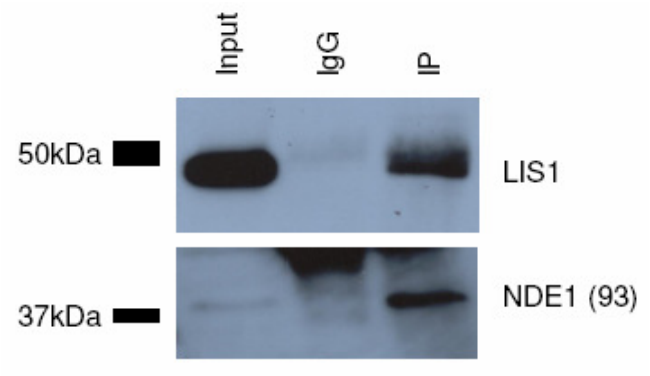

Figure 6.2.A: LIS1 was co-immunoprecipitated from a COS7 lysate using the 93 antibody, indicating that endogenous LIS1 and NDE1 can complex.

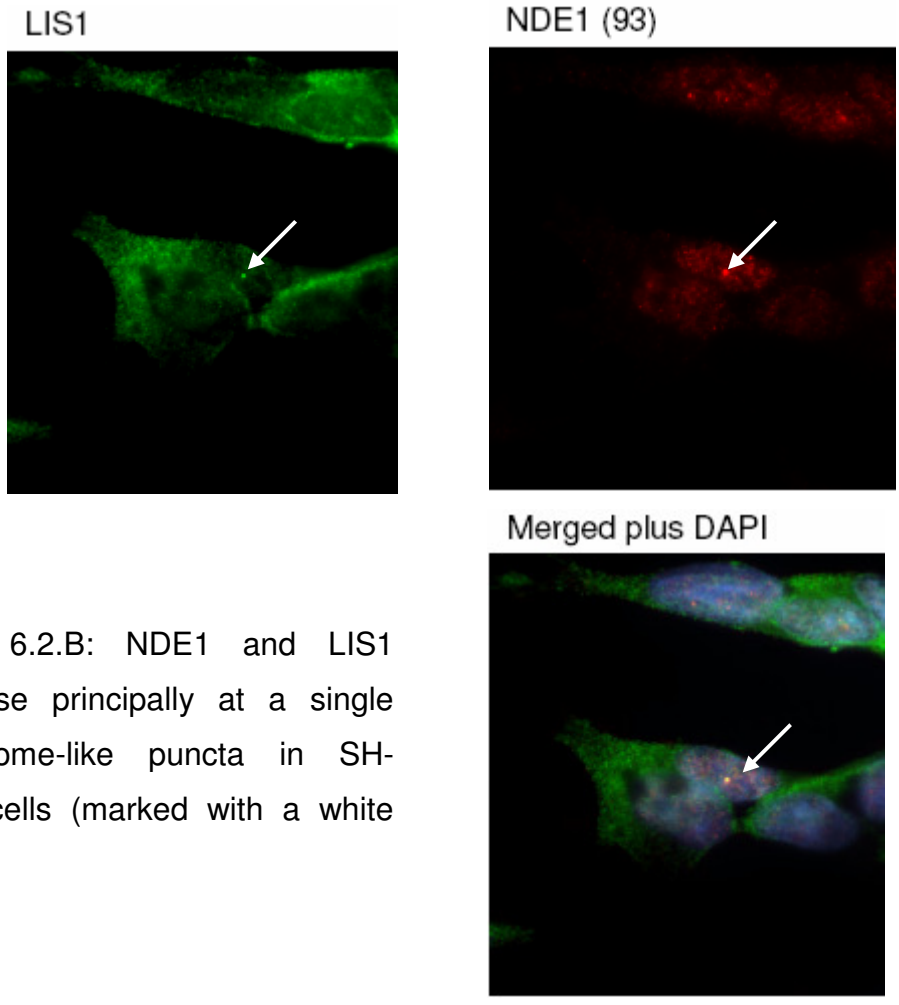

Figure 6.2.B: NDE1 and LIS1 colocalise principally at a single centrosome-like puncta in SH-SY5Y cells (marked with a white arrow)

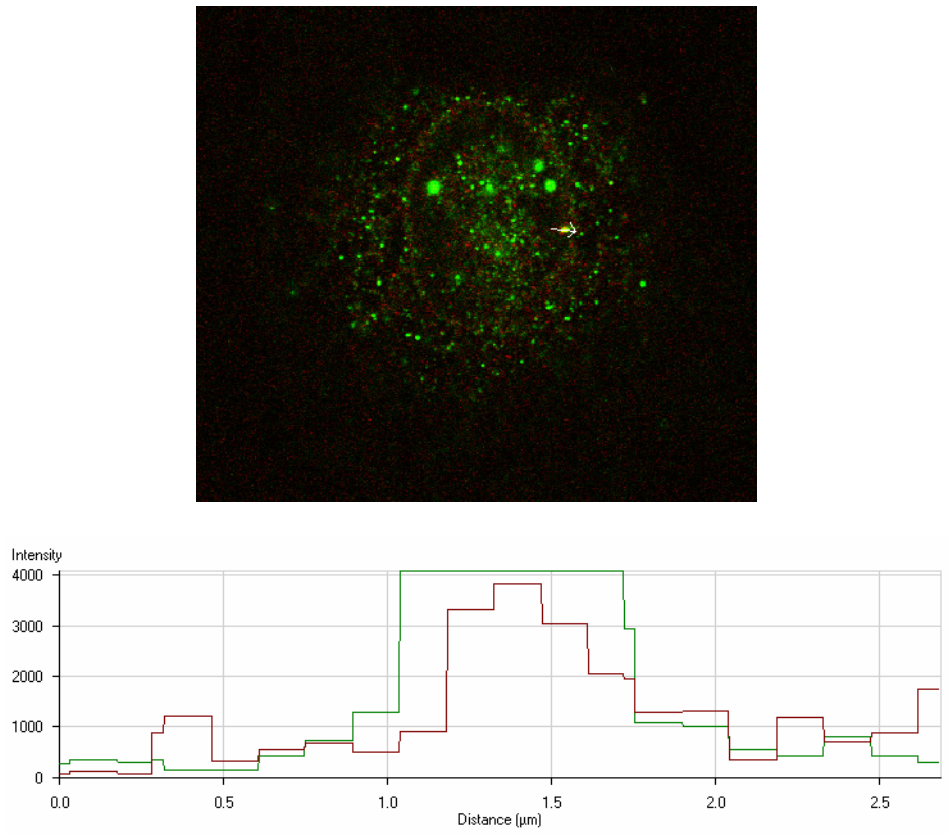

Figure 6.2.C: Sample confocal microscopy image of LIS1 (red) and NDE1 93 (green) in COS7 cells. Graph shows intensities of the two antibodies along the white arrow in the image above. At the large perinuclear puncta, colocalisation of the two proteins is clearly seen.

6.2.3 LIS1 and NDE1 colocalisation by confocal microscopy

In order to confirm the colocalisation of LIS1 and NDE1 to this centrosome-like puncta, confocal microscopy was utilised with assistance from Becky Carlyle. The NDE1 93 and LIS1 antibodies were this time used to stain COS7 cells. Colocalisation was again repeatably seen to occur at a single centrosome-like puncta (see figure 6.2.C), but this was not visible in all cells.

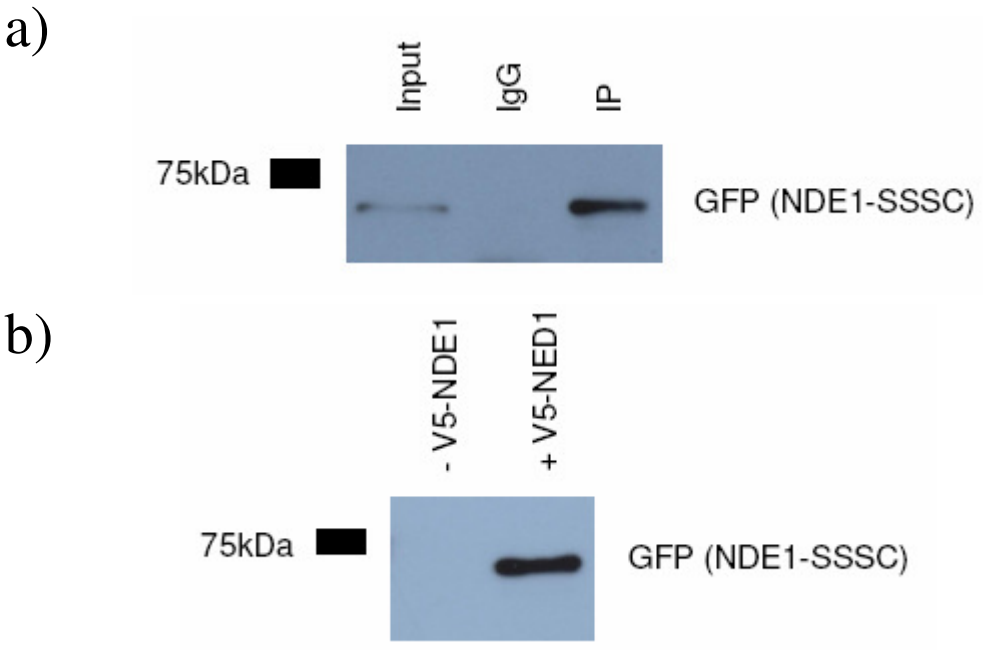

Figure 6.3.A: a) V5-NDE1-SSSC and GFP-NDE1-SSSC were over-expressed in COS7 cells and immunoprecipitated using an anti-V5 antibody. GFP-NDE1 was co-immunoprecipitated. b) *In vitro* transcribed and translated GFP-NDE1-SSSC can be co-immunoprecipitated by an anti-V5 antibody in the presence of V5-NDE1-SSSC, but not in its absence.

6.3 NDE1 and NDEL1 complexes

6.3.1 NDE1 forms homodimers

NDEL1 molecules have been previously been shown to form homodimers (Efimov and Morris 2000; Sasaki *et al.* 2000; Maiolica *et al.* 2007). In order to investigate whether NDE1 does the same, V5-NDE1-SSSC and GFP-NDE1-SSSC were over-expressed in COS7 cells. By using an anti-V5 antibody it was possible to co-immunoprecipitate the GFP-tagged NDE1 (see figure 6.3.A.a), suggesting that the two NDE1 proteins formed a complex together within the cell. This is in agreement with a similar experiment performed elsewhere (Feng and Walsh 2004). The use of such protein tags for immunoprecipitation experiments is well established and so it seems highly unlikely that the interaction is due to V5-GFP interactions, nevertheless this possibility cannot be formally discounted without an additional negative control.

However, this result alone merely shows that two or more NDE1 monomers can co-exist in the same complex, not necessarily that they bind directly to each other. If both bound simultaneously to a third protein, for example a LIS1 dimer, then they would still be able to co-immunoprecipitate each other from cell lysates. Therefore, in order to demonstrate direct binding, an alternative to a cell lysate is required. An *in vitro* transcription and translation system was therefore used to produce V5-NDE1-SSSC and GFP-NDE1-SSSC in a cell free environment. These two pools of protein were mixed and immunoprecipitation was performed using an anti-V5 antibody. As a negative control, GFP-NDE1-SSSC alone was used. GFP-NDE1-SSSC could indeed be co-immunoprecipitated using this system, but only in the presence of V5-NDE1-SSSC (see figure 6.3.A.b). Given the lack of other proteins present compared to in a cell lysate, it can be concluded that NDE1 self-association probably occur through direct interaction of NDE1 monomers. Based on a published structural analysis of NDEL1 (Derewenda *et al.* 2007), in which X-ray defraction was used in order to study the N-terminal coiled-coil segment of NDEL1 and NDEL1 multimers, it appears likely that this interaction occurs principally in the form of a dimer.

6.3.2 NDE1 exists in a complex with NDEL1

Both NDE1 and NDEL1 have been shown to form dimers and the self-association domain of NDEL1 (Sasaki *et al.* 2000) is well conserved in NDE1 (75.2% identity, 96.2% similarity from NDEL1 amino acids 57-189). It is therefore reasonable to predict that NDE1 and NDEL1 proteins may also be able to bind to each other. GFP-NDEL1-PLSV and V5-NDE1-SSSC were therefore over-expressed in COS7 cells. NDE1 was immunoprecipitated using an anti-V5 antibody, and GFP-NDEL1 was seen to be co-immunoprecipitated with it (see figure 6.3.B.a), implying that NDE1 and NDEL1 can co-exist in the same protein complex.

To see if endogenous protein behaves in the same way, the 93 antibody was used to immunoprecipitate NDE1 from an SH-SY5Y lysate. By using the 231 antibody,

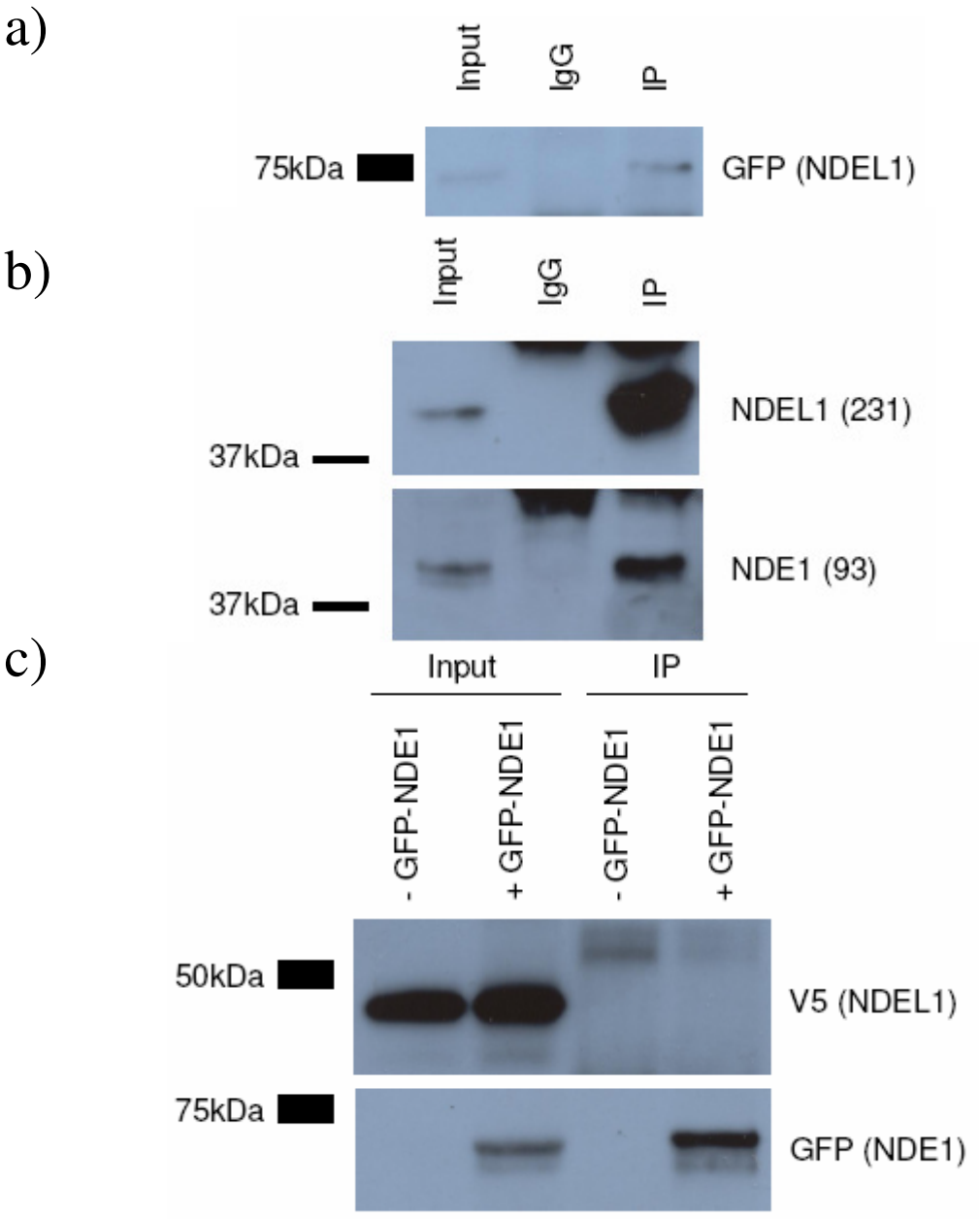

Figure 6.3.B: a) V5-NDE1-SSSC can co-immunoprecipitate GFP-NDEL1-PLSV using an anti-V5 antibody when both are over-expressed in COS7. b) Endogenous NDEL1 (antibody 231) can be co-immunoprecipitated from an SH-SY5Y lysate using an endogenous anti-NDE1 antibody (93). c) V5-NDEL1-PLSV is not seen to co-immunoprecipitate by GFP-NDE1-SSSC using an anti-GFP antibody when the two proteins are transcribed and translated *in vitro*. The immunoprecipitation of GFP-NDE1-SSSC is confirmed to have worked.

NDEL1 was seen to have been co-immunoprecipitated (see figure 6.3.B.b), showing that endogenous NDE1 and NDEL1 complex together. A similar result has since been published elsewhere using independent antibodies (Burdick *et al.* 2008). Surprisingly, it appeared to be considerably easier to co-immunoprecipitate NDE1 and NDEL1 using endogenous protein than it was using the tagged over-expressed protein. While co-immunoprecipitation experiments using different antibodies are not directly comparable, this nevertheless presented the possibility that an additional cellular factor is required for them to complex, a factor which is limiting when over-expressed NDE1 and NDEL1 form a complex.

To further investigate this phenomenon, V5-NDEL1-PLSV and GFP-NDE1-SSSC were produced using the *in vitro* transcription and translation system. Immunoprecipitating using an anti-GFP antibody, only GFP-NDE1-SSSC, and not V5-NDEL1-PLSV, was precipitated (see figure 6.3.B.c). This experiment was repeated three times, each with the same negative result. It therefore appears that it is not possible for NDE1-NDEL1 interactions to occur under these conditions, despite NDE1 self association interactions being detected using the same system (see figure 6.3.A.b). This suggests that NDE1-NDEL1 complexes are of a different form to NDE1-NDE1 or NDEL1-NDEL1 complexes, as will be discussed in section 6.7.1.

6.3.3 Comparison of NDE1 and NDEL1 localisations

When over-expressed in HEK293T cells, V5 and GFP tagged NDE1-SSSC and NDEL1-KMLL are found to colocalise, principally at a perinuclear structure which resembles the centrosome (see figure 6.3.C.a). This pattern was not dependent on which protein was labelled with which tag. It cannot be presumed that these localisations are reflective of endogenous protein, however.

As NDE1 antibody 93 and NDEL1 antibody 231, were raised in rabbits, a direct comparison of the staining patterns of the two is not possible. A small amount of the NDE1 93 antibody was therefore conjugated directly to a green fluorescent tag. This conjugated antibody, 93-488, produces a similar expression pattern to 93 but shows

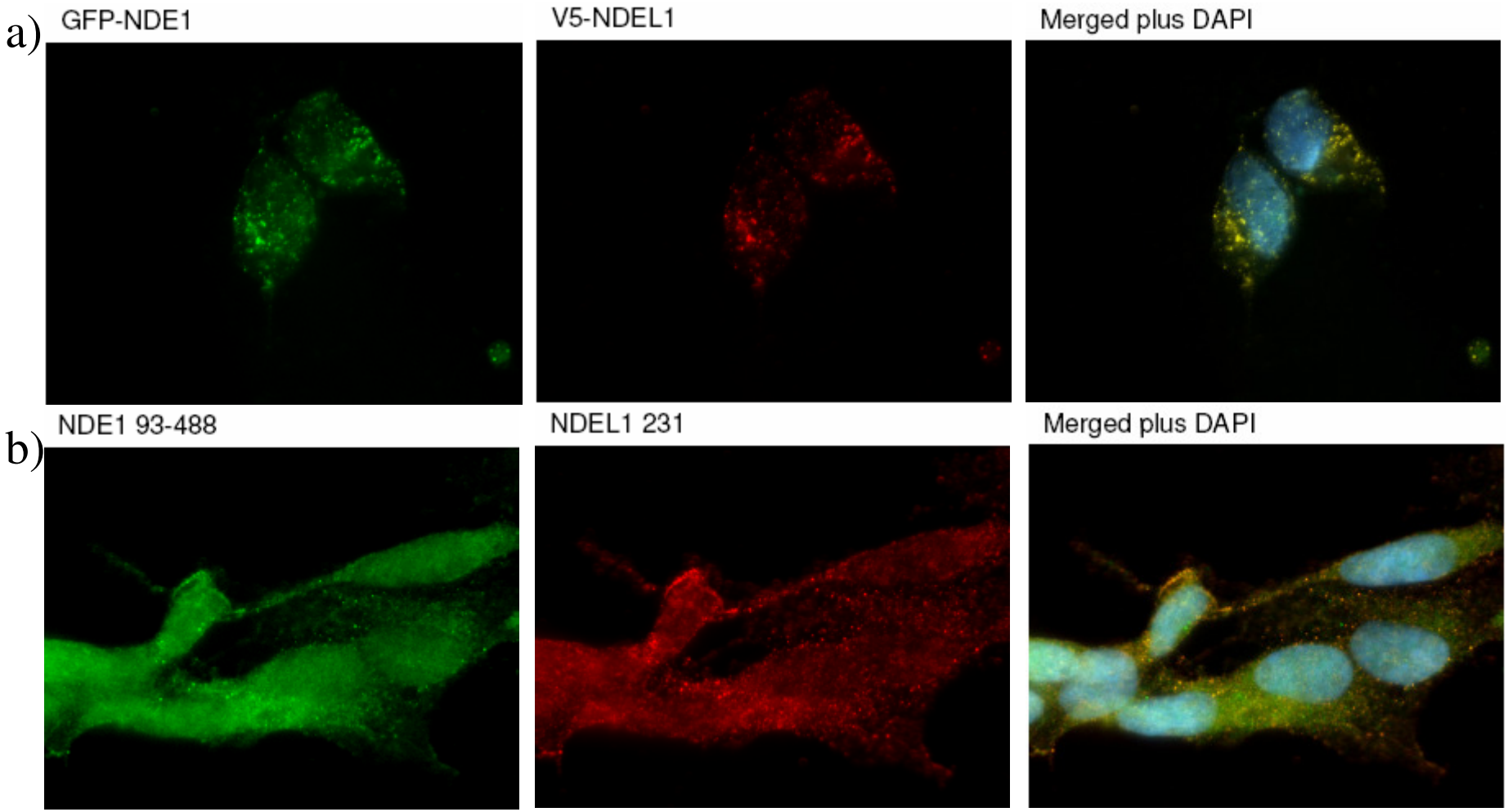

Figure 6.3.C: a) GFP-NDE1-SSSC and V5-NDEL1-PLSV colocalise in HEK293T cells. b) The 93-488 (NDE1) and 231 (NDEL1) antibodies colocalise extensively but not completely in SH-SHY5Y cell bodies.

nuclear NDE1 in a diffuse, rather than punctate, pattern. When the 93-488 and 231 antibodies were compared in SH-SY5Y cells (see figure 6.3.C.b), wide-spread NDE1-NDEL1 colocalisation was seen. Specifically, the two proteins were seen together in the cell body and at the centrosome. Without γ-tubulin staining, it was not possible to determine whether this localisation was across the whole centrosome or just at a single centriole. NDE1 expression at the nucleus appeared to be greater than that of NDEL1, relative to their expression elsewhere in the cell.

6.3.4 Partial colocalisation of NDE1 and NDEL1 by confocal microscopy

In order to further investigate the expression patterns of the 93-488 and 231 antibodies, the cells were viewed by confocal microscopy, with assistance from Becky Carlyle. Looking at SH-SY5Y cells, the NDE1 and NDEL1 antibodies were repeatably seen to colocalise at a large perinuclear structure which can be presumed to be the centrosome (see figure 6.3.D.a).

Interestingly, when the intensities of the antibody fluorescence were measured along a line crossing the nucleus (see figure 6.3.D.b), it was seen that the 93-488 antibody shows a stronger staining pattern than 231 within this organelle. In comparison, 231 showed the stronger signal at the nuclear periphery. Both proteins appear to be present at the nucleus, however.

6.4 The NDE1-DISC1 interaction

6.4.1 Confirmation that NDE1 binds directly to DISC1

As a first step towards confirming that DISC1 and NDE1 interact, as had been shown through yeast-two-hybrid screening (Millar *et al.* 2003; Brandon *et al.* 2004), FLAG-tagged DISC1 and V5-tagged NDE1-SSSC were over-expressed in COS7 cells. The V5-NDE1 could be co-immunoprecipitated with the FLAG-DISC1 using an anti-FLAG antibody (figure 6.4.A.a), implying that the two over-expressed proteins were able to complex with each other, in agreement with results that have since been published elsewhere (Burdick *et al.* 2008).

a)

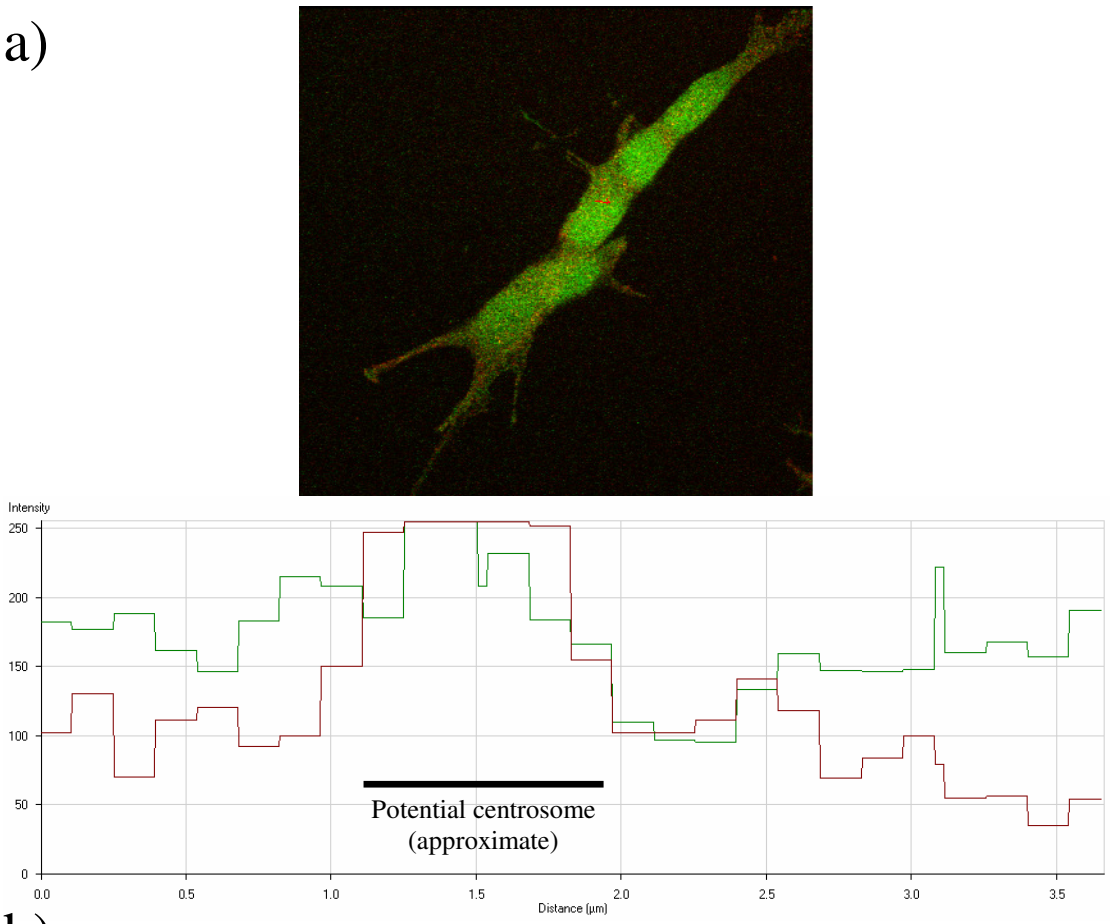

b)

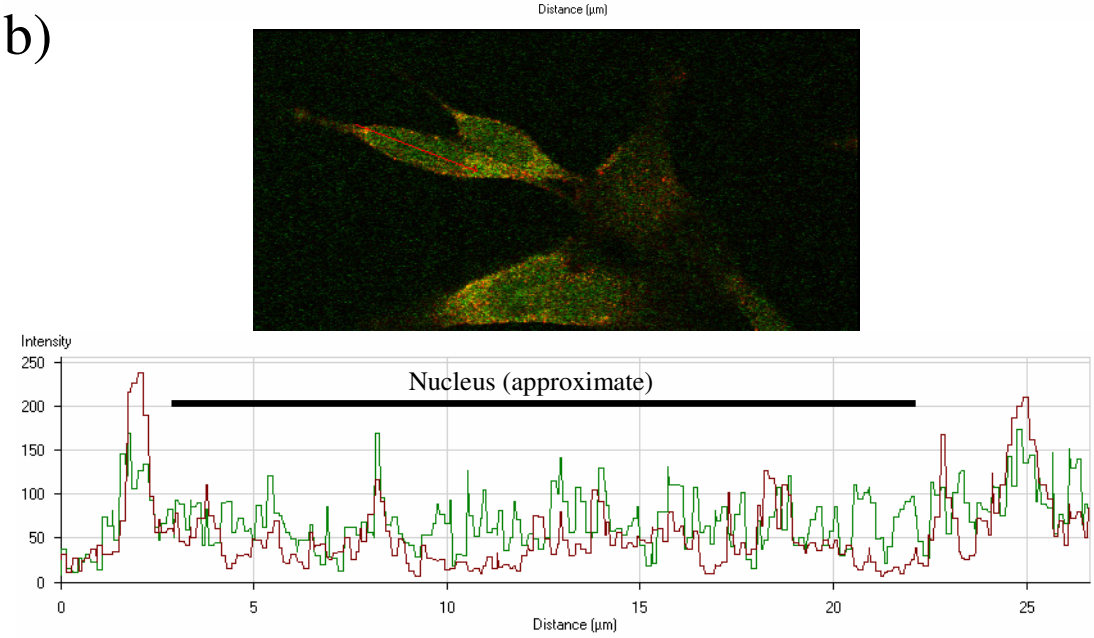

Figure 6.3.D: Confocal microscopy of NDE1 93-488 (green) and NDEL1 231 (red) in SH-SY5Y cells. Graphs show intensities of each antibody along the red line marker on the corresponding image. Estimates of the positions of the nucleus and centrosome-like puncta are marked on the graph.

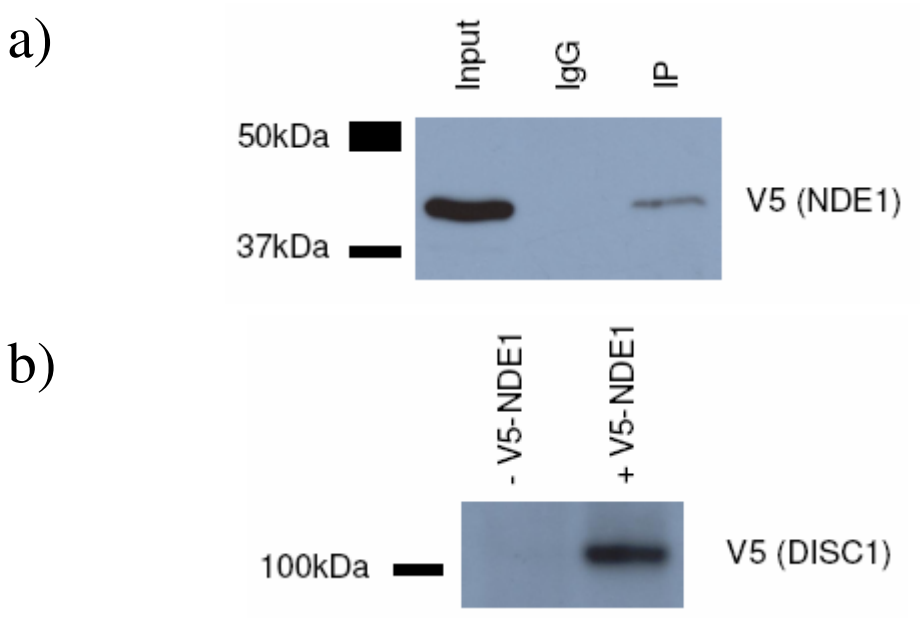

Figure 6.4.A: a) V5-NDE1-SSSC was co-immunoprecipitated by FLAG-DISC1 using an anti-FLAG antibody when both were over-expressed in COS7 cells. b) V5-DISC1 was co-immunoprecipitated with GFP-NDE1-SSSC using an anti-GFP antibody and *in vitro* transcribed and translated protein.

In order to determine if this is a direct interaction (rather than simultaneous binding of DISC1 and NDE1 to a third protein), *in vitro* transcribed and translated V5-DISC1 and GFP-NDE1-SSSC were mixed together. V5-DISC1 could be co-immunoprecipitated using an anti-GFP antibody in the presence of GFP-NDE1-SSSC, but not in its absence (figure 6.4.A.b). This strongly implies that DISC1 and NDE1 bind directly to each other as suggested by the yeast-two-hybrid results.

6.4.2 NDE1 binds multiple isoforms of endogenous DISC1

The DISC1 protein is known to exist as a number of different species of varying sizes (James *et al.* 2004). In order to determine which endogenous DISC1 isoforms NDE1 interacts with, the 93 antibody was used to immunoprecipitate NDE1 from an SH-SY5Y cell lysate. The αDISC1 antibody is raised against a C-terminal region of DISC1 and has been characterised previously (Ogawa *et al.* 2005), detecting multiple DISC1 species of the same size as those detected using other established antibodies (James *et al.* 2004). The α-DISC1 antibody was able to detect numerous species of

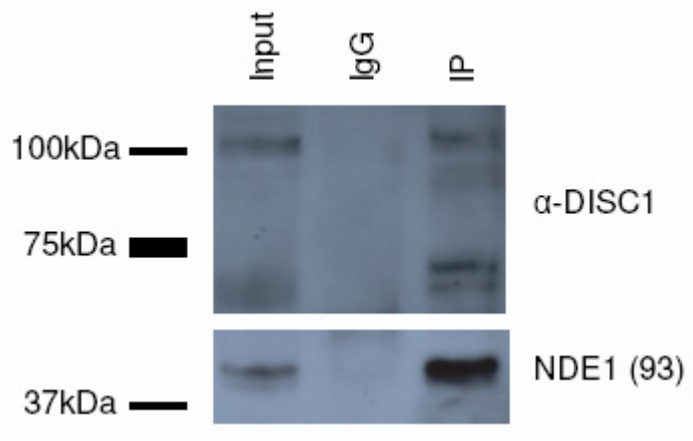

Figure 6.4.B: Multiple DISC1 isoforms co-immunoprecipitated using an anti-NDE1 antibody (93) from an SH-SY5Y lysate.

DISC1 which had co-immunoprecipitated with NDE1 (see figure 6.4.B). These included the full length (~100kDa) form, as well as species of sizes of 70-80kDa. It therefore appears that NDE1 can bind to multiple isoforms of DISC1 within the human cell. The nature of the species remains to be determined but could be analysed by, for example, mass spectroscopy.

6.4.3 NDE1 and DISC1 colocalise at a centrosome-like structure

DISC1 has been previously shown at the centrosome (Morris *et al.* 2003; James *et al.* 2004), where it colocalises with over-expressed NDEL1 (Kamiya *et al.* 2006). In order to determine if DISC1 and NDE1 also colocalised at this location, FLAG-DISC1 and V5-NDE1-SSSC were over-expressed in HEK293T cells. Colocalisation of V5 and FLAG antibodies in the cells was restricted, but was seen most clearly at a large puncta on the edge of the nucleus (see figure 6.4.C) which closely resembles the centrosome.

6.5 NDE1 exists in a complex with ATF4

6.5.1 NDE1 complexes with ATF4

Activating Transcription Factor 4 (ATF4) is a DISC1-interacting protein (Millar *et al.* 2003; Morris *et al.* 2003; Sawamura *et al.* 2008) which has been suggested to be associated with schizophrenia (Kakiuchi *et al.* 2007; Qu *et al.* 2008). In order to

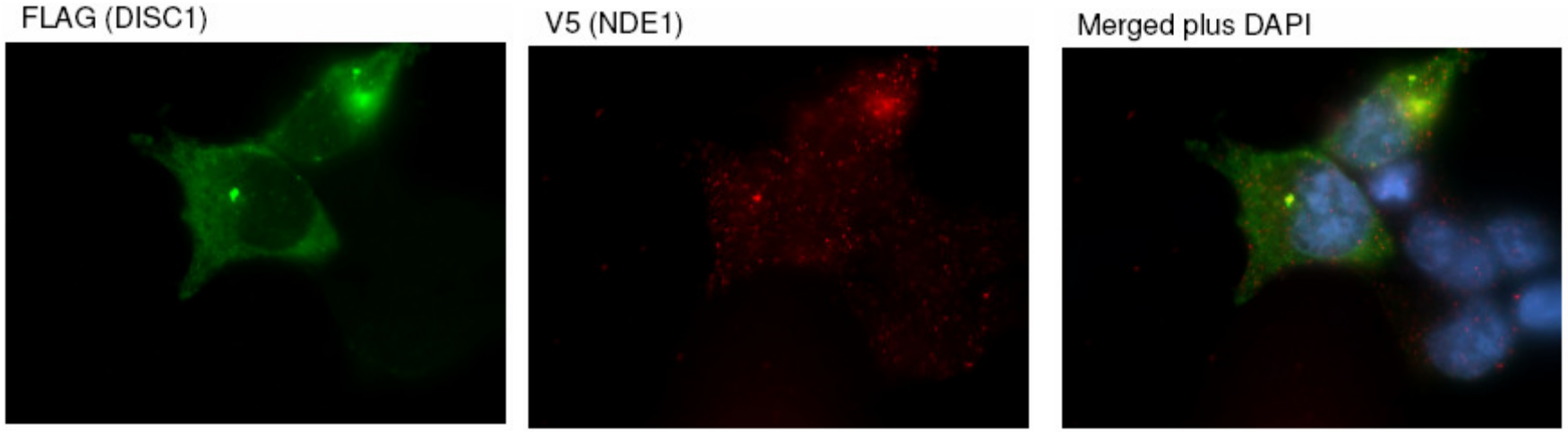

Figure 6.4.C: FLAG-DISC1 and V5-NDE1 (MBL antibody) colocalise at a centrosome-like puncta when over-expressed in HEK293T cells.

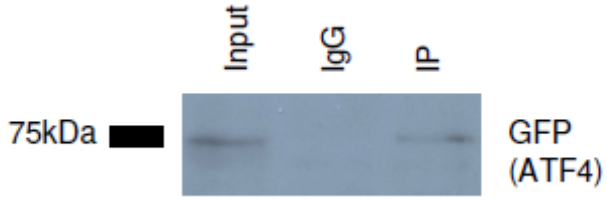

Figure 6.5.A: V5-NDE1-SSSC can co-immunoprecipitate GFP-ATF4 using an anti-V5 antibody when both are over-expressed in COS7 cells.

---

investigate whether NDE1 and ATF4 may bind to DISC1 simultaneously, COS7 cells were co-transfected with V5-tagged NDE1-SSSC and GFP-tagged ATF4. By using an anti-V5 antibody, it was possible to co-immunoprecipitate ATF4 with NDE1 (figure 6.5.A). It therefore appears that NDE1 and ATF4 can exist in the same complex.

6.5.2 NDE1 and ATF4 show some colocalisation

Staining SH-SY5Y cells with antibody 93 and an anti-ATF4 antibody, it could be seen that endogenous NDE1 and ATF4 colocalise in some cells (figure 6.5.B). Typically the two colocalised at one, or occasionally two, punctate structures in the nucleus. It would be interesting to know whether this was the same type of nuclear structure as that at which NDE1 and CENPA were seen to colocalise in section 5.5.1.1, a question which could be addressed using three-colour immunofluorescence.

6.6 NDE1 exists in a complex with PDE4B1

6.6.1 Over-expressed NDE1 can complex with PDE4B1

In order to test if NDE1 and PDE4B1 can exist in the same protein complex, for example by simultaneous binding to DISC1, PDE4B1 and V5-tagged NDE1-SSSC were over-expressed in COS7 cells. PDE4B could be immunoprecipitated using an anti-V5 antibody (figure 6.6.A), indicating that the two over-expressed proteins were indeed forming a complex together.

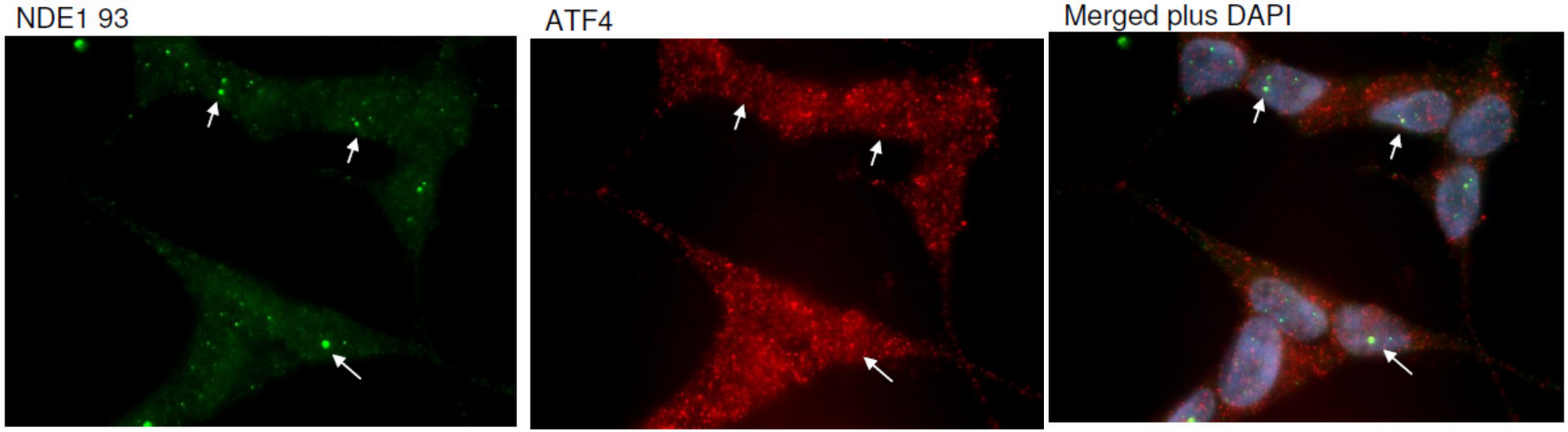

Figure 6.5.B: NDE1 (green) and ATF4 (red) colocalise at a nuclear punctate structure in some, but not all, SH-SY5Y cells. White arrows indicate points of colocalisation

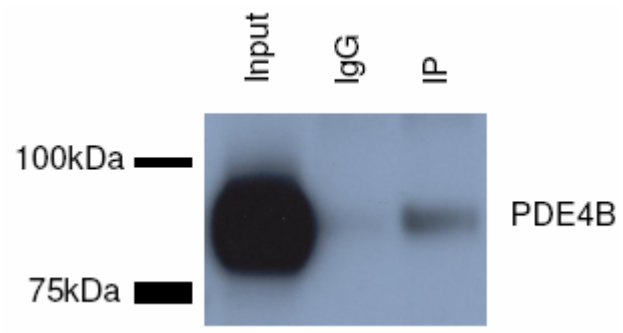

Figure 6.6.A: PDE4B1 (detected using a pan-PDE4B antibody) is seen to be co-immunoprecipitated with V5-NDE1-SSSC using an anti-V5 antibody when both are over-expressed in COS7 cells.

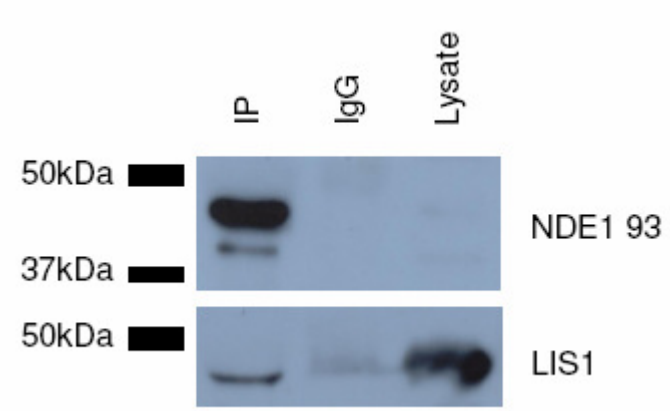

Figure 6.6.B: Endogenous PDE4B had previously been immunoprecipitated from an SH-SY5Y lysate by Sheila Christie and Kirsty Millar using a pan-PDE4B antibody. They showed DISC1 and NDEL1 to be co-immunoprecipitated. The membrane was now also probed using the NDE1 93 antibody and a commercial LIS1 antibody. Both proteins were seen to have been co-immunoprecipitated with PDE4B.

6.6.2 Endogenous PDE4B can complex with NDE1 and LIS1

Previously, Kirsty Millar and Sheila Christie performed an immunoprecipitation experiment from an SH-SY5Y lysate using an anti-PDE4B antibody, and showed that NDEL1 (231) is co-immunoprecipitated (Bradshaw *et al.* 2008). This suggests that PDE4B and NDEL1 exist in the same complex *in vivo*.

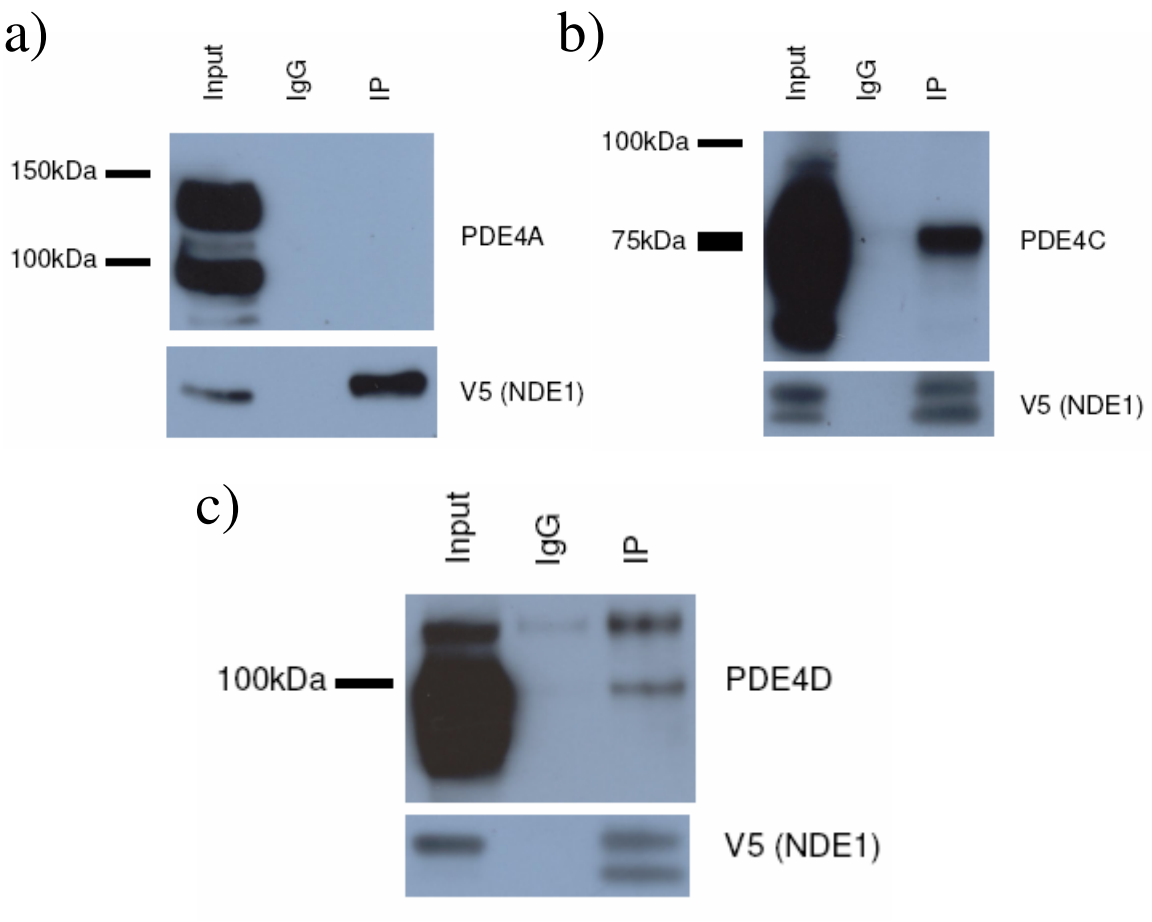

Figure 6.6.C: a) V5-NDE1-SSSC was not seen to co-immunoprecipitate with PDE4A10 when over-expressed in COS7 cells. b) V5-NDE1-SSSC and PDE4C2 were over-expressed in COS7 cells. A PDE4C protein co-immunoprecipitated with V5-NDE1. c) V5-NDE1-SSSC and PDE4D5 were over-expressed in COS7 cells. A PDE4D protein co-immunoprecipitated with V5-NDE1. All co-immunoprecipitations were done using an anti-V5 antibody.

This lysate and immunoprecipitate were once again Western blotted and this time stained using the 93 antibody. NDE1 is indeed clearly seen to be co-immunoprecipitated (see figure 6.6.B). It therefore appears that the complexing of NDE1 and PDE4B shown using over-expressed protein also occurs with endogenous protein. Additionally, LIS1 was co-immunoprecipitated, indicating that it also exists in a complex with PDE4B.

6.6.3 Over-expressed NDE1 can complex with a range of PDE4 proteins

There are four separate genes encoding PDE4 proteins in humans named *PDE4A-D* (Houslay and Adams 2003). Each of these then has a number of splice variants, for example PDE4B has five, termed PDE4B1-5 (Houslay and Adams 2003; Cheung *et al.* 2007). These isoforms can be divided into three broad categories based on a conserved configuration of functional domains. These categories are long, short and super-short. Given that NDE1 has been seen to complex with one long PDE4 isoform, PDE4B1, it is reasonable to hypothesise that it may be able to also complex with other long PDE4 isoforms.

Four sets of COS7 cells were co-transfected with V5-NDE1-SSSC and a representative long PDE4 isoform from one of PDE4A-D. Using an anti-V5 antibody, it was possible to co-immunoprecipitate PDE4B1, PDE4C2 and PDE4D5 with V5-NDE1 (see figure 6.6.C). In three attempts, however, PDE4A10 was not definitively co-immunoprecipitated. It remains unclear whether this is due to lack of a biological interaction, or simply due to technical problems. It therefore appears as if NDE1 is capable of forming a complex with a range of PDE4 long isoforms, but not necessarily with all of them. Results of a similar experiment, using NDEL1 rather than NDE1, have recently been published (Collins *et al.* 2008). They showed co-immunoprecipitation of over-expressed NDEL1 with PDE4A5, PDE4B1, PDE4C2 and PDE4D3.

6.7 Discussion

6.7.1 The nature and localisation of the NDE1-NDEL1 complex

In this chapter, NDE1 and NDEL1 have been demonstrated to co-exist in complexes by means of co-immunoprecipitation. An implication of this finding is it that the two proteins are capable of working cooperatively within the cell. It therefore follows that NDE1 and NDEL1 are likely to share some of the same cellular functions. It also adds further complexity to the issue of using antibodies to detect NDE1 and NDEL1 within the cell. Not only must it be clarified if the antibody detects NDE1,

NDEL1 or both, but is possible that any signal detected may be from a complex containing both proteins anyway.

Given that both NDE1 and NDEL1 form homo-dimers, and their close amino acid similarity, the existence of a NDE1-NDEL1 heterodimer can be predicted. However, while the NDE1-NDEL1 interaction appeared very strong using endogenous protein, it was relatively weak using over-expressed protein and was not visible at all *in vitro*. Given that robust NDE1-NDE1 self-association could be consistently shown using all three of these systems, it must be concluded that the NDE1-NDEL1 interaction is fundamentally different in nature to NDE1-NDE1 or NDEL1-NDEL1 self association. The simplest explanation for this would be that the two proteins do not interact directly, but instead simultaneously bind to a third protein such as LIS1 or DISC1. An alternative conclusion can be drawn by comparing their amino acid sequences and noting that the NDEL1 tetramerisation domain (Derewenda *et al.* 2007) is almost perfectly conserved in NDE1 (81% identity, 99% similarity), while the dimerisation domains differ to a greater extent (56% identity, 92% similarity). Thus NDE1 and NDEL1 may only be able to interact when homodimers of each protein bind to form a heterotetramer. In this case, the lack of binding *in vitro* would be explained by the lack of a cellular factor required to aid in the binding of the proteins, or if such a tetramer was a thermodynamically unfavourable configuration at the low protein concentrations present in such an experiment, compared to the much higher total protein content of a cell.

Some NDEL1 signal was detected in the nucleus using the NDEL1 231 antibody. This may represent NDE1 cross-reactivity, however it is also possible that NDEL1 could genuinely be present in this location. This could happen in two ways. Firstly, it is possible that there exists an additional, but not yet described, NDEL1 isoform which has an NLS sequence. Secondly, NDE1 and NDEL1 have been shown to complex together. It is therefore possible that a complex (such as a heterotetramer) containing NDE1-KMLL could be targeted to the nucleus, taking any NDEL1 proteins in the complex with it.

A caveat to co-immunoprecipitation analysis using over-expressed protein is that the possibility that protein tags (in this case V5 and GFP) interact with each other cannot be formally excluded without the use of an additional negative control in which the tags alone are expressed and immunoprecipitation performed. Similarly, the fact that the 93 antibody is successful in co-immunoprecipitating a variety of proteins raises the possibility that the co-immunoprecipitation may be an artefact of using the antibody. Again this could be discounted by the addition of an additional negative control, in this case demonstrating that 93 cannot co-immunoprecipitate some other protein. Nevertheless, the fact that the work with both the endogenous and over-expressed protein yields the same results (NDE1-NDEL1 interaction) implies that the interaction is genuine and not a false positive. The same is also true of other NDE1 interactions described in the chapter.

6.7.2 DISC1 interaction with NDE1 and NDEL1

The interaction of DISC1 with NDEL1 is very well established; however this is the first work to demonstrate a DISC1-NDE1 interaction using endogenous protein. Interestingly, NDE1 is seen to co-immunoprecipitate with several different DISC1 species, including the full length 100kDa species as well as the 75kDa and 71kDa species which may be localised to the mitochondria (Ozeki *et al.* 2003; James *et al.* 2004). This implies that NDE1 is likely to associate with DISC1 in multiple parts of the cell.

6.7.3 NDE1 as part of a DISC1 mega-complex

DISC1 is known to interact with NDE1 and NDEL1, each of which also show evidence of being associated with schizophrenia. However DISC1 interacts with other proteins, notably PDE4B, that have also been associated with major mental illness. It is highly implausible that DISC1 would be involved in multiple independent schizophrenia-related pathways. The alternative, however, would be that they are in fact not two distinct pathways, but part of the same one. It is therefore gratifying to learn that NDE1 and NDEL1 exist in a complex with PDE4B in the cell, possibly by binding simultaneously to DISC1. That LIS1 also co-immunoprecipitated with PDE4B implies that much of the NDE1-NDEL1-LIS1-

dynein complex may co-exist with PDE4B *in vivo* as part of a DISC1 "mega-complex".

It can be hypothesised that such a complex would consist of a central DISC1 multimer, with PDE4B and NDE1/NDEL1 attached to it. LIS1 is known to be able to bind directly to DISC1 (Camargo *et al.* 2007), but could also bind NDE1 or NDEL1 molecules in the complex.

Other proteins which are known to bind both DISC1 and at least one of NDE1 and NDEL1 are 14-3-3ε (Toyo-Oka *et al.* 2003; Camargo *et al.* 2007; Taya *et al.* 2007), pericentrin-B (Miyoshi *et al.* 2005; Guo *et al.* 2006), DBZ/Su48 (Hirohashi *et al.* 2006b; Camargo *et al.* 2007; Hattori *et al.* 2007) and PCM1 (Guo *et al.* 2006; Kamiya *et al.* 2008). It is therefore possible that any one of these could exist in a DISC1-NDE1/NDEL1 complex. There is however no evidence as yet to suggest that they might bind at the same time as PDE4B. A schematic of these, as well as other some other proteins which bind DISC1 and NDE1/NDEL1, is shown in figure 6.7.

A crucial next step is to determine the roles of the various proteins in such a mega-complex: Which serve regulatory functions and which have active roles in the cell? How do these functions interact with each other? One aspect of this will be addressed in the next chapter.

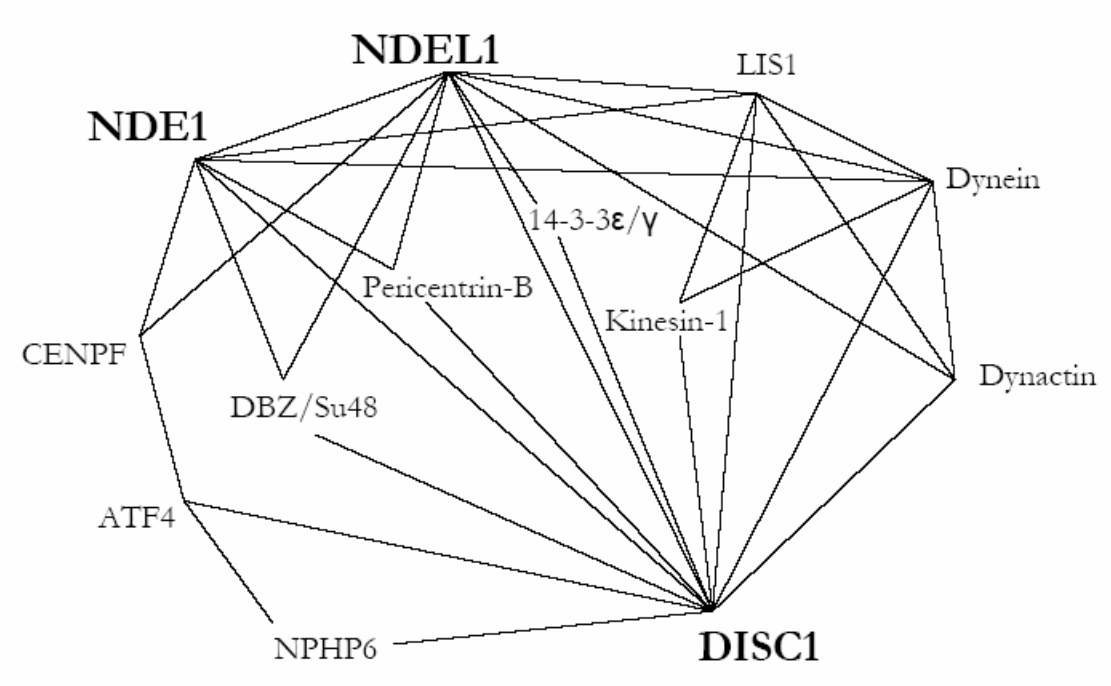

Figure 6.7: Known protein-protein interactions (black lines) involving DISC1 and at least one of NDE1 and NDEL1, as determined by a literature search. Data taken from the following papers: (Efimov and Morris 2000; Faulkner *et al.* 2000; Feng *et al.* 2000; Kitagawa *et al.* 2000; Niethammer *et al.* 2000; Sasaki *et al.* 2000; Sweeney *et al.* 2001; Millar *et al.* 2003; Morris *et al.* 2003; Ozeki *et al.* 2003; Toyo-Oka *et al.* 2003; Brandon *et al.* 2004; Kamiya *et al.* 2005; Miyoshi *et al.* 2005; Soukoulis *et al.* 2005; Guo *et al.* 2006; Hirohashi *et al.* 2006b; Kamiya *et al.* 2006; Ma *et al.* 2006; Sayer *et al.* 2006; Camargo *et al.* 2007; Hattori *et al.* 2007; Liang *et al.* 2007; Stehman *et al.* 2007; Taya *et al.* 2007; Vergnolle and Taylor 2007; Yamada *et al.* 2008)

Chapter 7 - NDE1 as a substrate of Protein Kinase A

7.1 NDE1 is phosphorylated by PKA

7.1.1 NDE1 phosphorylation is detectable with an anti-PKA substrate antibody

Bioinformatics analysis predicts that NDE1 is phosphorylatable by a number of different kinases (see table 4.4.B). One of these kinases, PKA, is of particular interest as it is cAMP-dependent and therefore influenced by cAMP phosphodiesterases such as PDE4B (see figure 1.2.D). As a result, it would be interesting to know whether NDE1 is indeed a substrate of PKA.

As an initial test, V5-NDE1-SSSC was over-expressed in COS7 cells and the cells were treated with the drugs IBMX and forskolin. Forskolin is known to increase cAMP production within cells through the activation of adenylyl cyclase, while IBMX is a phosphodiesterase inhibitor and thus reduces the rate of cAMP degradation. In combination, these drugs should raise the cellular levels of cAMP, increasing the activity of PKA. These cells were then lysed and immunoprecipitation performed using an anti-V5 antibody.

The immunoprecipitate was Western blotted and stained using an antibody raised against the phosphorylated peptide RRXp(S/T). This motif is known to be a canonical substrate site for PKA phosphorylation (Shabb 2001). Therefore this antibody should in theory show immunoreactivity to proteins which PKA has phosphorylated. NDE1 has one RRXS motif at amino acids 303-306, however it also has a highly similar KRXT motif at amino acids 128-131. The manufacturers of the PKA substrate antibody say that is should also be able to detect this phosphorylated motif. The antibody did indeed a band of the correct size to be NDE1 using the PKA substrate antibody, and an identical band when the gel re-stained using an anti-V5 antibody (see figure 7.1.A) suggesting that this band could be phosphorylated NDE1.

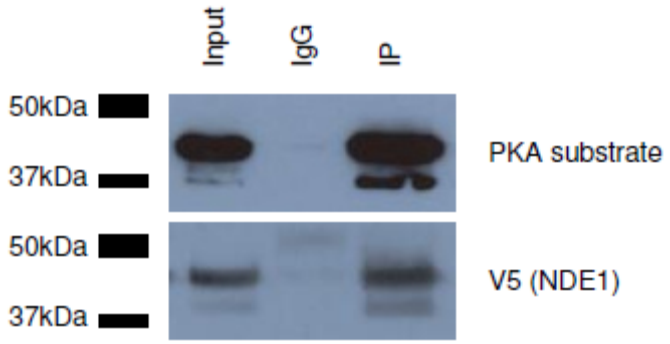

Figure 7.1.A: V5-NDE1-SSSC was over-expressed in COS7 cells. Cells were treated with IBMX and forskolin to increase PKA activity and lysates were immunoprecipitated using an anti-V5 antibody. Identical size bands were seen in both the lysate and immunoprecipitate using V5 and a phosphorylated PKA substrate antibody, suggesting the NDE1 to be phosphorylated. The smaller band may represent a form of NDE1 lacking a post-translational modification (such as additional non-PKA phosphorylation) or translated using the alternate start codon at methionine-23. That both antibodies are capable of detecting it suggests that it is unlikely to be non-specific binding of the antibodies to a non-NDE1 protein.

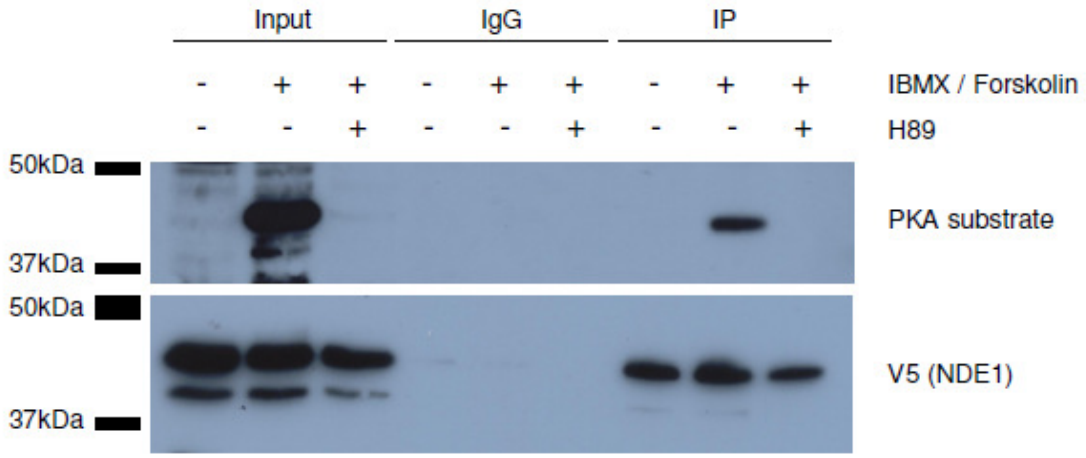

Figure 7.1.B: COS7 cells were transfected with V5-NDE1-SSSC and ensuing lysates were immunoprecipitated using an anti-V5 antibody. Cells treated with IBMX and forskolin to raise their cAMP levels showed considerably higher levels of phosphorylated V5, as visualised using a PKA substrate antibody. This effect was largely abolished in cells which were also treated with the PKA inhibitor H89. The V5 staining shows that this effect was not due to differing V5-NDE1 expression.

This is consistent with the idea of V5-NDE1 being phosphorylated at a location matching a PKA substrate motif, although further work is needed to confirm this.

7.1.2 NDE1 phosphorylation is cAMP and H89 sensitive

In order to confirm that the apparent phosphorylation seen on NDE1 was due to the action of PKA, and not by another kinase that uses a similar substrate motif, the above experiment was repeated using three parallel sets of COS7 cells. The first of these was mock treated, the second was treated with IBMX and forskolin while the third was treated with IBMX, forskolin and H89, an inhibitor of PKA activity.

A NDE1-sized band was again seen using the PKA substrate antibody following treatment with IBMX and forskolin (see figure 7.1.B). This band was greatly reduced or absent in cells that were mock treated or treated with H89 in addition to IBMX and forskolin. The levels of total V5-NDE1-SSSC, as determined using an anti-V5 antibody did not significantly vary. It therefore appears that this phosphorylation of NDE1 is sensitive to the levels of cAMP in the cell and can be inhibited by H89. Together this implies that NDE1 is being phosphorylated in a PKA-dependent manner. An alternative approach would have been the use of RNAi to block PKA expression in the cells, and thus PKA-dependant phosphorylation.

7.1.3 NDE1 can be phosphorylated by PKA *in vitro*

The tests performed so far have demonstrated that phosphorylation of NDE1 is PKA-dependent, but not necessarily that PKA is the kinase which phosphorylates NDE1. It is also possible that a kinase down-stream of PKA may instead perform the phosphorylation. Therefore, in order to determine whether PKA can phosphorylate NDE1 directly, GST and GST-tagged NDE1-SSSC were bacterially expressed and purified from pGEX-6P1 and pGEX-6P1-NDE1-SSSC plasmid vectors respectively (see section 5.2.). These were then treated with recombinant PKA and analysed by Western blotting using the PKA substrate antibody. GST-NDE1 clearly showed a phosphorylation signal, while a larger quantity of GST did not (see figure 7.1.C). This indicates that the site or sites of phosphorylation are found entirely within the

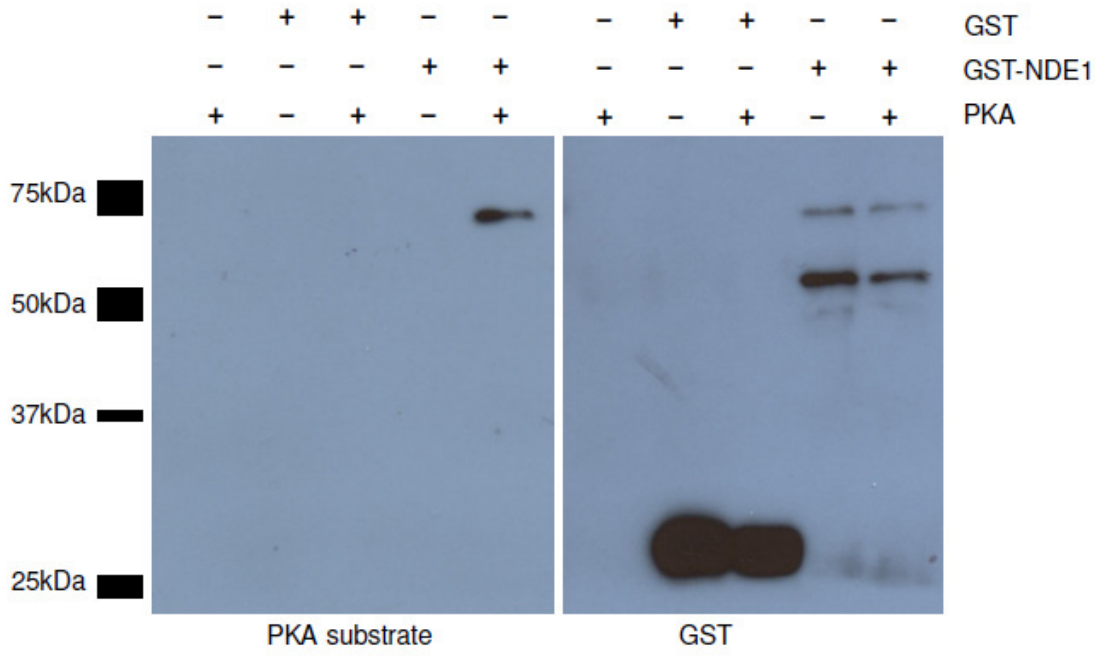

Figure 7.1.C: GST and GST-NDE1-SSSC were purified from transformed bacteria and treated with recombinant PKA. GST-NDE1 (~70kDa) is seen to be phosphorylated using the PKA substrate antibody, while a larger amount of GST (~28kDa) is not. This signal is dependent on PKA treatment. The additional products seen in the GST-NDE1 lanes may represent the results of premature translation termination, as the fact that they were successfully purified indicate that the GST tag is intact. These additional products do not appear to be phosphorylated, implying a C-terminal phosphorylation site.

---

amino acids derived from NDE1, rather than those from the GST tag. Neither PKA alone nor untreated GST-NDE1 produced a similar phosphorylation signal.

Together this indicates that PKA is capable of phosphorylating NDE1 directly *in vitro*, strongly suggesting that it is also responsible for the cAMP/H89-sensitive phosphorylation of NDE1 seen in COS7 cells.

7.2 Determining the PKA phosphorylated residues of NDE1

7.2.1 Site-directed mutagenesis of potential PKA phosphorylation sites

Plasmid constructs were created encoding mutant forms of NDE1 which lack potential PKA phosphorylation sites. A pDEST-40-NDE1-T131A construct was created by using the QuikChange II kit and the T131A F & R primers (see table 2.5.A) to perform a PCR reaction on the pDEST-40-NDE1-SSSC plasmid. These primers theoretically replaced threonine-131 of the *NDE1* gene with an alanine, as well as removing a BssHII restriction enzyme target site from the plasmid. Thus, digesting samples of different clones with BssHII and running them on an agarose gel allowed the clones to be screened for the T131A mutation. One of the colonies bearing the mutation (as confirmed by sequencing) was then grown and used to produce the mutant plasmid.

In a similar manner, a pDEST-40-NDE1-S306A construct was generated using the S306A F & R primers (see table 2.5.A), which mutated serine-306 to an alanine, while also removing an AleI site. Finally, the S306A primers were applied to the pDEST-40-NDE1-T131A plasmid in order to create a double-knockout pDEST-40-NDE1-T131A-S306A plasmid.

7.2.2 NDE1 is phosphorylated by PKA at serine-306

V5-tagged NDE1-S306A and wild type NDE1 constructs were transfected into parallel sets of COS7 cells. These were treated with IBMX/forskolin and an anti-V5 antibody was used to immunoprecipitate the over-expressed NDE1. Using the PKA substrate antibody, a marked decrease in phosphorylation of the S306A mutant was seen when compared to the wild-type construct (see figure 7.2.A.a).

Three further independent repeats of the experiment were performed (two of which were performed in part by Sheila Christie). The resulting blots were then scanned into a computer and densitometry was used to quantify the ratio of the PKA substrate and V5 antibody signals visible in the immunoprecipitate of each experiment. Using a one-tailed paired t-test, the difference in phosphorylation level between wild type

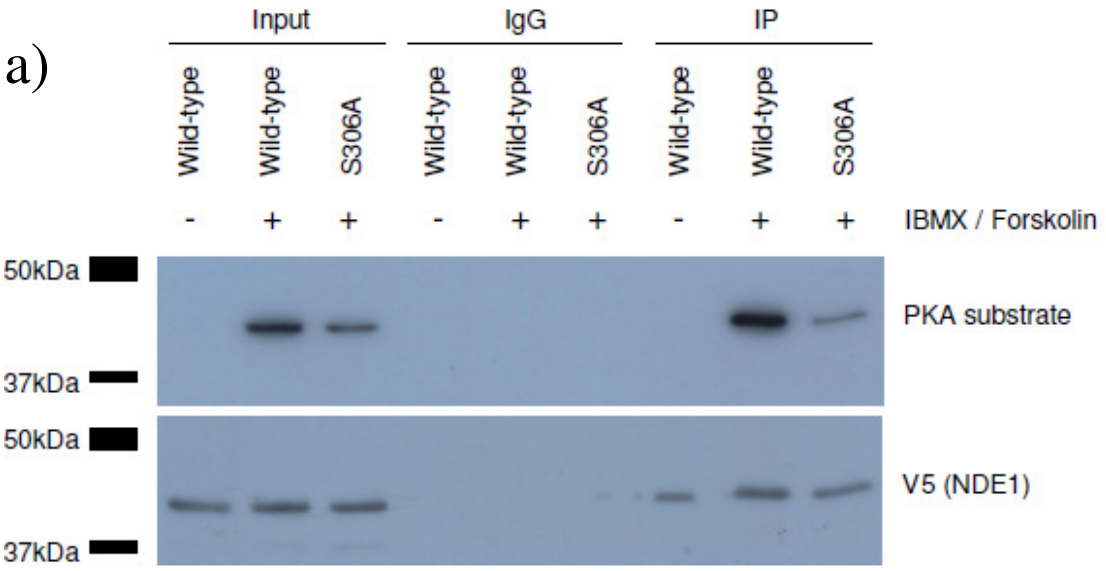

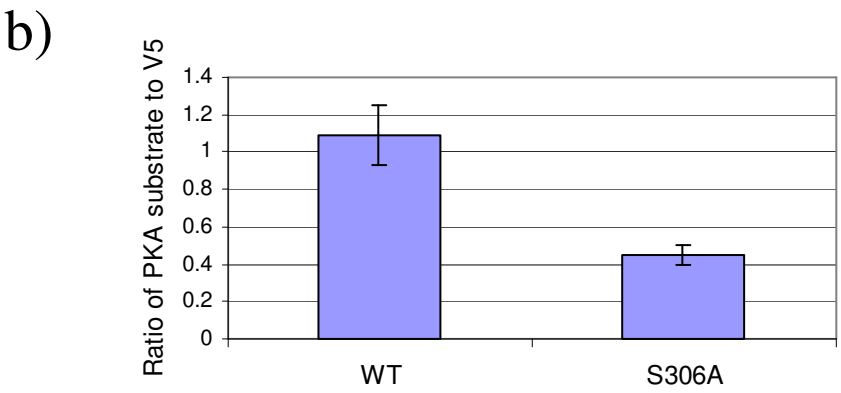

Figure 7.2.A: COS7 cells were transfected with V5-NDE1-SSSC constructs and the ensuing lysates immunoprecipitated using an anti-V5 antibody. a) Less phosphorylated NDE1 is detectable using the S306A mutant compared to wild-type NDE1, suggesting that serine-306 is a site of phosphorylation. b) Densitometry was performed in order to quantify four such experiments. The ratio of PKA substrate to V5 signal in the immunoprecipitate of each experiment was quantified and the difference between wild-type and S306A NDE1 was seen to be significant.

and mutant NDE1 was found to be significant (p=0.023, see figure 7.2.A.b). Densitometry was performed with Kirsty Millar.

This finding suggests that serine-306 is a major site of PKA phosphorylation on NDE1. That the S306A mutation does not abolish phosphorylation altogether, however, indicates that other sites of PKA phosphorylation also exist.

7.2.3 Potential phosphorylation of NDE1 by PKA at theroinine-131

The NDE1-T131A and wild type NDE1 constructs were then transfected into parallel sets of COS7 cells. IBMX/forskolin was applied and an anti-V5 antibody was used to immunoprecipitate the proteins. Using the PKA substrate antibody, a slight difference in V5-NDE1 phosphorylation was seen between the wild-type and mutant NDE1. Over four independent experiments this was not seen to be significant however (see figures 7.2.B.a and 7.2.B.c, two of the repeats performed in part by Sheila Christie). This would suggest that threonine-131 is unlikely to be a major site of PKA phosphorylation on NDE1.

The test was then repeated in order to compare the phosphorylation levels of NDE1-S306A single mutant and of the NDE1-T131A-S306A double mutant. This experiment was performed three times (the latter two with assistance from Sheila Christie) and the results were again analysed by densitometry. Consistently, the double mutant showed evidence of reduced phosphorylation when compared to the single mutant (see figure 7.2.B.b). The difference between the S306A and T131A-S306A mutants does not reach the boundary of statistical significance (p=0.091, see figure 7.2.B.c), although the difference between the double mutant and wild-type NDE1 (p=0.003) was a lot more significant than that between wild type and S306A (p=0.023). It therefore appears that threonine-131 may be an additional site of PKA phosphorylation on NDE1. Furthermore, that this was only clearly visible on the background of an S306A mutant presents the possibility that the phosphorylation status of one site may influence the phosphorylation potential of the other. Alternatively, this may be due to differences in the ability of the antibody to detect each site (see section 7.4.1). Densitometry was performed by Kirsty Millar.

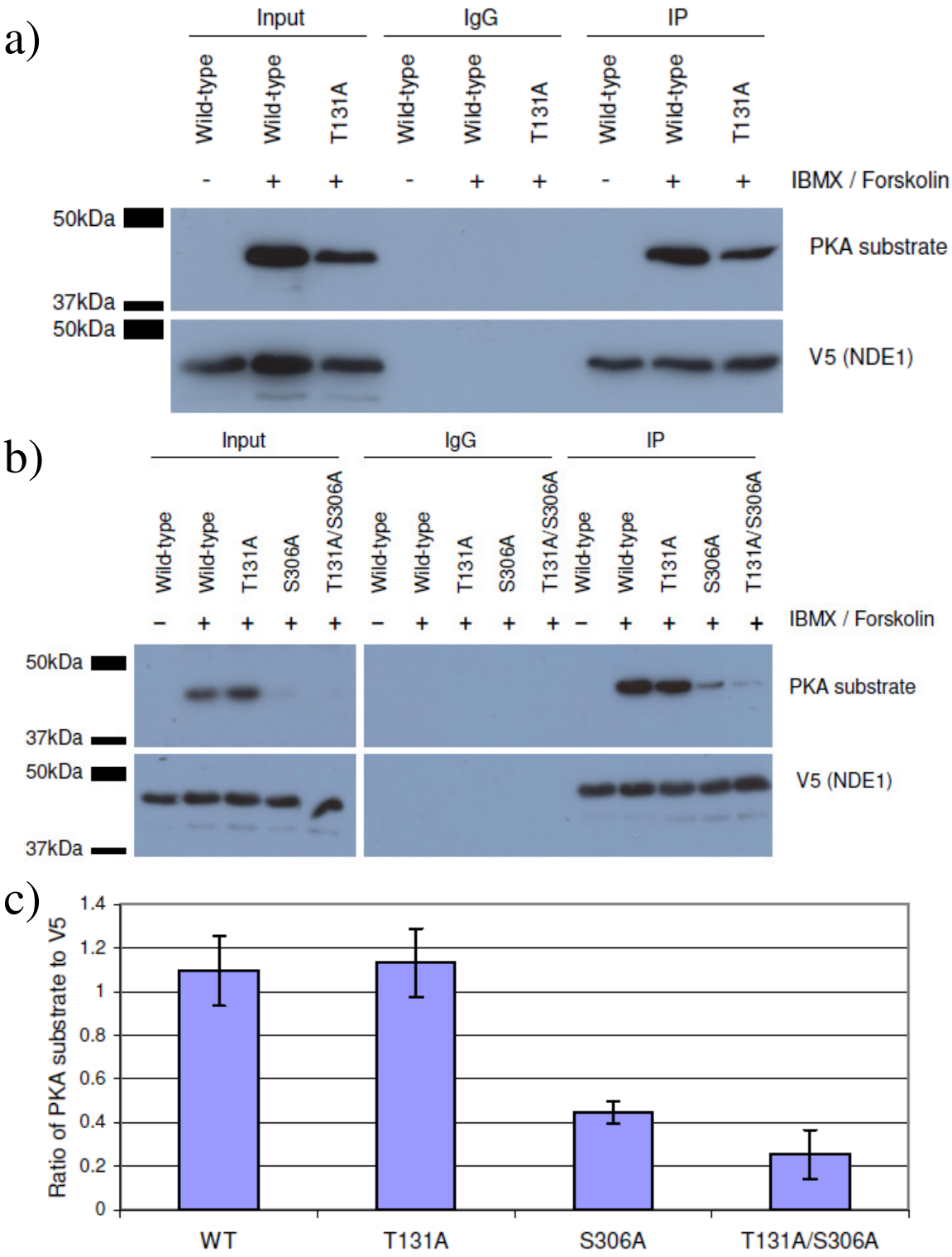

Figure 7.2.B: a) V5-NDE1-T131A shows a small change in level of phosphorylation compared to wild-type V5-NDE1 in COS7 cells following IBMX-forskolin treatment. b) This change is more obvious on the background of an S306A mutation in NDE1. c) Densitometry analysis of four independent experiments.

7.2.4 Predictions of other potential PKA sites on NDE1

That mutation of both serine-306 and threonine-131 did not completely abolish phosphorylation of V5-tagged NDE1 implies that one or more additional sites of PKA phosphorylation must exist. Therefore an alternative online phosphorylation site prediction program, NetPhosK 1.0 (Blom *et al.* 2004), was used to search for other, more weakly predicted, potential PKA phosphorylation sites in NDE1-SSSC.

In total, five other such sites were predicted (see table 7.2), although none of these conform precisely to the conventional RRX(S/T) PKA substrate motif (Shabb 2001) and it is therefore unclear which, if any, of these sites the PKA substrate antibody may be able to detect. No potential PKA phosphorylation sites are predicted to exist in the V5-tag.

7.3 Investigating the effects of PKA phosphorylation of NDE1

7.3.1 Predicting the effects of PKA phosphorylation on cellular NDE1

Threonine-131 is located in the N-terminal coiled-coil of NDE1, in domains that are known in NDEL1 to be involved in LIS1 binding and tetramerisation (Yan *et al.* 2003; Derewenda *et al.* 2007). Looking at the published structure of NDEL1 tetramers (Derewenda *et al.* 2007) it can be seen that the four threonine-131 residues are within very close proximity of each other and all point into the centre of the coiled-coil (see figure 7.3.A.a and 7.3.A.b). This suggests that phosphorylation of this residue would be highly unlikely to occur subsequent to multimerisation, and indeed it may prevent multimerisation all together. The threonine-131 residues of the NDEL1 dimer are approximately 10Å apart, while in a tetramer, they can come within 3Å of their counterparts running in the opposite direction. Given that a phosphate group has a diameter of 5.8Å, tetramerisation following threonine-131 phosphorylation would seem to be highly unlikely. Disruption of multimerisation in any way is likely to influence binding to LIS1, which is known to bind dimers rather

Site	Motif	NetPhosK score	Detectable by Scansite?	Location in NDE1
S94	**R**XX**S**	0.57	No	Coiled-coil (dimerisation site)
T131	**KR**X**T**	0.72	Yes	Coiled-coil (tetramerisation site)
S223	**R**XX**S**	0.77	No	Unstructured central region
S252	X**R**X**S**	0.78	No	Protein-binding α-helix
S273	**K**XX**S**	0.53	No	Protein-binding α-helix
S306	**RR**X**S**	0.85	Yes	Unstructured C-terminal tail
S307	**R**XX**S**	0.70	No	Unstructured C-terminal tail

Table 7.2: Sites of NDE1-SSSC predicted to be PKA phosphorylated using the program NetPhosK 1.0 (Blom *et al.* 2004). Score is a rating from 0 to 1 of the likelihood that the site is phosphorylated *in vitro*. The default cut-off value of 0.50 is used. Two of the sites are also detectable by Scansite 2.0 using its default stringency setting of "Medium" (see table 4.4.B)

---

than monomers of NDEL1 (Tarricone *et al.* 2004). Threonine-131 is also conserved in NDEL1.

Serine-306 is located near the C-terminus of the protein, immediately after the short predicted coil domain. It is possible that it is close enough to this coil to affect the binding of NDE1 to DISC1, dynein, dynactin and/or pericentrin-B, all of which are known to interact with NDE1 and/or NDEL1 in this region (Sasaki *et al.* 2000; Brandon *et al.* 2004; Liang *et al.* 2004; Guo *et al.* 2006). Additionally serine-306 lies within the NLS which was predicted to be found in NDE1-KMLL (figure 7.3.A.c). It is therefore possible that it could alter the cellular localisation of this isoform. This residue is not conserved in NDEL1.

7.3.2 Generation of a phospho-mimic NDE1 construct

The residues aspartic acid and glutamic acid are chemically similar to phosphorylated serine and threonine residues respectively in terms of their size and charge. It is therefore possible to use mutant proteins, bearing either a serine to aspartic acid mutation or a threonine to glutamic acid one, as a model for a constitutively phosphorylated wild type protein. Therefore a construct encoding V5-NDE1 with a T131E mutation was generated in order to mimic PKA phosphorylated

a)

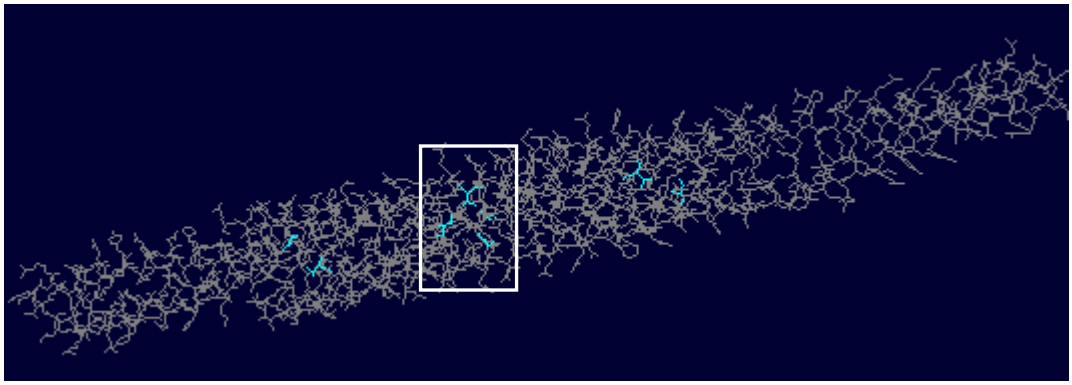

b)

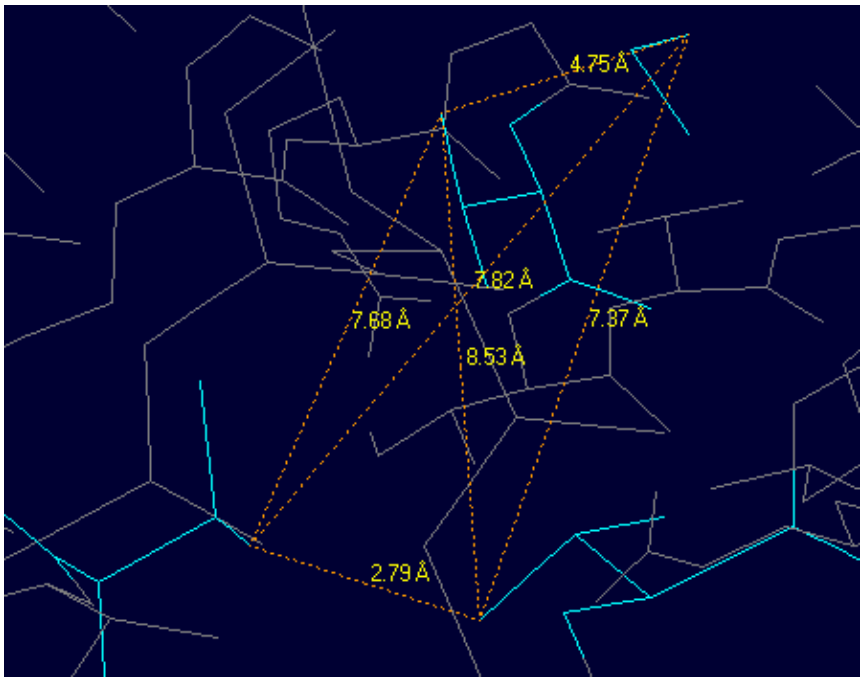

c)

PASGRSSKNRDGGE**RR**P**S**STSVPLGD**K**GLG**KR**LEFGKPPSHMS

Figure 7.3.A: a) The structure N-terminal coiled-coil regions of four NDEL1 molecules in a tetramer (Derewenda *et al.* 2007). All threonine residues are indicated in blue, with threonine-133 residues are indicated by a white box. b) Focus on the four threonine-133 residues. Distances between the oxygen atoms (to which the phosphate group would bind) are indicated. Structures viewed using Deep View/Swiss-Pdb View 3.7. c) The amino acid sequence of NDE1-KMLL around serine-306 (blue), with the basic residues of the putative NLS (red) and residues which are part of the unique C-terminal tail of NDE1-KMLL (underlined).

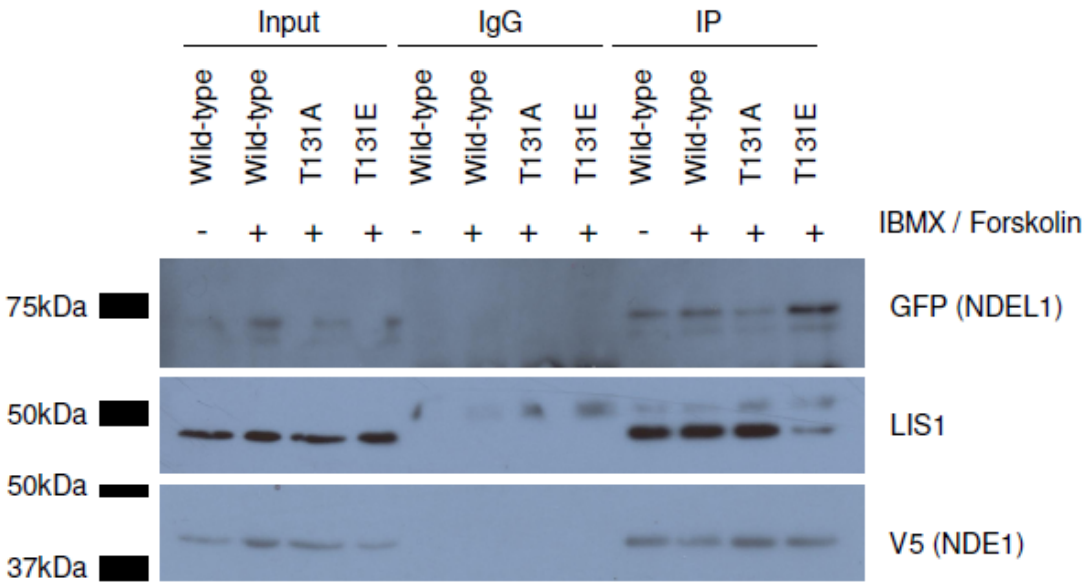

Figure 7.3.B: COS7 cells were transfected with V5-NDE1-SSSC (either wild-type or mutant) plus GFP-NDEL1-PLSV. Cells were IBMX/forskolin or mock treated and were immunoprecipitated using an anti-V5 antibody. GFP-NDEL1 is preferentially co-immunoprecipitated by the NDE1-T131E mutant compared to wild-type NDE1 and the T131A mutant. In contrast, endogenous LIS1 is preferentially co-immunoprecipitated by wild-type NDE1 and T131A compared to the T131E mutant. The overall level of V5-NDE1 is approximately consistent over the four samples. This blot is representative of two experiments. The 50kDa band visible in the LIS1 blot is IgG.

NDE1. The mutation was generated as in section 7.2.1, using the T131E F & R primers (see table 2.5.A).

7.3.3 Mock phosphorylation of NDE1 threonine-131 affects its interactions with LIS1 and NDEL1

In section 6.7.1, it was theorised that while NDE1 could form homodimers with itself, NDE1-NDEL1 interactions could only occur through tetramerisation. Therefore, in order to test the effect of threonine-131 phosphorylation on NDE1 tetramerisation, the NDE1-NDEL1 interaction was investigated.

COS7 cells were co-transfected with constructs encoding GFP-NDEL1-PLSV and V5-NDE1-SSSC, with the NDE1 being either wild-type or carrying one of the T131A or T131E mutations. Cells were IBMX/forskolin treated and an anti-V5 antibody used to immunoprecipitate the NDE1. In two independent experiments, NDEL1 was seen to co-immunoprecipitate more strongly with NDE1-T131E than it did with wild type NDE1 or NDE1-T131A (figure 7.3.B). The amount of NDE1 immunoprecipitated meanwhile remained largely unchanged. This suggests that the interaction of NDE1 with NDEL1 may be PKA sensitive.

The same immunoprecipitates were then also stained using an anti-LIS1 antibody. Strikingly, the amount of LIS1 co-immunoprecipitated by the NDE1-T131E mutant was considerably less than by wild-type NDE1 or NDE1-T131A (figure 7.3.B). While these findings are still preliminary, and further repeats are needed to be certain, this suggests that the phosphorylation status of threonine-131 may play a key role in determining whether NDE1 is preferentially a LIS1 or NDEL1 interacting protein.

7.4 Discussion

7.4.1 The mechanism of PKA-phosphorylation of NDE1

NDE1 has been demonstrated to be phosphorylated at PKA substrate-consensus sites. That this phosphorylation is sensitive to cAMP levels and to an inhibitor of PKA, combined with the fact that recombinant PKA can phosphorylate NDE1 *in vitro*, strongly implies that the kinase responsible is PKA.

NDE1 phosphorylation by PKA occurs at multiple sites, the most prominent of these being serine-306, at the C-terminal unstructured tail of NDE1 and proximal to the helical region implicated in DISC1, dynein, dynactin and pericentrin-interaction (Sasaki *et al.* 2000; Brandon *et al.* 2004; Liang *et al.* 2004; Guo *et al.* 2006). Threonine-131, found in coiled-coil region implicated in tetramerisation an LIS1-interaction (Yan *et al.* 2003; Derewenda *et al.* 2007), also appears to be a phosphorylation site, although this result did not meet statistical significance. That

mutation of both these sites did not completely abolish PKA-phosphorylation implies that other lesser-used sites of phosphorylation also exist. Potential locations for the remaining PKA phosphorylation site(s) are at serines-94, 223, 252, 273 and 307.

Interestingly, the potential phosphorylation of NDE1 at threonine-131 was only visible when an S306A mutation was also introduced. Assuming that threonine-131 is a genuine site of phosphorylation, there are several potential explanations for this. Firstly, phosphorylation of serine-306 may cause a configurational shift in the structure of NDE1, altering the feasibility of the threonine-131 being phosphorylated. A more likely explanation, however, would be that serine-306 is phosphorylated at a considerably higher frequency than threonine-131 and thus the signal from serine-306 phosphorylation masks any alteration of the phosphorylation status at the other site. This is very plausible as the position of threonine-131 within the coiled-coil is likely to prevent the residue from being accessible to PKA after it has formed a dimer. Additionally, the fact that the PKA substrate antibody was raised against the RRXp(S/T) motif means that it may well detect phosphorylation at serine-306 (RRXpS) more strongly than phosphorylation at threonine-131 (KRXpT), potentially preventing alterations in the threonine-131 site from being easily detectable.

Given that the primary site of PKA-phosphorylation on NDE1, serine-306, is not conserved in NDEL1, it appears unlikely that NDEL1 is also PKA phosphorylated to a similar degree as NDE1. Phosphorylation of NDEL1 at a site equivalent to threonine-131 remains a possibility and has been suggested to occur in a recent study (Collins *et al.* 2008).

7.4.2 Threonine-131 of NDE1 as a potential protein-interaction "switch"

In the previous chapter, phosphodiesterase 4 molecules were shown to exist in complex with NDE1, implying the existence of DISC1 complexes *in vivo* containing both PDE4B and NDE1/NDEL1. PDE4s are involved in regulation levels of cAMP within the cell and may therefore influence the activity of cAMP-dependent kinases such as PKA. The discovery that NDE1 is phosphorylated by PKA therefore

suggests for the first time a functional link between PDE4s and DISC1's centrosomal protein interactors.

NDE1 is PKA phosphorylated on serine-306. The effect of this phosphorylation on NDE1 is not yet known, but may influence the protein-protein interactions which occur at its C-terminal helix. In NDE1-KMLL, this site is also within a predicted nuclear-localisation signal and therefore may influence cellular localisation of the protein. Determining the exact effect of this phosphorylation should therefore by a major goal of future work.

Threonine-131 also appears to be a PKA phosphorylation site for NDE1, although additional work is required in order to be certain of this. Based on the published model for NDEL1 (Derewenda *et al.* 2007) this site is likely to be buried within a coiled-coil and therefore inaccessible to PKA after dimerisation has occurred. It is possible, however, that phosphorylation could still occur while NDE1 was a monomer. This theory is consistent with the fact that threonine-131 phosphorylation was seemingly less common than serine-306 phosphorylation.

Through use of a mock-phosphorylated NDE1 mutant (a T131E mutation), it was suggested that threonine-131 is important for determining the protein-interaction partners of NDE1. Mock-phosphorylation led to NDE1 preferentially binding to NDEL1 and is therefore likely to also affect NDE1 tetramerisation, although the ability of NDE1 to form dimers makes this difficult to study using this technique. The mock-phosphorylation also led to reduced LIS1 binding. It is interesting to note that phosphorylation of T131 appears to increase NDE1/NDEL1 interaction, whereas it had been previously predicted to block the interaction (see section 7.3.1). This effect would presumably be caused by the phosphorylation altering the coiled-coil, either forcing it to be looser or else breaking the α-helix around it, altering the overall configuration of the coil and favouring the interaction of NDEL1 over LIS1. While these results are still preliminary and in need of further replication, a model for the mechanism of this phosphorylation can be proposed. NDE1 monomers would be phosphorylated or dephosphorylated depending on the local cAMP concentration.

Once dimerisation occurred, the phosphorylation status of the component monomers would "set" the binding affinities of the resulting dimer for LIS1, NDEL1 and potentially other protein interactors.

It is also interesting to note that in a recent publication, mutation of alanine-131 of NDEL1 to an aspartic acid dramatically increased the strength of NDEL1-NDEL1 interactions on a peptide array (Collins *et al.* 2008). This residue is immediately adjacent to threonine-132, the NDEL1 equivalent of threonine-131 on NDE1. Given the similarity between aspartic acid and the glutamic acid which was mutated into NDE1-T131E, it is perhaps unsurprising that the two mutations have similar effects. This further reinforces the theory that this region of NDE1/NDEL1 plays a significant role in determining their propensity to form either homotetramers or heterotetramers with each other.

It has previously been reported that DISC1 binds preferentially to the inactive form of PDE4B and that, for certain isoforms, binding of DISC1 to PDE4 is PKA-dependent (Millar *et al.* 2005b; Murdoch *et al.* 2007). Combined with the potential for PKA-dependent NDE1-LIS1 and NDE1-NDEL1 interactions, this suggests that regulation of the DISC1 complex, which includes PDE4B and NDE1, is likely to be highly complex (figure 7.4) and further study is needed in order to understand this better.

Determining whether this "mock-phosphorylation" truly resembles the role of PKA phosphorylation at threonine-131 *in vivo* remains a priority for future work. Should this mechanism be seen to truly represent NDE1 within the cell, further analysis of how these NDEL1/LIS1 binding switches works remain an important steps in future study of NDE1. Regardless, the ability of the T131E mutant to alter protein interactions of NDE1 will make it a useful tool for future analysis of the protein.

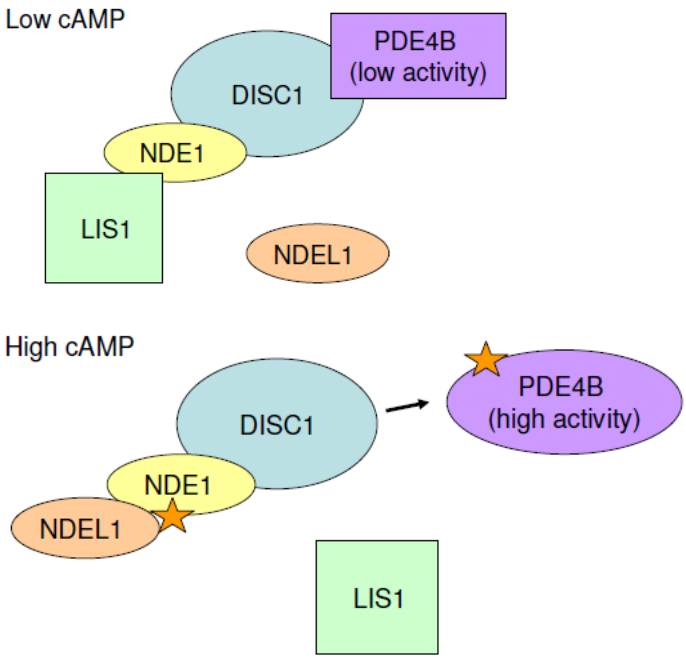

Figure 7.4: A crude schematic of the effect of local cAMP levels on the DISC1 complex. At low cAMP levels DISC1 (specifically the 71kDa form) binds to inactive PDE4B as well as NDE1. NDE1 meanwhile binds to LIS1, while NDE1-NDEL1 interactions are relatively weak. At high cAMP concentrations, PDE4B and NDE1 can become phosphorylated by PKA, as indicated by orange stars. This leads to PDE4B becoming active and disassociating from DISC1 (Millar *et al.* 2005b; Murdoch *et al.* 2007). Newly dimerised NDE1, meanwhile, now preferentially binds to NDEL1 over LIS1. Note: This diagram does not take into account the fact that both LIS1 and NDEL1 can also bind to DISC1 directly (Millar *et al.* 2003; Morris *et al.* 2003; Ozeki *et al.* 2003; Brandon *et al.* 2004; Camargo *et al.* 2007). The effect of cAMP on these interactions is yet to be determined.

Chapter 8 - Concluding Remarks

8.1 Studying NDE1

In this thesis the Nuclear Distribution Factor E (*Aspergillus nidulans*) homologue 1 (NDE1) protein has been studied. This protein is of considerable interest in the study of psychiatric illness due to its known neurodevelopmental function, its relationship with Disrupted-In-Schizophrenia 1 (DISC1) and evidence that genetic variation in *NDE1* may be associated with schizophrenia pathology.

In the opening chapter, three main goals were set out: to determine a basic biology of NDE1, to better understand its relationship with NDEL1 and to investigate the role of NDE1 in the DISC1 pathway, focusing specifically on its relationship with DISC1-interacting phosphodiesterases. Each of these points will be addressed in turn.

8.2 Establishing a basic biology of NDE1

Using bioinformatics analysis, I have predicted that the NDE1 dimer, like NDEL1, contains a major coil, but that in addition, both proteins have an a C-terminal protein-binding α-helix. The coil and the helix are predicted to be separated by a flexible disordered region which may allow for the binding of different combinations of protein interactors. Additionally, I have demonstrated experimentally that multiple splice forms of NDE1 (as well as at least two of NDEL1) are expressed in the brain. Most of the isoforms encoded by these splice forms are predicted to be full-length, differing only at the extreme C-terminus. This region may function as an isoform-specific regulatory domain, allowing for complex regulation of pools of NDE1 within the cell.

I have now established that endogenous NDE1 is found at the centrosome and can interact with LIS1, consistent with findings gained using over-expressed protein (Feng *et al.* 2000; Kitagawa *et al.* 2000). More surprising, however, was the novel identification of NDE1 in the nucleus using both over-expressed and endogenous NDE1. This is potentially an isoform-specific localisation as only two NDE1

isoforms are predicted to have nuclear localisation signals (for example the 95 antibody, which is specific for mouse Nde1-KMLL, detects a unique nuclear envelope expression pattern) and implies previously unknown functions for NDE1 within the cell.

8.3 The relationship between NDE1 and NDEL1

Structurally, NDE1 and NDEL1 are predicted to be highly similar, sharing both a highly conserved coiled-coil and α-helix. Similarly, they have been shown to share a number of "core" features including centrosomal localisation and the ability to interact with LIS1 and DISC1. Interestingly, their localisation patterns may not be identical, with NDE1 being potentially more highly expressed in the nucleus. Another potential difference between the two proteins is that both are predicted to have differing patterns of phosphorylation, and one such NDE1-specific phosphorylation site has been demonstrated experimentally, suggesting that post-translational regulation of the two proteins is likely to vary.

I have now shown that NDE1 and NDEL1 can form complexes in the cell. Such a complex is unlikely to be a simple heterodimer, but may take the form of a heterotetramer. That they interact at all, however, implies a previously unknown cooperative role for the proteins within the cell. For example, it is possible that the NLS motifs predicted on certain NDE1 isoforms could be used to localise NDE1-NDEL1 complexes to the nucleus. That the two proteins appear to show similar but not totally identical expression patterns within cultured cells indicates that NDE1-NDEL1 complexes do occur, but that they are also likely to function independently.

8.4 NDE1 within the DISC1 pathway

NDEL1 is a robustly established DISC1-interacting protein, and I have now demonstrated a similar relationship between NDE1 and DISC1. Intriguingly, NDE1 was seen to exist in a complex with other DISC1-interacting proteins including ATF4 and PDE4B1. That three schizophrenia-related proteins (DISC1, NDE1 and PDE4B1) co-complex suggests that this protein complex is functionally important for our understanding of major mental illness. Interestingly LIS1 was also seen to

form a complex with PDE4B. Should this prove to be the same complex that contains DISC1 and NDE1 also, then it would strongly suggest that the DISC1-NDE1-PDE4B exists at the centrosome.

PDE4 proteins are involved in the degradation of cAMP in a negative feedback mechanism involving cAMP-sensitive PKA (see figure 1.2.D). The discovery that PKA in turn can phosphorylate NDE1 provides, for the first time, a functional link between phosphodiesterases and the DISC1 pathway. Furthermore, the initial evidence suggesting that PKA phosphorylation affects the binding affinity of NDE1 for NDEL1 and LIS1 suggests that this process is likely to be of significant biological importance. That DISC1-PDE4B binding is also known to be cAMP-dependent (Millar *et al.* 2005b) suggests that regulation of the DISC1 complex, including both PDE4B and NDE1, by cAMP is likely to be highly regulated.

8.5 Future work

This thesis has answered a range of questions regarding NDE1, its role in the cell and relationship with the DISC1 pathway. However, other questions still remain and indeed several new ones have been generated. Issues which should be addressed in future work include the following:

1. Transcripts of several NDE1 and NDEL1 splice variants have been shown to exist in the brain. A logical next step would be to prepare plasmid constructs encoding each of these different isoforms. These could then be used to investigate differences between the isoforms in terms of cellular localisation, post-translational regulation and protein-protein interaction capabilities. A more long term approach would then be to generate custom antibodies against each isoform in order to study them in their endogenous state.
2. It has been predicted that both NDE1 and NDEL1 possess, in addition to their N-terminal coiled-coil region, a smaller α-helix near the C-terminus and an unstructured region linking the two. It would therefore be interesting to attempt to confirm these predictions through biophysical methods.

3. NDE1 and NDEL1 are predicted to be differentially regulated by phosphorylation. Phosphorylation of NDE1 by PKA at threonine-131 has been demonstrated, but it would also be useful to investigate the other potential phosphorylation events experimentally.
4. In chapter 5, NDE1-specific antibodies were used to investigate NDE1 localisation and it was seen to exist in the nucleus. This localisation ideally needs to be confirmed using independent antibodies. Use of isoform specific antibodies, such as those mentioned in point 1, would also be useful to test the prediction that this localisation is due to the potential nuclear localisation signals of two NDE1 isoforms.
5. The NDE1 antibodies described in this thesis have so far been used only in cell lines. It would be informative to make further use of them on tissue samples, and in particular in the brain.
6. A variety of DISC1-interacting proteins, including NDE1, NDEL1, LIS1 and PDE4B, have been demonstrated to exist in complex with each other, although it remains to be demonstrated whether all of these exist in a single "mega-complex" or not. This could be investigated, for example, through use of affinity chromatography followed by mass spectroscopy.
7. While threonine-131 appears to be a PKA phosphorylation site on NDE1, comparison of its phosphorylation status with that of wild-type NDE1 or NDE1-S306A (using a PKA substrate antibody) did not yield a significant p-value. It therefore must still be confirmed that this is a genuine phosphorylation site. Possible future steps include the use of a C-terminally truncated NDE1 construct containing only the coiled-coil regions, in order to decrease the signal caused by other PKA substrate sites on the protein. Alternatively, an N-terminally truncated mutant, which would lack the dimerisation domain and force NDE1 to exist as a monomer, may increase the amount of phosphorylation at threonine-131. Finally mouse Nde1, in which threonine-131, but not serine-306 is conserved, could be used to further investigate this.
8. NDEL1 has a threonine residue equivalent to threonine-131 of NDE1. It should therefore be determined whether NDEL1 is also a substrate of PKA.

9. Use of a NDE1-T131E mutant appeared to affect the binding affinity of NDE1 for NDEL1 and LIS1 in two independent tests. This result needs repeating further in order to confirm the functional consequences. Use of NDE1 deletion constructs such as those described in point 5 may help in this analysis.
10. If phosphorylation of threonine-131 of NDE1 does affect its ability to bind to LIS1 then it is likely to have dramatic effects on its cellular role, for example whether it is found at the microtubules. Further investigation of the T131E mutant, its cellular localisation and whether it forms complexes with proteins like dynein and possibly even DISC1, would be of great interest.
11. The PDE4 protein family are involved in cAMP degradation and therefore have an affect of cAMP-dependent PKA. It would therefore be interesting to know whether PDE4B or PDE4D activity had a direct effect on the level of NDE1 phosphorylation.
12. Serine-306 is known to be PKA phosphorylated on NDE1 and a corresponding site does not exist on NDEL1. Work is needed, however, to determine in what way this phosphorylation regulates the biology of NDE1 in the cell.
13. Finally, mutation of both threonine-131 and serine-306 did not completely abolish PKA phosphorylation of NDE1. It therefore still remains to be determined how many other PKA phosphorylation sites there are on NDE1 and where they are located.

8.6 Final comments

DISC1 is considered to be one of the most promising candidate genes for schizophrenia currently under investigation. As the DISC1 protein appears to function *in vivo* as a scaffold protein, understanding of its role within the cell can be gained through the study of its protein interaction partners. NDE1, like NDEL1 and PDE4B appears to be a promising DISC1-interaction protein, due to its known role in neurodevelopment and evidence associating it with schizophrenia. This thesis has attempted to close the gap in our understanding of NDE1 compared to these other DISC1-interactors and has furthermore shed light on mechanisms by which NDE1

interacts with both NDEL1 and PDE4B. That multiple schizophrenia-related proteins interact within the cell strongly suggests that the complex is likely to play a prominent role in the pathology of schizophrenia and that further study of it is of crucial importance.

References

Aberg, K, E Axelsson, P Saetre, L Jiang, L Wetterberg*, et al.* (2008). "Support for schizophrenia susceptibility locus on chromosome 2q detected in a Swedish isolate using a dense map of microsatellites and SNPs." Am. J. Med. Genet. **147B**(7): 1238-1244.

Altschul, SF, W Gish, W Miller, EW Myers and DJ Lipman (1990). "Basic local alignment search tool." J. Mol. Biol. **215**: 403-410.

Andrade, L, JJ Caraveo-anduaga, P Berglund, RV Bijl, R De Graaf*, et al.* (2003). "The epidemiology of major depressive episodes: results from the International Consortium of Psychiatric Epidemiology (ICPE) surveys " Int. J. Methods Psychiatr. Res. **12**(1): 3-21.

Anitha, A, K Nakamura, K Yamada, Y Iwayama, T Toyota*, et al.* (2007). "Gene and expression analyses reveal enhanced expression of Pericentrin 2 (PCNT2) in bipolar disorder." Biol. Psychiatry **63**(7): 678-685.

Arai, M, N Obata, TTJP Kockelkorn, K Yamada, T Toyota*, et al.* (2007). "Lack of association between polymorphisms in the 5' upstream region of the DISC1 gene and mood disorders." Psychiatr. Genet. **17**: 357.

Austin, CP, B Ky, L Ma, AJ Morris and J Shugrue (2004). "Expression of Disrupted-In-Schizophrenia-1, a schizophrenia associated gene, is prominant in the mouse hippocampus throughout brain development." Neuroscience **124**: 3-10.

Avramopoulos, D, VL Willour, PP Zandi, Y Huo, DF MacKinnon*, et al.* (2004). "Linkage of bipolar affective disorder on chromosome 8q24: follow-up and parametric analysis." Mol. Psychiatry **9**(2): 191-196.

Baala, L, S Audollent, J Martinovic, C Ozilou, M-C Babron*, et al.* (2007). "Pleiotropic effects of CEP290 (NPHP6) mutations extend to Meckel syndrome." Am. J. Hum. Genet. **81**(1): 170-179.

Balczon, R, L Bao and W Zimmer (1994). "PCM-1, A 228-kD centrosome autoantigen with a distinct cell cycle distribution." J. Cell Biol. **124**(5): 783-793.

Beard, MB, JC O'Connell, GB Bolger and MD Houslay (1999). "The unique N-terminal domain of the cAMP phosphodiesterase PDE4D4 allows for interaction with specific SH3 domains." FEBS Letters **460**(1): 173-177.

Beausoleil, SA, J Villen, SA Gerber, J Rush and SP Gygi (2006). "A probability-based approach for high-throughput protein phosphorylation analysis and site localization." Nat. Biotechnol. **24**(10): 1285-1292.

Beckwith, SM, CH Roghi, B Liu and N Ronald Morris (1998). "The "8-kD" cytoplasmic dynein light chain is required for nuclear migration and for dynein heavy chain localization in Aspergillus nidulans." J. Cell Biol. **143**(5): 1239-1247.

Bernardi, R and PP Pandolfi (2007). "Structure, dynamics and functions of promyelocytic leukaemia nuclear bodies." Nat. Rev. Mol. Cell Biol. **8**(12): 1006-1016.

Biamonti, G (2004). "Nuclear stress bodies: a heterochromatin affair?" Nat. Rev. Mol. Cell Biol. **5**(6): 493-498.

Biedler, JL, S Roffler-Tarlov, M Schachner and LS Freedman (1978). "Multiple neurotransmitter synthesis by human neuroblastoma cell lines and clones." Cancer Res. **38**(11): 3751-3757.

Blackwood, DHR, A Fordcye, T Walker, DM St.Clair, DJ Porteous and WJ Muir (2001). "Schizophrenia and affective disorders - Cosegregation with a translocation at chromosome 1q42 that directly disrupts brain-expressed genes: Clinical and P300 findings in a family." Am. J. Hum. Genet. **69**: 428-433.

Blasius, TL, D Cai, GT Jih, CP Toret and KJ Verhey (2007). "Two binding partners cooperate to activate the molecular motor Kinesin-1." J. Cell Biol. **176**(1): 11-17.

Blom, N, T Sicheritz-Ponten, R Gupta, S Gammeltoft and S Brunak (2004). "Prediction of post-translational glycosylation and phosphorylation of proteins from the amino acid sequence." Proteomics **4**(6): 1633-1649.

Böhm, D, K Hoffmann, F Laccone, B Wilken, P Dechent*, et al.* (2006). "Association of Jacobsen syndrome and bipolar affective disorder in a patient with a de novo 11q terminal deletion." Am. J. Med. Genet. **140**(4): 378-382.

Bolger, GB, S Erdogan, RE Jones, K Loughney, G Scotland*, et al.* (1997). "Characterization of five different proteins produced by alternatively spliced mRNAs from the human cAMP-specific phosphodiesterase PDE4D gene." Biochem. J. **328**: 539-548.

Bradshaw, NJ, S Christie, DC Soares, BC Carlyle, DJ Porteous and JK Millar (2009). "NDE1 and NDEL1: Multimerisation, alternate splicing and DISC1 interaction." Neurosci. Lett. **449**(3): 228-233.

Bradshaw, NJ, F Ogawa, B Antolin-Fontes, JE Chubb, BC Carlyle*, et al.* (2008). "DISC1, PDE4B, and NDE1 at the centrosome and synapse." Biochem. Biophys. Res. Comm. **377**(4): 1091-1096.

Brandon, NJ, EJ Handford, I Schurov, J-C Rain, M Pelling*, et al.* (2004). "Disrupted in Schizophrenia 1 and Nudel form a neurodevelopmentally regulated protein complex: implications for schizophrenia and other major neurological disorders." Mol. Cell. Neurosci. **25**: 42-55.

Brandon, NJ, I Schurov, LM Camargo, EJ Handford, B Duran-Jimeriz*, et al.* (2005). "Subcellular targetting of DISC1 is dependant on a domain independant of the Nudel binding site." Mol. Cell. Neurosci. **28**: 613-624.

Brennan, MD and J Condra (2005). "Transmission disequilibrium suggests a role for the sulfotransferase-4A1 gene in schizophrenia." Am. J. Med. Genet. **139B**(1): 69-72.

Brito, GC, AA Fachel, AL Vettore, GM Vignal, ERP Gimba*, et al.* (2008). "Identification of protein-coding and intronic noncoding RNAs down-regulated in clear cell renal carcinoma." Mol. Carcinog. **47**(10): 757-767.

Burdick, KE, A Kamiya, CA Hodgkinson, T Lencz, P DeRosse*, et al.* (2008). "Elucidating the relationship between DISC1, NDEL1, and NDE1 and the risk for schizophrenia: Evidence of epistasis and competitive binding." Hum. Mol. Genet. **17**(16): 2462-2473.

Burmeister, M, MG McInnis and S Zollner (2008). "Psychiatric genetics: progress amid controversy." Nat. Rev. Genet. **9**(7): 527-540.

Byrne, M, E Agerbo, B Bennedsen, WW Eaton and PB Mortensen (2007). "Obstetric conditions and risk of first admission with schizophrenia: A Danish national register based study." Schizophr. Res. **97**(1-3): 51-59.

Cahana, A, T Escamez, RS Nowakowski, NL Hayes, M Giacobini*, et al.* (2001). "Targeted mutagenesis of Lis1 disrupts cortical development and LIS1 homodimerization." Prot. Natl. Acad. Sci. USA **98**(11): 6429-6434.

Cahana, A, XL Jin, O Reiner, A Wynshaw-Boris and C O'Neill (2003). "A study of the nature of embryonic lethality in LIS1-/- mice." Mol. Rep. Dev. **66**(2): 134-142.

Callicott, JH, RE Straub, L Pezawas, MF Egan, VS Mattay*, et al.* (2005). "Variation in DISC1 affects hippocampal structure and function and increases risk for schizophrenia." Prot. Natl. Acad. Sci. USA **102**(24): 8627-8632.

Camargo, ACM, H Caldo and PC Emson (1983). "Degradation of neurotensin by rabbit brain endo-oligopeptidase A and endo-oligopeptidase B (proline-endopeptidase)." Biochem. Biophys. Res. Comm. **116**(3): 1151-1159.

Camargo, ACM, R Shapanka and LJ Greene (1973). "Preparation, assay, and partial characterization of a neutral endopeptidase from rabbit brain." Biochemistry **12**(9): 1838-1844.

Camargo, LM, V Collura, J-C Rain, K Mizuguchi, H Hermjakob*, et al.* (2007). "Disrupted in Schizophrenia 1 Interactome: evidence for the close connectivity of risk genes and a potential synaptic basis for schizophrenia." Mol. Psychiatry **12**(1): 74-86.

Camp, NJ, MR Lowry, RL Richards, AM Plenk, C Carter*, et al.* (2005). "Genome-wide linkage analyses of extended Utah pedigrees identifies loci that influence recurrent, early-onset major depression and anxiety disorders." Am. J. Med. Genet. **135B**(1): 85-93.

Cannon, M, PB Jones and RM Murray (2002). "Obstetric complications and schizophrenia: Historical and meta-analytic review." Am. J. Psychiatry **159**(7): 1080-1092.

Cannon, SC and SM Strittmatter (1993). "Functional expression of sodium channel mutations identified in families with periodic paralysis." Neuron **10**(2): 317-326.

Cannon, TD, W Hennah, TGM van Erp, PM Thompson, J Lonnqvist*, et al.* (2005). "Association of DISC1/TRAX haplotypes with schizophrenia, reduced prefrontal gray matter, and impaired short- and long-term memory." Arch. Gen. Psychiatry **62**(11): 1205-1213.

Carter, CJ (2006). "Schizophrenia susceptibility genes converge on interlinked pathways related to glutamatergic transmission and long-term potentiation, oxidative stress and oligodendrocyte viability." Schizophr. Res. **86**(1-3): 1-14.

Carter, CJ (2007). "Multiple genes and factors associated with bipolar disorder converge on growth factor and stress activated kinase pathways controlling translation initiation: Implications for oligodendrocyte viability." Neurochem. Int. **50**(3): 461-490.

Caspi, M, FM Coquelle, C Koifman, T Levy, H Arai*, et al.* (2003). "LIS1 Missense Mutations: Variable phenotypes result from unpredicatble alterations in biochemical and cellular properties." J. Biol. Chem. **278**(40): 38740-38748.

Chen, Q-Y, Q Chen, G-Y Feng, K Lindpaintner, L-J Wang, *et al.* (2007). "Case-control association study of Disrupted-in-Schizophrenia-1 (DISC1) gene and schizophrenia in the Chinese population." J. Psychiatr. Res. **41**(5): 428-434.

Cheung, Y-F, Z Kan, P Garrett-Engele, I Gall, H Murdoch, *et al.* (2007). "PDE4B5, a novel, super-short, brain-specific cAMP phosphodiesterase-4 variant whose isoform-specifying N-terminal region is identical to that of cAMP phosphodiesterase-4D6 (PDE4D6)." J. Pharmacol. Exp. Ther. **322**(2): 600-609.

Chiba, S, R Hashimoto, S Hattori, M Yohda, B Lipska, *et al.* (2006). "Effect of antipsychotic drugs on DISC1 and dysbindin expression in mouse frontal cortex and hippocampus." J. Neural Transm. **113**(9): 1337-1346.

Chubb, JE, NJ Bradshaw, DC Soares, DJ Porteous and JK Millar (2008). "The DISC locus in psychiatric illness." Mol. Psychiatry **13**: 36-64.

Cichon, S, J Schumacher, DJ Muller, M Hurter, C Windemuth, *et al.* (2001). "A genome screen for genes predisposing to bipolar affective disorder detects a new susceptibility locus on 8q." Hum. Mol. Genet. **10**(25): 2933-2944.

Clapcote, SJ, TV Lipina, JK Millar, S Mackie, S Christie, *et al.* (2007). "Behavioral phenotypes of Disc1 missense mutations in mice." Neuron **54**: 387-402.

Clapcote, SJ and JC Roder (2006). "Deletion polymorphism of Disc1 is common to all 129 mouse substrains: Implications for gene targeting studies of brain function." Genetics **173**(4): 2407-2410.

Cockell, MM, K Baumer and P Gonczy (2004). "Lis-1 is required for dynein-dependent cell division processes in C. elegans embryos." J. Cell Sci. **117**(19): 4571-4582.

Coeytaux, K and A Poupon (2005). "Prediction of unfolded segments in a protein sequence based on amino acid composition." Bioinformatics **21**: 1891-1900.

Cokol, M, R Nair and B Rost (2000). "Finding nuclear localization signals." EMBO Rep. **1**: 411-415.

Collins, DM, H Murdoch, AJ Dunlop, E Charych, GS Baillie, *et al.* (2008). "Ndel1 alters its conformation by sequestering cAMP-specific phosphodiesterase-4D3 (PDE4D3) in a manner that is dynamically regulated through Protein Kinase A (PKA)." Cell. Signal. **20**(12): 2356-2369.

Coquelle, FM, M Caspi, FP Cordelieres, JP Dompierre, DL Dujardin, *et al.* (2002). "LIS1, CLIP-170's key to the dynein/dynactin pathway." Mol. Cell. Biol. **22**(9): 3089-3102.

Curtis, D, G Kalsi, J Brynjolfsson, M McInnis, J O'Neill, *et al.* (2003). "Genome scan of pedigrees multiply affected with bipolar disorder provides further support for the presence of a susceptibility locus on chromosome 12q23-q24, and suggests the presence of additional loci on 1p and 1q." Psychiatr. Genet. **13**(2): 77-84.

Dammermann, A and A Merdes (2002). "Assembly of centrosomal proteins and microtubule organization depends on PCM-1." J. Cell Biol. **159**(2): 255-266.

Datta, SR, A McQuillin, M Rizig, E Blaveri, S Thirumalai, *et al.* (2008). "A threonine to isoleucine missense mutation in the pericentriolar material 1 gene is strongly associated with schizophrenia." Mol. Psychiatry **doi: 10.1038/mp.2008.128**.

Davies, G, J Welham, D Chant, EF Torrey and J McGrath (2003). "A systematic review and meta-analysis of northern hemisphere season of birth studies in schizophrenia." Schizophr. Bull. **29**(3): 587-593.

Deane, CM, L Salwinski, I Xenarios and D Eisenberg (2002). "Protein interactions: Two methods for assessment of the reliability of high throughput observations." Mol. Cell. Proteomics **1**(5): 349-356.

Demirhan, O and D Tastemir (2003). "Chromosome aberrations in a schizophrenia population." Schizophr. Res. **65**(1): 1-7.

Derewenda, U, C Tarricone, WC Choi, DR Cooper, S Lukasik*, et al.* (2007). "The structure of the coiled-coil domain of NDEL1 and the basis of its interaction with LIS1, the causal protein of Miller-Dieker lissencephaly." Structure **15**(11): 1567-1581.

Detera-Wadleigh, SD, JA Badner, WH Berrettini, T Yoshikawa, LR Goldin*, et al.* (1999). "A high-density genome scan detects evidence for a bipolar-disorder susceptibility locus on 13q32 and other potential loci on 1q32 and 18p11.2." Proc. Natl. Acad. Sci. USA **96**(10): 5604-5609.

Devon, RS, KL Evans, JC Maule, S Christie, S Anderson*, et al.* (1997). "Novel transcribed sequences neighbouring a translocation breakpoint associated with schizophrenia." Am. J. Med. Genet. **74**(1): 82-90.

Di Giorgio, A, G Blasi, F Sambataro, A Rampino, A Papazacharias*, et al.* (2008). "Association of the SerCys DISC1 polymorphism with human hippocampal formation gray matter and function during memory encoding." Eur. J. Neurosci. **28**(10): 2129-2136.

Di Giovanni, S, AI Faden, A Yakovlev, JS Duke-Cohan, T Finn*, et al.* (2004). "Neuronal plasticity after spinal cord injury: identification of a gene cluster driving neurite outgrowth." FASEB J. **19**(1): 153-154.

Diviani, D, LK Langeberg, SJ Doxsey and JD Scott (2000). "Pericentrin anchors protein kinase A at the centrosome through a newly identified RII-binding domain." Curr. Biol. **10**(7): 417-420.

Dosztányi, Z, V Csizmók, P Tompa and I Simon (2005a). "IUPred: web server for the prediction of intrinsically unstructured regions of proteins based on estimated energy content." Bioinformatics **21**: 3433-3434.

Dosztányi, Z, V Csizmók, P Tompa and I Simon (2005b). "The pairwise energy content estimated from amino acid composition discriminates between folded and intrinsically unstructured proteins." J. Mol. Biol. **347**: 827-839.

Dosztányi, Z and P Tompa (2008). "Prediction of protein disorder." Methods Mol. Biol. **426**: 103-115.

Dougherty, MK and DK Morrison (2004). "Unlocking the code of 14-3-3." J. Cell Sci. **117**(10): 1875-1884.

Doxsey, SJ, P Stein, L Evans, PD Calarco and M Kirschner (1994). "Pericentrin, a highly conserved centrosome protein involved in microtubule organization." Cell **76**(4): 639-650.

Duan, X, JH Chang, S Ge, RL Faulkner, JY Kim*, et al.* (2007). "Disrupted-In-Schizophrenia 1 regulates integration of newly generated neurons in the adult brain." Cell **130**(6): 1146-1158.

Dudai, Y, YN Jan, D Byers, WG Quinn and S Benzer (1976). "dunce, a mutant of Drosophila deficient in learning." Proc. Natl. Acad. Sci. USA **73**(5): 1684-1688.

Dunker, AK, Z Obradovic, P Romero, EC Garner and CJ Brown (2000). "Intrinsic protein disorder in complete genomes." Genome Inform. Ser. Workshop Genome Inform. **11**: 161-171.

Efimov, VP and NR Morris (2000). "The LIS1-related NUDF protein of *Aspergillus nidulans* interacts with the coiled-coil domain of the NUDE/RO11 protein." J. Cell Biol. **150**(3): 681-688.

Ekelund, J, W Hennah, T Hiekkalinna, A Parker, J Meyer*, et al.* (2004). "Replication of 1q42 linkage in Finnish schizophrenia pedigrees." Mol. Psychiatry **9**(11): 1037-1041.

Ekelund, J, I Hovatta, A Parker, T Paunio, T Varilo*, et al.* (2001). "Chromosome 1 loci in Finnish schizophrenia families." Hum. Mol. Genet. **10**(15): 1611-1617.

Ekelund, J, D Lichtermann, I Hovatta, P Ellonen, J Suvisaari*, et al.* (2000). "Genome-wide scan for schizophrenia in the Finnish population: evidence for a locus on chromosome 7q22." Hum. Mol. Genet. **9**(7): 1049-1057.

Ekholm, JM, T Kieseppa, T Hiekkalinna, T Partonen, T Paunio*, et al.* (2003). "Evidence of susceptibility loci on 4q32 and 16p12 for bipolar disorder." Hum. Mol. Genet. **12**(15): 1907-1915.

Elefteriou, F, JD Ahn, S Takeda, M Starbuck, X Yang*, et al.* (2005). "Leptin regulation of bone resorption by the sympathetic nervous system and CART." Nature **434**: 514-520.

Evans, KL, J Brown, Y Shibasaki, RS Devon, L He*, et al.* (1995). "A contiguous clone map over 3 Mb on the long arm of chromosome 11 across a balanced translocation associated with schizophrenia." Genomics **28**(3): 420-428.

Ewald, H, TA Kruse and O Mors (2003). "Genome wide scan using homozygosity mapping and linkage analyses of a single pedigree with affective disorder suggests oligogenic inheritance." Am. J. Med. Genet. **120B**(1): 63-71.

Ewald, H, FP Wikman, BM Teruel, HN Buttenschön, M Torralba*, et al.* (2005). "A genome-wide search for risk genes using homozygosity mapping and microarrays with 1,494 single-nucleotide polymorphisms in 22 eastern Cuban families with bipolar disorder." Am. J. Hum. Genet. **133B**(1): 25-30.

Fatemi, SH, DP King, TJ Reutiman, TD Folsom, JA Laurence*, et al.* (2008). "PDE4B polymorphisms and decreased PDE4B expression are associated with schizophrenia." Schizophr. Res. **101**(1-3): 36-49.

Faulkner, NE, DL Dujardin, C-Y Tai, KT Vaughan, CB O'Connell*, et al.* (2000). "A role for the lissencephaly gene LIS1 in mitosis and cytoplasmic dynein function." Nat. Cell Biol. **2**(11): 784-791.

Faulkner, RL, M-H Jang, X-B Liu, X Duan, KA Sailor*, et al.* (2008). "Development of hippocampal mossy fiber synaptic outputs by new neurons in the adult brain." Proc. Natl. Acad. Sci. USA **105**(37): 14157-14162.

Feng, Y, EC Olson, PT Stukenberg, LA Flanagan, MW Kirschner and CA Walsh (2000). "LIS1 regulates CNS lamination by interacting with mNudE, a central component of the centrosome." Neuron **28**(3): 665-679.

Feng, Y and CA Walsh (2004). "Mitotic spindle regulation by Nde1 controls cerebral cortical size." Neuron **44**(2): 279-293.

Fletcher, JM, K Evans, D Baillie, P Byrd, D Hanratty*, et al.* (1993). "Schizophrenia-associated chromosome 11q21 translocation: Identification of flanking

markers and development of chromosome 11q fragment hybrids as cloning and mapping resources." Genomics **52**(3): 478-490.

Flory, MR and TN Davis (2003). "The centrosomal proteins pericentrin and kendrin are encoded by alternatively spliced products of one gene." Genomics **82**(3): 401-405.

Flory, MR, MJ Moser, RJJ Monnat and TN Davis (2000). "Identification of a human centrosomal calmodulin-binding protein that shares homology with pericentrin." Proc. Natl. Acad. Sci. USA **97**(11): 5919-5923.

Fox, AH, YW Lam, AKL Leung, CE Lyon, J Andersen*, et al.* (2002). "Paraspeckles: a novel nuclear domain." Curr. Biol. **12**(1): 13-25.

Fujita, T, AD Maturana, J Ikuta, J Hamada, S Walchli*, et al.* (2007). "Axonal guidance protein FEZ1 associates with tubulin and kinesin motor protein to transport mitochondria in neurites of NGF-stimulated PC12 cells." Biochem. Biophys. Res. Comm. **361**(3): 605-610.

Furuyashiki, T, K Fujisawa, A Fujita, P Madaule, S Uchino*, et al.* (1999). "Citron, a rho-target, interacts with PSD-95/SAP-90 at glutamatergic synapses in the thalamus." J. Neurosci. **19**(1): 109-118.

Gallinat, J, M Bauer and A Heinz (2008). "Genes and neuroimaging: advances in psychiatric research." Neurodegener. Dis. **5**(5): 277-285.

Garner, CC, A Garner, G Huber, C Kozak and A Matus (1990). "Molecular cloning of microtubule-associated protein 1 (MAP1A) and microtubule-associated protein 5 (MAP1B): identification of distinct genes and their differential expression in developing brain." J. Neurochem. **55**(1): 146-154.

Gasteiger, E, C Hoogland, A Gattiker, S Duvaud, MR Wilkins*, et al.* (2005). Protein identification and analysis tools on the ExPASy server. The Proteomics Protocols Handbook. J. M. Walker, Humana Press**:** 571-607.

Geiser, JR, EJ Schott, TJ Kingsbury, NB Cole, LJ Totis*, et al.* (1997). "Saccharomyces cerevisiae genes required in the absence of the CIN8-encoded spindle motor act in functionally diverse mitotic pathways." Mol. Biol. Cell **8**: 1035-1050.

Gejman, P, M Martinez, Q Cao, E Friedman, W Berrettini*, et al.* (1993). "Linkage analysis of fifty-seven microsatellite loci to bipolar disorder." Neuropsychopharmacology **9**(1): 31-40.

Gill, M, H Vallada, D Collier, P Sham, P Holmans*, et al.* (1996). "A combined analysis of D22S278 marker alleles in affected sib-pairs: Support for a susceptibility locus for schizophrenia at chromosome 22q12." Am. J. Med. Genet. **67**(1): 40-45.

Gill, S, T Schroer, I Szilak, E Steuer, M Sheetz and D Cleveland (1991). "Dynactin, a conserved, ubiquitously expressed component of an activator of vesicle motility mediated by cytoplasmic dynein." J. Cell Biol. **115**(6): 1639-1650.

Gluzman, Y (1981). "SV40-transformed simian cells support the replication of early SV40 mutants." Cell **23**(1): 175-182.

Gottesman, II, P McGuffin and AE Farmer (1987). "Clinical genetics as clues to the "real" genetics of schizophrenia (a decade of modest gains while playing for time)." Schizophr. Bull. **13**(1): 23-48.

Green, EK, N Norton, T Peirce, D Grozeva, G Kirov*, et al.* (2006). "Evidence that a DISC1 frame-shift deletion associated with psychosis in a single family may not be a pathogenic mutation." Mol. Psychiatry **11**: 798-799.

Griffith, E, S Walker, CA Martin, P Vagnarelli, T Stiff, *et al.* (2008). "Mutations in pericentrin cause Seckel syndrome with defective ATR-dependent DNA damage signaling." Nat. Genet. **40**(2): 232-236.

Guerrini, R and C Marini (2006). "Genetic malformations of cortical development." Exp. Brain Res. **173**(2): 322-333.

Guo, J, Z Yang, W Song, Q Chen, F Wang, *et al.* (2006). "Nudel contributes to microtubule anchoring at the mother centriole and is involved in both dynein-dependent and -independent centrosomal protein assembly." Mol. Biol. Cell **17**(2): 680-689.

Gurling, HM, H Critchley, SR Datta, A McQuillin, E Blaveri, *et al.* (2006). "Genetic association and brain morphology studies and the chromosome 8p22 pericentriolar material 1 (PCM1) gene in susceptibility to schizophrenia." Arch. Gen. Psychiatry **63**(8): 844-854.

Hamshere, ML, P Bennett, N Williams, R Segurado, A Cardno, *et al.* (2005). "Genomewide linkage scan in schizoaffective disorder: significant evidence for linkage at 1q42 close to DISC1, and suggestive evidence at 22q11 and 19p13." Arch. Gen. Psychiatry **62**(10): 1081-1088.

Hashimoto, R, T Numakawa, T Ohnishi, E Kumamaru, Y Yagasaki, *et al.* (2006). "Impact of the DISC1 Ser704Cys polymorphism on risk for major depression, brain morphology, and ERK signaling." Hum. Mol. Genet. **15**(20): 3024-3033.

Hattori, M, H Adachi, M Tsujimoto, H Arai and K Inoue (1994). "Miller-Dieker lissencephaly gene encodes a subunit of brain platelet-activating factor." Nature **370**: 216-218.

Hattori, T, K Baba, S Matsuzaki, A Honda, K Miyoshi, *et al.* (2007). "A novel DISC1-interacting partner DISC1-Binding Zinc-finger protein: implication in the modulation of DISC1-dependent neurite outgrowth." Mol. Psychiatry **12**(4): 398-407.

Hayashi, MAF, RS Pires, NA Reboucas, LRG Britto and ACM Camargo (2001). "Expression of endo-oligopeptidase A in the rat central nervous system: a non-radioactive in situ hybridization study." Mol. Brain Res. **89**(1-2): 86-93.

Hayashi, MAF, FCV Portaro, MF Bastos, JR Guerreiro, V Oliveira, *et al.* (2005). "Inhibition of NUDEL (nuclear distribution element-like)-oligopeptidase activity by disrupted-in-schizophrenia 1." Proc. Natl. Acad. Sci. USA **102**(10): 3828-3833.

Haynes, C, CJ Oldfield, F Ji, N Klitgord, ME Cusick, *et al.* (2006). "Intrinsic disorder is a common feature of hub proteins from four eukaryotic interactomes." PLoS Comput. Biol. **2**(8): e100.

Hegyi, H, E Schad and P Tompa (2007). "Structural disorder promotes assembly of protein complexes." BMC Struc. Biol. **8**(7): 65.

Hennah, W, P Thomson, A McQuillin, N Bass, A Loukola, *et al.* (2008). "DISC1 association, heterogeneity and interplay in schizophrenia and bipolar disorder." Mol. Psychiatry **doi:10.1038/mp.2008.22**.

Hennah, W, L Tomppo, T Hiekkalinna, OM Palo, H Kilpinen, *et al.* (2007). "Families with the risk allele of DISC1 reveal a link between schizophrenia and another component of the same molecular pathway, NDE1." Hum. Mol. Genet. **6**(5): 453-462.

Hennah, W, T Varilo, M Kestila, T Paunio, R Arajarvi, *et al.* (2003). "Haplotype transmission analysis provides evidence of association for DISC1 to schizophrenia and suggests sex-dependent effects." Hum. Mol. Genet. **12**(23): 3151-3159.

Hikida, T, H Jaaro-Peled, S Seshadri, K Oishi, C Hookway, *et al.* (2007). "Dominant-negative DISC1 transgenic mice display schizophrenia-associated phenotypes detected by measures translatable to humans." Proc. Natl. Acad. Sci. USA **104**(36): 14501-14506.

Hinnebusch, AG (2006). "eIF3: a versatile scaffold for translation initiation complexes." Trends Biochem. Sci. **31**(10): 553-562.

Hirohashi, Y, Q Wang, Q Liu, X Du, H Zhang, *et al.* (2006a). "p78/MCRS1 forms a complex with centrosomal protein Nde1 and is essential for cell viability." Oncogene **25**(35): 4937-4946.

Hirohashi, Y, Q Wang, Q Liu, B Li, X Du, *et al.* (2006b). "Centrosomal proteins Nde1 and Su48 form a complex regulated by phosphorylation." Oncogene **25**(45): 6048-6055.

Hirokawa, N and Y Noda (2008). "Intracellular transport and kinesin superfamily proteins, KIFs: structure, function, and dynamics." Physiol. Rev. **88**(3): 1089-1118.

Hirotsune, S, MW Fleck, MJ Gambello, GJ Bix, A Chen, *et al.* (1998). "Graded reduction of Pafah1b1 (Lis1) activity results in neuronal migration defects and early embryonic lethality." Nat. Genet. **19**(4): 333-339.

Hodgkinson, CA, D Goldman, F Ducci, P DeRosse, DA Caycedo, *et al.* (2006). "The FEZ1 gene shows no association to schizophrenia in Caucasian or African American populations." Neuropsychopharmacology **32**(1): 190-196.

Hodgkinson, CA, D Goldman, J Jaeger, S Persaud, JM Kane, *et al.* (2004). "Disrupted in Schizophrenia 1 (DISC1): Association with schizophrenia, schizoaffective disorder, and bipolar disorder." Am. J. Hum. Genet. **75**(5): 862-872.

Honda, A, K Miyoshi, K Baba, M Taniguchi, Y Koyama, *et al.* (2004). "Expression of fasciculation and elongation protein zeta-1 (FEZ1) in the developing rat brain." Mol. Brain Res. **122**(1): 89-92.

Hong, CJ, DL Liao, HL Shih and SJ Tsai (2004). "Association study of PICK1 rs3952 polymorphism and schizophrenia." Neuroreport **15**(12): 1965-1967.

Houslay, MD and DR Adams (2003). "PDE4 cAMP phosphodiesterases: modular enzymes that orchestrate signalling cross-talk, desensitization and compartmentalization." Biochem. J. **370**: 1-18.

Hovatta, I, T Varilo, J Suvisaari, JD Terwilliger, V Ollikainene, *et al.* (1999). "A genomewide screen for schizophrenia genes in an isolated Finnish subpopulation, suggesting multiple susceptability loci." Am. J. Hum. Genet. **65**: 1114-1124.

Howell, BJ, DB Hoffman, G Fang, AW Murray and ED Salmon (2000). "Visualization of Mad2 dynamics at kinetochores, along spindle fibers, and at spindle poles in living cells." J. Cell Biol. **150**(6): 1233-1250.

Howell, BJ, BF McEwen, JC Canman, DB Hoffman, EM Farrar, *et al.* (2001). "Cytoplasmic dynein/dynactin drives kinetochore protein transport to the spindle poles and has a role in mitotic spindle checkpoint inactivation." J. Cell Biol. **155**(7): 1159-1172.

Huston, E, S Lumb, A Russell, C Catterall, AH Ross*, et al.* (1997). "Molecular cloning and transient expression in COS7 cells of a novel human PDE4B cAMP-specific phosphodiesterase, HSPDE4B3." Biochem. J. **328**: 549-588.

Hwu, H-G, C-M Liu, CS-J Fann, W-C Ou-Yang and SF-C Lee (2003). "Linkage of schizophrenia with chromosome 1q loci in Taiwanese families." Mol. Psychiatry **8**: 445-452.

Ikeda, M, T Hikita, S Taya, J Uraguchi-Asaki, K Toyo-oka*, et al.* (2008). "Identification of YWHAE, a gene encoding 14-3-3epsilon, as a possible susceptibility gene for schizophrenia." Hum. Mol. Genet. **17**(20): 3212-3222.

Ikuta, J, A Maturana, T Fujita, T Okajima, K Tatematsu*, et al.* (2007). "Fasciculation and elongation protein zeta-1 (FEZ1) participates in the polarization of hippocampal neuron by controlling the mitochondrial motility." Biochem. Biophys. Res. Comm. **353**(1): 127-132.

Ishizuka, K, J Chen, S Taya, W Li, JK Millar*, et al.* (2007). "Evidence that many of the DISC1 isoforms in C57BL//6J mice are also expressed in 129S6//SvEv mice." Mol. Psychiatry **12**(10): 897-899.

Jacobs, PA, M Bruntion, A Frackiewicz, M Newton, PJL Cook and EB Robson (1970). "Studies on a family with three cytogenetic markers." Ann. Hum. Genet. **33**(4): 325-336.

Jainchill, JL, SA Aaronson and GJ Todaro (1969). "Murine sarcoma and leukemia viruses: Assay using clonal lines of contact-inhibited mouse cells." J. Virol. **4**(5): 549-553.

James, R, RR Adams, S Christie, SR Buchanan, DJ Porteous and JK Millar (2004). "Disrupted in Schizophrenia 1 (DISC1) is a multicompartmentalized protein that predominantly localizes to mitochondria." Mol. Cell. Neurosci. **16**: 112-122.

Judd, LL and HS Akiskal (2003). "The prevalence and disability of bipolar spectrum disorders in the US population: re-analysis of the ECA database taking into account subthreshold cases." J. Affect. Disord. **73**(1-2): 123-131.

Kähler, AK, S Djurovic, B Kulle, EG Jönsson, I Agartz*, et al.* (2008). "Association analysis of schizophrenia on 18 genes involved in neuronal migration: *MDGA1* as a new susceptibility gene." Am. J. Med. Genet. **147B**(7): 1089-1100.

Kakiuchi, C, M Ishiwata, S Nanko, H Kunugi, Y Minabe*, et al.* (2007). "Association analysis of ATF4 and ATF5, genes for interacting-proteins of DISC1, in bipolar disorder." Neurosci. Lett. **417**(3): 316-321.

Kamiya, A, K Kubo, T Tomoda, M Takaki, R Youn*, et al.* (2005). "A schizophrenia-associated mutation of DISC1 perturbs cerebral cortex development." Nat. Cell Biol. **7**(12): 1167-1178.

Kamiya, A, PL Tan, K Kubo, C Engelhard, K Ishizuka*, et al.* (2008). "Recruitment of PCM1 to the centrosome by the cooperative action of DISC1 and BBS4: a candidate for psychiatric illnesses." Arch. Gen. Psychiatry **65**(9): 996-1006.

Kamiya, A, T Tomoda, J Chang, M Takaki, C Zhan*, et al.* (2006). "DISC1-NDEL1/NUDEL protein interaction, an essential component for neurite outgrowth, is modulated by genetic variations of DISC1." Hum. Mol. Genet. **15**(22): 3313-3323.

Kaneko, N, T Muratake, H Kuwabara, T Kurosaki, M Takei*, et al.* (2007). "Autosomal linkage analysis of a Japanese single multiplex schizophrenia

pedigree reveals two candidate loci on chromosomes 4q and 3q." Am. J. Med. Genet. **144B**(6): 735-742.

Kaneva, RP, VM Chorbov, VK Milanova, CS Kostov, KI Nickolov*, et al.* (2004). "Linkage analysis in bipolar pedigrees adds support for a susceptibility locus on 21q22." Psychiatr. Genet. **14**(2): 101-106.

Kasamatsu, A, Y Endo, K Uzawa, D Nakashima, H Koike*, et al.* (2005). "Identification of candidate genes associated with salivary adenoid cystic carcinomas using combined comparative genomic hybridization and oligonucleotide microarray analyses." Int. J. Biochem. Cell Biol. **37**(9): 1869-1880.

Kawauchi, T, K Chihama, Y Nabeshima and M Hoshino (2003). "The in vivo roles of STEF/Tiam1, Rac1 and JNK in cortical neuronal migration." EMBO J. **22**(16): 4190-4201.

Khattak, S, BR Lee, SH Cho, J Ahnn and NA Spoerel (2002). "Genetic characterization of Drosophila Mi-2 ATPase." Gene **293**(1-2): 107-114.

Khodjakov, A, CL Rieder, G Sluder, G Cassels, O Sibon and C-L Wang (2002). "De novo formation of centrosomes in vertebrate cells arrested during S phase." J. Cell Biol. **158**(7): 1171-1181.

Kholmanskikh, SS, JS Dobrin, A Wynshaw-Boris, PC Letourneau and ME Ross (2003). "Disregulated RhoGTPases and actin cytoskeleton contribute to the migration defect in Lis1-deficient neurons." J. Neurosci. **23**(25): 8673-8681.

Kilpinen, H, T Ylisaukko-oja, W Hennah, OM Palo, T Varilo*, et al.* (2008). "Association of DISC1 with autism and Asperger syndrome." Mol. Psychiatry **13**: 187-196.

Kim, H-J, HJ Park, KH Jung, JY Ban, J Ra*, et al.* (2007). "Association study of polymorphisms between DISC1 and schizophrenia in a Korean population." Neurosci. Lett. **430**(1): 60-63.

Kim, JC, JL Badano, S Sibold, MA Esmail, J Hill*, et al.* (2004). "The Bardet-Biedl protein BBS4 targets cargo to the pericentriolar region and is required for microtubule anchoring and cell cycle progression." Nat. Genet. **36**(5): 462-470.

Kim, PM, A Sboner, Y Xia and M Gerstein (2008). "The role of disorder in interaction networks: a structural analysis." Mol. Syst. Biol. **4**: 179.

Kim, YH, CY Choi and Y Kim (1999). "Covalent modification of the homeodomain-interacting protein kinase 2 (HIPK2) by the ubiquitin-like protein SUMO-1." Proc. Natl. Acad. Sci. USA **96**(22): 12350-12355.

Kirkpatrick, B, L Xu, N Cascella, Y Ozeki, A Sawa and RC Roberts (2006). "DISC1 immunoreactivity at the light and ultrastructural level in the human neocortex." J. Comp. Neurol. **497**(3): 436-450.

Kitagawa, M, M Umezu, J Aoki, H Koizumi, H Arai and K Inoue (2000). "Direct association of LIS1, the lissencephaly gene product, with a mammalian homologue of a fungal nuclear distribution protein, rNUDE." FEBS Lett. **479**(1-2): 57-62.

Klei, L, SA Bacanu, M Myles-Worsley, B Galke, W Xie*, et al.* (2005). "Linkage analysis of a completely ascertained sample of familial schizophrenics and bipolars from Palau, Micronesia." Hum. Genet. **117**(4): 349-356.

Koga, M, H Ishiguro, Y Horiuchi, T Albalushi, T Inada, *et al.* (2007). "Failure to confirm the association between the FEZ1 gene and schizophrenia in a Japanese population." Neurosci. Lett. **417**(3): 326-329.

Koike, H, PA Arguello, M Kvajo, M Karayiorgou and JA Gogos (2006). "Disc1 is mutated in the 129S6/SvEv strain and modulates working memory in mice." Proc. Natl. Acad. Sci. USA **103**(10): 3693-3697.

Kozak, M (1987). "An analysis of 5'-noncoding sequences from 699 vertebrate messenger RNAs." Nucleic Acids Res. **15**(20): 8125-8148.

Kubo, A, H Sasaki, A Yuba-Kubo, S Tsukita and N Shiina (1999). "Centriolar satellites: Molecular characterization, ATP-dependent movement toward centrioles and possible involvement in ciliogenesis." J. Cell Biol. **147**(5): 969-980.

Kuroda, Si, N Nakagawa, C Tokunaga, K Tatematsu and K Tanizawa (1999). "Mammalian homologue of the Caenorhabditis elegans UNC-76 protein involved in axonal outgrowth is a protein kinase C zeta -interacting protein." J. Cell Biol. **144**(3): 403-411.

Kvajo, M, H McKellar, PA Arguello, LJ Drew, H Moore, *et al.* (2008). "A mutation in mouse Disc1 that models a schizophrenia risk allele leads to specific alterations in neuronal architecture and cognition." Proc. Natl. Acad. Sci. USA **105**(19): 7076-7081.

Kwok, JBJ, LJ Adams, JA Salmon, JA Donald, PB Mitchell and PR Schofield (1999). "Nonparametric simulation-based statistical analyses for bipolar affective disorder locus on chromosome 21q22.3." Am. J. Med. Genet. **88B**(1): 99-102.

Lamond, AI and DL Spector (2003). "Nuclear speckles: a model for nuclear organelles." Nat. Rev. Mol. Cell. Biol. **4**(8): 605-612.

Larkin, MA, G Blackshields, NP Brown, R Chenna, PA McGettigan, *et al.* (2007). "ClustalW and ClustalX version 2." Bioinformatics **23**(21): 2947-2948.

Leliveld, SR, V Bader, P Hendriks, I Prikulis, G Sajnani, *et al.* (2008). "Insolubility of Disrupted-in-Schizophrenia 1 disrupts oligomer-dependent interactions with Nuclear Distribution Element 1 and is associated with sporadic mental disease." J. Neurosci. **28**(15): 3839-3845.

Lerer, B, RH Segman, A Hamdan, K Kanyas, O Karni, *et al.* (2003). "Genome scan of Arab Israeli families maps a schizophrenia susceptibility gene to chromosome 6q23 and supports a locus at chromosome 10q24." Mol. Psychiatry **8**(5): 488-498.

Li, C, PN Inglis, CC Leitch, E Efimenko, NA Zaghloul, *et al.* (2008). "An essential role for DYF-11/MIP-T3 in assembling functional intraflagellar transport complexes." PLoS Genet. **4**(3): e1000044.

Li, Q, D Hansen, A Killilea, H Joshi, R Palazzo and R Balczon (2001). "Kendrin/pericentrin-B, a centrosome protein with homology to pericentrin that complexes with PCM-1." J. Cell Sci. **114**(4): 797-809.

Li, W, Y Zhou, JD Jentsch, RAM Brown, X Tian, *et al.* (2007). "Specific developmental disruption of disrupted-in-schizophrenia-1 function results in schizophrenia-related phenotypes in mice." Proc. Natl. Acad. Sci. USA **104**(46): 18280-18285.

Liang, SG, AD Sadovnick, RA Remick, PE Keck, SL McElroy and JR Kelsoe (2002). "A linkage disequilibrium study of bipolar disorder and microsatellite markers on 22q13." Psychiatr. Genet. **12**(4): 231-235.

Liang, Y, W Yu, Y Li, Z Yang, X Yan*, et al.* (2004). "Nudel functions in membrane traffic mainly through association with Lis1 and cytoplasmic dynein." J. Cell Biol. **164**(4): 557-566.

Liang, Y, W Yu, Y Li, L Yu, Q Zhang*, et al.* (2007). "Nudel modulates kinetochore association and function of cytoplasmic dynein in M phase." Mol. Biol. Cell **18**(7): 2656-2666.

Linding, R, LJ Jensen, F Diella, P Bork, TJ Gibson and RB Russell (2003). "Protein disorder prediction: implications for structural proteomics." Structure **11**(11): 1453-1459.

Ling, L and DV Goeddel (2000). "MIP-T3, a novel protein linking tumor Necrosis Factor Receptor-Associated Factor 3 to the microtubule network." J. Biol. Chem. **275**(31): 23852-23860.

Lipska, BK, T Peters, TM Hyde, N Halim, C Horowitz*, et al.* (2006). "Expression of DISC1 binding partners is reduced in schizophrenia and associated with DISC1 SNPs." Hum. Mol. Genet. **15**(8): 1245-1258.

Liu, J, SH Juo, A Dewan, A Grunn, X Tong*, et al.* (2003). "Evidence for a putative bipolar disorder locus on 2p13-16 and other potential loci on 4q31, 7q34, 8q13, 9q31, 10q21-24, 13q32, 14q21 and 17q11-12." Mol. Psychiatry **8**(3): 333-342.

Liu, J, SH Juo, JD Terwilliger, A Grunn, X Tong*, et al.* (2001). "A follow-up linkage study supports evidence for a bipolar affective disorder locus on chromosome 21q22." Am. J. Hum. Genet. **105**(2): 189-194.

Liu, Y-L, CS-J Fann, C-M Liu, WJ Chen, J-Y Wu*, et al.* (2006). "A single nucleotide polymorphism fine mapping study of chromosome 1q42.1 reveals the vulnerability genes for schizophrenia, GNPAT and DISC1: Association with impairment of sustained attention." Biol. Psychiatry **60**(6): 554-562.

Logue, MW, LM Brzustowicz, AS Bassett, EW Chow and VJ Vieland (2006). "A posterior probability of linkage-based re-analysis of schizophrenia data yields evidence of linkage to chromosomes 1 and 17." Hum. Hered. **62**(1): 47-54.

Lowenstein, EJ, RJ Daly, AG Batzer, W Li, B Margolis*, et al.* (1992). "The SH2 and SH3 domain-containing protein GRB2 links receptor tyrosine kinases to ras signaling." Cell **70**(3): 431-442.

Lupas, A, M Van Dyke and J Stock (1991). "Predicting coiled-coils from protein sequences." Science **252**: 1162-1164.

Ma, L, Y Liu, B Ky, PJ Shughrus, CP Austin and JA Morris (2002). "Cloning and characterization of Disc1, the mouse ortholog of DISC1 (Disrupted-in-Schizophrenia 1)." Genomics **80**(6): 662-672.

Ma, L, X Zhao and X Xueliang Zhu (2006). "Mitosin/CENP-F in mitosis, transcriptional control, and differentiation." J Biomed. Sci. **13**: 205-213.

MacCallum, RM "Order/disorder prediction with self organising maps." http://www.forcasp.org/paper2127.html **(Retrieved 29-02-08)**.

Macgregor, S, PM Visscher, SA Knott, P Thomson, DJ Porteous*, et al.* (2004). "A genome scan and follow-up study identify a bipolar disorder susceptibility locus on chromosome 1q42." Mol. Psychiatry **9**(12): 1083-1090.

MacKenzie, SJ and MD Houslay (2000). "Action of rolipram on specific PDE4 cAMP phosphodiesterase isoforms and on the phosphorylation of cAMP-response-element-binding protein (CREB) and p38 mitogen-activated protein (MAP) kinase in U937 monocytic cells." Biochem. J. **347**: 571-578.

Maier, W (2008). "Common risk genes for affective and schizophrenic psychoses." Eur. Arch. Psychiatry Clin. Neurosci. **258**: S2: 37-40.

Maiolica, A, D Cittaro, D Borsotti, L Sennels, C Ciferri*, et al.* (2007). "Structural analysis of multi-protein complexes by cross-linking, mass spectrometry and database searching." Mol. Cell. Proteomics **6**(12): 2200-2211.

Marcheco-Teruel, B, TJ Flint, FP Wikman, M Torralbas, L González*, et al.* (2006). "A genome-wide linkage search for bipolar disorder susceptibility loci in a large and complex pedigree from the eastern part of Cuba." Am. J. Med. Genet. **141B**(8): 833-843.

Maziade, M, M-A Roy, YC Chagnon, D Cliche, J-P Fournier*, et al.* (2004). "Shared and specific susceptibility loci for schizophrenia and bipolar disorder: a dense genome scan in Eastern Quebec families." Nat. Psychaitry **10**(5): 486-499.

McCahill, A, T McSorley, E Huston, EV Hill, MJ Lynch*, et al.* (2005). "In resting COS1 cells a dominant negative approach shows that specific, anchored PDE4 cAMP phosphodiesterase isoforms gate the activation, by basal cyclic AMP production, of AKAP-tethered protein kinase A type II located in the centrosomal region." Cell. Sig. **17**(9): 1158-1173.

McGuffin, LJ, K Bryson and DT Jones (2000). "The PSIPRED protein structure prediction server." Bioinformatics **16**: 404-405.

McInnis, MG, TH Lan, VL Willour, FJ McMahon, SG Simpson*, et al.* (2003). "Genome-wide scan of bipolar disorder in 65 pedigrees: supportive evidence for linkage at 8q24, 18q22, 4q32, 2p12, and 13q12." Mol. Psychiatry **8**(3): 288-298.

Mili, S, K Moissoglu and IG Macara (2008). "Genome-wide screen reveals APC-associated RNAs enriched in cell protrusions." Nature **453**(7191): 115-119.

Millar, JK, J Brown, JC Maule, Y Shibasaki, S Christie*, et al.* (1998). "A long-range restriction map across 3 Mb of the chromosome 11 breakpoint region of a translotion linked to schizophrenia: localization of the breakpoint and the search for neighbouring genes." Psychiatr. Genet. **8**(3): 175-181.

Millar, JK, S Christie, S Anderson, D Lawson, DHW Loh*, et al.* (2001). "Genomic structure and localisation within a linkage hotspot of Disrupted In Schizophrenia 1, a gene disrupted by a translocation segregating with schizophrenia." Mol. Psychiatry **6**(2): 173-178.

Millar, JK, S Christie and DJ Porteous (2003). "Yeast two-hybrid screens implicate DISC1 in brain development and function." Biochem. Biophys. Res. Comm. **311**: 1019-1025.

Millar, JK, S Christie, CAM Semple and DJ Porteous (2000a). "Chromosomal location and genomic structure of the human translin-associated factor X gene (*TRAX; TSNAX*) revealed by intergenic splicing to *DISC1,* a gene disrupted by a translocation segregating with schizophrenia." Genomics **67**: 69-77.

Millar, JK, R James, S Christie and DJ Porteous (2005a). "Disrupted in Schizophrenia (DISC1): Subcellular targeting and induction of ring mitochondria." Mol. Cell. Neurosci. **30**(4): 477-484.

Millar, JK, BS Pickard, S Mackie, R James, S Christie, *et al.* (2005b). "DISC1 and PDE4B are interacting genetic factors in schizophrenia that regulate cAMP signalling." Science **310**: 1187-1191.

Millar, JK, JC Wilson-Annan, S Anderson, S Christie, MS Taylor, *et al.* (2000b). "Disruption of two novel genes by a translocation co-segregating with schizophrenia." Hum. Mol.Genet. **9**(9): 1415-1425.

Miyoshi, K, M Asanuma, I Miyazaki, FJ Diaz-Corrales, T Katayama, *et al.* (2005). "DISC1 localizes to the centrosome by binding to kendrin." Biochem. Biophys. Res. Comm. **317**: 1195-1199.

Miyoshi, K, A Honda, K Baba, M Taniguchi, K Oono, *et al.* (2003). "Disrupted-in-Schizophrenia 1, a candidate gene for schizophrenia, participates in neurite outgrowth." Mol. Psychiatry **8**: 685-694.

Moon, HJ, S-V Yim, WK Lee, Y-W Jeon, YH Kim, *et al.* (2006). "Identification of DNA copy-number aberrations by array-comparative genomic hybridization in patients with schizophrenia." Biochem. Biophys. Res. Comm. **344**(2): 531-539.

Mori, D, Y Yano, K Toyo-oka, N Yoshida, M Yamada, *et al.* (2007). "NDEL1 phosphorylation by Aurora-A Kinase is essential for centrosomal maturation, separation, and TACC3 recruitment." Mol. Cell. Biol. **27**(1): 352-367.

Morris, JA, G Kandpal, L Ma and CP Austin (2003). "DISC1 (Disrupted-In-Schizophrenia 1) is a centrosome-associated protein that interacts with MAP1A, MIPT3, ATF4/5 and NUDEL: regulation and loss of interaction with mutation." Hum. Mol.Genet. **12**(13): 1591-1608.

Moult, J, T Hubbard, K Fidelis and JT Pedersen (1999). "Critical assessment of methods of protein structure prediction (CASP): round III." Proteins **Suppl 3**: 2-6.

Muir, WJ, CM Gosden, AJ Brookes, J Fantes, KL Evans, *et al.* (1995). "Direct microdissection and microcloning of a translocation breakpoint region, t(1;11) (q42.2;q21), associated with schizophrenia." Cytogenet. Cell Genet. **70**(1-2): 35-40.

Murdoch, H, S Mackie, DM Collins, EV Hill, GB Bolger, *et al.* (2007). "Isoform-selective susceptibility of DISC1/Phosphodiesterase-4 complexes to dissociation by elevated intracellular cAMP levels." J. Neurosci. **27**(35): 9513-9524.

Nagase, T, K-i Ishikawa, M Suyama, R Kikuno, M Hirosawa, *et al.* (1998). "Prediction of the coding sequences of unidentified human genes. XII. The complete sequences of 100 new cDNA clones from brain which code for large proteins *in vitro*." DNA Res. **5**(6): 355-364.

Nair, R, P Carter and B Rost (2002). "NLSdb: database of nuclear localization signals." Nucleic Acids Res. **31**(1): 397-399.

Nakai, K and P Horton (1999). "PSORT: a program for detecting sorting signals in proteins and predicting their subcellular localization." Trends Biochem. Sci. **24**(1): 34-35.

Namba, R, JE Maglione, RR Davis, CA Baron, S Liu, *et al.* (2006). "Heterogeneity of mammary lesions represent molecular differences." BMC Cancer **6**: 275.

Newton, SS, EF Collier, AH Bennett, DS Russell and RS Duman (2004). "Regulation of growth factor receptor bound 2 by electroconvulsive seizure." Mol. Brain Res. **129**(1-2): 185-188.

Nguyen, MD, T Shu, K Sanada, RC Lariviere, H-C Tseng, *et al.* (2004a). "A NUDEL-dependent mechanism of neurofilament assembly regulates the integrity of CNS neurons." **6**(7): 595-608.

Nguyen, MD, T Shu, K Sanada, RC Larivière, HC Tseng, *et al.* (2004b). "A NUDEL-dependent mechanism of neurofilament assembly regulates the integrity of CNS neurons." Nat. Cell Biol. **6**(7): 595-608.

Niethammer, M, DS Smith, R Ayala, J Peng, J Ko, *et al.* (2000). "NUDEL is a novel Cdk5 substrate that associates with LIS1 and cytoplasmic dynein." Neuron **28**(3): 697-711.

Numata, S, JI Iga, M Nakataki, S Tayoshi, K Taniguchi, *et al.* (2008a). "Gene expression and association analyses of the phosphodiesterase 4B (PDE4B) gene in major depressive disorder in the Japanese population." Am. J. Med. Genet. **doi:10.1002/ajmg.b.30852**.

Numata, S, S-i Ueno, J-i Iga, H Song, M Nakataki, *et al.* (2008b). "Positive association of the PDE4B (phosphodiesterase 4B) gene with schizophrenia in the Japanese population." J. Psychiatr. Res. **43**(1): 7-12.

O'Donovan, MC, N Craddock, N Norton, H Williams, T Peirce, *et al.* (2008). "Identification of loci associated with schizophrenia by genome-wide association and follow-up." Nat. Genet. **40**(9): 1053-1055.

Obenauer, JC, LC Cantley and MB Yaffe (2003). "Scansite 2.0: Proteome-wide prediction of cell signaling interactions using short sequence motifs." Nucleic Acids Res. **31**(13): 3636-3641.

Obradovic, Z, K Peng, S Vucetic, P Radivojac and AK Dunker (2005). "Exploiting heterogeneous sequence properties improves prediction of protein disorder." Proteins **61**(S7): 176-182.

Ogawa, F, M Kasai and T Akiyama (2005). "A functional link between Disrupted-In-Schizophrenia 1 and the eukaryotic translation initiation factor 3." Biochem. Biophys. Res. Comm. **338**(2): 771-776.

Orthaus, S, C Biskup, B Hoffmann, C Hoischen, S Ohndorf, *et al.* (2008). "Assembly of the inner kinetochore proteins CENP-A and CENP-B in living human cells." Chem. Biochem. **9**(1): 77-92.

Owens, RJ, S Lumb, K Rees-Milton, A Russell, D Baldock, *et al.* (1997). "Molecular cloning and expression of a human phosphodiesterase 4C." Cell. Signal. **9**(8): 575-585.

Ozeki, Y, T Tomoda, J Kleiderlein, A Kamiya, L Bord, *et al.* (2003). "Disrupted-in-Schizophrenia-1 (DISC-1): Mutant truncation prevents binding to NudE-like (NUDEL) and inhibits neurite outgrowth." Proc. Natl. Acad. Sci. USA **100**(1): 289-294.

Palo, OM, M Antila, K Silander, W Hennah, H Kilpinen, *et al.* (2007). "Association of distinct allelic haplotypes of DISC1 with psychotic and bipolar spectrum disorders and with underlying cognitive impairments." Hum. Mol. Genet. **16**(20): 2517-2528.

Park, N, SH Juo, R Cheng, J Liu, JE Loth, *et al.* (2004). "Linkage analysis of psychosis in bipolar pedigrees suggests novel putative loci for bipolar disorder and shared susceptibility with schizophrenia." Mol. Psychiatry **9**(12): 1091-1099.

Paunio, T, J Ekelund, T Varilo, A Parker, I Hovatta, *et al.* (2001). "Genome-wide scan in a nationwide study sample of schizophrenia families in Finland

reveals susceptibility loci on chromosomes 2q and 5q." Hum. Mol. Genet. **10**(26): 3037-3048.

Pawlisz, AS, C Mutch, A Wynshaw-Boris, A Chenn, CA Walsh and Y Feng (2008). "Lis1-Nde1 dependent neuronal fate control determines cerebral cortical size and lamination." Hum. Mol. Genet. **17**(16): 2441-2455.

Pearson, WR and DJ Lipman (1988). "Improved tools for biological sequence comparison." Proc. Natl. Acad. Sci. USA **85**(8): 2444-2448.

Pedersen, AG and H Nielsen (1997). "Neural network prediction of translation initiation sites in eukaryotes: perspectives for EST and genome analysis." Proc. Int. Conf. Intell. Syst. Mol. Biol. **5**: 226-233.

Pedersen, CB and PB Mortensen (2001). "Evidence of a dose-response relationship between urbanicity during upbringing and schizophrenia risk." Arch. Gen. Psychiatry **58**(11): 1039-1046.

Pedrotti, B, R Colombo and K Islam (1994). "Microtubule associated protein MAP1A is an actin-binding and crosslinking protein." Cell Motil. Cytoskeleton **29**(2): 110-116.

Pedrotti, B and K Islam (1994). "Purified native microtubule associated protein MAP1A: kinetics of microtubule assembly and MAP1A/tubulin stoichiometry." Biochemistry **33**(41): 12463-12470.

Peng, K, P Radivojac, V S., AK Dunker and Z Obradovic (2006). "Length-dependent prediction of protein intrinsic disorder." BMC Bioinformatics **7**: 208.

Peri, S and A Pandey (2001). "A reassessment of the translation initiation codon in vertebrates." Trends Genet. **17**(12): 685-687.

Pickard, BS, MP Malloy, A Christoforou, PA Thomson, KL Evans*, et al.* (2006). "Cytogenetic and genetic evidence supports a role for the kainate-type glutamate receptor gene, GRIK4, in schizophrenia and bipolar disorder." Mol. Psychiatry **11**(9): 847-857.

Pickard, BS, JK Millar, DJ Porteous, WJ Muir and DHR Blackwood (2005). "Cytogenetics and gene discovery in psychiatric disorders." Pharmacogenetics J. **5**: 81-88.

Pickard, BS, PA Thomson, A Christoforou, KL Evans, SW Morris*, et al.* (2007). "The PDE4B gene confers sex-specific protection against schizophrenia." Psychiatr. Genet. **17**(3): 129-33.

Pletnikov, MV, Y Ayhan, O Nikolskaia, Y Xu, M Ovanesov*, et al.* (2008). "Inducible expression of mutant human DISC1 in mice is associated with brain and behavioral abnormalities reminiscent of schizophrenia." Mol. Psychiatry **13**: 173-186.

Pletnikov, MV, Y Xu, MV Ovanesov, A Kamiya, A Sawa and CA Ross (2007). "PC12 cell model of inducible expression of mutant DISC1: New evidence for a dominant-negative mechanism of abnormal neuronal differentiation." Neurosci. Res. **58**(3): 234-244.

Pombo, A, P Cuello, W Schul, JB Yoon, RG Roeder*, et al.* (1998). "Regional and temporal specialization in the nucleus: a transcriptionally-active nuclear domain rich in PTF, Oct1 and PIKA antigens associates with specific chromosomes early in the cell cycle." EMBO J. **17**(6): 1768-1778.

Prata, DP, A Mechelli, CHY Fu, M Picchioni, F Kane*, et al.* (2008). "Effect of disrupted-in-schizophrenia-1 on pre-frontal cortical function." Mol. Psychiatry **13**: 915-917.

Prilusky, J, CE Felder, T Zeev-Ben-Mordehai, EH Rydberg, O Man*, et al.* (2005). "FoldIndex(C): a simple tool to predict whether a given protein sequence is intrinsically unfolded." Bioinformatics **21**(16): 3435-3438.

Psychiatric GWAS Consortium (2008). "A framework for interpreting genome-wide association studies of psychiatric disorders." Mol. Psychiatry **doi:10.1038/mp.2008.126**.

Pulver, AE, M Karayiorgou, PS Wolyniec, VK Lasseter, L Kasch*, et al.* (1994). "Sequential strategy to identify a susceptibility gene for schizophrenia: Report of potential linkage on chromosome 22q12-q13.1: Part 1." Am. J. Med. Genet. **54**(1): 36-43.

Qu, M, F Tang, L Wang, H Yan, Y Han*, et al.* (2008). "Associations of ATF4 gene polymorphisms with schizophrenia in male patients." Am. J. Med. Genet. **147B**(6): 732-736.

Qu, M, F Tang, W Yue, Y Ruan, T Lu*, et al.* (2007). "Positive association of the *Disrupted-in-Schizophrenia-1* gene (*DISC1*) with schizophrenia in the Chinese han population." Am. J. Med. Genet. **144B**(3): 266-270.

Rauch, A, CT Thiel, D Schindler, U Wick, YJ Crow*, et al.* (2008). "Mutations in the Pericentrin (PCNT) gene cause primordial dwarfism." Science **319**(5864): 816-819.

Reardon, W, A Dunlop, ST Holden and R Blennerhassett (2007). "Bipolar affective disorder associated with 11q24.2 disruption--a second report." Am. J. Med. Genet. **143A**(12): 1263-1267.

Redon, R, S Ishikawa, KR Fitch, L Feuk, GH Perry*, et al.* (2006). "Global variation in copy number in the human genome." Nature **444**(7118): 444-454.

Reiner, O, R Carrozzo, Y Shen, M Wehnert, F Faustinella*, et al.* (1993). "Isolation of a Miller-Dicker lissencephaly gene containing G protein (beta)-subunit-like repeats." Nature **364**: 717-721.

Rena, G, F Begg, A Ross, C MacKenzie, I McPhee*, et al.* (2001). "Molecular cloning, genomic positioning, promoter identification, and characterization of the novel cyclic AMP-specific phosphodiesterase PDE4A10." Mol. Pharmacol. **59**(5): 996-1011.

Riley, BP, E Tahir, S Rajagopalan, M Mogudi-Carter, S Fauré*, et al.* (1997). "A linkage study of the N-methyl-D-aspartate receptor subunit gene loci and schizophrenia in southern African Bantu-speaking families." Psychiatr. Genet. **7**(2): 57-74.

Robbins, J, SM Dilworthtt, RA Laskey and C Dingwall (1991). "Two interdependent basic domains in nucleoplasmin nuclear targeting sequence: Identification of a class of bipartite nuclear targeting sequence." Cell **64**(3): 615-623.

Rush, J, A Moritz, KA Lee, A Guo, VL Goss*, et al.* (2005). "Immunoaffinity profiling of tyrosine phosphorylation in cancer cells." Nature. Biotech. **23**(1): 94-101.

Sachs, NA, A Sawa, SE Holmes, CA Ross, LE DeLisi and RL Margolis (2005). "A frameshift mutation in Disrupted in Schizophrenia 1 in an American family with schizophrenia and schizoaffective disorder." Mol. Psychiatry **10**: 758-764.

Saetre, P, I Agartz, A De Franciscis, P Lundmark, S Djurovic*, et al.* (2008). "Association between a disrupted-in-schizophrenia 1 (DISC1) single

nucleotide polymorphism and schizophrenia in a combined Scandinavian case-control sample." Schizophr. Res. **106**(2-3): 237-241.

Saha, S, D Chant, J Welham and J McGrath (2005). "A systematic review of the prevalence of schizophrenia." PLoS Med. **2**(5): 413-433.

Sakae, N, N Yamasaki, K Kitaichi, T Fukuda, M Yamada*, et al.* (2008). "Mice lacking the schizophrenia-associated protein FEZ1 manifest hyperactivity and enhanced responsiveness to psychostimulants." Hum. Mol. Genet. **17**(20): 3191-3203.

Sanders, AR, J Duan, DF Levinson, J Shi, D He*, et al.* (2008). "No significant association of 14 candidate genes with schizophrenia in a large european ancestry sample: Implications for psychiatric genetics." Am. J. Psychiatry **165**(4): 497-506.

Sasaki, S, D Mori, K Toyo-oka, A Chen, L Garrett-Beal*, et al.* (2005). "Complete loss of Ndel1 results in neuronal migration defects and early embryonic lethality." Mol. Cell. Biol. **25**(17): 7812-7827.

Sasaki, S, A Shionoya, M Ishida, MJ Gambello, J Yingling*, et al.* (2000). "A LIS1/NUDEL/cytoplasmic dyenin heavy chain complex in the developing and adult nervous system." Neuron **28**: 681-696.

Sawamura, N, T Ando, Y Maruyama, M Fujimuro, H Mochizuki*, et al.* (2008). "Nuclear DISC1 regulates CRE-mediated gene transcription and sleep homeostasis in the fruit fly." Mol. Psychiatry **13**(12): 1138-1148.

Sawamura, N, T Sawamura-Yamamoto, Y Ozeki, CA Ross and A Sawa (2005). "A form of DISC1 enriched in nucleus: Altered subcellular distribution in orbitofrontal cortex in psychosis and substancealcohol abuse." Proc. Natl. Acad. Sci. USA **102**(**4**): 1187-1192.

Sayer, JA, EA Otto, JF O'Toole, G Nurnberg, MA Kennedy*, et al.* (2006). "The centrosomal protein nephrocystin-6 is mutated in Joubert syndrome and activates transcription factor ATF4." Nat. Genet. **38**(6): 674-681.

Schurov, I, EJ Handford, NJ Brandon and PJ Whiting (2004). "Expression of disrupted in schizophrenia 1 (DISC1) protein in the adult and developing mouse brain indicates its role in neurodevelopment." Mol. Psychiatry **9**: 1100-1110.

Segurado, R, SD Detera-Wadleigh, DF Levinson, CM Lewis, M Gill*, et al.* (2003). "Genome scan meta-analysis of schizophrenia and bipolar disorder, part III: Bipolar disorder." Am. J. Hum. Genet. **73**(1): 49-62.

Semple, CAM, RS Devon, S Le Hellard and DJ Porteous (2001). "Identification of genes from a schizophrenia-linked translocation breakpoint region." Genomics **73**(1): 123-126.

Semple, DM, AM McIntosh and SM Lawrie (2005). "Cannabis as a risk factor for psychosis: systematic review." J. Psychopharmacol. **19**(2): 187-194.

Sette, C and M Conti (1996). "Phosphorylation and activation of a cAMP-specific phosphodiesterase by the cAMP-dependant protein kinase." J. Biol. Chem. **271**(28): 16526-16534.

Severinsen, JE, TD Als, H Binderup, TA Kruse, AG Wang*, et al.* (2006a). "Association analyses suggest GPR24 as a shared susceptibility gene for bipolar affective disorder and schizophrenia." Am. J. Med. Genet. **141B**(5): 524-533.

Severinsen, JE, CR Bjarkam, S Kiar-Larsen, IM Olsen, MM Nielsen, *et al.* (2006b). "Evidence implicating BRD1 with brain development and susceptibility to both schizophrenia and bipolar affective disorder." Mol. Psychiatry **11**(12): 1126-1138.

Shabb, JB (2001). "Physiological substrates of cAMP-dependent protein kinase." Chem. Rev. **101**(8): 2381-2412.

Shen, S, B Lang, C Nakamoto, F Zhang, J Pu, *et al.* (2008a). "Schizophrenia-related neural and behavioral phenotypes in transgenic mice expressing truncated Disc1." J. Neurosci. **28**(43): 10893-10904.

Shen, Y, N Li, S Wu, Y Zhou, Y Shan, *et al.* (2008b). "Nudel binds Cdc42GAP to modulate Cdc42 activity at the leading edge of migrating cells." Dev. Cell **14**: 342-353.

Shim, SY, BA Samuels, J Wang, G Neumayer, C Belzil, *et al.* (2008). "Ndel1 controls the dynein-mediated transport of vimentin during neurite outgrowth." J. Biol. Chem. **283**(18): 12232-12240.

Shimizu, S, S Matsuzaki, T Hattori, N Kumamoto, K Miyoshi, *et al.* (2008). "DISC1-kendrin interaction is involved in centrosomal microtubule network formation." Biochem. Biophys. Res. Comm. **377**(4): 1051-1056.

Shinoda, T, S Taya, D Tsuboi, T Hikita, R Matsuzawa, *et al.* (2007). "DISC1 regulates Neurotrophin-induced axon elongation via interaction with Grb2." J. Neurosci. **27**(1): 4-14.

Shiomura, Y and N Hirokawa (1987). "The molecular structure of microtubule-associated protein 1A (MAP1A) in vivo and in vitro. An immunoelectron microscopy and quick-freeze, deep-etch study." J. Neurosci. **7**(5): 1461-1469.

Shu, T, R Ayala, M-D Nguyen, Z Xie, JG Gleeson and L-H Tsai (2004). "Ndel1 operates in a common pathway with LIS1 and cytoplasmic dynein to regulate cortical neuronal positioning." Neuron **44**(2): 263-277.

Silberberg, G, A Levit, D Collier, D St Clair, J Munro, *et al.* (2008). "Stargazin involvement with bipolar disorder and response to lithium treatment." Pharmacogenet. Genomics **18**(5): 403-412.

Smyth, C, G Kalsi, D Curtis, J Brynjolfsson, J O'Neill, *et al.* (1997). "Two-locus admixture linkage analysis of bipolar and unipolar affective disorder supports the presence of susceptibility loci on chromosomes 11p15 and 21q22." Genomics **39**(3): 271-278.

Song, W, W Li, J Feng, LL Heston, WA Scaringe and SS Sommer (2008). "Identification of high risk DISC1 structural variants with a 2% attributable risk for schizophrenia." Biochem. Biophys. Res. Comm. **367**(3): 700-706.

Sorokin, AV, ER Kim and LP Ovchinnikov (2007). "Nucleocytoplasmic transport of proteins." Biochemistry (Moscow) **72**(13): 1439-1457.

Soukoulis, V, S Reddy, RD Pooley, Y Feng, CA Walsh and DM Bader (2005). "Cytoplasmic LEK1 is a regulator of microtubule function through its interaction with the LIS1 pathway." Proc. Natl. Acad. Sci. USA **102**(24): 8549-8554.

St Clair, D, D Blackwood, W Muir, A Carothers, M Walker, *et al.* (1990). "Association within a family of a balanced autosomal translocation with major mental illness." Lancet **336**(8706): 13-16.

Stehman, SA, Y Chen, RJ McKenney and RB Vallee (2007). "NudE and NudEL are required for mitotic progression and are involved in dynein recruitment to kinetochores." J. Cell Biol. **178**(4): 583-94.

Stöber, G, K Saar, F Rüschendorf, J Meyer, G Nürnberg, *et al.* (2000). "Splitting schizophrenia: Periodic catatonia-susceptibility locus on chromosome 15q15." Am. J. Hum. Genet. **67**(5): 1201-1207.

Straub, RE, T Lehner, Y Luo, JE Loth, W Shao, *et al.* (1994). "A possible vulnerability locus for bipolar affective disorder on chromosome 21q22.3." Nat. Genet. **8**(3): 291-296.

Sullivan, PF (2008). "Schizophrenia genetics: the search for a hard lead." Curr. Opin. Psychiatry **21**(2): 157-160.

Susser, E, D St Clair and L He (2008). "Latent effects of prenatal malnutrition on adult health: the example of schizophrenia." Ann. NY Acad. Sci. **1136**: 185-192.

Suzuki, SO, RJ McKenney, S Mawarari, M Mizuhuchi, A Mikami, *et al.* (2007). "Expression patterns of LIS1, dynein and their interaction partners dynactin, NudE, NudEL and NudC in human gliomas suggest roles in invasion and proliferation." Acta Neuropathologica **113**(5): 591-599.

Sweeney, KJ, GD Clark, A Prokscha, WB Dobyns and G Eichele (2000). "Lissencephaly associated mutations suggest a requirement for the PAFAH1B heterotrimeric complex in brain development." Mech. Dev. **92**(2): 263-271.

Sweeney, KJ, A Prokscha and G Eichele (2001). "NudE-L, a novel Lis1-interacting protein, belongs to a family of vertebrate coiled-coil proteins." Mech. Dev. **101**(1-2): 21-33.

Szebenyi, G, F Bollati, M Bisbal, S Sheridan, L Faas, *et al.* (2005). "Activity-driven dendritic remodeling requires Microtubule-Associated Protein 1A." Curr. Biol. **15**(20): 1820-1826.

Szeszko, PR, CA Hodgkinson, DG Robinson, P DeRosse, RM Bilder, *et al.* (2008). "DISC1 is associated with prefrontal cortical gray matter and positive symptoms in schizophrenia." Biol. Psychol. **79**(1): 103-110.

Tai, C-Y, DL Dujardin, NE Faulkner and RB Vallee (2002). "Role of dynein, dynactin, and CLIP-170 interactions in LIS1 kinetochore function." J. Cell Biol. **156**(6): 959-968.

Takahashi, S, SV Faraone, J Lasky-Su and MT Tsuang (2005). "Genome-wide scan of homogeneous subtypes of NIMH genetics initiative schizophrenia families." Psychiatry Res. **133**(2-3): 111-122.

Tandon, R, MS Keshavan and HA Nasrallah (2008). "Schizophrenia, "Just the Facts" What we know in 2008. 2. Epidemiology and etiology." Schizophr. Res. **102**(1-3): 1-18.

Tarricone, C, F Perrina, S Monzani, L Massimiliano, M-H Kim, *et al.* (2004). "Coupling PAF signaling to dynein regulation: Structure of LIS1 in complex with PAF-acetylhydrolase." Neuron **44**(5): 809-821.

Tastemir, D, O Demirhan and Y Sertdemir (2006). "Chromosomal fragile site expression in Turkish psychiatric patients." Psychiatry Res. **144**(2-3): 197-203.

Taya, S, T Shinoda, D Tsuboi, J Asaki, K Nagai*, et al.* (2007). "DISC1 regulates the transport of the NUDEL/LIS1/14-3-3epsilon complex through kinesin-1." J. Neurosci. **27**(1): 15-26.

Taylor, MS, RS Devon, JK Millar and DJ Porteous (2003). "Evolutionary constraints on the Disrupted in Schizophrenia locus." Genomics **81**: 67-77.

Thompson, JD, DG Higgins and TJ Gibson (1994). "CLUSTAL W: improving the sensitivity of progressive multiple sequence alignment through sequence weighting, position-specific gap penalties and weight matrix choice." Nucleic Acids Res. **22**(22): 4673-4680.

Thomson, PA, SE Harris, JM Starr, LJ Whalley, DJ Porteous and IJ Deary (2005a). "Association between genotype at an exonic SNP in DISC1 and normal cognitive aging." Neurosci. Lett. **389**(1): 41-45.

Thomson, PA, NR Wray, KL Evans, S Le Hellard, A Condie*, et al.* (2005b). "Association between the TRAX/DISC locus and both dipolar disorder and schizophrenia in the Scottish population." Mol. Psychiatry: 1-12.

Tikole, S and R Sankararamakrishnan (2008). "Prediction of translation initiation sites in human mRNA sequences with AUG start codon in weak Kozak context: A neural network approach." Biochem. Biophys. Res. Comm. **369**(4): 1166-1168.

Tomppo, L, W Hennah, Pi Lahermo, A Loukola, J Ekelund*, et al.* (2006). "Association evidence from NUDEL and PDE4D support the DISC1-pathway concept in the etiology of schizophrenia." Am. J. Med. Genet. **141B**: 717.

Toth, C, SY Shim, J Wang, Y Jiang, G Neumayer*, et al.* (2008). "Ndel1 promotes axon regeneration via intermediate filaments." PLoS One **3**(4): e2014.

Toyo-Oka, K, D Mori, Y Yano, M Shiota, H Iwao*, et al.* (2008). "Protein phosphatase 4 catalytic subunit regulates Cdk1 activity and microtubule organization via NDEL1 dephosphorylation." J. Cell Biol. **180**(6): 1133-1147.

Toyo-Oka, K, S Sasaki, Y Yano, D Mori, T Kobayashi*, et al.* (2005). "Recruitment of katanin p60 by phosphorylated NDEL1, an LIS1 interacting protein, is essential for mitotic cell division and neuronal migration." Hum. Mol. Genet. **14**(21): 3113-3128.

Toyo-Oka, K, A Shionoya, MJ Gambello, C Cardoso, R Leventer*, et al.* (2003). "14-3-3epsilon is important for neuronal migration by binding to NUDEL: a molecular explanation for Miller-Dieker syndrome." Nat. Genet. **34**(3): 274-285.

Türeci, Ö, U Sahin, M Koslowski, B Buss, C Bell*, et al.* (2002). "A novel tumour associated leucine zipper protein targeting to sites of gene transcription and splicing." Oncogene **21**(24): 3879-3888.

Valente, EM, JL Silhavy, F Brancati, G Barrano, SR Krishnaswami*, et al.* (2006). "Mutations in CEP290, which encodes a centrosomal protein, cause pleiotropic forms of Joubert syndrome." Nat. Genet. **38**(6): 623-625.

Vallada, H, N Craddock, L Vasques, D Curtis, G Kirov*, et al.* (1996). "Linkage studies in bipolar affective disorder with markers on chromosome 21." J. Affect. Disord. **41**(3): 217-221.

Vergnolle, MAS and SS Taylor (2007). "Cenp-F links kinetochores to Ndel1/Nde1/Lis1/Dynein microtubule motor complexes." Curr. Biol. **17**(13): 1173-1179.

Verma, R, S Kubendran, SK Das, S Jain and SK Brahmachari (2005a). "SYNGR1 is associated with schizophrenia and bipolar disorder in southern India." J. Hum. Genet. **50**(12): 635-640.

Verma, R, M Mukerji, D Grover, C B-Rao, SK Das*, et al.* (2005b). "MLC1 gene is associated with schizophrenia and bipolar disorder in Southern India." Biol. Psychiatry **58**(1): 16-22.

Vucetic, S, H Xie, LM Iakoucheva, CJ Oldfield, AK Dunker*, et al.* (2007). "Functional anthology of intrinsic disorder. 2. Cellular components, domains, technical terms, developmental processes, and coding sequence diversities correlated with long disordered regions." J. Proteome Res. **6**(5): 1899-1916.

Wachtel, H (1983). "Potential antidepressant activity of rolipram and other selective cyclic adenosine 3',5'-monophosphate phosphodiesterase inhibitors." Neuropharmacology **22**(3, Part 1): 267-272.

Walss-Bass, C, AP Montero, R Armas, A Dassori, SA Contreras*, et al.* (2006). "Linkage disequilibrium analyses in the Costa Rican population suggests discrete gene loci for schizophrenia at 8p23.1 and 8q13.3." Psychiatr. Genet. **16**(4): 159-168.

Wang, Q, X Du, J Meinkoth, Y Hirohashi, H Zhang*, et al.* (2006). "Characterization of Su48, a centrosome protein essential for cell division." Proc. Natl. Acad. Sci. USA **103**(17): 6428-6435.

Ward, JJ, JS Sodhi, LJ McGuffin, BF Buxton and DT Jones (2004). "Prediction and functional analysis of native disorder in proteins from the three kingdoms of life." J. Mol. Biol. **337**(635-645).

Wellcome Trust Case Control Consortium (2007). "Genome-wide association study of 14,000 cases of seven common diseases and 3,000 shared controls." Nature **447**(7145): 661-678.

Wijsman, EM, EA Rosenthal, D Hall, ML Blundell, C Sobin*, et al.* (2003). "Genome-wide scan in a large complex pedigree with predominantly male schizophrenics from the island of Kosrae: evidence for linkage to chromosome 2q." Mol. Psychiatry **8**(7): 695-705.

Wohl, M and P Gorwood (2007). "Paternal ages below or above 35 years old are associated with a different risk of schizophrenia in the offspring." Eur. Psychiatry **22**(1): 22-26.

World Health Organisation (2004). Disease incidence, prevalance and disability. The global burden of disease, 2004 update, World Health Organisation Press**:** 27-38.

Wright, PE and HJ Dyson (1999). "Intrinsically unstructured proteins: re-assessing the protein structure-function paradigm." J. Mol. Biol. **293**(2): 321-331.

Xiang, X, AH Osmani, SA Osmani, M Xin and NR Morris (1995a). "NudF, a nuclear migration gene in *Aspergillus nidulans*, is similar to the human LIS-1 gene required for neuronal migration." Mol. Biol. Cell **6**: 297-310.

Xiang, X, C Roghi and N Morris (1995b). "Characterization and localization of the cytoplasmic dynein heavy chain in Aspergillus nidulans." Proc. Natl. Acad. Sci. USA **92**(21): 9890-9894.

Xiang, X, W Zuo, VP Efimov and NR Morris (1999). "Isolation of a new set of Aspergillus nidulans mutants defective in nuclear migration." Curr. Genet. **35**(6): 626-630.

Xie, H, S Vucetic, LM Iakoucheva, CJ Oldfield, AK Dunker*, et al.* (2007). "Functional anthology of intrinsic disorder. 1. Biological processes and functions of proteins with long disordered regions." J. Proteome Res. **6**(5): 1882-1898.

Yamada, K, K Nakamura, Y Minabe, Y Iwayama-Shigeno, H Takao*, et al.* (2004). "Association analysis of FEZ1 variants with schizophrenia in Japanese cohorts." Biol. Psychiatry **56**(9): 683-690.

Yamada, M, S Toba, Y Yoshida, K Haratani, D Mori*, et al.* (2008). "LIS1 and NDEL1 coordinate the plus-end-directed transport of cytoplasmic dynein." EMBO J. **27**(19): 2471-2483.

Yamaguchi, N, Y Takanezawa, H Koizumi, M Umezu-Goto, J Aoki and H Arai (2004). "Expression of NUDEL in manchette and its implication in spermatogenesis." FEBS Lett. **566**(1-3): 71-76.

Yan, XM, F Li, Y Liang, YD Shen, XS Zhao*, et al.* (2003). "Human Nudel and NudE as regulators of cytoplasmic dynein in poleward protein transport along the mitotic spindle." Mol. Cell. Biol. **23**(4): 1239-1250.

Zandi, PP, D Avramopoulos, VL Willour, Y Huo, K Miao*, et al.* (2007). "SNP fine mapping of chromosome 8q24 in bipolar disorder." Am. J. Med. Genet. **144B**(5): 625-630.

Zandi, PP, S Zöllner, D Avramopoulos, VL Willour, Y Chen*, et al.* (2008). "Family-based SNP association study on 8q24 in bipolar disorder." Am. J. Med. Genet. **147B**(5): 612-618.

Zhang, F, J Sarginson, C Crombie, N Walker, D St Clair and D Shaw (2006). "Genetic association between schizophrenia and the DISC1 gene in the Scottish population." Am. J. Med. Genet. **141B**(2): 155-159.

Zhang, J, G Han and X Xiang (2002). "Cytoplasmic dynein intermediate chain and heavy chain are dependent upon each other for microtubule end localization in Aspergillus nidulans." Mol. Microbiol. **44**: 381-392.

Zhang, J, S Li, R Fischer and X Xiang (2003). "Accumulation of cytoplasmic dynein and dynactin at microtubule plus ends in Aspergillus nidulans is kinesin dependent." Mol. Biol. Cell **14**(4): 1479-1488.

Zhang, X, M Tochigi, J Ohashi, K Maeda, T Kato*, et al.* (2005). "Association study of the DISC1/TRAX locus with schizophrenia in a Japanese population." Schizophr. Res. **79**(2-3): 175-180.

Zheng, Y, X Wang, N Gu, G Feng, F Zou*, et al.* (2006). "A two-stage linkage analysis of Chinese schizophrenia pedigrees in 10 target chromosomes." Biochem. Biophys. Res. Comm. **342**(4): 1049-1057.

Zhou, X, MA Geyer and JR Kelsoe (2008). "Does disrupted-in-schizophrenia (DISC1) generate fusion transcripts?" Mol. Psychiatry **13**(4): 361-363.

Appendix – Relevant publications

At the time of writing, three journal articles have been published relevant to this thesis. Details of these articles and my contribution to each of them are described below. Full versions of the articles and their supplementary online material follow.

The first article was published by Nature Publishing group, who grant permission to "reproduce the Contribution in whole or in part in any printed volume (book or thesis) of which they are the author(s)." The latter two articles were published by Elsevier, who grant "the right to include the journal article, in full or in part, in a thesis or dissertation".

Publication 1

"The *DISC* locus in psychiatric illness"

Jennifer E. Chubb, Nicholas J. Bradshaw, Dinesh C. Soares, David J. Porteous & J. Kirsty Millar

Molecular Psychiatry (2008) **13** (1) 36-64

My part of this review article was written alongside chapter 1 of this thesis. My principle contribution to the article was writing the section on NDE1, NDEL1 and LIS1.

Publication 2

"NDE1 and NDEL1: Multimerisation, alternate splicing and DISC1 interaction"

Nicholas J. Bradshaw, Sheila Christie, Dinesh C. Soares, Becky C. Carlyle, David J. Porteous and J. Kirsty Millar

Neuroscience Letters (2009) **449** (3) 228-233

This article contains work found in chapters 3-6 of this thesis. I performed all experiments described in the paper with the following exceptions: Both the V5 and GFP-tagged NDE1 and NDEL1 constructs were generated by Kirsty Millar and Sheila Christie, the NDE1-KMLL nuclear localisation signal was identified by

Dinesh Soares and confocal microscopy was performed with considerably assistance by Becky Carlyle. The manuscript was co-written by Kirsty Millar and me, with input from David Porteous and Dinesh Soares. Graphics were prepared by Sarah West.

Publication 3

"DISC1, PDE4B and NDE1 at the centrosome and synapse"

Nicholas J. Bradshaw*, Fumiaki Ogawa*, Beatriz Antolin-Fontes, Jennifer E. Chubb, Becky C. Carlyle, Sheila Christie, Antoine Claessens, David J. Porteous and J. Kirsty Millar

Biochemical and Biophysical Research Communications (2008) **377** (4) 1091-1096

This article contains work found in chapters 4, 6 and 7 of this thesis. The endogenous co-immunoprecipitation of PDE4B was performed by Sheila Christie and Kirsty Millar, with additional probings by Antoine Claessens and me. I performed all of the co-immunoprecipitation experiments involving over-expressed NDE1. Some of the colocalisation experiments within cell lines were performed by me and the remainder by Sheila Christie, with confocal microscopy being performed by Becky Carlyle. I performed all of the experiments relating to PKA phosphorylation of NDE1, with the exception of some repetitions of the phosphorylation mutant experiments, which were performed in part by Sheila Christie and the densitometry, which was performed with Kirsty Millar. I performed all of the bioinformatics analysis. The paper was co-written by myself, Kirsty Millar and Fumiaki Ogawa, with input by David Porteous, Christoph Grunewald and Shaun Mackie. Graphics were prepared by Kirsty Millar, Fumiaki Ogawa and Sarah West. *Fumiaki Ogawa and I are joint first authors.